UNIVERSITY OF LIVERPOOL

THE EFFECT OF CATHEPSIN L INHIBITOR ON NF-KB SIGNALLING PATHWAY AND POTENTIAL MODULATION BY THYMOQUINONE IN ADVANCED GLYCATION END PRODUCTS (AGES) -EXPOSED RETINAL PIGMENT EPITHELIUM CELLS (RPE)

Thesis submitted in accordance with the requirements of the University of Liverpool

for the degree of

Doctor of Philosophy

by

NUR MUSFIRAH BINTI MAHMUD

November 2019

DOCTOR OF PHILOSOPHY DECLARATION

I hereby declare that this dissertation is a record of work carried out in the Institute of Ageing and Chronic Disease at the University of Liverpool and Faculty of Medicine at University of Malaya during the period of November 2014 to October 2018. This dissertation is original in content except where otherwise stated.

November 2019

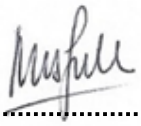

.....

(Nur Musfirah Binti Mahmud)

THE EFFECT OF CATHEPSIN L INHIBITOR ON NF-KB SIGNALLING PATHWAY AND POSSIBLE MODULATION BY THYMOQUINONE ON ADVANCED GLYCATION END PRODUCTS(AGES)-EXPOSED RETINAL PIGMENT EPITHELIUM (RPE) CELLS

ABSTRACT

The retinal pigment epithelium, or RPE, is a post-mitotic monolayer of cells responsible for maintaining retinal homeostasis. The RPE undergoes structural changes with age which results in impaired function and subsequently leads to development of age-related macular degeneration (AMD). Accumulation of advanced glycation endproducts (AGEs) is known to be one of the hallmarks of AMD. Activation of AGEs through binding to its receptor activates various signalling pathway including the inflammatory pathway, specifically the NF-κβ signalling pathway. In addition, accumulation of AGEs in Bruch's membrane (BrM) may alter RPE lysosomal activities by changing the expressions of key proteolysis effector proteins such as cathepsins. Decreased cathepsin L expression has been observed in AGEs-treated RPE cells in previous studies. In this study, we sought to understand the effects of AGEs on the NF-κβ signalling in a human RPE cell line (ARPE-19), and the response to an oxidative stressor, TNFα in the same environment. We also studied the role of cathepsin L on NF-κβ signalling pathway, and in its response to TNFα stimulus. Lastly we studied the effects of thymoquinone, which is a flavonoid with anti-oxidative properties, on TNFα-treated RPE cells. Our results showed downregulation of NF-κβ signalling in AGEs-exposed RPE cells. TNFα-induced stimulation caused an exaggerated response of NF-κβ activation in AGEs-exposed RPE cells compared to controls. Cathepsin L inhibition causes dampening of the NF-κβ signalling pathway, as shown in significant downregulation of p65 protein. The effects of TNFα was also blunted, further strengthening the role of cathepsin L in NF-κβ pathway. Lastly we found that thymoquinone had no significant effects on TNFα stimulation of RPE cells. Our findings supported the notion that ageing cells have exaggerated response to inflammatory stimuli and renders them more susceptible to cellular damage. This suggests a possible explanation of increased damage to oxidative stress in ageing RPE cells in AMD. In conclusion, the NF-κβ signalling pathway is involved in the response towards oxidative stress in our in vitro model of ageing RPE cells. Cathepsin L may have a role in reducing the effects of oxidative stress in ageing RPE cells also through NF-κβ signalling pathway.

PERANAN PERENCAT CATHEPSIN L DALAM JALUR ISYARAT NF-KB DAN KEBERANGKALIAN MODULASI OLEH THYMOQUINONE KEATAS SEL RETINA PIGMEN EPITHELIA YANG TERDEDAH KEPADA PRODUK AKHIR GLIKASI

Abstrak (Malay)

Retina Pigmen Epithelia, atau RPE, adalah salah satu lapisan sel yang tidak melalui fasa pembaharuan dan bertanggungjawab dalam mengekalkan fungsi retina. RPE melalui beberapa perubahan struktur ketika penuaan yang mengakibatkan kehilangan fungsi dan membawa kepada pembentukan penyakit "degenerasi macula berkaitan usia" atau lebih dikenali dengan singkatan AMD. Pengumpulan produk akhir glikasi atau "advanced glycation endproducts" (AGEs) merupakan salah satu petanda kepada AMD. AGEs diaktifkan melalui interaksinya kepada reseptor yang seterusnya mengaktifkan pelbagai laluan isyarat termasuk isyarat yang berkaitan dengan kesan keradangan, khususnya laluan isyarat NF-κβ. Tambahan pula, pengumpulan AGEs ini di dalam lapisan 'Bruch's membrane' boleh mengubah aktiviti lisosomal RPE dengan menukarkan ekspresi protein seperti 'cathepsin'. Penurunan expresi cathepsin L dalam sel-sel RPE yang dirawat AGEs telah ditemui di dalam kajian terdahulu. Di dalam kajian ini, kami cuba memahami kesan AGEs keatas laluan isyarat NF-κβ di dalam RPE sel (ARPE-19), dan tindak balasnya terhadap tekanan oksidatif, TNFα dalam persekitaran yang sama. Kami juga mengkaji peranan cathepsin L pada laluan isyarat NF-κβ, dan tindak balasnya terhadap rangsangan TNFα. Selain itu, kesan thymoquinone, yang merupakan flavonoid dengan bersifat anti-oksidatif, pada sel RPE yang dirawat TNFα turut dikaji. Kami mendapati bahawa terdapat penurunan isyarat NF-κβ dalam sel-sel RPE yang didedahkan kepada AGEs. Bagaimanapun, tindak balas berlebihan berlaku di dalam sel RPE apabila sel-sel tersebut dirangsang dengan TNFα. Tindak balas ini menjelaskan peningkatan kerosakan kepada tekanan oksidatif dalam penuaan sel-sel RPE di dalam AMD. Sekatan terhadap cathepsin L telah menyebabkan pengurangan tindak balas NF-κβ, seperti yang ditunjukkan dalam penurunan ketara protein p65. Kesan TNFα juga turut dikurangkan, menunjukkan kepentingan peranan cathepsin L dalam isyarat NF-κβ. Terakhir, kami mendapati bahawa thymoquinone tidak mempunyai kesan yang besar terhadap rangsangan TNFα terhadap laluan isyarat NF-κβ di dalam sel-sel RPE. Kesimpulannya, laluan isyarat NF-κβ terlibat dalam tindak balas terhadap tekanan oksidatif dalam model penuaan sel RPE ini. Selain itu, cathepsin L juga mempunyai peranan dalam mengurangkan kesan tekanan oksidatif dalam penuaan sel RPE juga melalui laluan isyarat NF-κβ.

ACKNOWLEDGEMENTS

Alhamdulillah, all praises to Allah for the strengths and His blessing in completing this thesis. Special appreciation and deepest gratitude goes to my supervisors, Assoc. Prof. Dr. Tengku Ain Tengku Kamalden, Prof Luminita Paraoan and Prof Malcolm Jackson for the continuous support, patience, motivation and knowledge throughout the research studies. My two years away from home has been a great time thanks to Prof Luminita and Prof Malcom, who has treat me full of care and makes me feels close to home and family. And to Dr. Ain, thank you for all your care while I am away and in UM. The trust given by my parents to allow me fly abroad was thanks to you too. Not to forget to all the UM's staff who has been helping me to enrol to the program.

A special thanks to Dr. Umar Shariff, Dr. Raheela Uwais, Dr. Paul Kay and Dr. Joe Butler for your warm welcome from my Day 1 in University of Liverpool. To my dear friend, Samantha McDonnell and Wasu Supharattanasitthi, we have started the journey together, although we finish it on our own sweet time, I would like you to know I appreciate every single moments we had together. To Syatirah and Faridah, thanks for all your help throughout the journey. To all friends, thank you for your understanding and encouragement during my hard times. The friendship that we built is something I would treasure throughout my life.

Last but not least, a remarkable special gratitude goes out to my family for their love and support through this journey, in fact throughout my whole life. Thank you, mum (Rahmah Abdullah) and dad (Mahmud Said) for giving me the strength to chase for my dreams. To my sister (Fatin) and brother (Faris), I could not thank you enough for being there, stand for the family while I am not able to do so.

Nur Musfirah Mahmud, October 2018

TABLE OF CONTENTS

LIST OF FIGURES

LIST OF TABLES

LIST OF SYMBOLS AND ABBREVIATIONS

For examples:

%	:	Percent
<	:	Less than
°C	:	Degree Celcius
µl	:	Microlitre
µm	:	Micrometer
µM	:	Micromolar
AGEs	:	Advanced Glycation Endproducts
AMD	:	Age Related Macular Degeneration
ARED	:	Age-Related Eye Disease
ATCC	:	American Type Culture Collection
ATP	:	Adenosine Triphosphate
BSA	:	Bovine Serum Albumin
cDNA	:	Complementary DNA
CML	:	N (Epsilon)-(Carboxymethyl) Lysine
CNTF	:	Ciliary Neurotrophic Factor
CNV	:	Choroidal Neovascularisation
CRALBP	:	Cellular retinaldehyde-binding protein
CRBP	:	Cellular Retinol Binding Proteins
ddCT	:	Delta-delta CT
DHA	:	Docosahexanoic Acid
DMEM	:	Dulbecco's Modified Eagle's Medium
DMSO	:	Dimethyl sulfoxide

DNA	:	Deoxyribonucleic Acid
ECM	:	Extracellular Matrix
EHS	:	Engelbreth-Holm-Swarm
ERK	:	Extracellular-Signal-Regulated Kinase
FBS	:	Fetal Bovine Serum
FDA	:	Food And Drug Administration
FGF	:	Fibroblast-Like Growth Factor
GA	:	Glycoaldehyde
GAPDH	:	Glyceraldehyde 3-Phosphate Dehydrogenase
GLUT	:	Glucose Transporter
IGF-1	:	Insulin-Like Growth Factor-1
IPM	:	Interphotoreceptor Matrix
IRBP	:	Interphotoreceptor Retinoid-Binding Proteins
Iκβα	:	Iκb Kinase
JNK	:	C-Jun N-Terminal Kinases
LAMP	:	Lysosomal-Associated Membrane Protein
LEDGF	:	Lens Epithelium-Derived Growth Factor
LPS	:	Lipopolysaccharides
LRAT	:	Lecithin Retinol Acyl Transferase
Lys	:	Lysine
MAPK	:	Classical Mitogen-Activated Protein Kinase
mm	:	Millimeter
Mrna	:	Messenger RNA
MSR	:	Macrophage Scavenger Receptors
NF-κβ	:	Nuclear Factor Kappa-Light-Chain-Enhancer Of Activated B Cells
ng	:	Nanogram

NPD1	:	Neuroprotectin D1
PBS	:	Phosphate Buffer Serum
PCR	:	Polymerase Chain Reaction
PDGF	:	Platelet-Derived Growth Factor
POS	:	Photoreceptor Outer Segment
pP65	:	Phosphorylated P65
qPCR	:	Realtime Polymerase Chain Reaction
RAGE	:	Receptor For Advanced Glycation Endproducts
RNA	:	Ribonucleic Acid
RPE	:	Retinal Pigment Epithelium
RPE65	:	Retinal pigment epithelium-specific 65 kDa protein
SEM	:	Standard Error of Mean
Ser	:	Serine
SOD	:	Superoxide Dismutase
TBE	:	Tris-Borate-EDTA
TBST	:	Tris-Buffered Saline Tween
TGF-β	:	Transforming Growth Factor-B
TIMP	:	Members Of The Interleukin Family, Tissue Inhibitor Of Matrix Metalloprotease
TLR	:	Toll-Like Receptor
TNFR	:	Tumor Necrosis Factor Receptor
TNFα	:	Tumor Necrosis Factor Alpha
UV	:	Ultraviolet
VEGF	:	Vascular Endothelial Growth Factor (VEGF) And Pigment Epithelium-Derived Factor
WHO	:	World Health Organisation

CHAPTER 1: LITERATURE REVIEW

1.1 Overview of the Eye

Human beings are equipped with five sensory organs which enable them to see, touch, smell, taste, and hear. The eye is the organ of sight providing vision by converting light into meaningful electrical impulses which are interpreted by the occipital region of the brain as images.

The eyeball has a non-spherical globular structure, located in the orbit of the skull measuring on average 24mm in its longest diameter (Westmoreland et al., 1998; Smerdon, 2000; Snell & Lemp, 2013). The anatomy of the eyeball is shown in Figure 1.1. The cornea forms a transparent window of the eyeball through which anterior segment structures, namely the iris, pupil and lens (DelMonte & Kim, 2011; Garhart & Lakshminarayanan, 2012). The iris is a contractile pigmented tissue with a central opening, or aperture called the pupil (Garhart & Lakshminarayanan, 2012). The contracting and dilating action of the iris controls the amount of light entering the eye by changing the size of the pupils (Kolb et al., 2007; Garhart & Lakshminarayanan, 2012). The visible white outer coat of the eye is called the sclera. Sclera provides a strong structural support to the eyeball (Snell & Lemp, 2013). The majority of the globe cavity is filled with a gelatinous fluid called vitreous humor. With 99% of water as its main constituent, the vitreous takes control two thirds of the eyeball's volume and weight (Garhart & Lakshminarayanan, 2012). The vitreous gel is in direct contact with the retinal layer on the posterior aspect of the eyeball. Among its main functions, vitreous pressure serves to maintain the globular shape of the eyeball (Snell & Lemp, 2013).

The posterior segment of the eyeball contains the optic nerve, choroid and retina. The optic nerve is the second cranial nerve and connects the eyeball to the brain

(Westmoreland et al., 1998). Its main function is in relaying visual information in the form of electrical impulses from the retina to the brain (Westmoreland et al., 1998; Ansari & Nadeem, 2016). The optic nerve mainly consists of the long axons of retinal ganglion cells (Ansari & Nadeem, 2016). The choroid is a vascular layer which lies between the retina and the sclera. It is comprised of 4 layers, namely Haller's, Sattler's, choriocapillaries and the innermost layer, called Bruch's membrane (Westmoreland et al., 1998; Snell & Lemp, 2013). The Bruch's membrane consists of collagen-rich extracellular matrix (Ansari & Nadeem, 2016). The Bruch's membrane separates the retina layer from the choroid and allows exchange of various molecules including oxygen, nutrient and waste product between the two layers (Snell & Lemp, 2013). The retina consists of the multi-layered neuroretina and the retinal pigment epithelium layers (Smerdon, 2000; Kolb et al., 2007). Detailed structures of the retina are discussed in section 1.2.

Light which passes through the eye is refracted or focused mainly by the cornea. The cornea focus the light through bending of light rays into the pupil, centre of the iris. Then light pass through the lens before hitting the photoreceptors on the retina, which in turn, generates specific electrical impulses. These electrical impulses are visual information, and is transmitted via the optic nerve to respective regions in the brain. The brain interprets these signals as meaningful 3-dimensional images (Kolb et al., 2007).

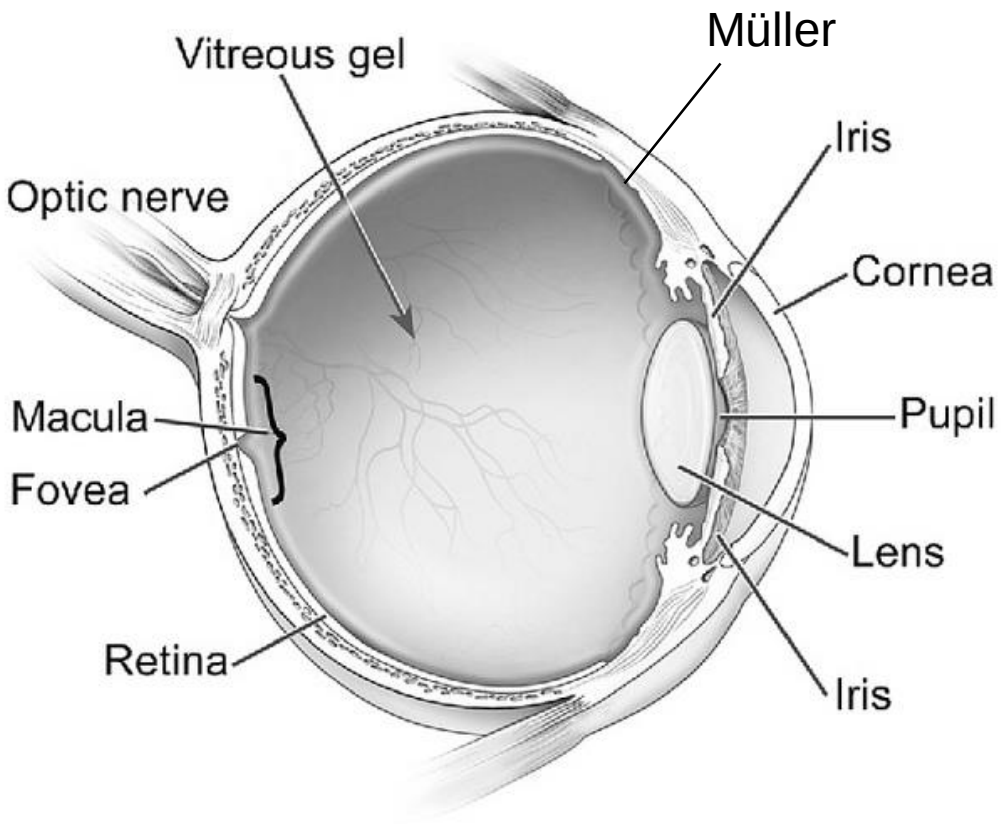

Figure 1.1 Gross anatomy of the human eyeball (Image modified from https://nei.nih.gov/photo/anatomy-of-the-eye).

1.2 Retina

The retina is light-sensitive tissue layer located at the back of the eye stretching from the optic nerve, to the ora serrata (refer to Figure 1.1). The thickness of the retina layer differs depending on its location. It is approximately 0.56mm thick near the optic disc area and 0.1mm as its approaches the ora serrata (Kolb et al., 2007; Snell & Lemp, 2013). The outer surface of the retina is in contact with the Bruch's membrane of the choroid and the inner surface directly surrounds the vitreous body (Ansari & Nadeem, 2016). Two specialised areas exist on the retina, namely macula lutea and fovea centralis. Macula lutea is an oval yellowish area at the centre posterior of the retina measuring 5mm in diameter, and is located approximately 3mm temporal to the optic disc (Snell & Lemp, 2013). Fovea centralis is a depressed area in the centre of macula lutea measuring about 1.5mm in diameter (Snell & Lemp, 2013; Ansari & Nadeem, 2016). Both of them are responsible in providing sharp acuity and colour vision (Westmoreland et al., 1998; Snell & Lemp, 2013).

The retina serves as a site for transforming light energy into a neural signal. The retina is made up of nine layer of inner neurosensory retina, also called neural retina, and an outer pigmented layer, the retinal pigment epithelium (RPE) (Snell & Lemp, 2013). The ten layers of retina and its cells composition is portrayed in Figure 1.2.

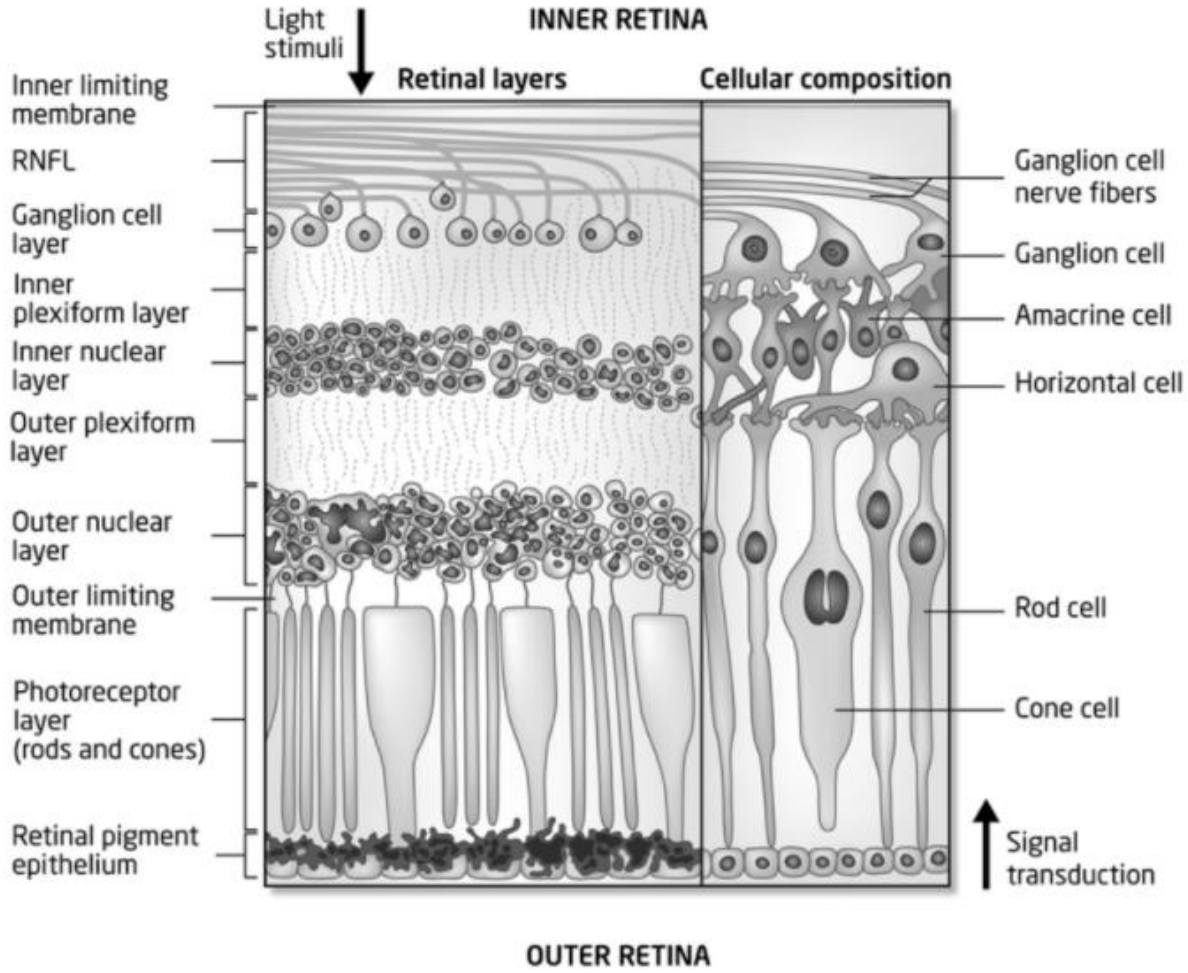

Figure 1.2 A representative image of the ten layers of retina and its different cells composition. Image retrieved from http://www.neurology.org/content/80/1/47/F1.

1.2.1 Neural Retina

Neural retina is a thin sensory tissue internally in contact to the vitreous body of the eyeball and externally attached to the RPE layer (Snell & Lemp, 2013). Neural retina covers the first nine layer of retina as counted from the inner retina surface (Refer to Figure 1,2). The neural retina is made up of three main groups of neurons namely photoreceptor, bipolar cells and ganglion cells (Westmoreland et al., 1998). These three cells carry neural signal in a three-step pathway through the retina.

1.2.1.1 Photoreceptor cells

Photoreceptor cells in the retina consist of rods and cones (Smerdon, 2000). Rods are responsible in providing vision in dim light and motion. In contrast to the rods, cones are involved in colour vision and visual acuity (Westmoreland et al., 1998; Garhart & Lakshminarayanan, 2012; Snell & Lemp, 2013). There are about 110-125 millions of rod and 6.3-6.8 millions of cones are present in the retina but its density varies across the (Snell & Lemp, 2013). Rods are absent at the fovea centralis area but cones present at its highest density in this area (Smerdon, 2000; Snell & Lemp, 2013).

Generally, rod cells are slim, measuring 100-120 µm in length. Cone cells are shorter in length measuring 65-75 µm (Snell & Lemp, 2013). Rods contain rhodopsin, photosensitive pigment aids in phototransduction, however this pigment is called as iodhopsin or photopsin in cones and these two pigments exist in the disc membrane of rods and cones (Remington & Goodwin, 2011). Rhodopsin is responsible for vision in dim light or dark light or vision in different shades of grey. The iodopsin or photopsin in cones is able to detect 3 different wavelength of light which is blue, red and green (Kolb, 2007b; Snell & Lemp, 2013).

Both rods and cones long body can be divided into four parts; outer segment, inner segment, cell body and synaptic body, as shown in Figure 1.3. The outer segment is the outer end of the photoreceptor facing the RPE layer and is in direct contact with the RPE microvilli. The outer segment of rod is made up of 600-1000 of membrane bound lamellae termed as disc (Remington & Goodwin, 2011; Snell & Lemp, 2013). New discs are formed at the base of the rod outer segment. With time, the outer segment discs are gradually pushed outwards towards the RPE microvilli. As the disc reached the tip of the outer segment, it will eventually be phagocytosed by the RPE. This forms the disc shedding and renewal process which is important to maintain the photoreceptor constant length and proper functions (Boesze-Battaglia & Goldberg, 2002; Strauss, 2005; Kevany & Palczewski, 2010; Snell & Lemp, 2013). Rod disc shedding processes does not occur continuously in 24-hour basis but once in early morning, once light hits the eye (LaVail, 1976; Strauss, 2005). Compared to rod discs, cone discs are not enclosed but are partially exposed to the surrounding fluids. Unlike in rods, shedding of cones tips occurs at the end of the day. Cone's discs are broader at the base and tapers closer to the tips. Rods have almost similar tapering disc shape throughout the outer segment (Strauss, 2005; Remington & Goodwin, 2011; Snell & Lemp, 2013).

The cilium acts as a connecting stalk between the outer segment and the inner segment (Boesze-Battaglia & Goldberg, 2002). It is made up of a series of nine microtubules without a central pair. The inner segment of rods and cones contains two parts; ellipsoid and myoid. The ellipsoid part resides next to the connecting stalk and the myoid is located closer towards the vitreous. The ellipsoid part contains mainly mitochondria to provide energy for the disc shedding and renewal process. Meanwhile myoids contains various organelles includes endoplasmic reticulum, free ribosomes and golgi bodies (Remington & Goodwin, 2011).

Extending from the inner segment are the outer fibre, cell body and inner fibre of the photoreceptors. The outer fibre joins the inner segment to cell body which contains the nucleus. Microtubules and specialised synaptic terminals reside in the inner fibre. The photoreceptors form synapses with the bipolar and horizontal cells (Remington & Goodwin, 2011).

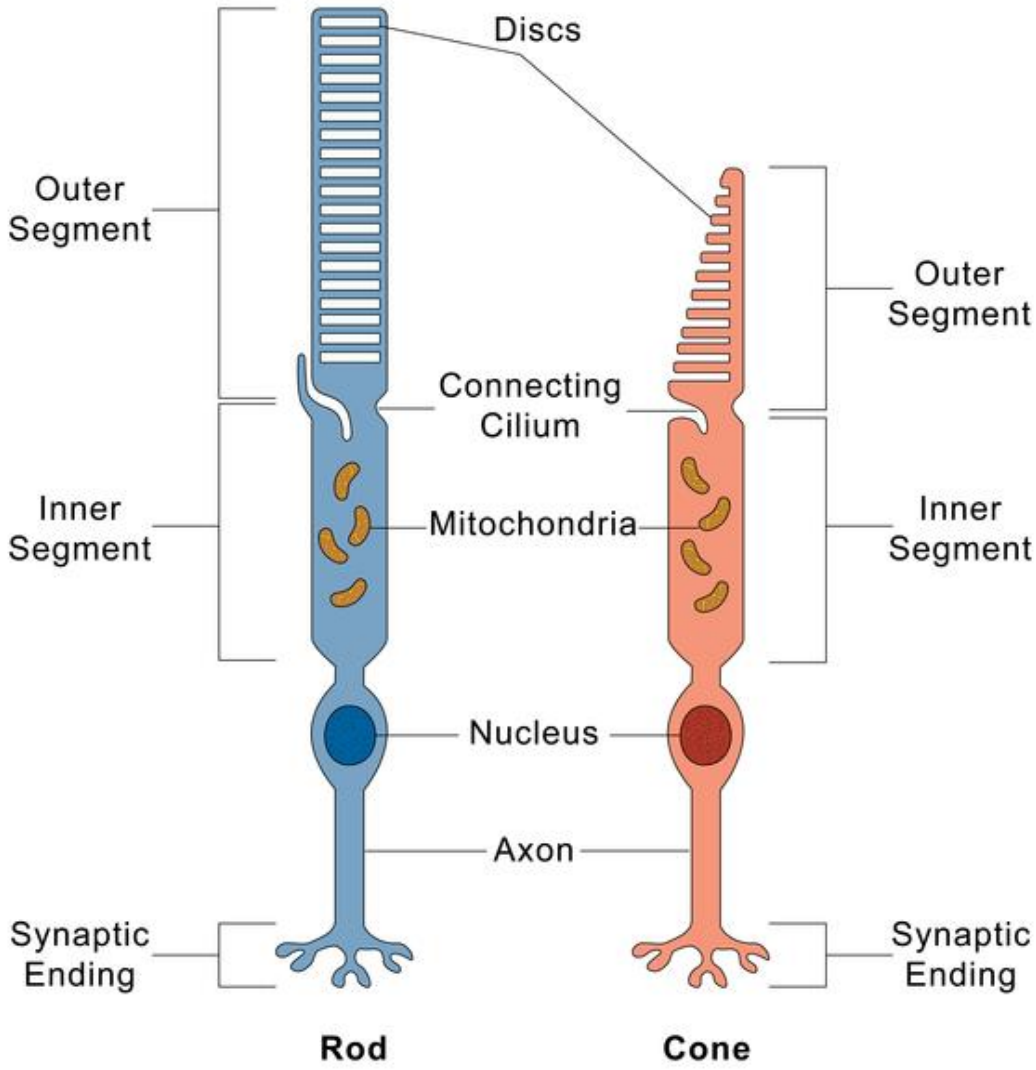

Figure 1.3 Structure of rods and cones of the retina. Image was retrieved from https://ghr.nlm.nih.gov/art/large/rod-and-cone-cells.jpeg.

1.2.1.2 Bipolar cells

The bipolar cell is a neuron with two extensions at respective ends (dendrites and axons). It has a large nucleus with minimal cell body cytoplasm. Bipolar cell dendrites synapses with photoreceptor and horizontal cells, meanwhile the axons synapses with the ganglion and amacrine cells (Figure 1.4). Eleven different types of bipolar cells have been characterised being associated with the photoreceptors (Westmoreland et al., 1998; Remington & Goodwin, 2011; Snell & Lemp, 2013; Euler et al., 2014). Bipolar cells can be classified into ON bipolar and OFF bipolar cells. The classification is based on their response to glutamate release by photoreceptors. ON bipolar cells depolarised during light onset, meanwhile the OFF bipolar cells depolarised in the dark (Euler et al., 2014).

Retinal bipolar cells facilitate the transmission of signals from photoreceptors to ganglion cells (Euler et al., 2014). It acts as the first elementary component of visual cycle. The bipolar cells gather and sort the signal from photoreceptor for further processing by the amacrine and retinal ganglion cells in the inner retina (Euler et al., 2014).

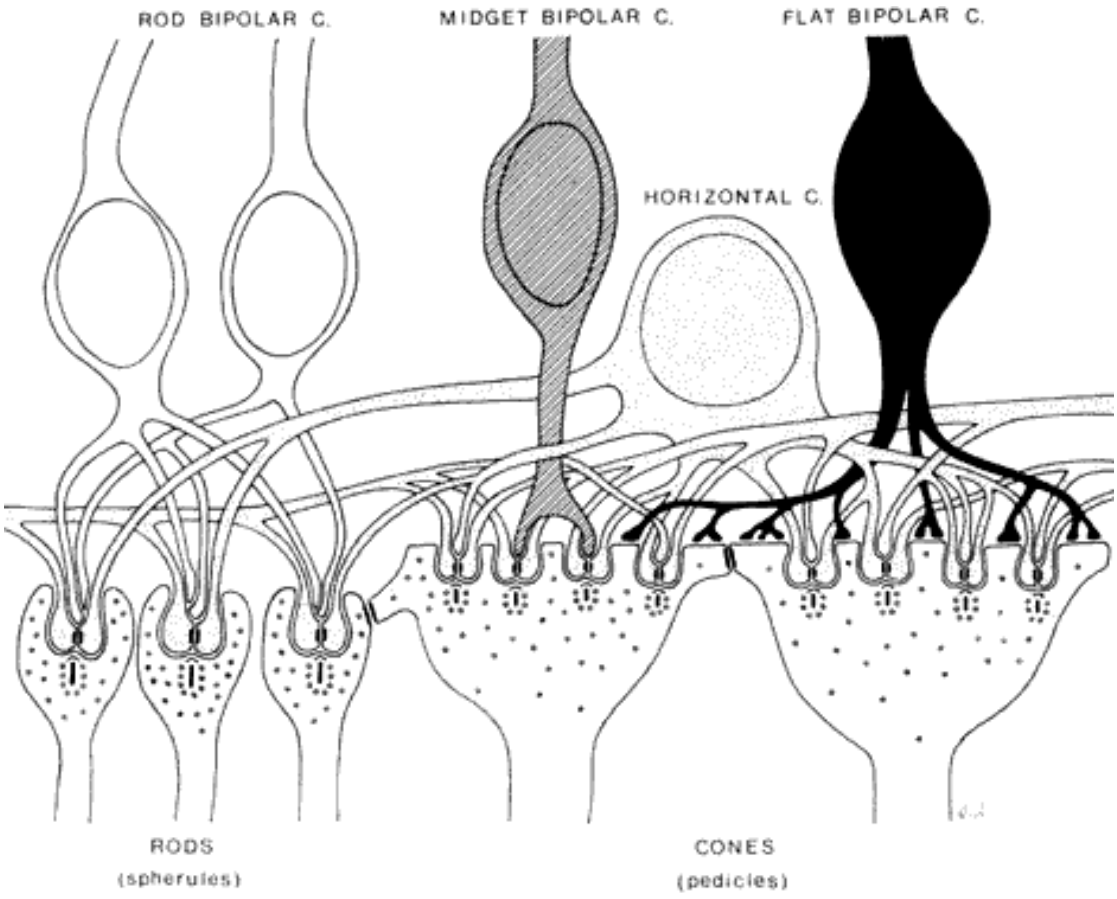

Figure 1.4 Image of bipolar cells which connects photoreceptors to the ganglion cells (Remington & Goodwin, 2011).

1.2.1.3 Retinal ganglion cells

Retinal ganglion cells (RGCs) are third-order neurons in the visual pathway and form the innermost layer of the neuroretina. The size of RGCs may vary between 10 to 36 µm diameters. RGCs are absent from the fovea but increases from the macula to the periphery retina (Remington & Goodwin, 2011; Snell & Lemp, 2013). It can exists either as bipolar (single axon and single dendrites) or multipolar (single axon and multiple dendrites) forms (Snell & Lemp, 2013). The RGCs' dendrites synapse with either the axons of bipolar or amacrine cells. Meanwhile the axons of the RGCs form a right-angle turn to become parallel to the retina surface in the nerve fibre layer and pass through the optic disc to form the optic nerve head (Snell & Lemp, 2013; Sanes & Masland, 2015).

1.2.1.4 Supporting cells

Apart from the three main neuronal cells present in the neuroretina; there are other supporting cells that aids in vision processing. Supporting cells such as horizontal cells, amacrine cells, Müller cells, microglial cells and astrocytes form the supporting cells in the retinal layer. Although some of them are not actively involved in visual processing, they provide structural and physiological support to the neurons in the retina (Westmoreland et al., 1998; Remington & Goodwin, 2011; Snell & Lemp, 2013)

Horizontal cells are located near to the terminal expansion of the photoreceptors. It exists as multipolar cell responsible in transmitting information in a horizontal direction parallel to the retinal surface between photoreceptor and bipolar cells (Poché & Reese, 2009). Horizontal cells have one axon and several short dendrites with branching terminals. The dendrites lay parallel on retinal surface creating synapses with photoreceptors, bipolar and other horizontal cells (Remington & Goodwin, 2011)

Amacrine cells have large cell bodies filled lobulated nuclei and branches of processes which form synapses with RGCs and axons of bipolar cells in the inner plexiform layer of the retina (Kolb et al., 1995). Amacrine cells responsible in modulation of information that received by ganglion cells (Kolb et al., 1995; Remington & Goodwin, 2011).

There are about 10 million Müller cells found in the mammalian retina (Remington & Goodwin, 2011). Müller cells transverses the entire thickness of the neuroretinal layer, from the inner to the outer limiting membrane (Kolb, 2007a). They provide important structural support to the retina. Additionally, Müller cells maintain homeostatic retinal processes such as regulating potassium ions concentration, controlling uptakes of neurotransmitter, maintaining the extracellular pH by absorbing

metabolic waste products, and glycogen synthesis and storage (Bringmann et al., 2006; Remington & Goodwin, 2011; Reichenbach & Bringmann, 2013; Snell & Lemp, 2013).

Last but not least are the microglial and astrocytes. Microglials are phagocytic cells found in the retina (Remington & Goodwin, 2011; Silverman & Wong, 2018). These microglial cells claimed to play a role in immunologic functions of the retina (Chen et al., 2002; Snell & Lemp, 2013; Rathnasamy et al., 2019). Their numbers are found to increase in response to tissue inflammation and injury (Remington & Goodwin, 2011). Astrocytes appear as star-shaped fibrous cells found in the nerve fibre layer and RGC layer (Kolb, 2007a; Remington & Goodwin, 2011; Tao & Zhang, 2014). They provide supportive network around the nerve fibres and retinal capillaries (Remington & Goodwin, 2011).

1.2.2 Pigmented cells

The pigmented part of retina is made up of retinal pigment epithelium (RPE), cobblestone like cells spreading as monolayers between the Bruch's membrane and the photoreceptors (Remington & Goodwin, 2011). The RPE will be discussed further in the next subchapter 1.4

1.2.3 Visual processing in retina

The retina is responsible in converting light energy to electrical signals to be sent to the brain for visual interpretation. As the light pass the globe, it is focused to the retinal layer at the back of the eye, where it is captured by the disc of the photoreceptor for further processes (Kolb et al., 2007). Rods is important in scotopic vision or black and white vision, meanwhile the cones is responsible for photopic vision or colour vision (Smerdon, 2000; Remington & Goodwin, 2011).

The photoreceptor pigment consist of two component, the 11-cis retinal and an opsin (Kolb et al., 1995; Tsin et al., 2018). In the presence of light, the photoreceptor pigment undergoes photobleaching process (Kolb et al., 1995). The 11-cis retinal double bond is broken creating all-trans retinal and transported to RPE for recycling. Meanwhile the free opsin molecules then undergoes series of conformational changes to metarhodopsin II. The metarhodopsin II binds to a G-couple protein (transducin) causing activation of phospodiesterase enzyme (PDE). PDE is responsible for cleavage of cyclic guanosine monophosphate (cGMP) into guanosine monophosphate (GMP) and cGMP is important to retain the opening of the sodium potassium gated channel. Thus, activation of PDE would leads to reduction in cGMP in the photoreceptor outer segment and closure of the sodium potassium channel. As a result, sodium ion can no longer enters the photoreceptor outer segment and it became hyperpolarised (-67mV of current) inducing reduction in glutamate release on the photoreceptor synaptic terminal. This process is called phototransduction. Finally, the slow release of glutamate would stimulates depolarisation of ON bipolar cells and hyperpolarisation OFF bipolar cells. Alternately, bipolar cells would then conveys the signal to the brain through ganglion cells and optic nerve for visual interpretation (Smerdon, 2000; Strauss, 2005; Remington & Goodwin, 2011).

In the less light, the two components of photoreceptor pigment are bound together leading to consistent production of cyclic cyclic guanosine monophosphate (cGMP). The cGMP keeps the sodium potassium channel to remains open and allow constant flow of sodium and calcium ion into the photoreceptor. This makes the photoreceptor to be in depolarised state at about -40mV of current. Depolarised photoreceptor allows increase released of neurotransmitter, glutamate, in the synaptic part of the photoreceptor, next to bipolar cells. Glutamate release would triggers the bipolar and

ganglion cells for further visual processing (Strauss, 2005; Remington & Goodwin, 2011).

1.3 Retinal Pigment Epithelium

1.3.1 RPE structure

The RPE is the outermost layer of the retina, sandwiched between the photoreceptor outer segments on its apical site and the Bruch's membrane of the choroid on its basal site (Sparrow et al., 2010). The RPE consists of a monolayer of densely packed cobblestone-like cells. The size and shape varies across the retina although they mostly appear to have hexagonal shape (Bhatia et al., 2016). Each RPE cell measures about 14 µm in diameter and 12 µm tall around the macula area and grows wider and flatter towards the periphery area (Boulton & Dayhaw-Barker, 2001; Cavallotti & Cerulli, 2008; Ao et al., 2018). The concentration of RPE is also varies, they are densely pack around the macula area and the numbers decrease greatly towards the periphery from approximately 4500 cells/mm^2 to 1500 cells/mm^2 respectively (Westmoreland et al., 1998; Kolb et al., 2007). The number of RPE cells started to decline after the age of 60 years old, at a rate of about 0.2-0.3% per year due to ageing (Panda-Jonas et al., 1996; Del Priore et al., 2002).

Nuclei of the RPE cells can be seen in the basal part of the cytoplasm. RPE has one nucleus but can become multinucleated with ageing (Chen et al., 2016b; Starnes et al., 2016). Melanin granules are present on the basal site of RPE surrounding the microvilli portion of the cells (Sparrow et al., 2010; Boulton, 2014). The microvilli sizes range between 5 to 7 µm in length (Snell & Lemp, 2013). The outer segment of rods and cones occupies the space between the RPE microvilli and this arrangement enables a very strong RPE-outer segment interaction (Sparrow et al., 2010; Remington & Goodwin, 2011). Detailed anatomy of the RPE cell is illustrated in Figure 1.6. The

microvilli with its surrounding inter-photoreceptor binding matrix acts as 'glue' between the RPE and the neural retina layer (Sparrow et al., 2010). Tight junctions between adjacent RPE cells membranes are formed by zonula adherens on the basal site and zonula occludens on the apical sites. These tight junctions form the retinal-blood barrier (Westmoreland et al., 1998).

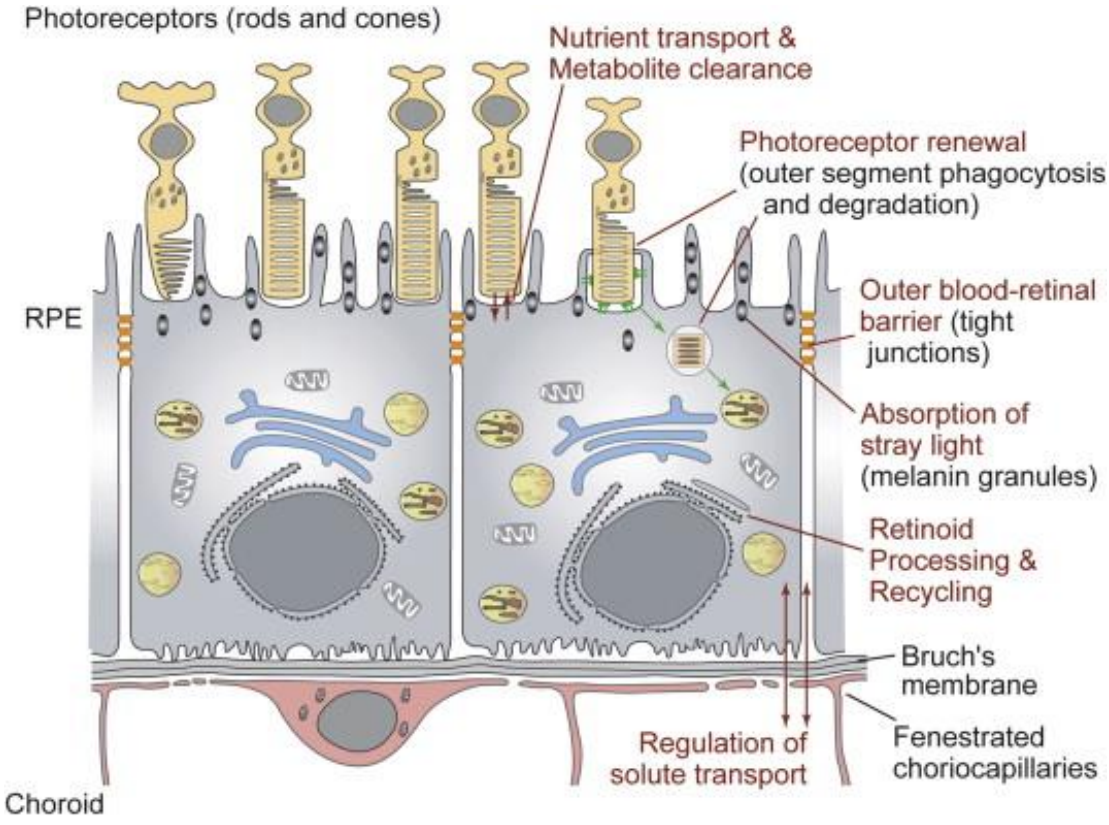

Figure 1.5 Detail anatomy of RPE cells and summary of its functions. Microvilli exists on the apical site of RPE interacting to the photoreceptors and basolaterally it forms a close proximity to the Bruch's membrane of the choroids (Lehmann, Benedicto, Philp, & Rodriguez-Boulan, 2014).

1.3.2 The functions of RPE

The RPE is important in maintaining the retinal homeostasis include aiding in absorption of scattered light, protection against photo oxidation, secretion growth factors, provide transepithelial transport, assisting in visual cycle and involved in phagocytosis of photoreceptor outer segments (Finnemann et al., 1997; Strauss, 2005; Kevany & Palczewski, 2010; Simo et al., 2010; Sparrow et al., 2010; Kay et al., 2013; Boulton, 2014)

1.3.2.1 Absorption of scattered light and protection against photooxidation

The retina has a high amount of polyunsaturated fatty acids and is exposed to a high amount of radiation from the light entering the eye (Saccà et al., 2018). Exposure to light radiation increases the production of oxidative stress and leads to photooxidation (Hammond et al., 2014; Ivanov et al., 2018) . To overcome this, the RPE has three lines of defence properties to protect the retina space from oxidative damage (Strauss, 2005).

The first line of defence is absorption of scattered light. The RPE is responsible in absorbing scattered light focused on the retina with its densely packed pigmented cells. Pigmented cells includes melanin and lipofuscin (Strauss, 2005; Sparrow et al., 2010). The RPE are the first cells in the body to become pigmented during embryogenesis through a process called melanogenesis (Strauss, 2005). This process produces the melanin pigment, which presents in the form of cytoplasmic granules, known as melanosome (Boulton, 2013, 2014). A high amount of melanin can be found on the apical site of the RPE which absorbs stray light that hit the retina and minimise light scattering within the eye (Sparrow et al., 2010). With ageing, the amount of melanin in the RPE is reduced due to fusion and removal by lysosomes (Sparrow et al., 2010). Lipofuscin is also an RPE pigment, which develops in later stages of life (Kennedy et al., 1995; Schraermeyer & Heimann, 1999). It is a by-product of incomplete digestion

of the photoreceptor outer segment by the RPE itself (Schraermeyer & Heimann, 1999). Lipofuscin consists of a mixture of lipids, proteins and fluorescent compound which aids in light absorption during visual cycle (Kennedy et al., 1995). Accumulation of lipofuscin results in more adverse effect than good especially with ageing. Unlike melanin, lipofuscin accumulates with age (Kennedy et al., 1995; Sparrow & Boulton, 2005). Excessive amount of lipofuscin in turn results in impairment of RPE cell functions, leading to poor vision in elderly and development of eye related diseases such as age related macular degeneration (AMD) (Kennedy et al., 1995; Katz, 2002; Sparrow & Boulton, 2005).

The second line of RPE defence is facilitated by the presence of antioxidant properties in RPE (Newsome et al., 1994; Strauss, 2005; Sparrow et al., 2010). The antioxidant properties help filter light with shorter wavelength which causes increase in oxidative stress (Newsome et al., 1994). There are two common carotenoids found in the RPE which possess antioxidant properties, ie. lutein and zeaxantin (Bian et al., 2012; Gong et al., 2017). Blue light exposure is believed to cause photooxidation of lipofuscin components resulting in toxic product accumulations (Strauss, 2005; Bian et al., 2012). About 60% of scattered and blue light are absorbed by melanin and the two carotenoids (Strauss, 2005). Studies have shown that intake of these antioxidants in daily diet can reduce the chances of developing age-related diseases includes the AMD (Carpentier et al., 2009; Bian et al., 2012; Khoo et al., 2019).

The third line of defence is the ability of the RPE cells to repair damaged DNA, lipids and proteins (Strauss, 2005). However, the mechanism behind this third line of defence remains poorly understood.

1.3.2.2 Secretion of growth factors

The RPE is also responsible in the production and secretion of various growth factors essential for the maintenance of retinal structural integrity and homeostasis (Strauss, 2005; Kay et al., 2013). Among the major growth factors secreted by the RPE are fibroblast growth factors (FGF-1, FGF-2, and FGF-5), transforming growth factor-β (TGF-β), insulin-like growth factor-1 (IGF-1), ciliary neurotrophic factor (CNTF), platelet-derived growth factor (PDGF), lens epithelium-derived growth factor (LEDGF), members of the interleukin family, tissue inhibitor of matrix metalloprotease (TIMP), vascular endothelial growth factor (VEGF) and pigment epithelium-derived factor (PEDF) (Martin et al., 1992; Guillonneau et al., 1998; Seidler et al., 1999; Strauss, 2005; Simo et al., 2010; Kay et al., 2013; Klettner et al., 2015). Among these growth factors, VEGF and PEDF are the most important growth factors in the retina. VEGF is secreted on the basal site of the RPE; meanwhile PEDF is secreted on the apical site (Strauss, 2005; Bhutto et al., 2006; Klettner et al., 2013; Klettner et al., 2015). PEDF maintains a normal retinal and choriocapillaries homeostasis. PEDF able to protect neurons cells against glutamate- and hypoxia- induced apoptosis as well as stabilising the endothelium cells of choriocapillaries (Strauss, 2005; Simo et al., 2010; Tian et al., 2017). In a normal eye, VEGF is secreted at a very low level and is essential for preventing endothelial apoptosis (Strauss, 2005; Simo et al., 2010; Ford et al., 2011). However, excessive secretion of VEGF can be easily triggered by hypoxia, a condition where oxygen is lacking in the environment (Yorston, 2014). Increased in VEGF secretion can be harmful to the eye. VEGF promotes abnormal growth of new vessel in order to accommodate the lack of oxygen (Yorston, 2014; Barquet, 2015). Consequently, this abnormal growth interferes with the retinal physiology leading to certain ocular conditions such as age-related macular degeneration, diabetic retinopathy and retinopathy of prematurity (Penn et al., 2008; Yorston, 2014; Barquet, 2015).

1.3.2.3 Transepithelial transport

The tight junction formation between RPE and its neighboring cells restricts movement of fluids and solutes in and out of the retina. To overcome this limitation of fluid movement, RPE facilitates the transport of fluids and solutes through a transepithelial transport system (Simo et al., 2010). Using this system, the RPE transports electrolytes and water from the subretinal space to the choroid and glucose and other nutrients from choroid to the photoreceptors (Boulton & Dayhaw-Barker, 2001; Strauss, 2005).

The RPE transport ions and water from subretinal spaces on the apical side to the blood stream of choriocapillaries on the basolateral space. This process occurs with aids of Na+-K+-ATPase channel on the apical sides. This channel helps provide energy for the transepithelial transport. Large amounts of fluids is generated in the retina due to the numerous metabolic processes and this affects the intraocular pressure (Simó, Villarroel, Corraliza, Hernández, & Garcia-Ramírez, 2010). Therefore, removal of excess fluid is essential to maintain normal homeostasis. Fluid from the inner retina is transported out by Müller cells, whereas fluid from the subretinal space is removed by aquaporins (Strauss, 2005).

Apart from that, the RPE helps transport glucose, retinol, ascorbic acids and fatty acids to the photoreceptors. RPE has high amounts of glucose transporters in both apical and basolateral membranes to performed this function. GLUT1 and GLUT3 are the two types of glucose transporters that are highly expressed in RPE cell membranes. GLUT3 mediates basic glucose transport while GLUT1 mediates glucose transport that is triggered by different metabolic demands (Simó et al., 2010; Strauss, 2005). The RPE transports retinoid from the vascular compartment to the photoreceptors to ensure continuing supply of retinol in visual cycle. The bulk of retinoid is exchanged between

RPE and photoreceptors during this cycle (Simó et al., 2010). Docosahexanoic acid (DHA) is a kind of fatty acids essential to maintain the RPE's functional integrity and acts as a precursor for neuroprotectin D1 (NPD1) (Strauss, 2005). NPD1 protects RPE cells from oxidative stress. DHA is synthesised in the liver from its precursor, linolenic acid, and is released into the blood circulation. The RPE mediates transport of DHA from the vascular compartment to the photoreceptors (Simó et al., 2010).

1.3.2.4 Retinoid reisomerisation for visual cycle

Light entering the eye is converted into visual information through a process known as visual cycle. Photoreceptors rely on the RPE to maintain its metabolic functions required for visual cycle (Strauss, 2005; Sparrow et al., 2010; Remington & Goodwin, 2011). The visual cycle process can be divided into two phases: phototransduction and reisomerization of all-trans retinal (Strauss, 2005).

The phototransduction takes place in the photoreceptor outer segment (Strauss, 2005; Snell & Lemp, 2013). However, due to photoreceptors lack in cis-trans-isomerase, which is an enzyme involved in the conversion, the reisomerisation of all-trans-retinal phases occurs in the RPE (Snell & Lemp, 2013). As previously mentioned in section 1.2.3, the photoreceptor pigment (rhodopsin or iodopsin) consists of opsin bound to 11-cis-retinal (Tsin et al., 2018). Once light hits the photoreceptor, the 11-cis-retinal undergoes photoisomerisation into all-trans-retinal. The opsin dissociates from the 11-cis-retinal and undergoes phototransduction, converting the light energy to electrical signal for visual interpretation by the brain (Strauss, 2005; Tsin et al., 2018). In the meantime, in order to maintain opsin's sensitivity to light, the all-trans-retinal is reduced to all-trans-retinol and then transported into the RPE for reisomeration to take place (Rando, 2001; Strauss, 2005).

The transport of all-trans-retinol into the RPE through interphotoreceptor matrix (IPM) is mediated by the inter-photoreceptor retinoid-binding proteins (IRBP) (Tsin et al., 2018). In the RPE, all-trans-retinol undergoes esterification by lecithin retinol acyltransferase (LRAT) into all-trans-retinyl-ester. LRAT linked all-trans-retinal to phospatidyl choline to generate all-trans-retinyl-ester (Rando, 2001; Strauss, 2005). These all-trans-retinyl-ester are the primary form of Vitamin A stored in the eye (Robison & Kuwabara, 1977). Besides, converting the all-trans-retinol, RPE also acts as a storage for the retinoids in the eye, in the form of all-trans-retinyl ester (Robison & Kuwabara, 1977; Bridges et al., 1982).

Later, the all-trans-retinyl-ester undergoes isomerization by isomerohydrolases RPE65 enzymes to form 11-cis-retinol (Rando, 2001; Tsin et al., 2018). Finally, the 11-cis-retinol is then oxidized into 11-cis retinal (Rando, 2001; Strauss, 2005). The 11-cis retinal is transported back into the photoreceptor outer segment to merged to opsin molecules and thus form a fully functional photoreceptor pigment (Strauss, 2005). The process of re-isomerisation of all-trans retinal is illustrated in Figure 1.6.

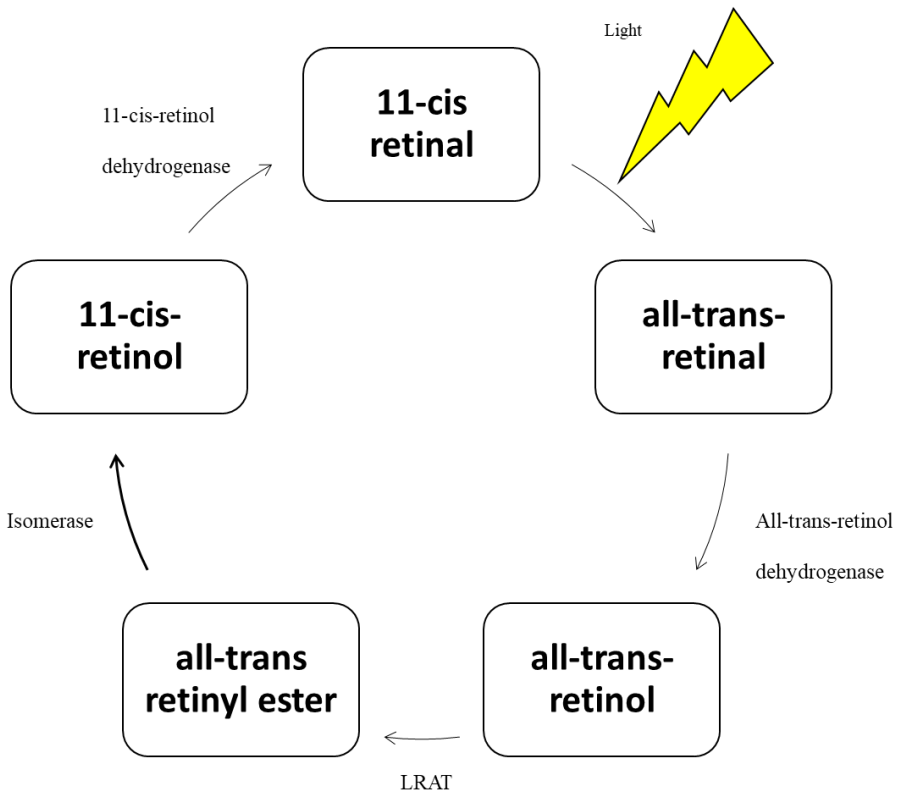

Figure 1.6 The visual cycle pathway. Image adapted from webvision.med

1.3.2.5 Phagocytosis of photoreceptor outer segments

Apart from the functions mentioned above, the RPE is also responsible in the digestion of photoreceptor outer segment (POS) disc (Sun et al.; Bosch et al., 1993; Ryeom et al., 1996; Nguyen-Legros & Hicks, 2000; Sun et al., 2007). In order to maintain the photoreceptor length and proper functions, the outer segment undergoes constant regeneration at the base and shedding at its tips (Nguyen-Legros & Hicks, 2000; Strauss, 2005). Approximately 10% of the photoreceptor outer segment length is shed and phagocytised by RPE daily (Bazan, 2007; Kevany & Palczewski, 2010). And about the same volume of the photoreceptor outer segment is regenerated every day (Kevany & Palczewski, 2010).

The rate of photoreceptor outer segment shedding was thought to be light and temperature dependent. Higher temperature and increase in the amount of light would

leads to increases of outer segment shedding (Besharse et al., 1977). The process of phagocytosis on POS is regulated based on light and dark cycle (LaVail, 1976; Strauss, 2005; Remington & Goodwin, 2011; Mazzoni et al., 2014). Rods outer segment discs are shed at the beginning of the circadian rhythm at the start of each day. In contrast, the cones outer segment discs shed at the end of the day with the onset of darkness (Strauss, 2005; Mazzoni et al., 2014). It is estimated that a single RPE is responsible for outer segment shedding and renewal of an average of 23 photoreceptors (Besharse et al., 1977).

Phagocytosis process by RPE occurs through four phases, namely recognition, ingestion, internalisation and digestion (Bosch et al., 1993; Kevany & Palczewski, 2010). Recognition or initiation of RPE phagocytosis occurs when shed photoreceptor outer segment binds to the microvilli on the apical sides of RPE cells (Kevany & Palczewski, 2010). The shed phtotoreceptor outer segment act as "eat me signal", initiate opsonisation through secretion of integrin ligand milk fat globule-EGF8 (MFG-E8) (Nandrot et al., 2007). The MFG-E8 localised to the neuroretina space and binds to alphavbeta5 (αvβ5), the only integrin present on the apical surface of RPE in human (Finnemann et al., 1997; Nandrot et al., 2007). Finnemann and collegues have shown that αvβ5 integrin is needed in the recognition phase (Finnemann et al., 1997; Mao & Finnemann, 2012). In vivo work has demonstrated the importance of these integrin. Mice with absence of αvβ5 shown to develop age-related blindness, believed to be due to impaired phagocytosis processes and accumulation of waste materials within and around the RPE (Finnemann et al., 1997; Nandrot et al., 2004; Kevany & Palczewski, 2010).

Upon binding of MFG-E8 to αvβ5, a series of signalling occurs leading to the second phase of the phagocytosis, which is the engulfment of the outer segment of RPE cells.

The signalling is govern by focal adhesion kinase (FAK) and MertK, which are receptors that reside in cytoplasm of the RPE (Kevany & Palczewski, 2010). The receptor itself does not physically move the outer segment into the RPE, but they may involve in the rearrangement of the plasma membrane layer that leads to engulfment by RPE. With the binding of MFG-E8 to αvβ5, the FAK is activated and signals phosphorylation of MertK. Subsequently, RPE increase expression of Insp3 and signal engulfment (Finnemann et al., 1997).

Engulfment is mainly governed by CD36. The unwanted outer segments are transferred from the apical space to the basal site of the RPE, where they undergoes degradation processed. The ingested photoreceptor is degraded by the lysosomal enzymes present in the RPE cytoplasm (Strauss, 2005; Kevany & Palczewski, 2010). Cathepsin D is one of the main lysosome enzymes involved in POS degradation in the RPE. The RPE is known to phagocytose more waste material compared to any other cells in the body (Rakoczy et al., 1997). A slight delay or inefficient degradation by RPE potentially leads to accumulation of harmful substances in the retina such as lipofuscin, which are implicated in the pathogenesis of certain eye diseases such as AMD (Bulloj et al., 2013).

1.4 Ageing and the RPE

Ageing is defined as "progressive accumulation of changes with time that are associated with or responsible for the ever-increasing susceptibility to disease and death which accompanies advancing age" (Harman, 1981). Recently, a new definition of ageing has been proposed. It is defined as "an age-dependent or age-progressive decline in intrinsic physiological function, leading to an increase in age-specific mortality rate (i.e., a decrease in survival rate) and a decrease in age-specific reproductive rate" (Flatt, 2012). With ageing, the level of damaged molecules increases as a result of increased production of harmful substances in the body such as oxidative stress which leads to loss of tissue or organ functions. The free radical theory of ageing was first introduced by Denham Harman which stated that formation of reactive oxygen species (ROS) through Haber-Weiss chemistry is a physiological phenomenon in cells (Harman, 1981). Later, the free radical theory was replaced by oxidative stress theory of ageing. This theory explains the fact oxidative damage may also be caused by non-free radical molecules cells (Bokov et al., 2004). This new theory of ageing is defined as an imbalance between the amount of oxidative stress in cells and the inherent ability of cells to repair damages caused by oxidative stress (Beatty et al., 2000; Burton & Jauniaux, 2011; Zafrilla et al., 2013). Ageing changes in the retina, mainly in RPE, are important contributions to the leading causes of blindness in developed countries. An excellent example is AMD, which is related to RPE changes associated with senescence. With aging, RPE undergoes various physiological and biochemical changes that will be further discussed in subchapter 1.4.1 to 1.4.6. Apart from that, it is important to note that, the neighbouring cells changes during aging also is affecting RPE homeostasis. Bruch's membrane, for instance, would experience increases in thickness, increases in protein crosslinking and increases in extracellular deposit accumulation as well as decreases in permeability (Zarbin, 2004). Additionally, choroid

would undergoes decreases in choriocapillaris number and lumen diameter (Snell & Lemp, 2013). These aforementioned changes that occurs during aging would lead to increase in inflammatory response which cause RPE cell death, that also can be seen in AMD condition (Zarbin, 2004). The effect of aging on RPE and its neighbouring cells and its correlation to AMD development is summarised in Figure 1.7.

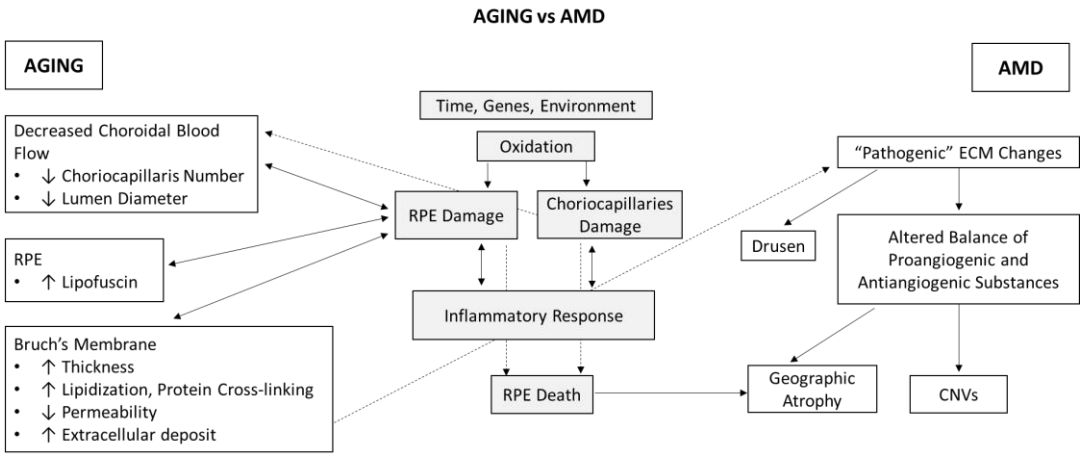

Figure 1.7 The effect of aging on RPE and its pathogenesis to AMD developments. Image retrieved from (Zarbin, 2004).

1.4.1 Physiological changes of RPE in ageing

RPE is a post-mitotic cell; cells do not divide throughout life. However, as ageing occurs, some RPE are loss as a normal part of retinal homeostasis and cannot be replaced, thus plays a major role in degenerative diseases such as AMD. Reduction in the number of RPE cells has been observed with increasing age, however the overall shape of the RPE cells remains the same (Bhatia et al., 2016). With the decrease in RPE cells, the ratio of RPE to photoreceptor is reduced and with the important function of RPE in maintaining the photoreceptor function, loss of RPE would also leads to photoreceptor's impairment and subsequently leads to impaired visual functions (Strauss, 2005).

Approximately 14cells/mm^2 were lost between the 2^{nd} and 9^{th} decade of human life (Gao & Hollyfield, 1992; Del Priore et al., 2002). Observation made on RPE cell count from a total of 53 human donor eyes showed that 0.3% of RPE cells were lost per year due to aging after 6^{th} decade of life (Panda-Jonas et al., 1996). However the decline in RPE cells differ across the entire RPE layer. Loss of RPE cells are higher in macula area and lesser in periphery area (Del Priore et al., 2002; Wang et al., 2012; Bhatia et al., 2016). Higher decline in macula area is possibly due to higher metabolic rate as light is mainly focused to macula area (Del Priore et al., 2002). High metabolic rate leads to increase in toxic waste accumulation which increase cell's burdens and leads to age related changes including apoptosis. In order to compensate for the loss of cells in macula, it is comprehensible that the peripheral RPE cells expand horizontally to fill the gap created by dead RPE cells (Bhatia et al., 2016). This is also a possible explanation to the observed increase in RPE size with ageing (Feeney-Burns et al., 1984; Del Priore et al., 2002).

The mechanism of cell death in ageing RPE is still debatable. Apoptosis, necrosis and autophagy are among the cells death mechanism associated with ageing RPE (Telegina et al., 2017b). However, most studies pointed that the cell death mechanism of RPE is regulated mainly via apoptosis. Apoptosis is a programmed cell death mechanism usually characterised by DNA fragmentation (Raff, 1992). High number of RPE apoptosis was observed with ageing, especially in individual suffers from AMD (Del Priore et al., 2002; Dunaief et al., 2002). Del Priore et al (2002) evaluated apoptosis of RPE in 22 human eyes age between 19-87 years old using detection of DNA fragmentation method (TUNEL labelling). Individual aged 60 and above was shown to have higher RPE apoptosis compared to younger ones. In addition they also showed higher apoptosis was detected in macula area as compared to periphery (Del Priore et al., 2002). The finding of this study was the supported by Bhattacharya et al (Bhattacharya et al., 2012). The study was carried out in primary RPE cells isolated from 8 postmoterm donors aged between 29- 94 years old also showed increased apoptosis with AGEs. In addition, they also observed compromised RPE's tight junction with ageing as observed through confocal microscopy (Bhattacharya et al., 2012). The decreased in tight junction properties can impaired the cells transepithelial transport system, thus impaired the RPE functions (Obert et al., 2017).

In addition to the decrease in RPE density, multinucleated cells has also been observed in the ageing RPE. Although most multinucleated RPE cell studies were reported from mouse models, several studies in different human tissues such as fibroblast and has shown similar possible changes (Holt & Grainger, 2011; Chen et al., 2016b; Starnes et al., 2016). A two-fold increase in multinucleated RPE cells was observed in senescent rat retinas as compared to younger ones (Telegina et al., 2017a). A study carried out in C57BL/6J mice showed that RPE cells became multinucleated with age (Chen et al., 2016b). It was shown that 80% of RPE cells in central retina

were multinucleated in majority of 24-month-old mice. It has been hypothesised that multinucleated RPE happens due to incomplete cell division. However, despite this noticeable change, multinucleated RPE cells were still able to perform its usual functions including phagocytic capability similar to younger healthy RPE cells (Chen et al., 2016b). However, study by (Starnes et al., 2016) from 19 human subjects showed multinucleated RPE is not correspond to increase age. However, there is lacking of evidence to conclude the association between ageing and multinucleated RPE.

1.4.2 Increase in oxidative stress level

Oxidative stress is termed as an imbalance in the production of harmful substances in cells and the cell's natural ability to prevent oxidative damage by utilising its anti-oxidative properties (Beatty et al., 2000; Burton & Jauniaux, 2011; Zafrilla et al., 2013). Oxidative stress is accompanied by the increase in reactive oxygen species (ROS) in the cells. ROS is highly reactive molecules that has the capabilities to alter DNA, protein and lipid, thus being a causative factor of ageing (Cui et al., 2012). In normal physiology, the ROS is maintained at a very low level, yet still measurable. However, with ageing, level of ROS increases and it is accompanies with decreases in antioxidant capacity (Cui et al., 2012). Increase of ROS with ageing has been observed in various cells including skin, dopaminergic neurons of the brain, cornea, lenses and aqueous humour, thus leads to various diseases pathologies (Starr & Starr, 2014; Cejka & Cejkova, 2015; Guo et al., 2018). Of interest, ROS formation in RPE is abundant. The formation of ROS in RPE is enhanced by various factors includes genetic, high oxygen consumption, high exposure to light, RPE phagocytosis and presence of polyunsaturated fatty acid (Beatty et al., 2000; Tokarz et al., 2013). These factors can be controlled by the presents of pigment and antioxidant properties, however, with age, the level of damage is higher than protective properties (Beatty et al., 2000).

Increase of ROS in RPE can leads to various changes such as inflammation, autophagy, lipid peroxidation, as well as oxidative nuclear and mitochondrial damage (Tokarz et al., 2013). Mitochondria can be found in abundance in RPE cytoplasm especially on the apical site. This is due to its energy demand required during phagocytosis of photoreceptor outer segments. Mitochondria is well-known as one of the major source of oxidative stress in cells. The oxidants generated by mitochondria accounts for up to 5% of oxidative stress generation (Liang & Godley, 2003; Lu et al., 2006). It has been shown that mitochondria are less numerous in older people and the mitochondrial functions are also impaired (Liang & Godley, 2003). Growing evidence has linked mitochondrial dysfunction to oxidative stress and subsequently neurodegenerative disease progression such as in Alzheimer's disease, Parkinson disease and Huntington's disease (Cui et al., 2012).

Apart from mitochondria, oxidative stress can also be raised by other sources, intra- and extra-cellularly. Ultraviolet light, smoking and excessive light exposure are some of potential external sources of oxidative stress to retinal cells. Physiologically, the RPE is exposed to a significant level of oxidative stress due to its high metabolic rate and consumption of oxygen, constant exposure to light and high levels of polyunsaturated fatty acids (Masuda et al., 2017). Examples of the oxidative stressor are superoxide anion, hydroxyl radical, and singlet oxygen. As ageing occurs, the amount of oxidative stress in RPE also increases (Masuda et al., 2017). Increase in oxidative stress in the RPE has been linked to accumulation of various lipids by-product including lipofuscin and drusens, which are discussed in sections 1.4.5 and 1.4.6 (Zafrilla et al., 2013). In addition phagocytosis process by the RPE is also another source of oxidative stress through oxidation of polyunsaturated fatty acids from the photoreceptor outer segments (Beatty et al., 2000).

Oxidative stress accumulation in cells is detrimental because it causes cellular damages to proteins, lipids and nucleic acids which may leads to activation of various inflammation pathways including NF-kB and MAPK (Wang et al., 1998; Beatty et al., 2000; Kauppinen et al., 2012). It has been shown that modulations of these cellular pathways are able to prevent cells death and apoptosis (Helenius et al., 1996; Wang et al., 1998). In order to overcome oxidative stress, cells are equipped with antioxidant properties, which will be discussed in detail in section 1.4.3.

1.4.3 Reduction of antioxidant level with age

Antioxidant is substance that has ability to eliminate potential harmful agent from the cells (Newsome et al., 1994). Examples of antioxidants are catalase and superoxide dismutase, two carotenoids found in RPE cells. Both catalase is responsible in breaking down toxic hydrogen peroxide into oxygen and water. In normal physiology, the RPE has six times higher catalase activity compared to other eye tissue (iris and vitreous). However, with ageing, catalase was shown to decrease greatly in both macula and periphery RPE by the 5^{th} decade of life (Liles et al., 1991). The protective effect of catalase in RPE was observed by in vitro experiments. Miceli et al (1994) tried to inhibit catalase in primary RPE cells. Results showed that inhibition of catalase cause increase in lipid peroxidation byproducts in RPE (Miceli et al., 1994). Recently, Rex et al (2004) used catalase overexpression to further study the important of catalase in RPE in vivo and in vitro. Overexpression of catalase was showed to protect the RPE and its neighbouring cells from hydrogen peroxide stimulation (Rex et al., 2004).

Working together with catalase is the SOD. SOD catalysed breakdown of superoxide into oxygen or hydrogen peroxide (Kasahara et al., 2005). Observations made in biopsy of RPE cells of 50-90 years-olds also showed that SOD actually reduced with aged and reduction is greater in AMD patient (Newsome et al., 1994; Kasahara et al., 2005). SOD

had been shown to protect the retina from oxidative damage in diabetic mice (Kanwar et al., 2007). SOD also has been shown to have a critical role in preventing apoptosis in RPE cells and a decrease in SOD level during ageing may actually be a contributory effect to AMD development (Kasahara et al., 2005; Kowluru et al., 2006). In addition, a high intake of antioxidant in daily diet has been shown to prevent age-related damages in RPE (Snodderly, 1995; VandenLangenberg et al., 1998; Yu et al., 2012; Tokarz et al., 2013).

Apart from the two aforementioned enzymatic antioxidant that present naturally in the RPE, vitamins also has antioxidant capability in protecting the RPE. Vitamin C and E are the examples of vitamins that has the antioxidant properties. Vitamin C or ascorbic acid is highly expressed in the RPE. They are thought to be responsible in protecting the RPE from light induced injury (Zafrilla et al., 2013). Vitamin C supplement albino rats were able to prevent reduction of docosahexanoic acid, reduce loss of rhodopsin and minimize photo-toxicity injury (Organisciak et al., 1985). Interestingly, vitamin C is thought to play a role in regeneration of vitamin E in RPE (Berman, 1994).

Vitamin E is a free radical scavenger which can protect cells from lipid free radicals and prevent lipid peroxidation (Tokarz et al., 2013). Based on analysis of vitamin A content in macular and retina from 70 donor eyes, vitamin E was found to be higher in RPE as compared to retina (Friedrichson et al., 1995). Interestingly, Vitamin E was observed to increase with aging from the 5^{th} decade of life onwards and started to decline again after 7^{th} decade of life. This trend was observed in RPE in the macula with less reduction after the 7^{th} decade in the RPE of the periphery (Friedrichson et al., 1995). Vitamin E deficient rats causes lipofuscin accumulation in the RPE, with concurrent damage of photoreceptors (Herrmann et al., 1984). In vivo experiments also

showed Vitamin E was able to reduce nitric oxide damage in rat's retinal homogenates. Taking the data together, it is noted that, vitamin E has an antioxidant properties to protect RPE cells.

1.4.4 Reduction of melanosomes

Melanosomes are enclosed lipid membrane organelle (Rózanowska et al., 1997). Melanosomes reside in the cytoplasm of RPE and having almost similar properties to the lysosome which contain acid hydrolases (Boulton et al., 1990; Różanowski et al., 2008). RPE melanosomes are either elliptical or spherical in shape. Elliptical melanosome's sizes are ranging between 1-2.5µm in diameter and 1.5- 1µum in width. Meanwhile the spherical melanosomes are between 0.5-2µm in diameter (Lu et al., 1998). Melanosomes can be abundantly found in the apical site RPE, where it has the highest photooxidation (Różanowski et al., 2008). In normal healthy individuals, melanosome is at its highest density around the macula area, and decreases through the posterior area (Różanowski et al., 2008) (Feeney-Burns et al., 1984).

Melanosomes contain melanin, a lysosome originated pigment. Melanin is synthesised on protein matrix at early age during embryogenesis and developed fully during the first year of human life (Różanowski et al., 2008). Melanin act as the first line of defences in RPE as its filter light that hits the retina, therefore reduce the amount of scattered light and improve visual acuity (Różanowski et al., 2008). Melanin also has been shown to store toxic waste by its ability to bind heavy metals such as mercury and selenium (Biesemeier et al., 2011).

Ageing process in the RPE is accompanied with loss of melanosomes granules and melanin (Różanowski et al., 2008; Boulton, 2013, 2014). Based on study on RPE cells from human donors, there was 2.5 fold decrease in melanosomes content in 90 years old RPE compared to 10 years old donor (Sarna et al., 2003). And in another

study, observation on human post-mortem eyes shows that about 35% reduction of melanosomes number was found in people age over 40 as compared to the younger ones (Feeney-Burns et al., 1984; Boulton, 2013). The loss of melanosomes differs throughout the RPE layer, but the distribution around the macula area are maintained throughout human life (Boulton & Wassell, 1998; Boulton, 2013). Due to its important function in reducing photooxidation, melanosomes and melanin loss in RPE may contribute to reduced RPE mitochondria activity and lysosomal destabilisation which subsequently leads to photoreceptor impairment (Różanowski et al., 2008). The loss of melanosomes are thought to be digested by the lysosomes during ageing. Besides, melanosomes loss may also occurs possibly due to fusion with lipofuscin molecules which has been found to predominantly formed at later stages of human life. The fusion molecule is known as melanolipofuscin (Feeney-Burns et al., 1984; Biesemeier et al., 2011).

1.4.5 Lipofuscin accumulation

Lipofuscin is a yellowish brown material accumulated with increasing age (Delori et al., 2001; Brunk & Terman, 2002). Lipofuscin is a photoinducible ROS generator consist of heterogenous group of autofluorescent lipid and proteins (Delori et al., 2001). Lipofuscin resides in lysosomal compartment of cells and lipofuscin granules occupy up to 20% of RPE cytoplasmic space as observed in individual over 70 years old (Delori et al., 2001; Sparrow & Boulton, 2005). Huge increase of lipofuscin accumulation was observed in RPE cells of 20-70 years old age group (Feeney-Burns et al., 1984; Delori et al., 2001). Although lipofuscin levels increase with age, the accumulation rates reduce after age of 80 years (Delori et al., 2001). Lipofuscin formation is a complex processes. Diet, oxygen, phagocytosis of photoreceptor, light exposure and antioxidant status are also affecting the liposfucin accumulation in RPE apart from increasing age (Boulton, 2014).

Lipofuscin formation is mainly associated with incomplete degradation of the photoreceptor outer segment and autophagic removal of aggregated proteins and lipids by the RPE (Kennedy et al., 1995). High accumulation of lipofuscin can be found around the posterior pole of the retina, where the highest amount of photoreceptor available (Kennedy et al., 1995). This supports the idea that lipofuscin is actually a result of waste accumulation from incomplete photoreceptor outer segment phagocytosis processes.

1.4.6 Drusen formation

In addition to lipofuscin accumulation in the RPE, drusens, which are yellow deposits, also accumulates between the basal lamina of RPE and the inner collagenous layer of Bruch's membrane which mainly of lipids, carbohydrates, and various intra- and extra-ocular components (Abdelsalam et al., 1999; Sarks et al., 1999; Hageman et al., 2001; Buschini et al., 2011). With the close contact of RPE and Bruch's membrane, integration of drusen may affect the RPE homeostasis. Drusens are commonly observed in individuals over the age of 60 years old (Sarks et al., 1999). Increased drusen density has been correlated with increasing age (Sarks et al., 1999; Imamura et al., 2006). Drusens not only cause physiology changes to RPE and Bruch's membrane but also can change contrast sensitivity, macular recovery function and central visual field sensitivity (Hageman et al., 2001).

A key component in drusen is amyloid beta plaques which accumulate along Bruch's membrane and photoreceptor outer segment of RPE. Apart from that, metalloproteinase 3 inhibitors, fibronectin, vitronectin, integrins, lipoproteins and advanced glycation endproducts are also present in drusen deposits (Buschini et al., 2011). Drusen is clinically classified as hard and soft drusen. Hard drusens is a small in size with sharp borders. Soft drusens has less-defined borders and larger in size compared to hard

drusens (Hageman et al., 2001; Buschini et al., 2011; Klein et al., 2015). Despite their morphological changes, the composition of both hard and soft drusens remained the same. Apart from that, drusen also is classified based on size either as small, intermediate or large drusen (Cheung & Eaton, 2013). Drusen with a diameter less than 64µm is considered small and between 64-124µm is considered intermediate. Anything that is larger than 124µm is considered as large drusen (Cheung & Eaton, 2013). The main concern with drusen formation is that it could contribute to visual loss such as seen in AMD patients.

1.5 Age-related Macular Degeneration

Age-related macular degeneration (AMD) is the leading cause of blindness in developed countries. According to World Health Organisation (WHO), AMD is ranked as the third leading cause of blindness after cataract and glaucoma. AMD is a multifactorial disease with family history, smoking, obesity and hypertension as its risk factor (Group, 2000; Lambert et al., 2016). However, ageing is considered to be the main risk factor for the disease (Group, 2000). It affects individual age above 55 but are more prominent in individuals above the age of 75 old (Kawasaki et al., 2008; Cheung & Eaton, 2013; Wong et al., 2014). Loss of vision is the worst outcome from AMD as a result of abnormalities in the photoreceptor, RPE, Bruch's membrane and/or choroidal complex (Majji et al., 2000; Bonilha, 2008; Bhutto & Lutty, 2012; Sadigh et al., 2013; Ablonczy et al., 2014; Gheorghe et al., 2015; Folgar et al., 2016; Inana et al., 2018; Farazdaghi & Ebrahimi, 2019).

AMD is responsible to 8.7% of blindness worldwide among people over the age of 60 years old (Gehrs et al., 2006; Ayoub & Patel, 2009; Wong et al., 2014). According to systematic review and meta-analysis, the prevalence of AMD is expected to increase to 196 million by 2020 and 288 million by 2040 (Wong et al., 2014). Regional study on

prevalence of AMD in 2014 shown that AMD are more common among Caucasians (12.3%) compared to Asians (7.4%) (Joachim et al., 2014; Wong et al., 2014). However, by 2040, AMD prevalence in Asian is expected to account for 113 million putting Asian to be the first followed by Caucasians (69 million) (Wong et al., 2014).

Drusen formation (discussed in subchapter 1.4.6) is known to be the earliest clinical hallmark for AMD which can be visualised through funduscopy examination (Nozaki et al., 2006; Cheung & Eaton, 2013; Klein et al., 2015). Location, size and pigmentation of drusen determines the classification of AMD. According to Age-related Eye Disease Study (AREDS), AMD is classified into 5 categories as listed in Table 1.1 below (Cheung & Eaton, 2013).

Table 1.1 Characteristic of drusen and its classification in AMD.

Category	**Characteristic of drusen**	**AMD classification**
Category 1	no drusen or non-extensive small drusen	No AMD
Category 2	extensive small drusen or non-extensive intermediate drusen or pigment abnormalities in at least one eye	Early AMD
Category 3	large drusen, extensive intermediate drusen, or noncentral geographic atrophy in at least one eye	Intermediate AMD
Category 4	AMD (geographic atrophy), or VA of less than 20/ 32 attributable to lesions of nonadvanced AMD, such as large drusen in the fovea, in at least one eye	Advanced AMD
Category 5	Neovascular AMD	Advanced AMD

Individuals that develop early AMD may experience symptoms such as blurred vision, decrease contrast sensitivity, difficulty in dark adaptation, and needs for bright light or extra magnification to read small text (Cheung & Eaton, 2013). The symptoms in early AMD may aggravate leading to degeneration of RPE and photoreceptor cells, subsequently progressing into intermediate or advanced AMD (Waugh et al., 2018).

Advanced AMD can be clinically categorised into two main forms, dry and wet form (Bressler et al., 1988). Dry AMD falls into Category 4, meanwhile wet AMD into Category 5 (Cheung & Eaton, 2013). Dry AMD is more common, however, wet AMD is much severe (Zarbin, 2004; Cheung & Eaton, 2013). The two form of AMD is illustrated in Figure 1.8 and will be discussed further in the next subchapter.

The cause of AMD is still unknown, however, AMD development is believed to link to various endogenous and exogenous factors. Smoking (Thornton et al., 2005; Khan et al., 2006; Velilla et al., 2013), light exposure (Delcourt et al., 2001; Chalam et al., 2011), nutrient intake (Kim et al., 2017; Chapman et al., 2019), stress (Beatty et al., 2000), sociodemography (age, sex, ethnicity, socioeconomy) (Fraser-Bell et al., 2005; Vanderbeek et al., 2011; Wong et al., 2014; Lambert et al., 2016), genetics (Sergejeva et al., 2016) and other health related disease can actually increase the chances of getting AMD (Group, 2000; Lambert et al., 2016). However inflammation and oxidative stress is thought to influence its pathogenesis at it most (Kaarniranta et al., 2011; Cheung & Eaton, 2013).

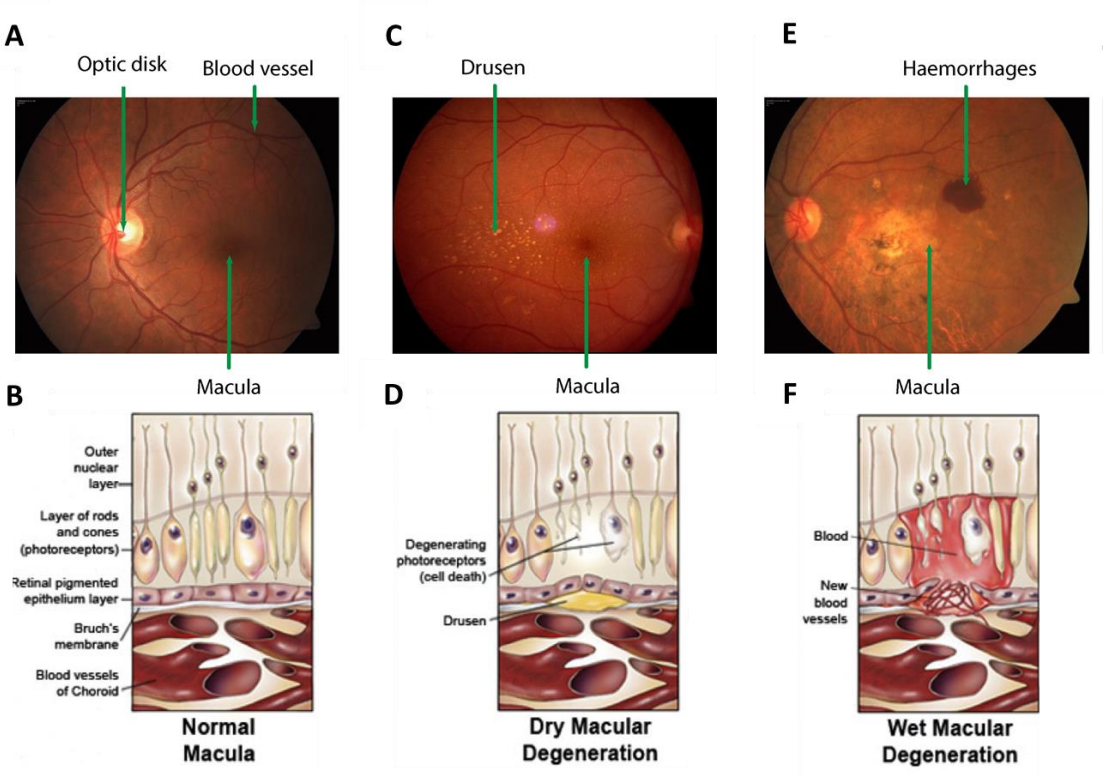

Figure 1.8 Differences between dry AMD and wet AMD. (A)(B) Normal, (C)(D) Dry AMD, (E)(F) Wet AMD. Images retrieved and modified from http://www.fabiobioletto.it (Mookiah et al., 2014).

1.5.1 Dry AMD

Dry AMD accounts for 90% of all AMD cases (Buschini et al., 2011; Cheung & Eaton, 2013). Usually, individuals suffers from dry AMD would experience a blurry vision in early development and worsen as time goes by. Dry AMD progresses slowly yet may still lead to visual loss in advanced stages (Buschini et al., 2011). Development of dry AMD initiated through building of lipids and proteins accumulation which leads to thickening of the Bruch's membrane known as drusen (Wang et al., 2009; Curcio & Johnson, 2013). The deposits also shown to interfere with the transport system between RPE and Bruch's membrane, thus increase the stress in RPE (Bowes Rickman et al., 2013). In turns, RPE would suffers from increase lipofuscin formation due to impaired lysosomal capacity of the cells. Decreased in lysosomal activity has been found in AMD eye (Wang et al., 2009). Characterisation of drusen in dry AMD can be referred to Table 1.1 (Category 3 and 4) and the appearance of drusen in the eye is portrayed in Figure

1.8 C and D (Mookiah et al., 2014). Drusen is not unique for AMD but the presence of drusen is the earliest visible clinical diagnosis of AMD (Sarks et al., 1999). Over the time, accumulation of drusen may leads to deterioration of macula and degeneration of RPE and photoreceptor cells which resulted in central scotoma or central field loss in the individual's vision (Refer to Figure 1.9) (Bowes Rickman et al., 2013). Central scotoma refers to formation of blind spot on the centre of the vision which may interferes with one's daily activities (Fletcher et al., 2012).

Figure 1.9 The difference in vision of normal individual and individual with AMD. Central scotoma forms in vision of AMD (Image retrieved and modified from own collection).

1.5.2 Wet AMD

Wet AMD is also known as exudative AMD or neovascular macular degeneration. Wet AMD is the advanced form of AMD. Visual loss in wet AMD occurs much faster compared to the dry form. Large, soft confluent drusen is usually found in AMD patient compared to in normal ageing (Friedman et al., 2004; Donoso et al., 2006; Buschini et al., 2011). Large confluent soft drusen is more common in wet AMD patients compared to dry AMD (Friedman et al., 2004). The classification of drusen in wet AMD can be

referred to Table 1.1 (Category 5). Wet AMD only accounts for 10-15% of all cases in population, however it is responsible for more than 80% of visual loss due to AMD (Kolb et al., 1995; Bowes Rickman et al., 2013; Cheung & Eaton, 2013; Michalska-Małecka et al., 2015). Vision loss in wet AMD is due to abnormal growth of blood vessels beneath the retina that is stretched from the choroidal space. The process is known as choroidal neovascularisation. The abnormal growth can rapidly invades the neural retinal space through Bruch's membrane (Donoso et al., 2006; Kaarniranta et al., 2011; Cheung & Eaton, 2013). These blood vessels that form in these spaces are very fragile, thus can leads to increase chances of haemorrhage resulting in accumulation of blood or serum beneath RPE (Hernández-Zimbrón et al., 2018). In addition, the haemorrhage also leads to raise in macula from its normal position, thus causing central vision loss (Hernández-Zimbrón et al., 2018). This changes also may affect RPE and photoreceptors cells, resulting in permanent visual loss (Kaarniranta et al., 2011).

Large, soft confluent drusen is usually found in AMD patient compared to in normal ageing (Friedman et al., 2004; Donoso et al., 2006; Buschini et al., 2011). Large confluent soft drusen is more common in wet AMD patients compared to dry AMD (Friedman et al., 2004). Apart from that, dry AMD also can be seen through death of photoreceptor cells.

1.5.3 RPE changes in AMD

RPE dysfunction has been shown to be associated with the development of AMD (Zarbin, 2004). Advanced Glycation Endproducts (AGEs) accumulates with age and be considered as one of the hallmark of RPE ageing. Accumulation of AGEs has been shown to be higher in elderly AMD patients compared to normal elderly people (Schutt et al., 2003). AGEs accumulate intra- and extra-cellularly. Intracellular AGEs can directly alter the protein function of the RPE cells, whereby extracellular AGES alter cell matrix and cell-cell interaction (Kasper & Funk, 2001).

AGEs plays an important role in formation of choroidal neovascularization, a hallmark of wet AMD. AGEs has been shown to be present in drusens and lipofuscin granules in RPE epithelial cells (Figure 1.10) (Stitt, 2001, 2005). Lipofuscin accumulates in the lysosomes and is associated with a decrease in lysosomal enzymes activity in the RPE (Schutt et al., 2003). Decreased lysosomal enzymes activity leads to reduction in photoreceptor outer segment phagocytosis, which in turns leads to increase in the accumulation of unwanted waste materials in the RPE (Brunk & Terman, 2002). Cathepsin D, a lysosomal protease enzyme has been found to be present in RPE and is commonly linked to phagocytose function of the RPE (Hayasaka et al., 1975; Hayasaka, 1983; Rakoczy et al., 1997). It has been shown that 80% of photoreceptor outer segment is digested by cathepsin D and the expression of cathepsin D in cells decline with age (Hayasaka et al., 1975; Rakoczy et al., 1997; Rakoczy et al., 1999). In addition to cathepsin D, another lysosomal protease enzyme, cathepsin L was also found to have an important role in maintaining RPE homeostasis (Shimada et al., 2010). Both cathepsins work optimally at an acidic environment. However, long term exposure of cathepsin L to acidic pH may cause denaturation. Denatured cathepsin L is a target for cleavage by cathepsin D. This demonstrates the important interaction between the two cathepsin in

the RPE (Turk et al., 2012). Interestingly, cathepsin D and L has been shown to reduce the toxicity of the AGEs in RPE (Grimm et al., 2012).

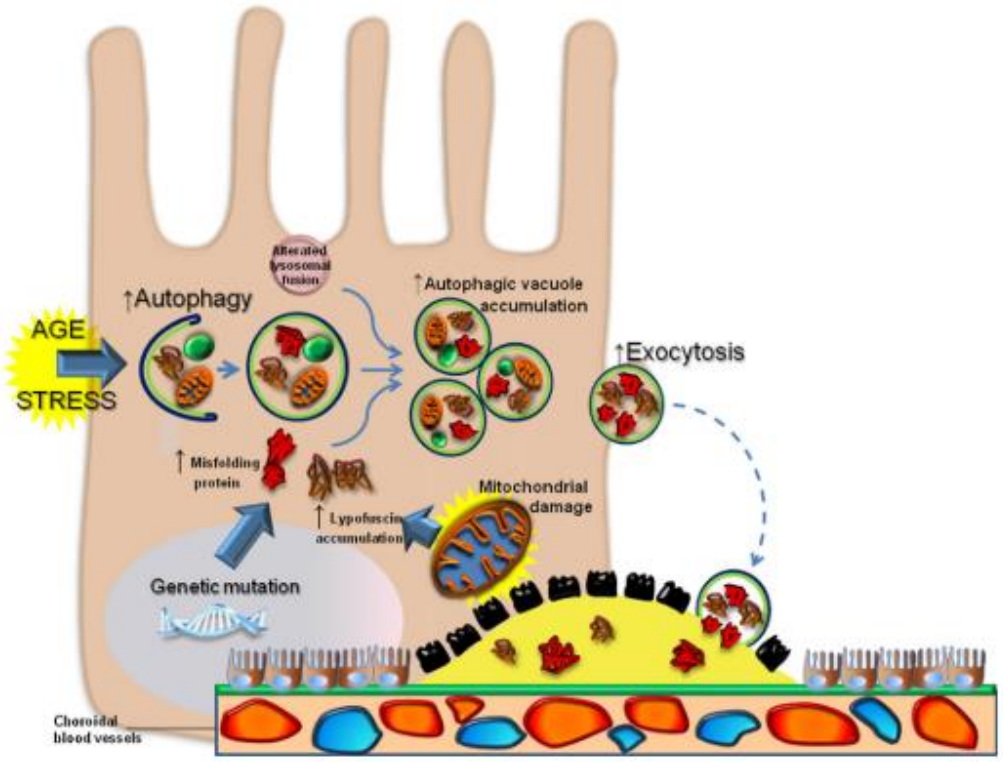

Figure 1.10 The involvement of AGEs and formation of drusen seen as hallmark of AMD disease. Image retrieved from (Buschini et al., 2011)

AGEs is activated through binding to its receptor such as RAGE. The binding of AGEs activates the NF-kB pathway, the most common signalling pathway linked to oxidative stress and inflammation in cells (Glenn & Stitt, 2009). Figure 1.11 shows a schematic representation of AMD pathogenesis. Activation of NF-kB signalling leads to transcription of many genes including tumour necrosis factor (TNF), interleukins, interferon-γ and various cell adhesion molecules (Kasper & Funk, 2001; Glenn & Stitt, 2009). Drusens accumulate between Bruch's membrane (BM) and RPE cells which decreases the delivery of oxygen from choriocapillaris to RPE cells and induces hypoxia. Increased in VEGF leads to neovascularization of blood vessels from the

choriocapillaries into RPE space resulting in permanent visual loss. Interestingly, NF-kB has been found to modulate apoptosis through release of cathepsins from the lysosomes into the cytoplasm, where they induce apoptosis (Liu et al., 2003).

Dysfunction of the RPE is an early change in AMD, and subsequent degeneration of RPE is the main cause of permanent vision loss as this causes photoreceptor damage (Bhutto & Lutty, 2012; Golestaneh et al., 2017). Oxidative stress is thought to be the main causative factor in AMD progression. Increased oxidative stress in ageing RPE causes age related changes including decrease in melanosomes, reduction in antioxidant properties, and increase in drusen formation (Rózanowska et al., 1997; Delori et al., 2001).

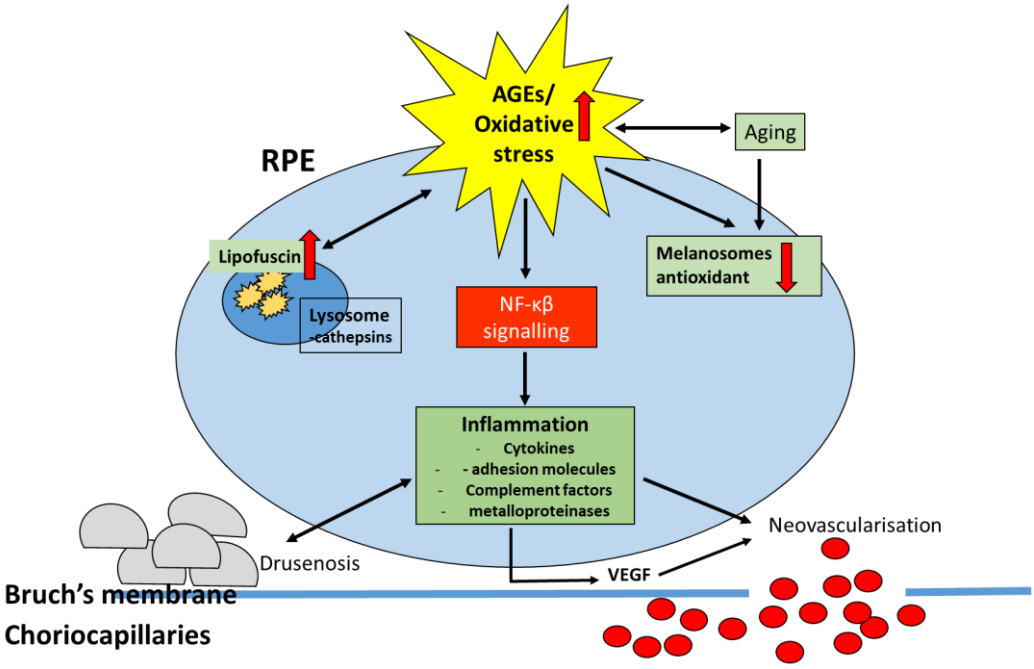

Figure 1.11 Schematic presentation of AMD pathogenesis in relation to AGEs, cathepsin and NF-κβ signalling pathway in RPE cells. Image modified from (Arjamaa et al., 2009; Kaarniranta & Salminen, 2009).

Being a postmitotic cell, study of the molecular mechanism of AGEs, lysosomal regulation and its interaction with NF-kB signalling pathway in RPE is thought to be an important subject in order to understand how age-related changes in RPE could affect its function and lead to pathogenesis of AMD.

1.5.4 Current available treatment for AMD

Currently, there is no cure for AMD. Current definitive treatment options aim at only delaying the disease progression. There is no treatment that could reverse photoreceptors or RPE damage once it has occurred (Cheung & Eaton, 2013). Anti VEGF injections is one of the current mainstay of treatment for AMD for treating choroidal neovascular membrane. Examples of available anti-VEGF treatment are pegaptanib, bevacizumab, ranibizumab and aflibercept (Kaarniranta et al., 2011; Cheung & Eaton, 2013). Pegaptanib is RNA aptamer that has ability to bind to heparin domain of VEGF. It is the first anti-VEGF agent approved by FDA in 2004 to treat neovascular AMD. Bevacizumab and ranibizumab are sharing the same chemical structure. Bevacizumab is a full length monoclonal antibody developed to treat metastatic colorectal cancer. Derived from bevacizumab, ranibizumab is specifically designed to treat AMD. It is an antibody fragment that binds and inhibits VEGF isoforms. It has 5-20 times higher potential in binding VEGF and has been approved by US Food and Drug Administration (FDA) in 2006. Aflibercept is the most recent of all anti-VEGF which received FDA approval for AMD (Cheung & Eaton, 2013). These injections are repeated every 4-6 weeks for as long as is required, as the anti-VEGF effects are only temporary. These injections are costly and cumulative cost for treatment impose a significant economic health burden to the ageing population (Masuda et al., 2014).

Thus, with improved healthcare and longer life expectancies, the prevalence of AMD is increasing, and will eventually pose a serious public health problem in developed countries. This highlights the importance of studies into the mechanism of disease pathways and discovery of newer molecules which may potentially be additional therapeutic targets in combating AMD.

1.6 Lysosomal regulation in RPE cells

Lysosomes were first discovered by Christian de Duve in 1955 (de Duve et al., 1955). Lysosomes are specialised membrane-enclosed organelles made up of phospholipid bilayer that can fuse with other membrane-bound organelles (de Duve et al., 1955; Appelqvist et al., 2013). Lysosomes are widely found in almost all eukaryotic cells except the red blood cells. They contained acid hydrolases include proteases, peptidases, glycosidase, nucleases, sulfatases, lipases and phosphatases that are working together to degrades most macromolecules in cells (Carmona-Gutierrez et al., 2016).

These enzymes are produced in the endoplasmic reticulum and packaged in the Golgi apparatus by forming buds on the Golgi wall. This is also known as primary lysosomes. The secondary lysosomes are formed when primary lysosomes fuse with the cell's vacuoles containing cellular materials and debris to be digested (Repnik et al., 2012).

Due to its action of degrading materials, the lysosome plasma membrane is protected by membrane proteins such as LAMP-1 and LAMP-2 (Repnik et al., 2012). Lysosomes measure approximately up to one micrometer (1µM) (Appelqvist et al., 2013). Lysosomes are involved in various cellular processes such as endocytosis, phagocytosis, membrane repair, pathogen defences, and cell signalling and cell death (Rudzińska et al., 2019).

The main function of lysosomes is in the proteolysis, which is degradation of proteins molecules in cells. Figure 1.12 shows the involvement of lysosomes intracellular processes such as cell death, autophagy and ECM degradation (Rudzińska et al., 2019). It was also reported that lysosomes are also involved in cellular processes such as membrane repair and immune response. Among all the lysosomal enzymes found, cathepsins family are the most significant group of lysosomes (Repnik et al., 2012; Turk et al., 2012).

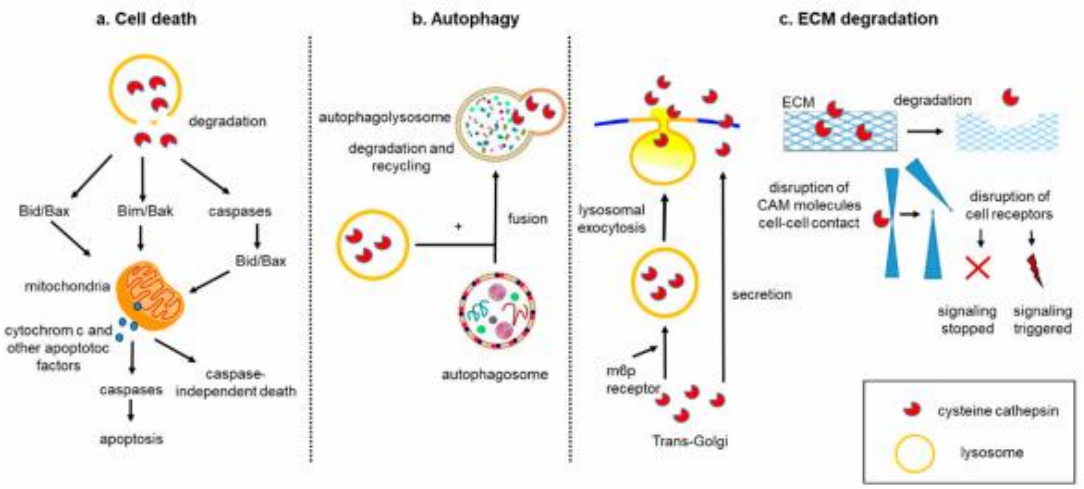

Figure 1.12 Role of lysosomes and lysosomal enzymes on cell death, autophagy and ECM degradation. Image taken from (Rudzińska et al., 2019).

1.6.1 Cathepsin family

Cathepsins comprised of three major groups which are serine protease (cathepsin A and G), aspartyl cathepsin (Cathepsin D and E) and cysteine cathepsin (cathepsins B, C, F, H, K, L O, S, V, W, X/Z) (Turk et al., 2012; Stoka et al., 2016). The list of cathepsins according to its group classification is presented in Figure 1.13. These group classifications are based on the amino acids found on their active sites either it is serine, aspartyl or cysteine (Turk et al., 2012). The cysteine cathepsin is the largest group of all and it will later be review in the next section.

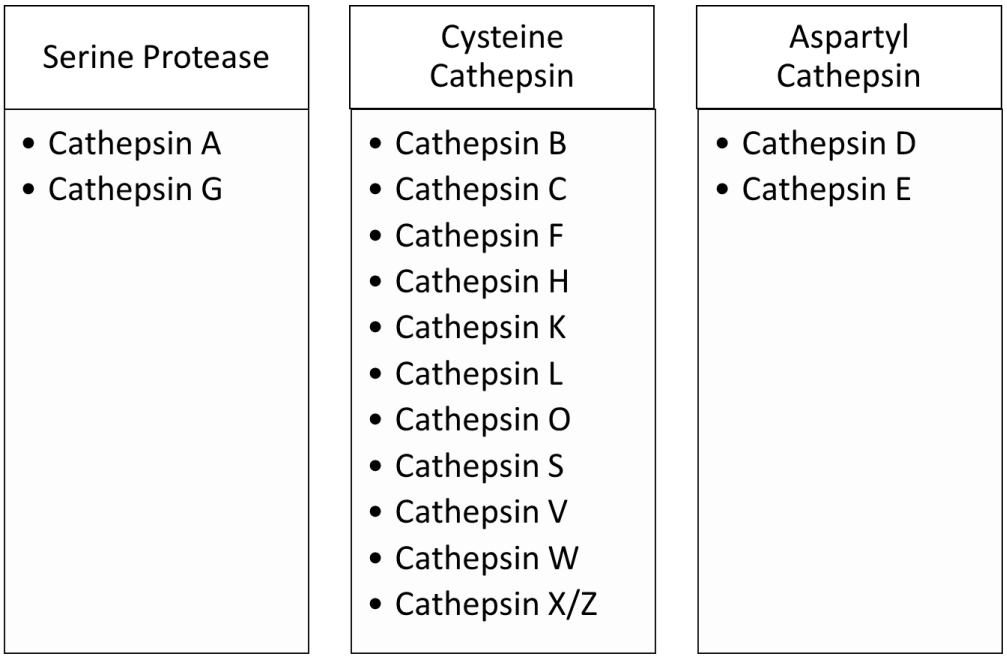

Figure 1.13 List of cathepsins according its group classification. Image modified from information provided by (Turk et al., 2012).

Cathepsin family can be found either as endopeptidases or exopeptidases (Repnik et al., 2012). Endopeptidase cathepsins act by hydrolysing the internal peptide bond of proteins whereas exopeptidase hydrolysing peptide from C- or N-terminal proteins. Cathepsins are mainly endopeptidase, however some do exert exopeptidase properties such as cathepsin X and cathepsin C (Turk et al., 2001).

Cathepsins have been shown to be involved in cellular processes including lysosomal cell death, ageing, autophagy and neurodegeneration, all of which are common processes in the development of AMD (Stoka et al., 2005; Stoka et al., 2016). It is believed that their actions are influenced by gene expression, zymogen processing, endogenous inhibitors and pH stability (Turk et al., 2012).

Due to its important function in cellular homeostasis, dysregulation of lysosomal expression and activities could affect cellular homeostasis. Lysosomal membrane permeabilisation (LMP) is one of the effects caused by cathepsin dysregulation where the protease enzymes in lysosomes are released into the cytosol, resulting in the activation of cell death pathway (Stoka et al., 2005). The occurrence of LMP can be activated by oxidative stress which is highly available in ageing cells (Repnik et al., 2012). The activity of these potentially hazardous proteases can be inhibited by protein inhibitors such as cystatins, serpins and Hsp70 which will be discussed in section 1.6.3.

1.6.1.1 Cysteine Cathepsin

Cysteine cathepsins are the most active proteases in the body. Eleven cathepsins has been characterized which are cathepsin B, C, F, H, K, L, O, S, V, W and X/Z (Im & Kazlauskas, 2007; Turk et al., 2012). Schematic representative and endopeptidase/exopeptidases grouping of cysteine cathepsins is represented in Figure 1.14. Cysteine cathepsins works best at a slightly acidic pH and completely unstable at pH above 7 with an exception of cathepsin S which can remain stable at above pH 7 (Turk et al., 2012). Cathepsin B and L are the major forms of cathepins and are well-characterised mammalian lysosomal cysteine proteases (Brix et al., 2008; Verma et al., 2016). Some human cathepsins such as cathepsin B, H and L are ubiquitously expressed in cells, whilesome are cell-specific (cathepsin F, K, S, V, X, and W) (Brix et al., 2008). Cathepsin L has been found in hair, heart, skin and bone cells (Roth et al., 2000; Spira

et al., 2007). Cathepsin L inhibition in mouse model has demonstrated that lacking in cathepsin L can caused skin epidermal hyperplasia, gradual hair loss and baldness (Roth et al., 2000). Cathepsins S, K and V are reported to be involved in extracellular matrix remodelling, possibly by regulating cleavage of extracellular matrix proteins such as laminin, elastin and collagen (Brix et al., 2008). Cathepsin V found uniquely in thymus, testis, breast and colorectal carcinomas (Brömme & Wilson, 2011). Cathepsin W which also exerts cell-specific expression, is found in $CD8^+$ T cells and is believed to play a role in T cell-mediated cytotoxicity (Stoeckle et al., 2009).

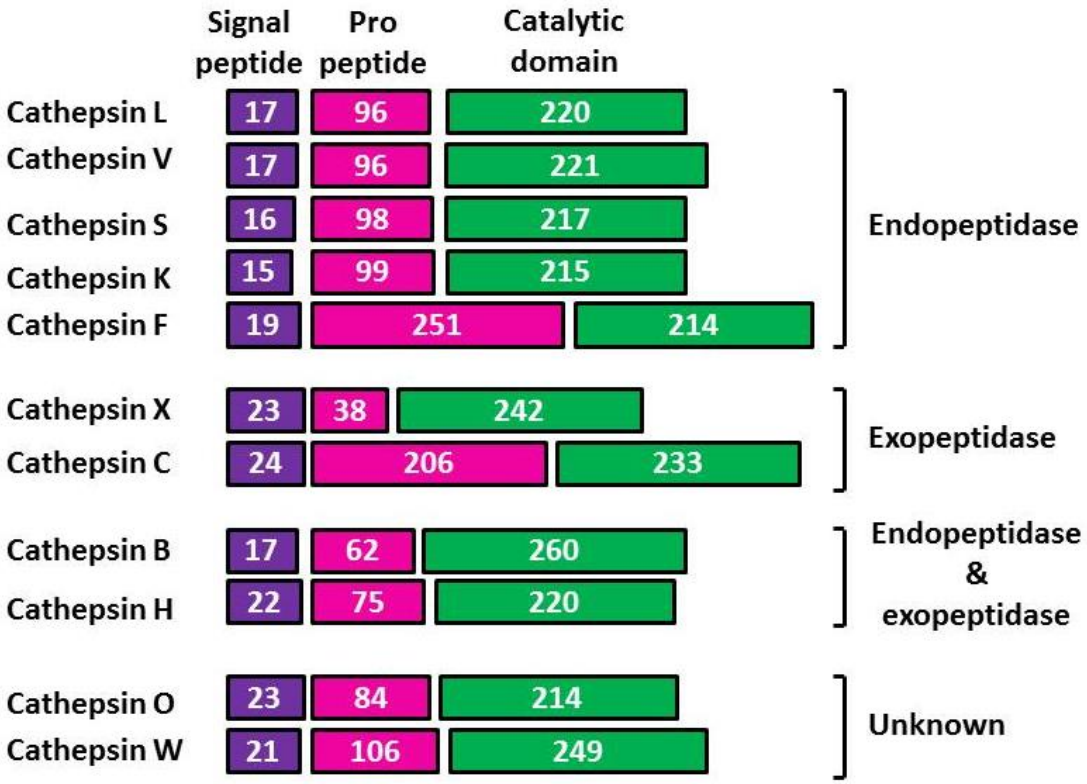

Figure 1.14 Schematic representation cysteine cathepsins and it structure. Cysteine cathepsins can exist either as endopeptidase, exopeptidase or both. Numbers in the block represent number of amino acid length of each peptide. The signal peptide is cleave upon translocation into ER meanwhile the propeptide is cleave with increasing acidic environement in the lysosomal system leaving the catalytic domain which acts as mature cathepsins . Image modified from (Brömme & Wilson, 2011).

1.6.2 Processing and regulation of cathepsins

Each cathepsins are encoded by a very unique gene. The process of cathepsin synthesis is shown in Figure 1.15. Cathepsins are synthesised as inactive pre-procathepsins in the membrane bound ribosomes tagged to an N-terminal propeptide. This is subsequently activated and transported to endoplasmic reticulum and Golgi apparatus (Im & Kazlauskas, 2007). Transportation of cathepsins from endoplasmic reticulum to Golgi occurs with the aid of mannose-6-phopshate (M6P) (Filocamo & Morrone, 2011). M6P is responsible as a tag for the cathepsins, to allow activation by acidic pH (Turk et al., 2012). Cathepsins are activated instantly upon packing into lysosomes. Activation by cleavage may occur either through autocatalytic activation or by the action of other proteases such as cathepsin L (Repnik et al., 2012). Autocatalytic activation only occurs with endopeptidases cathepsins, which are regulated by an acidic environment. Activation of exopeptidases enzymes such as cathepsin X and C are facilitated by endopeptidases enzymes such as cathepsin L and S. Upon activation, these enzymes are ready to carry out its function in proteolysis (Im & Kazlauskas, 2007; Brix et al., 2008).

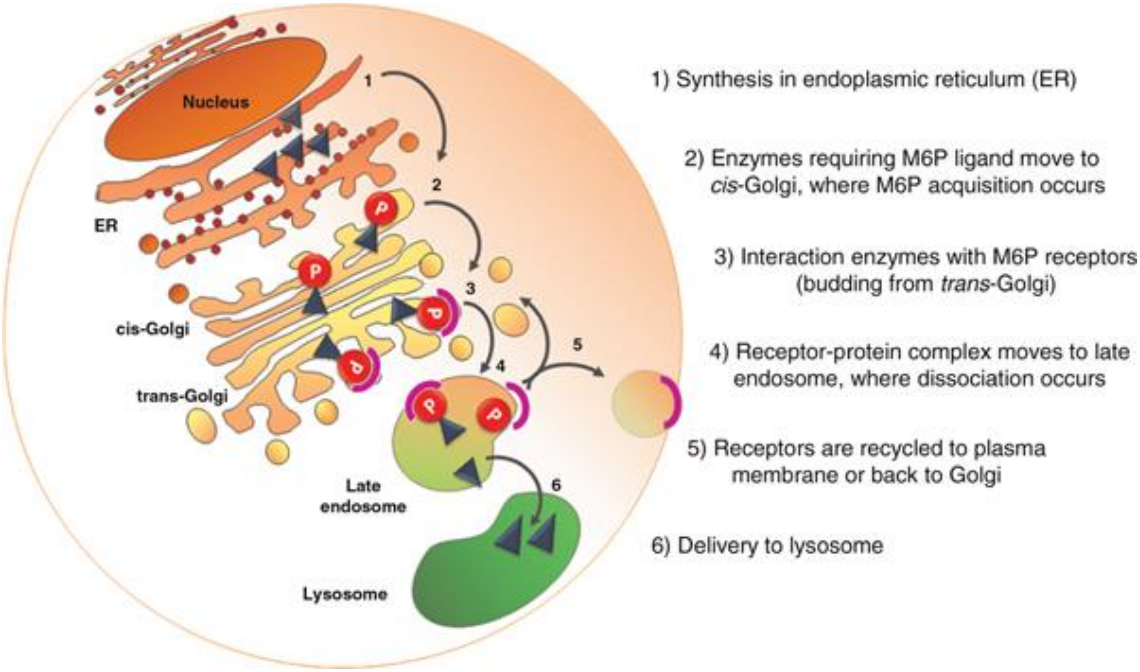

Figure 1.15 Cathepsin synthesis and packaging into lysosome. Image retrieved from (Filocamo & Morrone, 2011).

1.6.3 Cathepsin Inhibitor

Cathepsins are present in very high concentrations in the lysosomes. Inappropriate action of cathepsins can cause a damaging effect to the cells. Thus it is important to have an inhibitor that can control the regulation of cathepsins in cells. The three most prominent cathepsin inhibitors are cystatins, serpins and Hsp70. Cystatins are specific endogenous cysteine proteases inhibitors that capable of blocking protease activities prior to being released into the cytoplasm following lysosomal damage (Stoka et al., 2005). Cystatin B and C targets cathepsins B, H, L and S in their mode of action (Alizadeh et al., 2006). Many studies have showed the involvement of cystatin C as a protective agent in neurodegeneration diseases (Paraoan et al., 2000; Xu et al., 2005; Gauthier et al., 2011; Watanabe et al., 2014). It is possible that cystatin C acts through inhibition of cathepsins activity. Recent evidence has shown the association of cystatin C in AMD patients (Paraoan et al., 2010; Kay et al., 2013).

Apart from cathepsin, serpins are the largest group of protease inhibitors identified on animals, plants, bacteria, archea and poxviruses (Law et al., 2006). It is known to inhibit serine and cycteine cathepsins (Higgins et al., 2010; Guo et al., 2015). The main function of serpins is to perform an inhibitory function, however, some human serpins can also acts as hormone transporter and tumour suppressor (Law et al., 2006). Serpin cause inhibition of cathepsins through conformational switch mechanism. This resulted in damaged inactive enzymes. In addition, the action of serpins on proteases can be enhanced by presence of cofactor such as glycosaminoglycans (Higgins et al., 2010).

Hsp70 is a heat shock protein 70 resides at the lysosomal membrane. Under normal cell conditions, Hsp70 remains in the lysosomes and localised in the cytoplasm under stress stimulation. The presence of Hsp70 in tumour cells has been shown to protect the cells from cells death. The inhibition may occur via inhibition of LMP or cysteine cathepsins. Hsp70 has also been shown to protect the RPE cells from cell death. mRNA depletion in RPE cells has been shown to increase cell death significantly (Nylandsted et al., 2004). The mechanism on how the Hsp70 protect the RPE remains unclear.

1.6.4 Modulation of lysosomal cathepsins by oxidative stress and regulation in ageing

Oxidative stress has been observed to be one of the critical factor in age-related diseases and pathogenesis of neurodegenerative diseases including Alzheimer's and AMD (Gómez-Sintes et al., 2016). Higher oxidative stress levels has been detected in AMD patient's compared to healthy individuals (Zafrilla et al., 2013). The Age-related Eye Disease (ARED) study demonstrated that intake of vitamin supplements can reduce severity and progression of AMD (Alizadeh et al., 2006). In the RPE, lysosomal enzymes are more active than any other tissue in the body (Alizadeh et al., 2006). Lysosomal cathepsins are important in the degradation of cells organelles, membrane proteins and protein turnover. Within the eyes, cathepsins are found in cornea, optic nerve, choroid and the RPE (El-Hifnawi et al., 1995; Im & Kazlauskas, 2007)

Being a postmitotic cell, the RPE needs lysosomal cathepsins to help them maintain normal physiological and biochemical functions throughout the human life. Having an important role in phagocytosis and degradation of POS, it is suggested that lysosomal dysregulation with ageing contributes to RPE dysfunction leading to increase in lipofuscin formation and drusen deposit on the RPE environment (Guha et al., 2014). Figure 1.16 shows a summary on the effect of cathepsin impairment in ageing RPE.

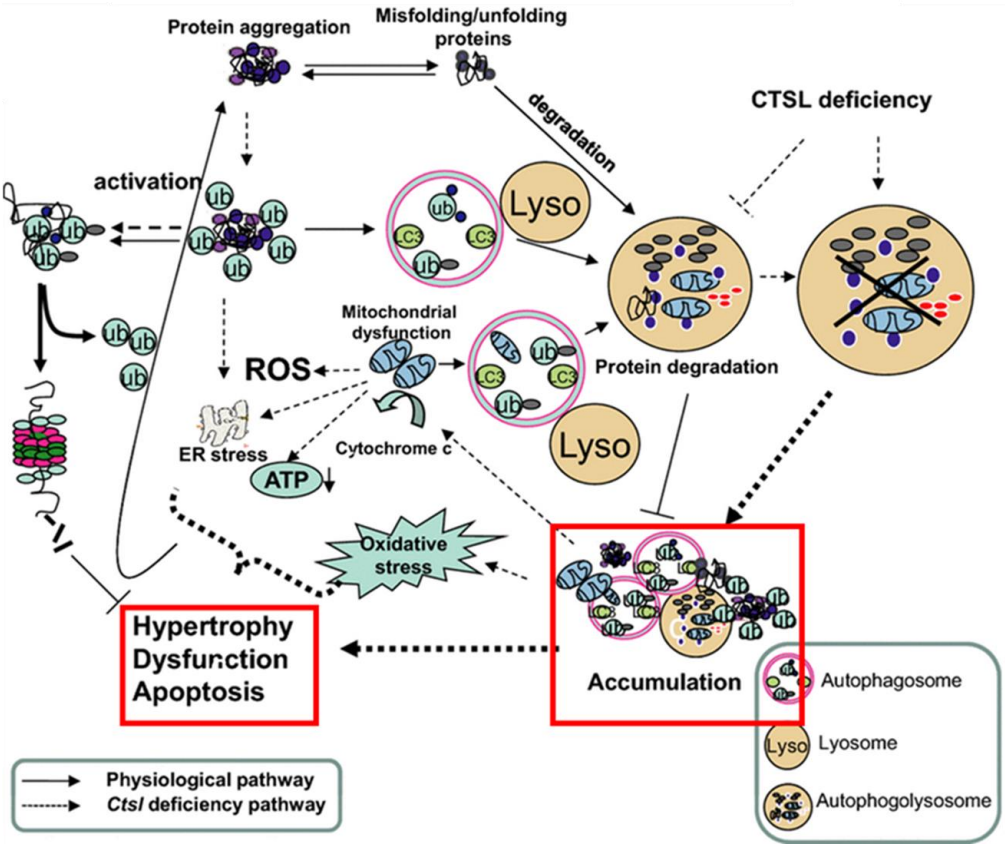

Figure 1.16 Effect of cathepsin pathway impairment in ageing RPE (Image retrieved and modified from (Sun et al., 2013)).

1.7 Advanced Glycation Endproducts

Advanced Glycation Endproducts (AGEs) are a heterogeneous group of molecules formed through a complex series of nonenzymatic process called Maillard reaction by interaction of aldehyde or carbonyl sugar with amino group of proteins, lipids or nucleic acids (Goldin et al., 2006; Luevano-Contreras & Chapman-Novakofski, 2010). To date, more than twenty types of AGEs has been characterised in human tissues and mostly are closely linked to ageing. Among AGEs present are Nε-(carboxymethyl) lysine (CML), Nε-carboxyethyllysine (CEL), pentosidine, methylglyoxal lysine dimer (MOLD), and glyoxal lysine dimer (GOLD) (Goldin et al., 2006; Glenn & Stitt, 2009).

AGEs have been implicated in the pathogenesis of a range of disease processes, which being widely study is its role in development of diabetes complications (Sato et al., 2001; Stitt, 2001; Ahmed, 2005; Ramasamy et al., 2005; Goh & Cooper, 2008; Grzebyk et al., 2013). However, research development has started to link AGEs with other age related diseases and degenerative disorders such as atherosclerosis (Basta et al., 2004; Chang et al., 2011), Alzheimer's (Sasaki et al., 1998; Ko et al., 2015; Drenth et al., 2017), osteoarthritis (Saudek & Kay, 2003; DeGroot et al., 2004; Trellu et al., 2017) and pulmonary fibrosis (Ding et al., 2015; Haider et al., 2019). In the eye specifically, apart from diabetic retinopathy, AGEs also linked to AMD (Ishibashi et al., 1998; Howes et al., 2004). Loss of vision in both of this eye disease are irreversible, though patient with AMD has higher chances of visual loss (Frohlich, 2005).

AGEs formation require three steps, which are described below (Figure 1.17) (Goldin et al., 2006; Luevano-Contreras & Chapman-Novakofski, 2010; Kandarakis et al., 2014; Guilbaud et al., 2016):

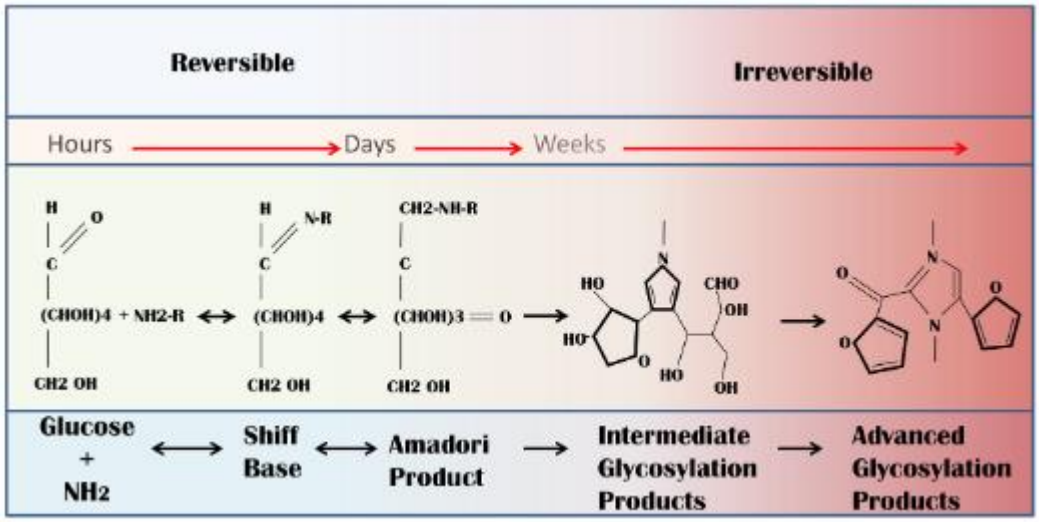

Figure 1.17 Formation of AGEs (Kandarakis et al., 2014).

i. Schiff base

Schiff base is formed when an aldehyde group of a sugar molecule react with the amino group of an amino acid introducing a double bond formation between the carbon of the aldehyde group and nitrogen from the amino group.

ii. Amadori formation

This stage involved further arrangement of hydrogen atoms from the hydroxyl group adjacent to the carbon nitrogen double bond. The hydrogen atom is transferred to the nitrogen atom to form ketone or also known as Amadori product.

iii. AGEs

Further oxidation and dehydration of the Amadori products later results in the irreversible form of proteins bound to AGEs. The first two stages in AGEs formation is reversible while the final product is irreversible.

AGEs formation can be triggered either internally or externally, depending on oxidative stress level, protein longevity, dietary content with AGEs, level of antioxidant

and modification rate of protein and lipids (Gkogkolou & Böhm, 2012; Vistoli et al., 2013; Guilbaud et al., 2016). Internally, metabolism product such as α-oxoaldehydes (glycoaldehyde, methyl gloxal, gloxal and 3-deoxyglucosone) exists at high amount in cells exposed to high glucose condition (Thorpe & Baynes, 2003; Vistoli et al., 2013). This metabolic by-product acts as reactive intermediates in AGEs formation (Nagai et al., 2000). Maillard reaction of glycoaldehyde may give rise to AGEs product known as carboxymethyl lysine (Zhang et al., 2009). Externally, AGEs can be generated by food intake (Nowotny et al., 2018). Microwave cooking has been recognised as one of dietary source of AGEs (Sharma et al., 2015). Restriction of heat processed food to normal mice showed a decrease in AGE and oxidative stress level (Kandarakis et al., 2014) .

AGEs accumulation in cells not only cause irreversible changes to extracellular matrix but also can activate various pro-inflammatory signalling pathway (Thorpe & Baynes, 2003; Glenn & Stitt, 2009). Among pathway pronounced to be associated with AGEs are JNK, MAPK, ERK and NF-kB signalling (Ott et al., 2014; Chen et al., 2016a). Activation of these signalling pathways are depending on binding of AGEs to its receptor.

1.7.1 Receptor for AGEs

Activation of AGEs are based on binding to its receptor (Bierhaus et al., 2005). There are more than one receptor in which AGEs can bind to includes receptor for advanced glycation endproducts (RAGE), macrophage scavenger receptors (MSRs), oligosaccharyl transferase-48 (OST48,also known as AGE-R1), 80 K-H phosphoprotein (or AGE-R2), galectin-3(AGE-R3), lectin-like oxidized low density lipoprotein receptor-1(Lox-1), fasciclin EGF-like, laminin-type EGF-like, link domain-containing scavenger receptor-1/2 (FEEL1/2) and CD36 (Kasper & Funk, 2001; Bierhaus et al., 2005; Glenn & Stitt, 2009; Xie et al., 2013; Kandarakis et al., 2014). Amongst all, RAGE is the most widely studied and can be found in various cell types includes in neurons, hepatocytes, monocytes and endothelial cells (Kandarakis et al., 2014). However the expressions may vary in human cells.

RAGE is a member of immunoglobulin superfamily of cells surface molecules with size of 35kDa (Kandarakis et al., 2014). RAGE structure has three main domains; a V-type domain responsible for ligand binding and two C-type domains linked to one transmembrane domain and one short intracellular negatively charged c-terminal tail (Bierhaus et al., 2005). Binding of AGEs occur on the V-domain (Schmidt et al., 2000; Bierhaus et al., 2005). The V-domain is positively charged which attract a negatively charged AGE-modified protein (Schmidt et al., 2000). Binding of AGEs to V-domain triggers downstream signalling pathway via its short intracellular negatively charged c-terminal tail affecting major cellular function such as adhesion, migration and proliferation (Younessi & Yoonessi, 2011; Xie et al., 2013).

The expression of RAGE is low in normal physiological conditions and can be upregulated in response to immune reaction upregulated (Kasper & Funk, 2001). In addition, RAGE also has been found to be upregulated in response to high oxidative

stress status (Nedić et al., 2013). Hypoxia exposure in tumour cells such as in prostate cancer cells, breast cancer cells, MDA-MB-231, MCF-7 and HeLa cells have shown increased in RAGE expression (Tafani et al., 2011a; Tafani et al., 2011b). RAGE ligand binding has been implicated with inflammation and cell migration processes as described in RAGE knockout mice (Kandarakis et al., 2014; Derk et al., 2018). It is believed that implication of these mentioned cellular processes possibly cause through activation of signalling pathway such as Nuclear Factor κ light chain enhancer of activated B cells (NF-κB) signalling pathway (Tafani et al., 2011b; Lin et al., 2012). Apart from NF-κB, the binding of ligand to RAGE can also activates other signalling such as ERK, JNK, MAPK pathway (Refer to Figure 1.18), subsequently altered stress related gene expression (Ott et al., 2014). The level of RAGE in cells can also be controlled by the aforementioned signalling pathways, thus provide a sustained ligand availability (Howes et al., 2004).

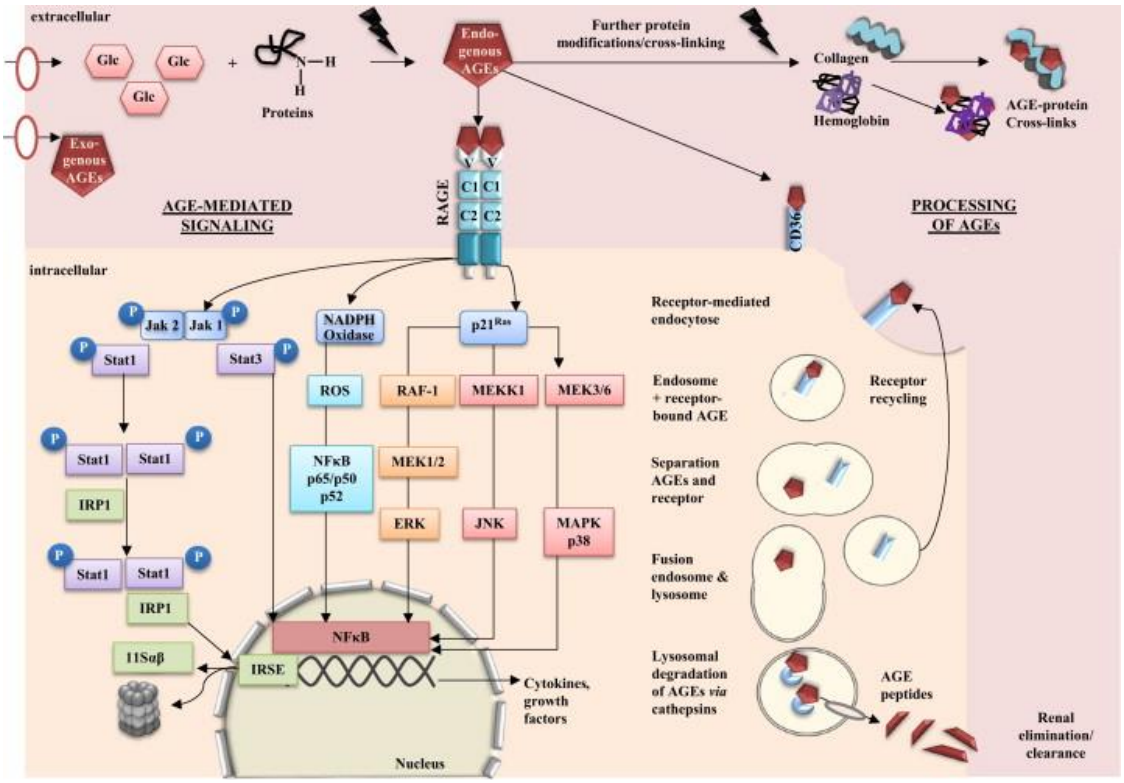

Figure 1.18 Signalling pathways associated with binding of AGEs to RAGE (Ott et al., 2014).

1.7.2 AGEs and ageing

AGEs is postulated to accelerate the process of ageing (Semba et al., 2010). AGEs accumulate as a result of oxidative stress and it also has the ability to induce oxidative stress (Kasper & Funk, 2001). AGEs form slowly in cells and accumulate in the Bruch's membrane, an extracellular matrix with mainly collagen as its major composition (Semba et al., 2010). AGEs has been shown to accumulate in RPE and Bruch's membrane (Handa et al., 1998; Handa et al., 1999; Howes et al., 2004; Tian et al., 2005; Yamada et al., 2006). Many studies has elucidated the increase in AGEs content in Bruch's membrane and RPE in AMD patients compared to normal ageing patients (Handa et al., 1999; Schutt et al., 2003; Howes et al., 2004; Yamada et al., 2006; Glenn et al., 2009; Glenn & Stitt, 2009; Ni et al., 2009).

AGEs can alters the RPE and Bruch's membrane functions. First of all, AGEs has been shown to play a significant role in induction of CNV, a hallmark of advanced for of AMD (Rudolf et al., 2005; Bhutto & Lutty, 2012). It is believed AGEs promotes CNV through upregulation of VEGF (Tong & Yao, 2006; Sun et al., 2017). Overexpression of RAGE i*n vivo* in ARPE-19 cells, confirm increase in secretion of VEGF (Ma et al., 2007). Secondly, AGEs interfere with RPE-Bruch's membrane functions through formation of drusen. Study on post-mortem eyes confirm the presence of AGEs in drusen (Ishibashi et al., 1998). In addition, accumulation of AGEs also caused significant increase in Bruch's membrane thickness. Study has shown that Bruch's membrane can thicken up to 135% in period of 100 years due to age related changes, which includes due to AGEs accumulation (Bhutto & Lutty, 2012). This increase in thickness interferes with the membrane's stiffness and permeability, thus impaired the Bruch's membrane function. This is supported by in vivo study, where mice fed with AGEs enhanced dietary shown to portray age-related Bruch's membrane defect (Ida et al., 2004; Tian et al., 2005).

AGEs affect disease progression by two general mechanism either by modifying molecules leading to formation of non-degradable aggregates or impairing normal cellular function through receptor-mediated activation (Howes et al., 2004). These two modes of action by AGEs can leads to cellular dysfunction and possible cell death.

Formation of non-degradable proteins aggregates in the AMD patients can be seen through drusen formation. Drusen is considered as an important hallmark in AMD disease (Howes et al., 2004; Yamada et al., 2006). Elevated levels of AGEs has been demonstrated in drusen of patients with AMD disease compare to normal ageing individuals (Ishibashi et al., 1998; Schutt et al., 2003).

AGEs can also impair the normal cellular function through binding to receptors. In support with increase AGEs in ageing retina, study focusing on the level of AGEs receptor, RAGE in ageing retina has shown a significantly high expression of this receptor on retina surface (Howes et al., 2004; Ma et al., 2007; Yamada et al., 2006). RAGE is known to be present in RPE and to be highly upregulated in AMD (Howes et al., 2004; Ma et al., 2007).

AGEs have been shown to inhibit lysosomal enzymes activity on other tissues.A previous study on lysosomal cathepsin B, H and L on kidney proximal tubule cells exposed to AGE-BSA showed a decreased pattern in its activity in a dose dependent manner (Sebeková et al., 1998). In addition, reduction in cathepsin S, G and D mRNA expression was also observed in RPE exposed to BSA-induced AGEs (Glenn et al., 2009).

AGEs also can stimulate various signals in the RPE. This include increase in cytokines levels such as VEGF expression which is known to be one of the stimulating factors in AMD development (Witmer et al., 2003; Howes et al., 2004; Rudolf et al.,

2005; Bhutto & Lutty, 2012). In normal conditions, VEGF is secreted to help maintaining the physiological function of choriocapillaris (Spilsbury et al., 2000; Saint-Geniez et al., 2009; Ford et al., 2011). However, overexpression of VEGF in ageing RPE has been shown to induce choroidal neovascularisation (Spilsbury et al., 2000; Wang et al., 2003). Treatment of ARPE-19 cells with AGE-BSA has shown to increase the level of VEGF secreted in the media suggesting the important of AGE ligand binding to RAGE in accumulation of VEGF (Ma et al., 2007). The exact mechanism of expression and secretion of VEGF in the RPE remains unclear. Yet, it is possible that increase in VEGF expression and secretion is governed by AGEs through various adaptor molecules and signalling such as ERK1, ERK2 and JNK/MAPK which later activates the main inflammatory associated pathway, NF-κβ (Tian et al., 2005; Ma et al., 2007).

1.8 Nuclear Factor κ light chain enhancer of activated B cells (NF-κB)

Nuclear Factor κ light chain enhancer of activated B cells (NF-κβ) is transcription factor commonly associated with immune responses and inflammation. It was firstly described as a tissue specific B-cells nuclear factor which activated the immunoglobulin k-light chain intron enhancer during B-lymphocyte development (Sen & Baltimore, 1986; Hayden & Ghosh, 2004; Oeckinghaus & Ghosh, 2009; Gupta et al., 2010). More than 150 candidate genes includes for cytokines, immunoreceptor, cell adhesion, cell migration and antigen presentation has been found to be associated with NF-κβ activation following various activation source (Tieri et al., 2012). The NF-κβ can exist eother as homo or heterodimeric molecules composed of 5 proteins; p65 (RelA), p50, cReI, p52 and ReI B (Aradhya & Nelson, 2001). Among all, p65/p50 heterodimer is the most characterised form of NF-κβ (Oeckinghaus & Ghosh, 2009). In the cells, the NF-κβ exists as inactive molecules sequestered in the cytoplasm through binding to an inhibitory molecule, IκBs (Iκβα, Iκββ, Iκβγ, Iκβε, Bcl3, p100 and p105) (Oeckinghaus & Ghosh, 2009; Sun, 2017). The activation of the NF-κβ is highly depending to the phosphorylation of IκBs protein. The IκB molecules and NF-κβ interaction sealed the nuclear localisation of NF-κβ proteins into the nucleus (Tak & Firestein, 2001; Brasier, 2006; Hoesel & Schmid, 2013).

The NF-κβ can be activated by various stimuli internal and externally. Growth factors, cytokines, bacterial lipopolysaccharides, UV and oxidative stressor are part of various stimuli which triggers the activation of NF-κβ molecules. Activation and translocation of NF-κβ molecules involved a series of phosphorylation and ubiquitination processes before proceed to gene transcription through binding of the

NF-κβ dimer to the κβ sites of DNA sequences (Figure 1.19) (Brasier, 2006).

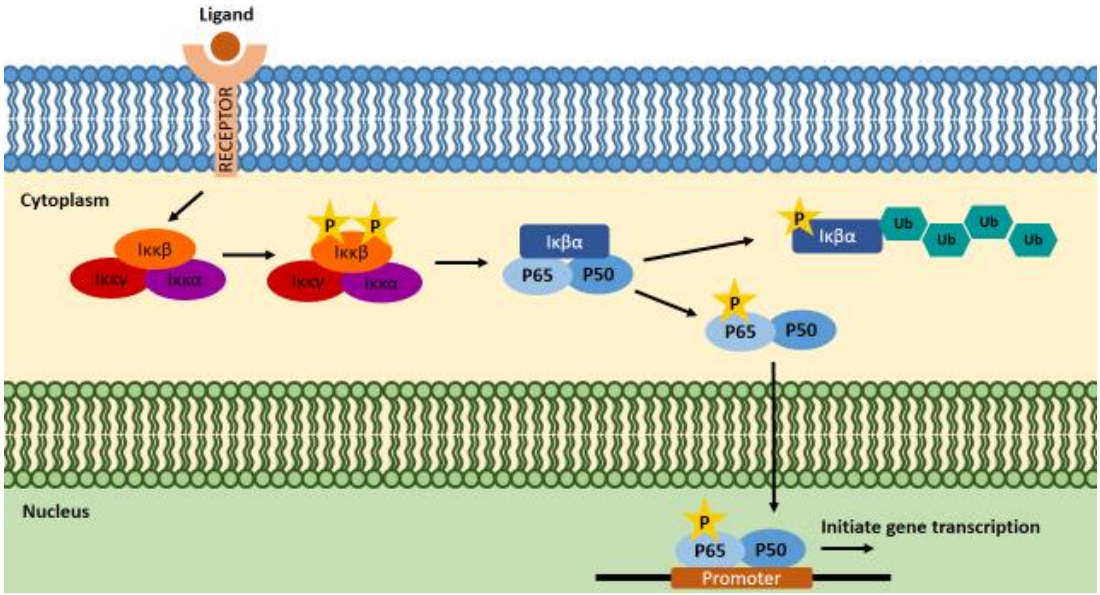

Figure 1.19 Schematic diagram of NF-kB signaling pathway. Image was from own drawing.

Following binding of stimuli to its receptor, the IκB will be phosphorylated by IκB kinase complex (IKK) (Karin, 1999). These proteins interaction unmasked the NF-κβ and induced translocation of the NF-κβ proteins into the nucleus. In the meantime, the IκB undergoes series of ubiquitination and finally is sent for degradation by the 26S proteasome (Sun, 2017). Translocated NF-κβ will induce gene transcription of specific proteins including the Ikβα, which portraits a negative feedback loop for the NF-kβ activation (Fraternale et al., 2013).

Activation of NF-κβ is classified into two main pathways which are canonical (classical) and non-canonical (alternative) pathway (Brasier, 2006). The canonical pathway mediates inflammatory responses, whereas the non-canonical pathway helps in immunity regulations, virus induced stress response and metabolic system (Cardozo et al., 2001; Brasier, 2006) (Allan R. Brasier, 2006; Cardozo et al., 2001). As an important signalling pathway, misregulation of this pathway may later leads to chronic

inflammation, cancer and other immune related diseases (Brasier, 2006; Hoesel & Schmid, 2013; Sun, 2017). Canonical activation of NF-κβ is considered as quick and reversible response; meanwhile it became slower and irreversible through non – canonical pathway (Gilmore, 2006).

In the canonical pathway, binding of ligand to cell surface receptor leads to recruitment of adaptor proteins which in turns recruit the IKK complex protein. Recruitment of IKK proteins leads to phosphorylation and ubiquitination of the IkBα which later cause the translocation of NF-kβ molecules into the nucleus and initialise the gene transcriptions. Phosphorylation and degradation of IKB inhibitor is thought to be the hallmark for this canonical pathway activation. Canonical activation activates p65, c-ReI, Rel B and p50 NF-kβ dimers (Brasier, 2006; Gilmore, 2006).

On the contrary, the non-canonical pathway activates p100/RelB activation. Non-canonical pathway can be activated by ligand such as B-cells activating factor (BAFF), lymphoxin B, cd40 ligand, human T-cells leukemia and Epstein Barr Virus (EBV). Receptor activation in non-canonical pathway recruits the NF-kβ inducing kinase (NIK) protein that will later cause phosphorylation of the IKKα. In turn, IKKα phosphorylates p100 leading to processing of p52/RelB heterodimer and finally translocation of that heterodimer into the nucleus. The non-canonical pathway relies on the phosphorylation of p100 by IKK instead of Iκβα as in canonical pathway (Gilmore, 2006).

Interestingly, canonical pathway can also be activated by the non-canonical pathway. TNFα binding to ligand was found to activate NF-kβ p65 mediated by this non-canonical pathway (Gupta et al., 2010).

1.8.1 NF-kB key regulator

1.8.1.1 NF-kβ receptor

Ligand binding is the first step in activation of NF-kβ signalling pathway and more than one receptor is responsible for this process (Oeckinghaus & Ghosh, 2009; Oeckinghaus et al., 2011; Liu et al., 2017). Toll-like Receptor (TLR), Tumor necrosis factor receptor 1 (TNFR1) and RAGE are among the important receptor for NF-kβ (Oeckinghaus & Ghosh, 2009).

TLRs is a family of receptors consisting of 13 members with leucine-rich repeat motifs in their extracellular domain (Verstrepen et al., 2008). The extracellular domain helps recognise extracellular ligand such as LPS, flagellin, viral double stranded RNA and unmethylated CpG motifs, which is highly found in bacterial DNA (Hemmi et al., 2000; Verstrepen et al., 2008). To date, eight TLRs have been reported and registered in GenBank. TLR2 is responsible for peptidoglycan from bacterial infections meanwhile TLR 3 has been found to be involved in binding the double stranded DNA from viral infections (Alexopoulou et al., 2001). TLR 4 is found to be responsible for immune response and LPS respectively meanwhile TLR9 is involves in CpG-containing bacterial DNA (Hemmi et al., 2000).

In contrast to the TLRs, RAGE activates NF-kβ through binding with AGEs ligand (Bierhaus et al., 1997; Bierhaus et al., 2001; Chavakis et al., 2004; Bierhaus et al., 2005). RAGE-mediated NF-kβ activation is associated with autoregulatory feedback loop, whereby ligation leads to new synthesis of NF-kβ p65. With high accumulation on NF-kβ p65 in cells, the amount of Iκβα in cells might not be able to retain the p65 in cytoplasm. In the end, translocation of p65 occurs and gene transcription by NF-kB continues and activates various proinflammatory responses (Chavakis et al., 2004; Bierhaus et al., 2005).

1.8.1.2 IKKs

Three types of IKKs has been studied, IKKα, IKKβ and IKKγ. IKKγ is also known as NEMO which responsible in activation of non-canonical NF-κβ pathway. IKKα and IKKβ acts a kinase catalytic subunit whereby IKKγ serves as regulatory subunit of the other two IKKs. IKKs exist as homo or heterodimer complex in the cytoplasm. IKKα: IKKβ heterodimer are predominantly found in cells (Oeckinghaus & Ghosh, 2009; Oeckinghaus et al., 2011).

Studies has shown that both IKKα and IKKβ to have a significant similarity in their sequences with protein kinase domain at their N-terminus, leucine zipper and helix-loop helix kinases at the COOH terminus (Oeckinghaus & Ghosh, 2009). The facts that these two IKKs shared the same sequences, research has been carried out to find out the importance of having both IKKs in the cells. Limb abnormalities and epidermal hyperproliferation were detected in IKKα knockout mice, meanwhile lethal embryonic phenotype were identified in IKKβ knockout mice (Hu et al., 1999; Takeda et al., 1999). After all, phosphorylation of IKKα and IKKβ is serine specific, and IKKβ activation is much more pronounced in canonical NF-κβ pathway through Iκβα activity regulation (Karin, 1999). Being a subunit regulator, the IKKγ is responsible in assembling IKKα and IKKβ in non-canonical pathway. Phosphorylation of IKKγ can occur either at serine or threonine site (Karin, 1999). Study has shown that IKKγ deficient mice are unable to activate IKK upon stimulation by human T-cell leukemia virus type 1 (Rothwarf et al., 1998; Uhlik et al., 1998; Yamaoka et al., 1998).

Interestingly, it has been shown that IKKs not only can phosphorylate IKBα and allows nuclear translocation of canonical NF-kB, but it can also phosphorylate p65 prior nuclear localisation. It is possible that phosphorylation of IKB and p65 by IKK occurs simultaneously by the same protein kinases (Sakurai et al., 1999). It has been speculated

that the phosphorylation by IKK occurs by different molecules of IKKs since they exist as homo or heterodimer complex. One IKK molecules phosphorylates IKB and send it for degradation, and the other is responsible in p65 phosphorylation prior nuclear localisation (Karin, 1999; Sakurai et al., 1999).

1.8.1.3 IκBs

IκBs act as an inhibitor of NF-κβ activation in cells. It is actually a small family of proteins consisting of six or more ankyrin repeats, an N-terminal regulatory domain and a C-terminal domain (Karin, 1999). Among all seven IκBs recognised in cells, Iκβα is studied at its best.

Iκβα is degraded by 26s proteasome upon activation by NF-κβ activators especially TNFα and IL-1B. The rate of Iκβα degradation can occur within minutes of ligand binding to surface receptors. IKKs are the one responsible for Iκβα phosphorylation before degradation. Two conserved serine sites have been recognised by IKK as Iκβα phosphorylation site in human, the Ser32 and Ser36 (Cardozo et al., 2001).

Phosphorylated Iκβα does not dissociate from NF-κβ complex instantly. Further polyubiquitination follows before Iκβα degradation takes place. Major ubiquitination sites in human Iκβα studied are Lys21 and Lys22. Iκβα ubiquitination occurs through a series of enzymatic reaction involving the present of E1, E2 and E3 enzyme-substrate reaction. This process is ATP dependent (Palombella et al., 1994).

1.8.1.4 P65

Although five NF-kB molecules exist in cells, P65 is abundantly founds. As P65 exists in dimer form, up to 15 heterodimer combination of NF-κβ molecules can be formed. Among all, p65/p50 dimer is the most abundant in all types of cells and well-studied (Oeckinghaus & Ghosh, 2009). NF-kB p65 is activated by phosphorylation and it is highly depending on the Iκβα degradation (Karin, 1999). P65 has 10 possible phosphorylation sites including Ser276, Ser529, and Ser536 (Sakurai et al., 1999; Okazaki et al., 2003; Oeckinghaus & Ghosh, 2009). Phosphorylation of P65 at its Ser536 is always been associated with binding of AGEs and RAGE (Peng et al., 2016). Apart from that, activation of P65 at Ser536 can also be initiated by LPS and TNFα stimuli (Oeckinghaus & Ghosh, 2009).

1.8.2 Negative Feedback loop of NF-κβ

Apart from its normal function in transcribing various cytokines, growth factors and cell survival regulators, NF-κβ activation can also acts as a negative feedback loop where activation of p65 can be abolished. Four steps are involved in this negative feedback loop regulation (Brasier, 2006). The first step is transcription of Iκβα by activated p65. This feedback loop of NF-κβ- Iκβα is addressed in the activation through TNFα stimulus (Beg & Baltimore, 1996; Brasier, 2006). Feedback loops activity is believed to occur to control the nuclear abundance of p65 in cells and restore the cells homeostasis, in which impairment can leads to chronic inflammation (Brasier, 2006). This feedback loops regulation begins when free p65 enters the nucleus to start transcription, instead of synthesis its direct targets, p65 induces the synthesis of ankyrin-repeat containing proteins. The ankyrin repeat containing protein will capture and inactivate the p65 (Beg & Baldwin, 1993; Beg & Baltimore, 1996). TNFα stimulation shows rapid synthesis of Iκβα through negative feedback loops. The reaction can occur within 1hour post TNFα exposure. Instead of Iκβα, negative feedback loop can also

synthesis Bcl-3 protein, however the reaction upon TNFα stimulation is much slower between 3-9hours post treatment (Brasier et al., 2001).

Secondly, p65 negative feedback loop mediate IKKs level. This process is held by A20 protein, a ubiquitin ligase associated with degradation of RIP through ubiquitin proteasome pathway (Wertz et al., 2004). TNFα induces cells in vivo in absent of A20 can actually induces chronic activation of NF-kB and end up with inflammation (Lee et al., 2000; Wertz et al., 2004). Negative feedback regulation would not happen without this secondary step. A20 deficient mouse demonstrated unsuccessful termination of p65 binding with IKBα autoregulation alone (Lipniacki et al., 2004; Wertz et al., 2004).

The third level is controlling the p65 activating receptor and its signalling receptor. The negative feedback loop control TRAF-1, TNFR1 associated receptor which influence caspase activation. It is believed that the feedback loop disrupt TNFR coupling with IKK (Brasier, 2006).

The fourth and final level is the control of negative feedback loop at the TNF mRNA stability mediated by tristetraprolein (TTP), a zinc finger protein (Brasier, 2006). TTP is responsible in degradation of AU-rich elements, which present in TNFα. Absent of TTP in mice resulted in chronic inflammation disease. Meanwhile increase in TNF secretion demonstrated by TTP deficient macrophages (Carballo et al., 1998). This supports the role of TTP in terminating TNF-induced NF-κβ through TNF mRNA degradation.

1.8.3 NF-κβ in ageing and RPE

NF-κβ signalling pathway is a very complex pathway interacting with various other pathways to modulate cellular processes including cells survival and proliferation. Apart from that, NF-κβ signalling also important in activation of inflammation cascade and it is particularly sensitive to oxidative stress stimulation. The complexity of NF-κβ signalling is shown in Figure 1.20. In ageing, activation of NF-κβ is higher due to increase in oxidative stress level (Helenius et al., 1996; Donato et al., 2007). Study in older endothelial cells has showed higher nuclear NF- κβ as compared to young ones (Donato et al., 2007). The same type of study carried out in cardiac muscle of male and female mouse also exhibit a massive increasing trend of NF-κβ binding activity in older mouse of both gender compared to younger ones (Helenius et al., 1996). Increase in binding activity possibly due to increase in NF- κβ nuclear translocation. To support the study, further investigation was carried out to see the changes in expression of NF- κβ inhibitor (Ikβα) and IκB kinase (Iκκ). Reduced expression of Ikβα was detected in older endothelial cells as compared to the young ones supporting the idea that increase in nuclear NF- κβ is due to decrease in its inhibitory proteins (Donato et al., 2008). In contrast, no change in Iκβa levels observed in cardiac muscle of old mouse (Helenius et al., 1996).

Next, researchers sough to find out how does oxidative stress accumulation during ageing affect the NF- κβ activation. Sprague-Dawley rats were administered with LPS, and the nuclear and cytoplasmic level of NF- κβ from its adrenal gland was measured. Marked increase of NF- κβ binding activity was observed in LPS stimulated rats compared to unstimulated rats in both young and old rats. Interestingly, the binding activity is reduced as the rats aged (Medicherla et al., 2002). This might be the effect of ageing itself which may triggers feedback loop of the NF- κβ transcription, end up with more Iκβa being synthesis to hold the NF- κβ proteins in the cytoplasm. In addition, the

expression of NF- κβ inhibitors may also be altered due to ageing processes. Or else, there might be possibilities that the cells are actually rich in antioxidants, which can inhibit NF- κβ activation.

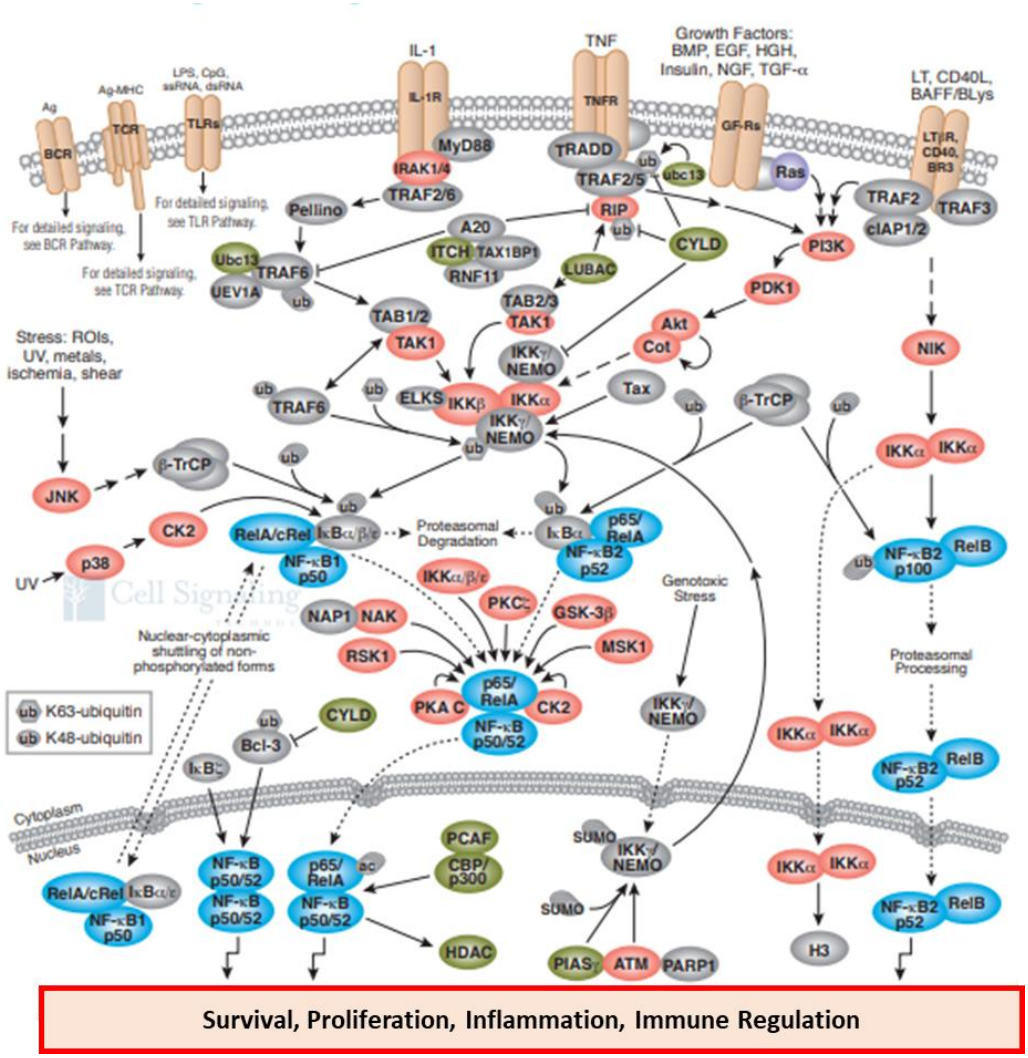

Figure 1.20 Complexity of NF- κβ signalling. Image retrieved from https://www.cellsignal.com/contents/science-cst-pathways-immunology-inflammation/nf-b-signaling/pathways-nfkb .

In the RPE, as it undergoes ageing, they are highly subjected to oxidative stress damage due to high oxygen exposure, long term light exposure and presence of high polyunsaturated fatty acids in the POS. It is believe that increase in this oxidative stress during ageing is the culprit of inflammation which subsequently leads to AMD progression. It is interesting to know that, increase oxidative stress in RPE leads to

accumulation of AGEs that may binds to RAGE, activates the NF-κβ signalling pathway and provoke cell death (Basta et al., 2002; Glenn & Stitt, 2009).

In conclusion, NF- κβ activity is cell specific and it can even exert a dual function, for cell survival and induce cell death. Presence of NF- κβ inhibitors and antioxidant also play roles in controlling the amount of nuclear NF- κβ and NF- κβ binding activity. However, presence of oxidative stress can further alter the expression, activation and binding activity of NF- κβ in ageing conditions.

1.9 Thymoquinone

1.9.1 Thymoquinone structure

Thymoquinone or 2-isopropyl-5methyl-1,4-benzoquinone is a major constituent in *Nigella sative*, a herbs which is broadly used in the Middle East and North America (Badary et al., 2003). The chemical structure of thymoquinone is as shown below in Figure 1.21.

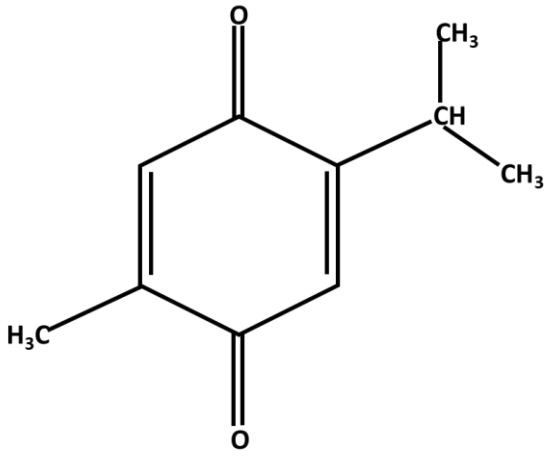

Figure 1.21 Structure of Thymoquinone (Silachev et al., 2015).

Thymoquinone has been recognised to exert an anti-inflammatory properties and analgesic effect (Sayed & Morcos, 2007; Losso et al., 2011). The rise of study on thymoquinone effect on various conditions and diseases shows the importance of this compound as a therapeutic target (Budancamanak et al., 2006; El Gazzar et al., 2006; Chehl et al., 2009; Kanter, 2009; Losso et al., 2011; Woo et al., 2012).

1.9.2 Protective effect of thymoquinone on AGEs

Losso et al. (2011) assessed the potential inhibitory effect of thymoquinone against AGEs from serum samples of diabetic patients through the use of hemoglobin-δ-gluconolactone, human serum albumin-glucose and the *N*-acetyl-glycyl-lysine methyl ester-ribose assay. The results suggested that 10uM and 20uM thymoquinone doses are able to suppress AGEs formation (Losso et al., 2011). Thymoquinone has been shown to suppress AGEs in blood plasma by 78% with a concentration as lower as 10mM (Losso et al., 2011). In another study investigating the neuroprotective effect of thymoquinone against AGEs was through measuring the induction of NF-κβ activation (Sayed & Morcos, 2007). This will be discussed in 1.9.3.

1.9.3 Protective effect of thymoquinone against NF-κβ activation.

Ability of thymoquinone to exert anti-inflammatory properties are already widely studied (El Gazzar et al., 2006; El Gazzar et al., 2007; Sayed & Morcos, 2007; Ragheb et al., 2009; Umar et al., 2012). To further characterise its anti-inflammatory properties, the neuroprotective effect of this compound on NF- κβ pathway was tested by measuring the level of inflammatory cytokines secreted.

In one of the many studies, BV2 microglial cells was stimulated with LPS upon thymoquinone incubation. LPS-induced NF- κβ activation was studied by measuring the secretion of TNFα and other NF- κβ related inflammatory cytokines such as IL-6 and IL-1β (Nagi et al., 1999; Wang et al., 2015; Velagapudi et al., 2017b). All above-mentioned NF- κβ related cytokines were shown to significantly reduce its level in range of dose between 2.5uM to 12uM of thymoquinone. In addition, exposure of LPS on rat basophil cell lines showed marked increase in TNFα production, and thymoquinone was able to reverse this effect with as low as 10uM concentration (El Gazzar et al., 2007). Study on the effect of thymoquinone on NF- κβ signalling and

TNFα cytokines release in the rat's liver also portray the same results as mentioned above (Sayed & Morcos, 2007).

Having the understanding that thymoquinone is able to reduce the release of pro-inflammatory cytokines through activation of NF- κβ, later leads the researchers to study the mechanism behind the attenuation effect of thymoquinone on the inflammatory cytokines secretions. El-Gazzar et al (2007), Wang et al (2015) and Velagapudi et al (2017) has tried measuring NF- κβ alteration in different stages of NF-κβ pathway. El-Gazzar et al (2007) shows that thymoquinone alters LPS-induced TNFa production and proves that the alteration was not due to inhibition of DNA binding by thymoquinone. On contrary, Velagapudi et al (2017) shows that there is a possibility that thymoquinone may acts on the P65 DNA binding capability and thus reduce the release of pro-inflammatory cytokines. In addition, Wang et al (2015) and Velagapudi et al (2017) suggest that alteration of NF- κβ by thymoquinone may also be mediated through inhibition of Iκβα phosphorylation or P65 phosphorylation (Wang et al., 2015; Velagapudi et al., 2017b). Up to date, there is still no solid conclusion on the mechanism of action of thymoquinone on the NF- κβ signalling pathway. However, with these current findings, possible role of thymoquinone in treating inflammatory related diseases such as seen in AMD which mediated by NF- κβ signalling is interesting to be explored.

1.10 Research Aims and Objectives

The main goal of this study was to understand the molecular mechanism linking age-related stressors, particularly AGEs, to lysosomal regulation and NF-kB signalling pathway in RPE cells, in order to provide a deeper understanding of the pathogenesis of AMD disease. We hypothesise that cathepsin L is involved in the NF-κβ signalling pathway in AMD model of ageing RPE cells. Our specific objectives were:

1. To investigate the effect of AGEs on NF-κβ signalling pathway in RPE cells
2. To study the effect of cathepsin L inhibition on the NF- κβ signalling pathway in RPE cells
3. To determine the effect TNFα on the NF-κβ signalling key effectors in both cathepsin L inhibited and AGEs-exposed RPE cells
4. To study the effect of thymoquinone on the NF-κβ signalling in AGEs-exposed RPE cells

CHAPTER 2: MATERIALS AND METHODS

2.1 Materials and Reagents

2.1.1 Cell Lines

ARPE-19 (ATCC® CRL-2302™) and HeLa (ATCC® CCL-2™) cell lines were purchased from the American Type Culture Collection (ATCC) (Virginia, USA).

2.1.2 Cell Culture Media and Additives

Dulbecco's Modified Eagle's Medium/F12 (DMEM/F12), Dulbecco's Modified Eagle's Medium (DMEM), Fetal Bovine Serum (FBS), L-glutamine, Trypsin solution and Phosphate Buffer Saline (PBS) were from Sigma-Aldrich, (Dorset, England). Matrigel™ Basement Membrane Matrix which in AGEs experiments were obtained from Corning (Tewksbury, MA).

2.1.3 Cell Culture Treatment Reagents

Cathepsin L Inhibitor III and TNF-alpha were obtained from Merck Millipore (Hertfordshire, UK) and Life Technologies (Carlsbad, California) respectively. Glycoaldehyde Dimer, Sodium Borohydride and Thymoquinone were all from Sigma-Aldrich Company Ltd (Dorset, England).

2.1.4 qPCR Reagents

RNeasy Plus Mini Kit for RNA isolation and RNAse Free water for RNA elution and cDNA synthesis preparation were purchased from Qiagen Ltd (Hilden, Germany). RevertAid First Strand cDNA synthesis was obtained from Thermo Fisher Scientific (Vilnius, Lithuania). Primers used for real-timr PCR (qPCR) were purchased from Integrated DNA Technology (IDT) (Singapore Science Park, Singapore). qPCR was measured using StepOnePlus^{TM} Real-Time PCR System (Applied Biosystem, UK) with aid of Quantinova SYBR Green PCR kit (Qiagen Ltd, Hilden, Germany). Molecular

Weight Marker for gel electrophoresis was purchased from Promega, Wisconsin, USA. The electrophoresis gel were stained with GelRed Nucleic Acid Gel Stain from Biotium (California, USA) and the image was viewed under UV using BIORAD GelDoc system (Milan, Italy).

2.1.5 Western Blot Reagents

Protein samples for Western Blot was quantified using Qubit® protein Assay (Thermo Fisher Scientific, Waltham, USA). Western Blot was carried out in BIORAD system (Hampstead, UK). The primary rabbit antibodies to NF-κB p65, IκBα and cathepsin L used were purchased from Abcam (Cambridge, UK). Anti- Phosphorylate NF-kB p65 Antibody was from Cell Signalling Technology (Massachusetts, USA). Anti- GAPDH primary antibody was obtained from Sigma-Aldrich Company Ltd (Dorset, England). Both secondary antibodies, Anti-Rabbit IgG (whole molecule) Peroxidase Antibody and Anti-Mouse IgG (whole molecule) Peroxidase Antibody were from Sigma-Aldrich Company Ltd (Dorset, England). Protein molecular weight marker and Pierce™ Western Blot Kit, ECL substrate were from Thermo Fisher Scientific, (Massachusettes, USA).

2.1.6 Others

Cathepsin L Activity Assay Kit was obtained from Abcam, (Cambridge, UK). MTT (3, 4, 5-dimethylthiazol-2-yl-2, 5-diphenyltetrazolium bromide) were from Thermo Fisher Scientific (Massachusettes, USA). Other chemicals and reagent were purchased from Sigma-Aldrich Company Ltd (Dorset, England) at its best quality available unless stated otherwise.

2.2 Cell Culture and Treatments

Method used on this project is summarised in the flow chart below (Figure 2.1):

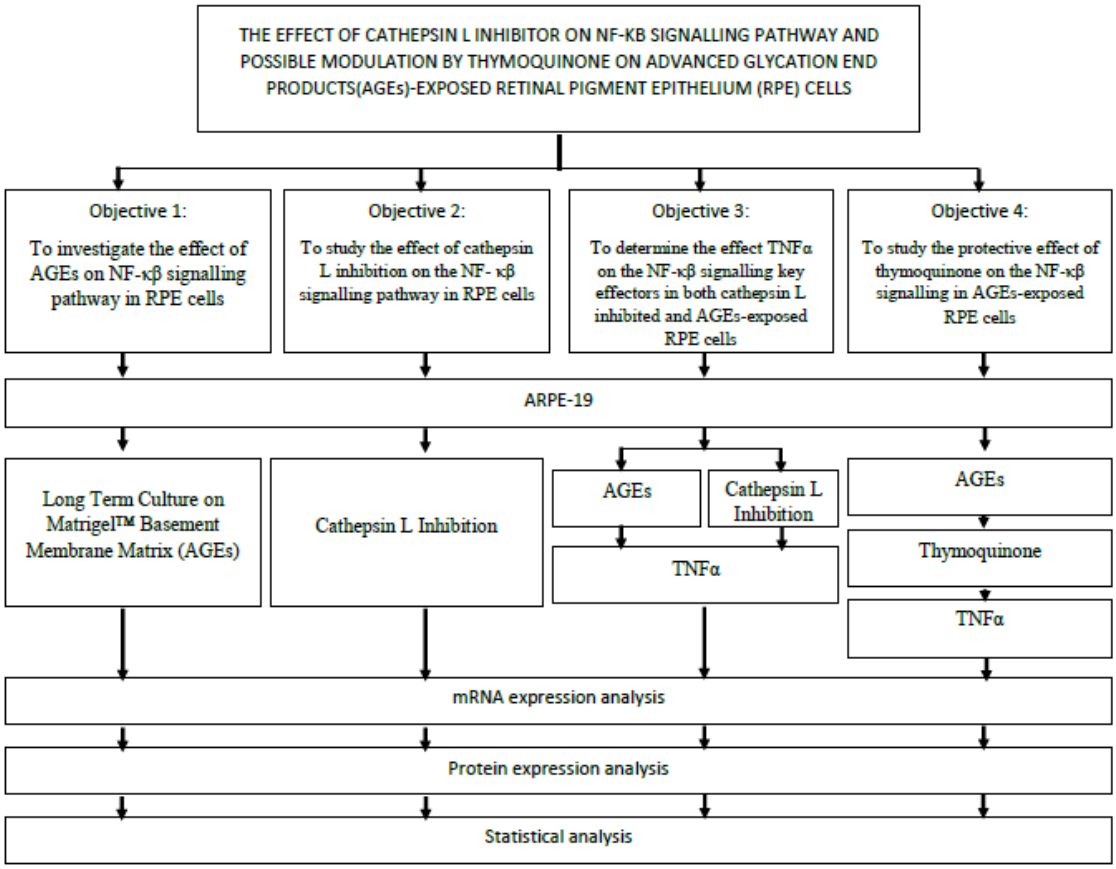

Figure 2.1 Experimental design of the study.

2.2.1 Maintenance of cell lines

All experiments were carried out using human-derived immortalised cell lines. The main cell line used to establish cultures of human RPE for this project was ARPE-19 (ATCC® CRL-2302™) cells. The ARPE-19 cells are retinal pigment epithelium cells derived by Amy Aotaki-Keen in 1986 from the normal eyes of a 19 years old male who died through a head trauma in a vehicle accident. The ARPE-19 was maintained in 1:1 mixture of Dulbecco's modified Eagles medium and Ham's F12 medium with 2mM L-glutamine, 15mM HEPEs, and sodium bicarbonate and supplemented with 10% (v/v) of fetal bovine serum.

Hela (ATCC® CCL-2™) cells were used as a control on most of the experiments in this project. Hela cells were derived from a 31 years old female adult with adenocarcinoma disease. Cells were grown in Dulbecco's Modified Eagle's Medium supplemented with 2mM L-glutamine and 10% (v/v) FBS.

Both cell lines were incubated at 37°C with 5% CO_2. Cells were fed in every three days and passaged when they reached 80-90% confluency. To allow cells detachment for splitting, the cells were washed three times with Phosphate Buffer Saline (PBS) followed by 1x trypsin incubation at 37°C for 3-5 minutes. The reaction was quenched using complete media at a ratio of 1:3 trypsin:media. The suspension was centrifuged at 1000rpm for 3-5 minutes at room temperature and the pellets were re-suspended in appropriate volume of fresh complete media. Cells were split at 1:3 to 1:5 for ARPE-19 cells and 1:2 to 1:6 ratio for Hela cells in 75 cm^2 flask as recommended by ATCC. The seeding capacity was further seized down or up based on container size wherever applicable. For all experimental procedure, ARPE-19 cells were seeded in 2ml supplemented media at density of $1x10^4$ cells per well in 6-well plates unless stated otherwise. Meanwhile due to its rapid growth, Hela cells were seeded at a density of $5x10^3$ in 6-well plates. For freezing down, medium consists of 50:50 DMEM/F12:FBS with 5% (v/v) DMSO was used. The cells suspension were allowed to freeze in -80˚C freezer overnight in a specialised box which slowly freeze down cells at a rate of 1˚C/ minute. Frozen cells were then placed in liquid nitrogen tank for long term storage.

2.2.2 Preparing Long Term Culture on Matrigel™ Basement Membrane Matrix

Matrigel™ Basement Membrane Matrix is a solubilised gelatinous basement membrane extracted from Engelbreth-Holm-Swarm (EHS) mouse sarcoma cells. Matrigel™ is widely used as a substrate for cell culture as it contains many extracellular matrix proteins and constituent that is similar to many tissues in its natural environment.

In this case, the Matrigel™ was used to mimic the BrM layers, where the RPE cells sets. The protocol used in this study has been established in few research groups (Glenn et al., 2009b; Kay et al., 2014). This ageing model is illustrated in Figure 2.2.

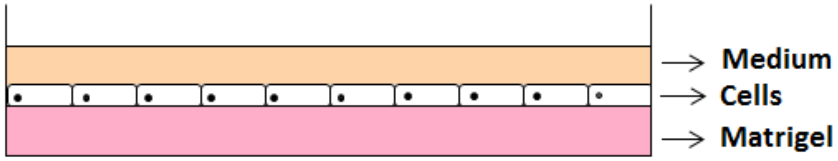

Figure 2.2 The illustration of the ageing models used in the experiment.

Basically, 6-well plates were used in this protocol. Firstly, 500µl of the diluted Matrigel™ was carefully pipetted and spread to each well. Air bubbles were removed out from the wells. Matrigel™ was allowed to polymerise for one hour at 37°C. Followed with a through washing with PBS to remove excess Matrigel™. Glycoaldehyde was used to induce AGEs formation to the Matrigel™ by four hours incubation in 2ml of 100mM glycoaldehyde at 37°C. For control matrices, 2ml of 100mM glycoaldehyde was replaced with 2ml of PBS.

Following the four hours incubation, the Matrigel™ was washed again with PBS to remove excess glycoaldehyde and the reaction was terminated by overnight incubation at 4°C with 2ml of 50mM sodium borohydride. On the next day, the Matrigel™ was washed again to remove all the remaining chemical that can affect the subsequent experiments. ARPE-19 cells were seeded at 1 x 10^4 cells on the Matrigel™ and allowed to grow for fourteen days. Each experiment was designed with at least two individual replicates with three independent replicates.

At early days, the cells were fed in every three days with DMEM/F12 with 10% FCS and changed to 2% FCS on the fifth days post seeding to help them formed stable

monolayers of cells. At the end of the 14th days, the cells were trypsinised, and lysed. Total RNA and total protein were extracted stored in -80°C for further use.

2.2.3 Cathepsin L Inhibition

ARPE-19 cells were seeded at density of 1x10^4 cells in a 6-well plate and allowed to grow in DMEM/F12 media with 10% FCS to confluent for four days. The cells were treated with 40µM of Cathepsin L inhibitor III for 8 hours at 37°C followed by through washing with PBS. Cells were lysed to get the RNA and proteins for further analysis using qPCR and immunoblotting. Samples were stored in -80°C and -20°C freezer until further use.

2.2.4 TNFα Treatment

Following AGEs or Cathepsin L treatment, ARPE-19 were further treated with oxidative stressor, TNFα at a concentration of 10ng/ml for 2 hours at 37°C. Cells were then washed thoroughly with PBS and lysed to get the RNA and protein for further qPCR and Western blotting analysis. Samples were stored at -80 and -20°C freezer until further use.

2.2.5 Thymoquinone Treatment

ARPE-19 cells were treated with 0.1uM and 10uM of thymoquinone. DMSO was used was a vehicle to transport the thymoquinone into the cells. Thus, DMSO at final concentration of 0.1% was added into the control well. Cells were incubated with thymoquinone for 6 hours and later, they were lysed to get RNA and proteins for further analysis. Samples were stored at -80 and -20°C respectively.

2.3 Cathepsin L Activity Assay

Cathepsin L Activity Assay Kit was used in this experiments. The cathepsin L activity assay kit is a fluorescent-based assay that designed for quantitative measurement of cathepsin L activity in cells.

Samples were prepared using the manufacturer's protocol. Media was removed and cells were washed three times with PBS before harvesting. Cells were trypsinised, centrifuged and suspended in 200µl of lysis buffer from the kit. The suspension was incubated 10 minutes on ice followed by five minutes maximum speed centrifugation. The supernatant was collected into new sterile tube and the pellet was discarded. Protein content was measured and the samples are ready to be tested.

Appropriate amount of protein samples were added to a 96-well plate and respective amount of lysis buffer were added to get a total amount of 50µl. Then, 50µl of assay buffer was added to each well. For a positive control buffer, 45µl assay buffer and 5µl of reconstituted positive control provided with the kit were added. For a negative control, only assay buffer were used in total of 50µl. Finally, 1µl of DTT and 2µl of 10mM AC-FR-AFC substrates were added to each wells. Samples were then incubated at 37°C and the fluorescent was read using a fluorescent plate reader (Promega, Madison, USA) at 1hour and 2 hours post incubation with a 400nm excitation filter and 505nm emission filter. Relative percentage of cathepsin L activity was determined by comparing the relative fluorescence unit (RFU) with the level of the negative control samples.

2.4 Cell Viability Assay

MTT Assay was used to assess the viability of cells in this project. MTT is a calorimetric assay used to measure the metabolic activity of cells. Actively metabolising cells will convert the water soluble MTT reagent to an insoluble purple formazan. The formed formazan is then solubilised and its concentration is determined using spectrophotometer. The concentration of formazan determine the amount of active cells in the well.

Basically, 10ul of MTT reagent (MTT 3-(4,5-dimethylthiazol-2-yl)-2,5-diphenyltetrazolium bromide) was added to the medium of the cells. The cells were incubated with the reagent for four hours at 37˚C. The media was removed and the formazan formed was dissolved in DMSO by 10 minutes incubation at 37˚C. The plate was read in a spectrophotometer at 540nm absorbance.

2.5 mRNA Expression Analysis

2.5.1 Total RNA Isolation

The RNeasy Plus Mini Kit was used to isolate RNA from the cells. The basic principle of this RNeasy Plus Mini kit is the cells will be lysed in a highly denatured guanidine-isothiocyanate-containing buffer, Buffer RLT Plus. Firstly, cells were trypsinised and centrifuged to obtain the cell pellets. Later, 350µl of the Buffer RLT plus was added and mixed well through pipetting followed by 30 seconds of vortexing.

Homogenised lysate was then transferred into a gDNA eliminator spin column to eliminate genomic DNA. It was followed by 30 seconds centrifugation at speed of 10000rpm. The spin column was discarded and 350µl of 70% ethanol was added into the flow-through. Ethanol acts as binding agent for the RNA. The mixture (700µl) was then transferred into an RNeasy spin column and centrifuged at 10000rpm for

15seconds. In this step, total RNA binds to the membrane. This step was repeated until all the mixture has been processed. The flow-through was discarded.

The next step involved washing processes to remove possible traces of contaminants which has passed the membrane. 700µl of Buffer RW1 was added into the same spin column and centrifuged for 15 seconds at 10000rpm. Next, the spin column was washed twice with 500µl of Buffer RPE followed with centrifugation steps as a speed of 10000 for 15 seconds and 2 minutes respectively to remove ethanol traces from the membrane. The spin column was transferred into new collection tube and briefly centrifuge for another one minute to remove any possible carryover that may affect the downstream reactions.

Finally, the RNeasy spin column was transferred into a new collection tube and 50µl of RNase free water was added directly onto the column membrane. The tube was centrifuged again for one minute to elute the RNA. The extracted mRNA is now ready for cDNA synthesis.

2.5.2 Purity testing of the total RNA

Total RNA was measured using a NanoDrop™ Spectrophotometer 2000. The spectrophotometer probe was first clean with RNAse free water and the system is initialised. In this case, the setting was change to RNA and the RNase free water was set up as blank. Next, sample was added onto the probe and the RNA concentration was measured. The A260/A280 and A260/A230 ratios were recorded as well as the concentration of RNA stated. In interpreting the results, pure RNA will have an A260/280 ratio of 2.1. A260/280 ratio which is less than 1.8 indicates potential DNA or protein contamination. The A260/230 ratio for RNA should also be above 2.0. Lower A230/260 is due to contamination from the washing solutions, chaotropic salts, phenols or proteins.

2.5.3 cDNA synthesis

Total extracted RNA was used to synthesise cDNA using the manufacturer's protocol provided with the RevertAid First Strand cDNA synthesis kit and was performed in a thermo cycler (Applied Biosystem, USA). Briefly, the following reagents were added into a 1.5ml centrifuge tube in the indicated order (Table 2.1):

Table 2.1 cDNA synthesis components

Component	**Amount**	**Final concentration**
Template RNA	1ug	1µg
Oligo dT Primer	1uL	5µm
Nuclease Free Water	Maximum of 12uL	-
5x Reaction Buffer	4uL	1x
Ribolock RNase Inhibitor (20U/ul)	1uL	10U/µl
10mM dNTP Mix	2uL	1mM
RevertAid M-MuLV RT(200U/uL)	1uL	10U/µl
TOTAL VOLUME	**20uL**	

It is important to note that master mix must contain all components required for a successful cDNA synthesis. The mixture were mixed gently by flicking the tube and followed by a brief centrifuge to allow the liquid to be collected at the base of the tube.

The PCR was carried out at 42˚C for 1hour. Later, the reaction was terminated by heating at 70˚C for 5 minutes. The reverse transcription reaction product is directly used for qPCR and stored in -20˚C until further use in qPCR.

2.5.4 Real Time PCR (qPCR)

2.5.4.1 Primer Design

Primers pairs for the sequence of interest (Cathepsin L, NF-kB p65, Iκβα, β-actin and α-tubulin) were designed and synthesised based on human sequences obtained from Genebank. Primers were designed to be in between 18-22bp with melting temperature between 52˚C-64˚C and GC% content between 35%-65%. Primers chosen were also considered to avoid self-complementary. To obtain optimum PCR conditions, the primers were tested at different annealing temperatures. The primer pairs for the gene of interest and internal control were shown in Table 2.2. Selected primers were then blasted in the https://www.ncbi.nlm.nih.gov/tools/primers-blast/primertool.cgi to check primer specificity.

Table 2.2 List of primers used in qPCR analysis

Primer	Template	5' → 3' sequence	Length	Product length
Iκβα	Forward	GAAGTGATCCGCCAGGTGAA	20	186
	Reverse	CTCACAGGCAAGGTGTAGGG	20	
p65	Forward	CCAGACCAACAACAACCCCT	20	188
	Reverse	TCACTCGGCAGATCTTGAGC	20	
Cathepsin L	Forward	CTAATGACACCGGCTTTGTGG	21	200
	Reverse	TTCAAATCCGTAGCCAACCACC	22	
β- actin	Forward	CACCATTGGCAATGAGCGGTTC	22	135
	Reverse	AGGTCTTTGCGGATGTCCACGT	22	
β- tubulin	Forward	CTGGACCGCATCTCTGTGTACT	22	117
	Reverse	GCCAAAAGGACCTGAGCGAACA	22	

2.5.4.2 Optimisation of primer annealing temperature

The annealing temperature of each primer sets were optimised through gradient temperature PCR. Different annealing temperatures were set for each primer depending on its annealing temperature obtain from the NCBI primer design webpage (https://www.ncbi.nlm.nih.gov/tools/primer-blast/). PCR product was run through gel electrophoresis to validate a single product obtained. The best annealing temperature of each primer was chosen based on the single band in melting curve in qPCR analysis and the brightest single band from the gel electrophoresis.

2.5.4.3 Optimisation of cDNA amount in qPCR

Serial dilution of cDNA was performed to obtain different concentration of cDNA to be used in optimisation. The cDNA concentrations used were 100ng, 50ng, 25ng, 12.5ng, 6.25 ng (dilution factor of 2). qPCR reactions were set up and qPCR was run using optimised annealing temperature. Non template controls wells were included in the set up to look of contamination. There should not be any amplification occurs in the non-template control wells. The presence of amplification indicates contamination in reactions. The qPCR products were then run through agarose gel electrophoresis to check for primer specificity.

2.5.4.4 Real Time PCR

The real time PCR was carried out in ABI Step-One Plus Real Time PCR system (Applied Biosystem, UK) using the QuantiNova SYBR Green PCR Kit (Qiagen, Germany) according to manufacturer's protocol. The reactions for the real time PCR were prepared as listed in Table 2.3 below. The plate was run in a real time thermal cycle with conditions listed in Table 2.4. No template control was added to the PCR plate as a negative control. Water was added to the negative control well replacing cDNA samples. Any amplification in the negative control well suggests the presence of contamination. To further confirm the absence of amplification, samples can be run through 1% (w/v) agarose gel electrophoresis.

Table 2.3 Real-time PCR components

Component	Volume per reaction	Final concentration
2x QuantiNova SYBR Green PCR Master Mix	10µl	1x
QN ROX Reference Dye	2µl	1x
Primer Forward	Variable	0.25 µM
Primer Reverse	Variable	0.25 µM
RNase Free Water	Variable	-
cDNA template (added last)	Variable	12.5ng/reaction
Total reaction volume	20µl	-

Table 2.4 Real-time PCR cycler conditions

Step	Time	Temperature
Activation step	2 minutes	95˚C
Denaturation	5 seconds	95˚C
Annealing/ extension	10 seconds	60˚C
Number of cycles	40 cycles	

The qPCR samples were kept at -20˚C for further use in agarose gel electrophoresis to confirm primer specificity if necessary.

2.5.5 Gel Electrophoresis

Gel electrophoresis is a commonly method used in separation of DNA fragment based on its size. DNA is added to one end of the gel and electric current is applied to the gel (negative pole on the well side). The DNA fragment will then pushed through the gel pores, which acts as a molecular sieve. Since DNA is negatively charged, it will moved towards the positive end of the gel. Smaller DNA size travels quicker as it has less resistance compared to a bigger size of DNA.

In this project, agarose gel was prepared in concentration of 1-1.5% gels to compensate the DNA fragment size. Agarose powder were weighed and dissolved in a flask containing 100ml of 1x Tris Borate EDTA (TBE) electrophoresis buffer. The flask was swirled to help dissolving the gel. The solution was then heated in a microwave until gel powder completely dissolved. Later, it was allowed to cool down to approximately 55˚C, 10ul GelRed was added into the gel and mixed well through swirling. GelRed was added to aids in the visualization of the DNA bands. Gel casting trays was set up while waiting for the gel to cool down. Then, gel was poured into the casting tray. Comb was inserted and the gel was allowed to solidify at room temperature for 15-30 minutes.

Once the gel has solidify, it was transfer to electrophoresis chamber and covered with 1x TBE buffer. Comb was gently removed to avoid defect to the gel. Samples were loaded to the well with DNA ladder as a reference bands. The samples were diluted in 0.5x loading buffer before loading. Loading buffer aids in visualizing the movement of samples during electrophoresis and thus prevent over-run of the electrophoresis. Electrophoresis was performed at 90V for 30minutes to one hour depending on the size of the DNA fragment. The gel were then visualized under ultraviolet rays in a BioRad ChemiDOC^{TM} imager (BioRad, Hampstead, UK).

2.5.6 Analysing qPCR results

qPCR data was saved in the form of StepOne Software and excel files. Melt curve was observed to check for presence of primer dimer or other sources of contamination. PFAFFL quantification method was used to quantify the relative expression of the gene of interest and its value was normalised to the geometric mean of the housekeeping genes, beta actin and beta tubulin. The samples were run through qPCR in three technical replicates per run with at least three independent replicates of experiments. Non parametric T-Test or One Way Annova quantifications were used to test for significance data. P-value of <0.050 was considered as statistically significant.

2.6 Protein expression analysis

2.6.1 Preparation of whole cell lysate

Samples for western blot analysis were prepared in 100µl Laemmli lysis buffer for each well of 6-well plates. The cells were detached either using cell scrappers or trypsin digestion. Initially, cells were washed three times with PBS and 100µl of lysis buffer was added to the cells. The cells were scrapped out by using cell scrappers. For harvesting cells using trypsin digestion, after washing with PBS, 1x trypsin was added to each well for 2-3 minutes. Cells were centrifuged at 1000rpm for 1 minute. Supernatant was removed and the pellet was resuspended in 100µl lysis buffer. Lysate was passed through 21G needles for 10-15times to shear the cell membranes and make it less viscous. The lysate was then heated at 95°C for 5 minutes. Total proteins in the sample were quantified by Qubit® Protein Assay as described in 2.7.2 to enable equal loading. The lysate is now ready for downstream immunoblotting procedures and stored at -20˚C for short term storage.

2.6.2 Quantification of total protein in cell lysate

The total protein content of cell lysate and conditioned media samples was determined by the Qubit® Protein Assay Kit using the Qubit® Fluorometer 2.0 (Thermo Fisher Scientific, Waltham, USA). The protein assay reagent was prepared by diluting a stock of Qubit® solution 1:200 in the provided dilution buffer. For protein measurement, a final volume of 200µl was recommended by the manufacturer. The cell lysate was diluted 1:10 in sterile double distilled water before mixed with the protein assay reagent. The mixture was vortexed briefly and incubated at room temperature for 15 minutes. Calibration of the Qubit® Fluorometer 2.0 was performed routinely before it is used to read the samples protein content to ensure an accurate reading. The protein readings were then used to ensure equal loading of proteins in immunoblotting or other relevant experiments.

2.6.3 SDS Gel electrophoresis and Western Blot

Western blot or also known as immunoblotting were carried out to identify specific protein of interest in a whole lysate. The first phase in western blot is the SDS PAGE gel electrophoresis. Proteins were separated based on their molecular weight and transferred to a solid support such as nitrocellulose membrane or PVDF before probing with a specific antibody for protein detection. Western blot is a semi quantitative technique for proteins detection. Samples were resolved by SDS-polyacrylamide gel electrophoresis alongside with protein molecular weight marker. SDS PAGE gel were prepare according to Table 2.5. Resolving gel used for protein separation contained 10% acrylamide, unless stated.

Table 2.5 Components for making resolving gel.

Components	10% Gel	
	Volume	Final concentration
dH_2O	4.17 ml	-
Resolving gel buffer	2.5 ml	0.75M
30% Acrylamide	3.33 ml	10% (v/v)
10% SDS	0.1 ml	0.1% (v/v)
10% APS	0.1 ml	0.1% (v/v)
TEMED	0.01 ml	0.1% (v/v)

The mixture was added into gel plate till ¾ full and a layer of absolute ethanol was added on top to help removed any bubbles in the gel. The alcohol was poured off when the gel get solidify. Traces of alcohol left were washed off slowly with distilled water and the water was blotted dry with paper towel.

Stacking gel is used to improve protein separation contained 4% acrylamide. The mixtures for the stacking gels are listed in Table 2.6 below.

Table 2.6 Components for making stacking gel

Components	4% Gel	
	Volume	Final concentration
dH_2O	1.85 ml	-
Stacking gel buffer	2.5 ml	0.25M
30% Acrylamide	0.65 ml	4% (v/v)
10% SDS	0.05 ml	0.1% (v/v)
10% APS	0.05 ml	0.1% (v/v)
TEMED	0.01 ml	0.01% (v/v)

The stacking gel solution was poured on top of the plates and a comb was inserted without introducing any air bubbles. Once the gel solidified, the comb was removed and the gel was placed in Mini-PROTEAN 4 cells system (BioRAd, Hampstead, UK). The wells were cleaned with pipette tips to remove any excess gels.

Appropriate amount of cell lysates were added to the wells alongside with protein marker and gel electrophoresis were carried out at 90-110V in 1x running buffer for 1hour and 30 minutes. Then, the gel was removed from the glass plate cascade and soaked in transfer buffer for few minutes before placed in transfer sandwich. A nitrocellulose membrane (VWR, Leichestershire, UK) was soaked in the transfer buffer 10 minutes before used. The gel and nitrocellulose membrane were sandwiched together with three layers of filter paper (VWR, Leichestershire, UK) and a sponge pad on each side. The sandwiched set is illustrated in Figure 2.3. It is necessary to make sure no air bubbles trapped in between the sandwich to ensure a proper transfer of proteins.

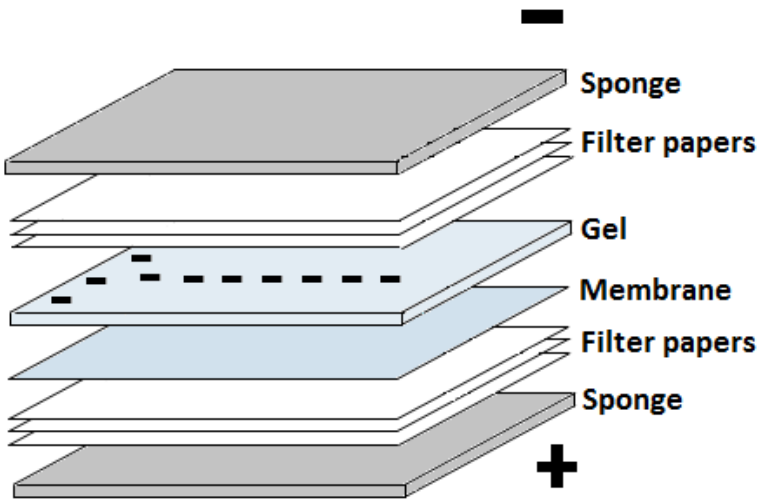

Figure 2.3 Transfer sandwich arrangements in Western blotting.

The transfer sandwich was then placed in transfer chamber and ran at 100V for 1hour and 30 minutes in transfer buffer. A block of ice was placed in the chamber to control the temperature during the transfer.

After the transfer process, the nitrocellulose membrane was stained with Ponceau S (Sigma Aldrich, Dorset, UK) solution to test the transfer efficiency. The stain was then removed by two time washes with 1x TBST. One hour incubation of the membrane with 5% blocking buffer at room temperature with gentle agitation was carried out to block unoccupied binding space and improve the sensitivity of this protocol. This also helped in reduces background interference without altering or obscuring the epitope binding sites.

Following to that, the membrane was incubated with primary antibody overnight at 4°C with gentle agitation. Primary antibodies used were listed in Table 2.7. Antibodies were prepared in either 5% milk blocking buffer or 5% BSA. The membrane was washed three times with 1x TBST to remove unbound antibody and was then incubated 1hour at room temperature with gentle agitation in an appropriate secondary antibody

diluted in 5% milk blocking buffer. Secondary antibodies used were listed in Table 2.8. Unbound antibody was washed once again three times with 1x TBST.

Protein detection was carried out using an enhanced chemiluminescent (ECL) substrate kit in BioRad ChemiDOC^{TM} imager (BioRad, Hampstead, UK). A mixture of ECL containing 1:1 ratio of reagent 1 and reagent 2 was applied to the membrane for 2-3 minutes. A clear plastic enclosed was used to put the membrane in to prevent membrane's drying while the imaging was carried out. Band intensity values was obtained using the BioRad Image Lab Program (BioRad, Hampstead, UK) and quantified. In this project, glyceraldehyde 3-phosphate dehydrogenase (GAPDH) was used as a normaliser during quantification and to determine equal loading.

Table 2.7 List of primary antibodies used

Antibody	Derived	Dilution	Diluent
Anti NF-kB P65 Ab16502 Abcam, Cambridge, UK	Rabbit polyclonal	1:500	5% (w/v) BSA in 1x TBST
Anti Phospho-NF-kB P65 (Ser536) 92H1	Rabbit monoclonal	1:500	5% (w/v) BSA in 1x TBST
Anti IKB-α Ab32518	Rabbit monoclonal	1:500	5% (w/v) BSA in 1x TBST
Anti GAPDH Ab8245	Mouse Monoclonal	1:30000	5% (w/v) Milk in 1x TBST
Anti Cathepsin L Ab103574	Mouse Monoclonal	1:500	5% (w/v) Milk in 1x TBST

Table 2.8 List of secondary antibody used

Antibody	Derived	Dilution
Anti Mouse IgG (whole molecule)-peroxidase antibody A9044 Sigma Aldrich, Dorset, UK	Rabbit	1:2000
Anti Rabbit IgG (whole-molecule)-peroxidase antibody A0545 Abcam, Cambridge, UK	Goat	1:1000

2.6.4 Western Blot Imaging and data analysis

Western blot imaging was carried out using ChemiDoc™ XRS+ System with Image Lab™ Software. The images were captured and save in the Image Lab format. These raw images were used for further quantification using the Image Lab software which was freely supplied with the equipment. Formula used to calculate proteins data are as follow:

a) Normalised protein expression:

$$\frac{Average\ value\ of\ protein\ of\ interest}{Average\ value\ of\ GAPDH}$$

b) Ratio of pP65/Iκβα and P65/Iκβα:

$$\frac{Normalised\ protein\ expression\ of\ pP65\ or\ P65}{Normalised\ protein\ expression\ of\ P65\ or\ I\kappa\beta\alpha}$$

c) Fold increase or decreased in Western blot data was determined by the amount of decrease or increase of samples compared to control. It was calculated by:

$$\frac{(Value\ of\ protein\ in\ treated\ cells - Value\ of\ protein\ in\ control)}{Value\ of\ protein\ in\ control}$$

d) Percentage increase/ decrease:

$$Value\ from\ (c)\ \times 100$$

2.7 Statistical analysis

Data analysis was performed using commercial software Microsoft Excel (Version 2010, Microsoft UK Ltd, Reading, UK) and GraphPad Prism (Version 6.1, GraphPad Software, Inc., USA). Non-parametric T-test and non-parametric One-way ANNOVA was performed. A p value <0.050 is considered to be statistically significant.

CHAPTER 3: RESULTS

3.1 Effect of AGEs on NF-κβ signalling key effectors in RPE cells

3.1.1 Cell density and morphological changes of control cells vs. AGEs treated RPE cells

Extracellular matrix (ECM) was used in this experiment to mimic the Bruch's membrane that relies on the posterior part of the retina. The ECM was chemically treated using 0.1M glycoldehyde to induce ageing conditions. Control cells were treated in PBS instead of glycoaldehyde to mimic young Bruch's membrane. ARPE-19 cells were seeded onto this membrane to model the actual closed relationship between Bruch's membrane and RPE in the eye. It was allowed to grow for 14-days. The two-week's time point was chosen in this experiment to allow the cells to become a confluent monolayer, thus being comparable to one another, as the AGEs-exposed cells has a slower growth rate.

At day 0, ARPE-19 cells were seeded at the same density on both control and treated ECM. Cells seeded on control ECM (Control) had a higher rate of population as compared to treated ECM (AGEs-treated cells). The comparison of the growth rate of the two groups are shown in Figure 3.1. By day 7, control cells started to becomes 90% confluent whereby AGES-treated cells were only at 60% confluency. However by day 14, both groups are already confluent and became tightly packed although in a closer look, control cells appeared more packed than the AGEs-treated cells. In addition, the morphology between the two cells also appeared to be slightly different as the control groups had a typical ARPE-19 characteristic with a cobblestones monolayer, while the AGEs-treated cells had lesser cobblestones appearance. This observation in AGEs-treated cells matches the behaviour of ageing cells in normal retina; where the RPE cells can expand to fill the gap left by the dead RPE cells and have larger size.

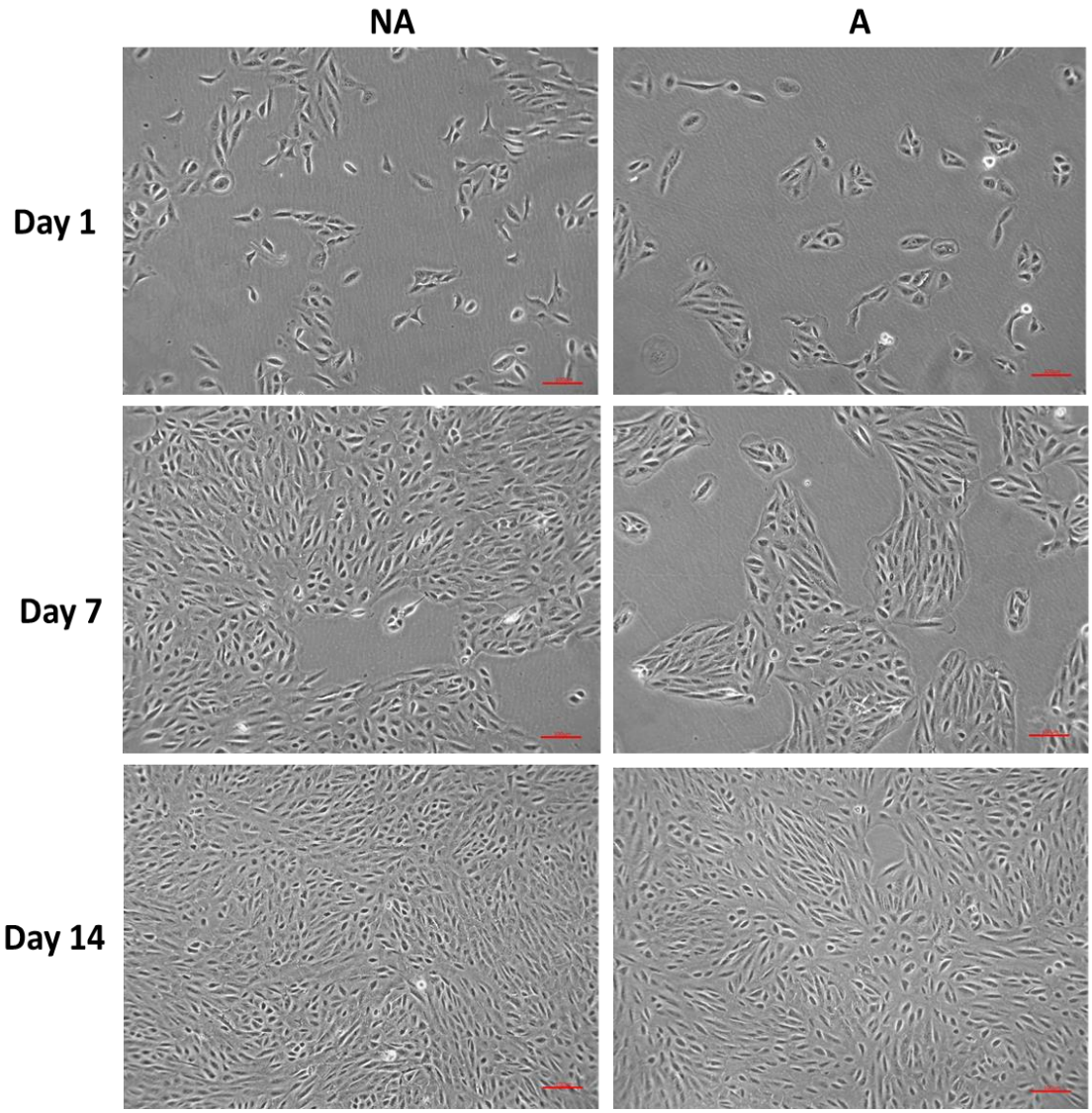

Figure 3.1 Morphology of RPE cells in non-AGEs (NA) and AGEs (A) condition from Day 1 (24 hours post seeding) to Day 14 (day of harvesting). Scale bar = 100µm.

3.1.2 Effect of AGEs exposure on mRNA expression level of NF-kB key effectors

To study the effect of AGEs, ARPE-19 cells were prepared as described in section 2.2.2. The mRNA is then harvested and samples were analysed through qPCR using primers listed in Table 3.1. First, the primers were tested for its efficiency using a random sample. Efficiency between ranges between 90-110% was considered optimum. The primers efficiency is listed in Figure 3.1 below. β-actin and β-tubulin were used as housekeeping genes. To confirm the specificity of the primers, the melt curve peak in the qPCR analysis was observed, and the samples were performed using an electrophoresis gel. The formation of a single band confirmed the specificity of the primer. PFAFFL quantification method was used to quantify the relative expression of the gene of interest and its value was normalised to the geometric mean of the housekeeping genes. The samples were run through qPCR in three technical replicates per run with at least three independent replicates of experiments.

Table 3.1 Efficiency of primers used in qPCR analysis

Primer	**Efficiency (%)**
P65	107
Iκβα	104
β-actin	94
β-tubulin	110

Following optimisation of primers, RPE cells exposed to AGEs were analysed for P65, Iκβα and phosphorylated P65 proteins and mRNA expressions. As described in the methodology sections the RPE cells were plated on AGEs-treated matrix for 14 days before cells were harvested for protein and gene analysis. The mRNA expression results are illustrated in Figure 3.2 and Figure 3.3.

Exposure to AGES did not show any significant changes to P65 and Iκβα mRNA expression, although the levels showed a decrease level compared to control with p=0.100 and 0.200, respectively.

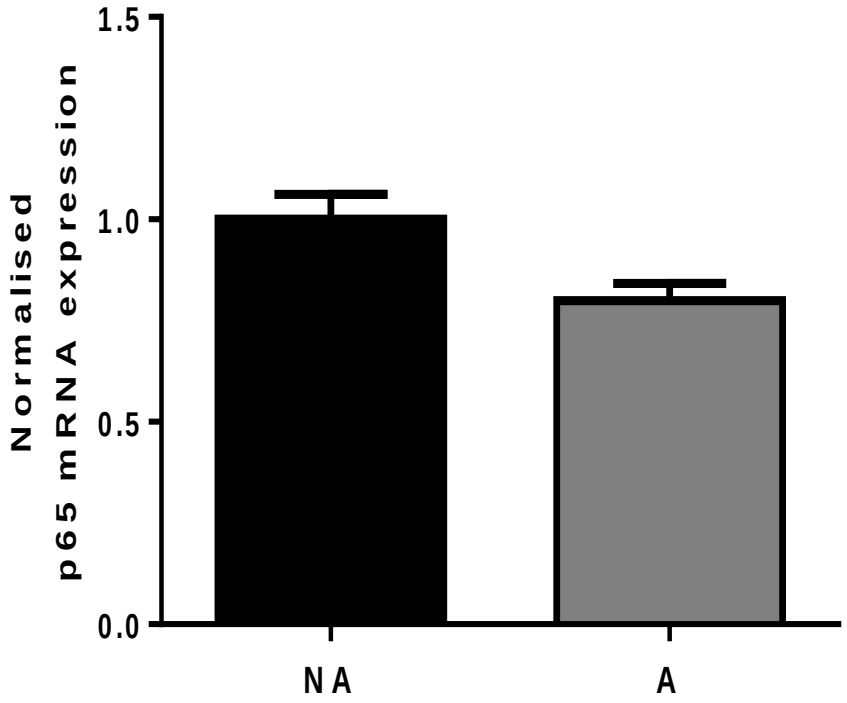

Figure 3.2 The mRNA expression of P65 in RPE cells exposed to AGEs (A) compared to control cells (NA). P65 mRNA expression was normalised to β-actin and β-tubulin. Data are shown as mean with error bar indicating ± SEM where n=9 (T- test, p=0.100).

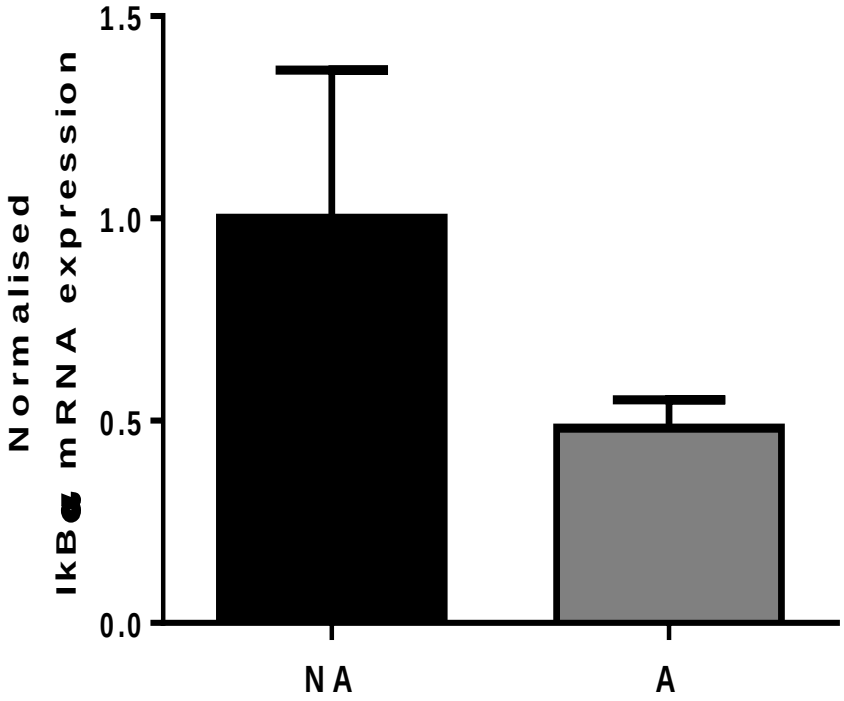

Figure 3.3 The mRNA expression of Iκβα in RPE cells exposed to AGEs (A) compared to control cells (NA). Iκβα mRNA expression was normalised to β-actin and β-tubulin. Data are shown as mean where error bar indicating ± SEM where n=9 (T-test, *p*=0.200).

3.1.3 Alteration of the NF-kB key effectors proteins by AGEs in RPE cells

From the mRNA analysis, the total p65 and Iκβα showed decreasing trends although these values were not statistically significant. Therefore, to further study the effect of AGEs on the NF-κβ signalling, the possible changes were quantified at protein levels using P65, Iκβα and pP65 antibodies. GAPDH was used as an internal loading control and normaliser.

Five independent replicates (n=5) were carried out in this experiment with the initial two replicates being carried out with help by a fellow postgraduate student in the group, Mr Umar Shariff. The collated data and consistency of each independent experiments were closely monitored. The representative blots are displayed in Figure 3.4. A band for total protein P65 and pP65 was observed at 70kDa and a band at approximately 37kDa was detected for Iκβα and GAPDH.

AGEs was shown to significantly decrease the level of both P65 and Iκβα proteins when compared to control cells (Figure 3.5 and Figure 3.6). There was a 25% decrease in P65 (p=0.009) level and 30% decrease in Iκβα (p=0.029) levels in RPE cells exposed to AGEs, compared to control. In addition, a significant decrease was also observed in the level of phosphorylated P65 (pP65) in AGEs-exposed RPE cells as compared to control cells (Figure 3.7). About 58% reduction was seen from this data with p=0.035.

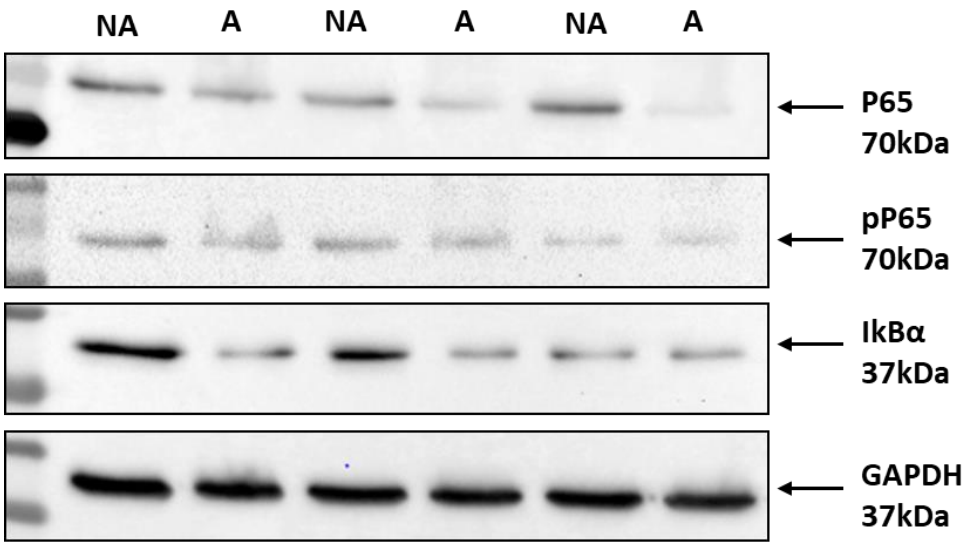

Figure 3.4 Representative western blot image of control vs AGEs-exposed cell lysates from one independent replicates with three technical replicates. The membrane was probe with Anti-P65 (1:500 dilution), Anti Iκβα (1:500 dilution) and phosphorylated p65 (pP65) (1:500 dilution). GAPDH (1:30,000 dilution) was used as a loading control.

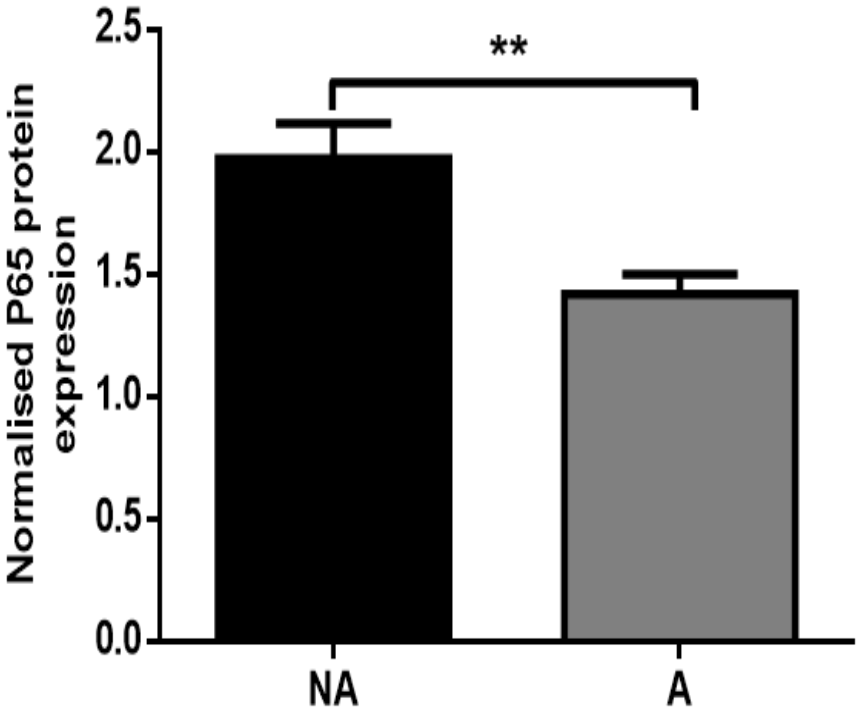

Figure 3.5 Normalised P65 protein expression in ARPE-19 cells exposed to AGEs (A) as compared to control (NA). Graph represents mean value of P65 protein expression normalised to GAPDH with error bars indicating ±S.E.M with n=5 (T-test, **p=0.009).

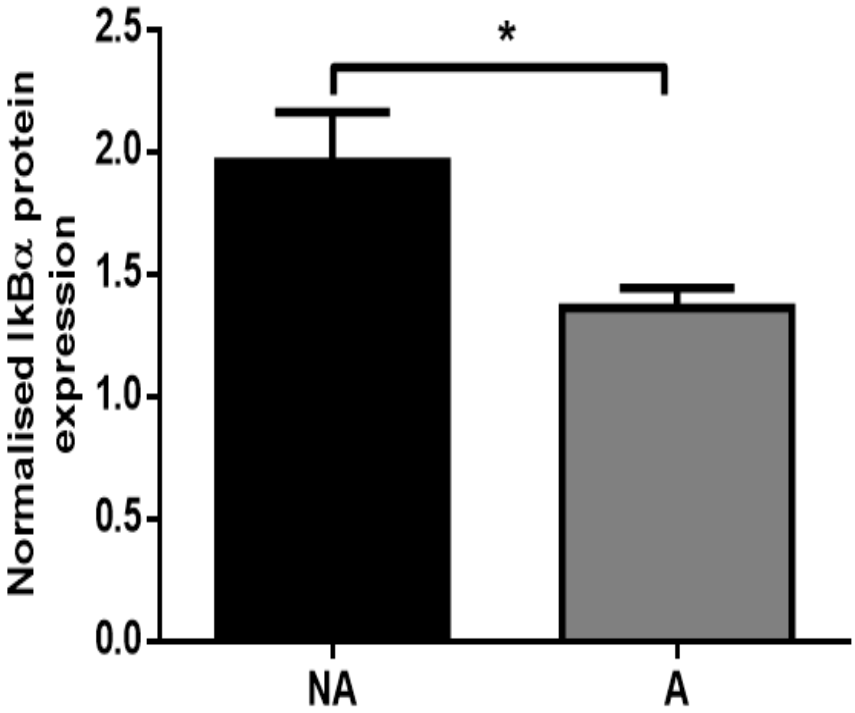

Figure 3.6 Normalised Iκβα protein expression in ARPE-19 cells exposed to AGEs (A) as compared to control (NA). Graph represents mean value of Iκβα protein expression normalised to GAPDH as loading control with error bars indicating ±S.E.M with n=5 (T-test, *p=0.029).

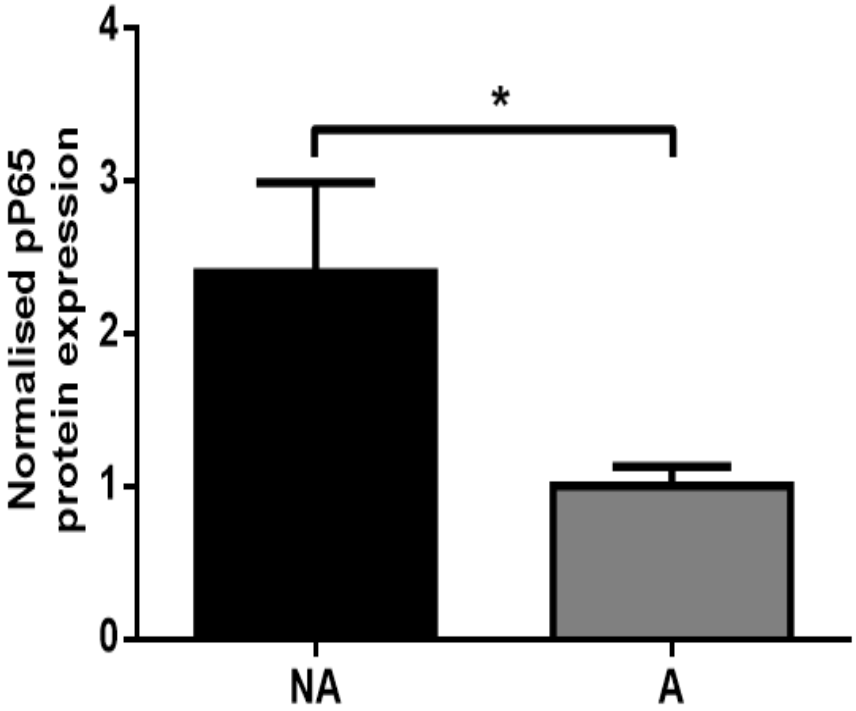

Figure 3.7 Normalised phosphorylated P65 (pP65) protein expression in ARPE-19 cells exposed to AGEs (A) as compared to control (NA). Graph represents mean value of pP65 protein expression normalised to GAPDH as loading control with error bars indicating ±S.E.M with n=5 (T-test, *p=0.035).

3.1.4 Ratio of NF-κβ activation in AGEs-treated cells vs control

To determine the effects of ageing on NF-κβ activation, the ratio of pP65/ p65 was calculated. However, the ratio was not statistically significant although the graph showed a decreasing trend (34% reduction) with p=0.310 (Figure 3.8). The ratio of P65/Iκβα was also calculated to see possibilities of negative feedback loops, as it is known that NF-κβ signalling can transcript genes for its own. The data observed showed no difference on the P65/Iκβα expression, p=0.618 (Figure 3.9), this can be possibly explained by the absence of negative feedback loop in NF-κβ signalling in AGEs-exposed RPE cells.

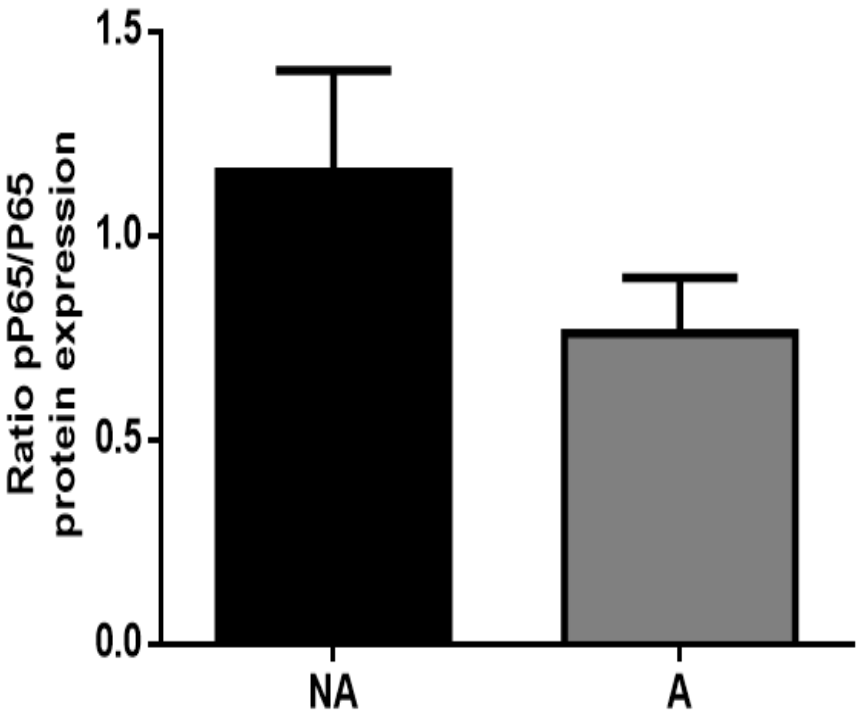

Figure 3.8 Ratio of pP65/P65 protein expression in control (NA) and AGEs-exposed (A) RPE cells. Graph represents mean with error bars indicating ± SEM with n=5 (T-test, p=0.310).

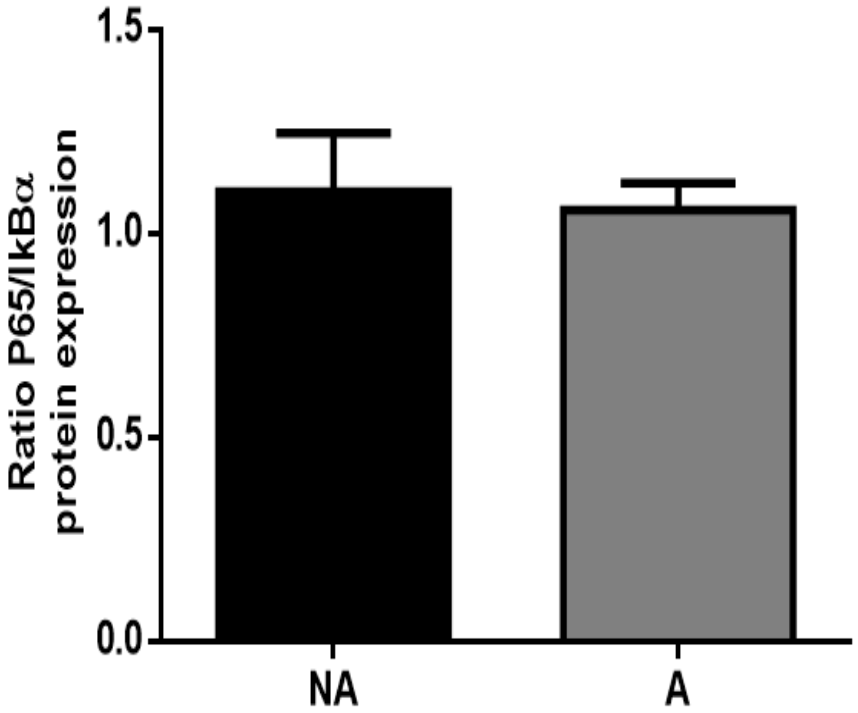

Figure 3.9 Ratio of P65/ Iκβα protein expression in control (NA) and AGEs-exposed (A) RPE cells. Graph represents mean with error bars indicating ± SEM with n=5 (T-test, *p*=0.618).

3.2 Effect of lysosomal cathepsin L inhibition on NF-κβ signalling in RPE cells

3.2.1 Optimisation of cathepsin L Inhibitor

Cathepsin L in ARPE-19 cells was inhibited through the use of cathepsin L inhibitor III. ARPE-19 cells were allowed to grow to desired confluency in culture and increasing concentrations of cathepsin L inhibitor (10μM, 25μM and 40μM) were later added at different time points (1hour, 2 hour, 4 hour and 8 hour). Activity of cathepsin L in the RPE was assessed by measuring the cathepsin L activity in the cells. Cells were harvested and prepared as mentioned in section 2.4. The relative percentage of cathepsin L activity was calculated. Significant decrease in cathepsin L activity was observed up to 8 hours post-treatment at inhibitor concentrations of 25μM and 40μM. However, the 40 μM concentration appeared to have a persistence decreased in cathepsin L activity in all time points tested. Hence, the 40μM concentration of cathepsin L inhibitor at 8 hours incubation time point was therefore used in subsequent experiments to ensure effective and sustained cathepsin L inhibition (Figure 3.10).

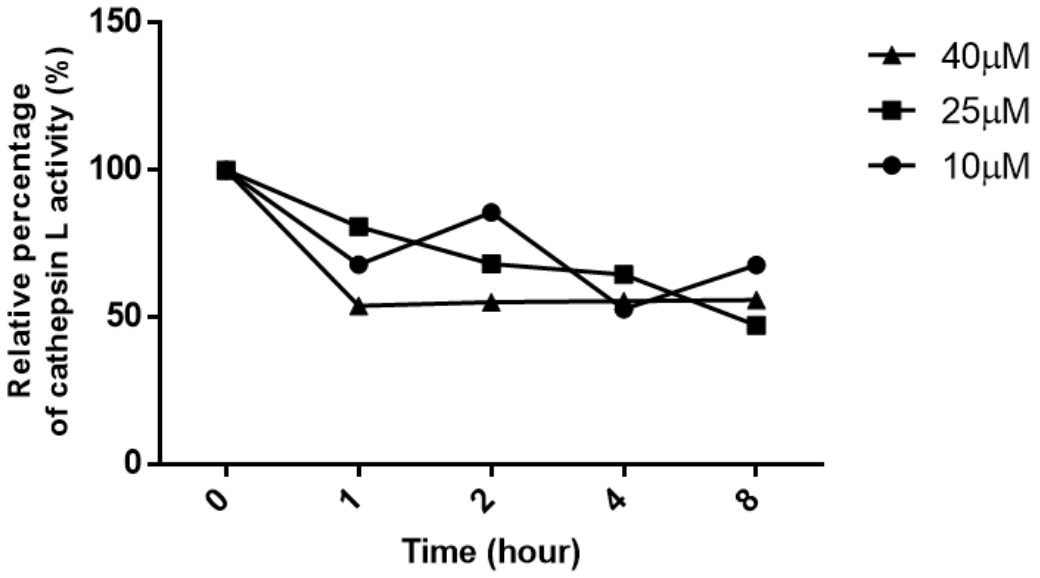

Figure 3.10 Evaluation of cathepsin L inhibitor III concentration and exposure time for effective enzymatic activity inhibition in ARPE-19 cells. Graph represent the average relative percentage of cathepsin L activity with error bar indicating ± SEM using two-way repeated measures ANOVA, where n=2.

3.2.2 Effect of Cathepsin L Inhibition on mRNA expression of NF-kB key effector

To study the effect of cathepsin L on the NF-κβ signalling, ARPE-19 cells were cultured and upon reaching confluency, 40μM of cathepsin L inhibitor III was added to the media for 8 hours. RNA was isolated and analysed through qPCR analysis. No alteration of mRNA expression was observed in both P65 and Iκβα, after the inhibition of cathepsin L in ARPE-19 cells (Figure 3.11 and Figure 3.12). Although the data showed a decreasing trend with 20% decrease in P65 level and 40% decrease in Iκβα level, the numbers were not statistically significant with a *p*-value of 0.944 and 0.200 respectively.

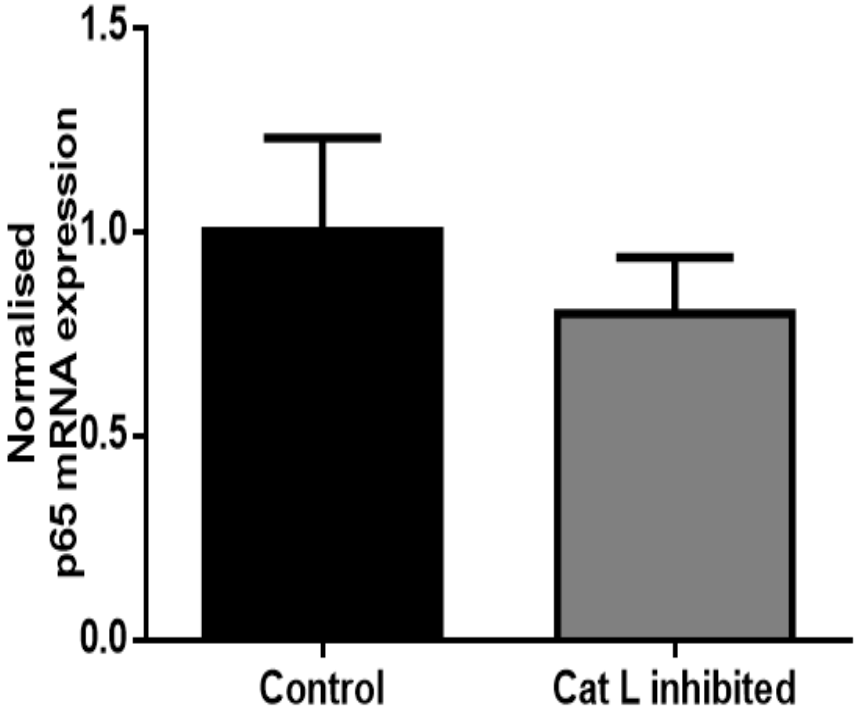

Figure 3.11 mRNA expression level of P65 in control and cathepsin L inhibited (CatL Inhibited). Graph represents the average mRNA expression of P65 normalised to to β-actin and β-tubulin with error bars indicating ± SEM, where n=5 (T-test, *p*=0.944).

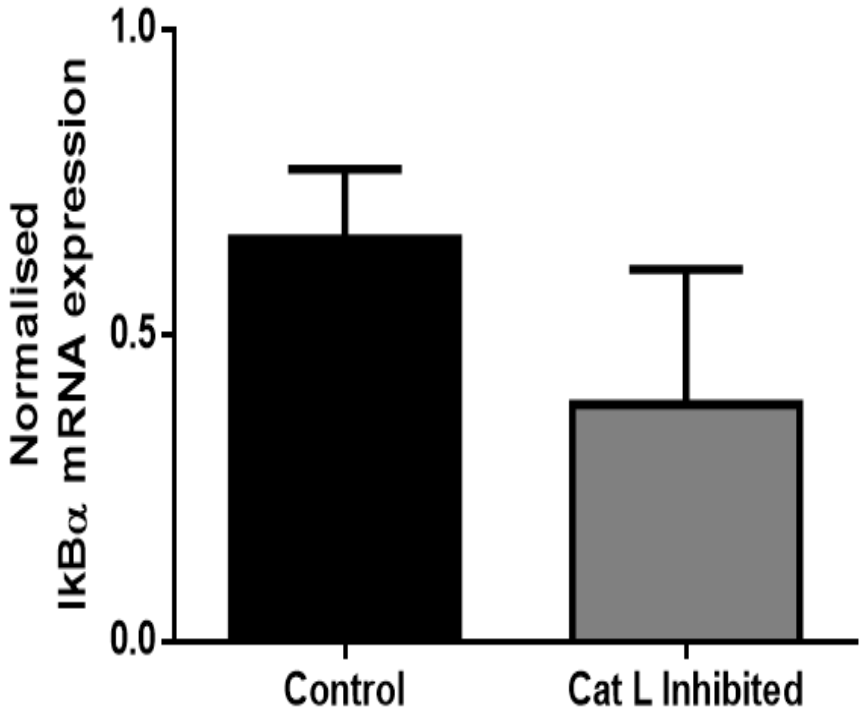

Figure 3.12 mRNA expression level of Iκβα in control and cathepsin L inhibited ARPE-19 cells (CatL Inhibited). Graph represents the average mRNA expression of Iκβα normalised to to β-actin and β-tubulin with error bars indicating ± SEM, where n=5 (T-test, *p*=0.200).

3.2.3 Effect of cathepsin L inhibition on NF-κβ key effector proteins

The effect of cathepsin L inhibition on the NF-κβ key effector protein was further evaluated using Western Blotting. Figure 3.13 shows a representative blot of P65, Iκβα and pP65 in cathepsin L inhibited and control ARPE-19 cells. A significant reduction (approximately 40%) in total P65 protein level was observed in cathepsin L-inhibited cells compared to control with a *p*-value of 0.018 (Figure 3.14). In contrast, cathepsin L inhibition did not cause any significant effects on the level of Iκβα proteins (p=0.131) (Figure 3.15), although a reduction of approximately 30% in cathepsin L inhibited cells was observed, as opposed to control. Additionally, there was no significant changes in the level of pP65 protein (p=0.952), as seen in Figure 3.16.

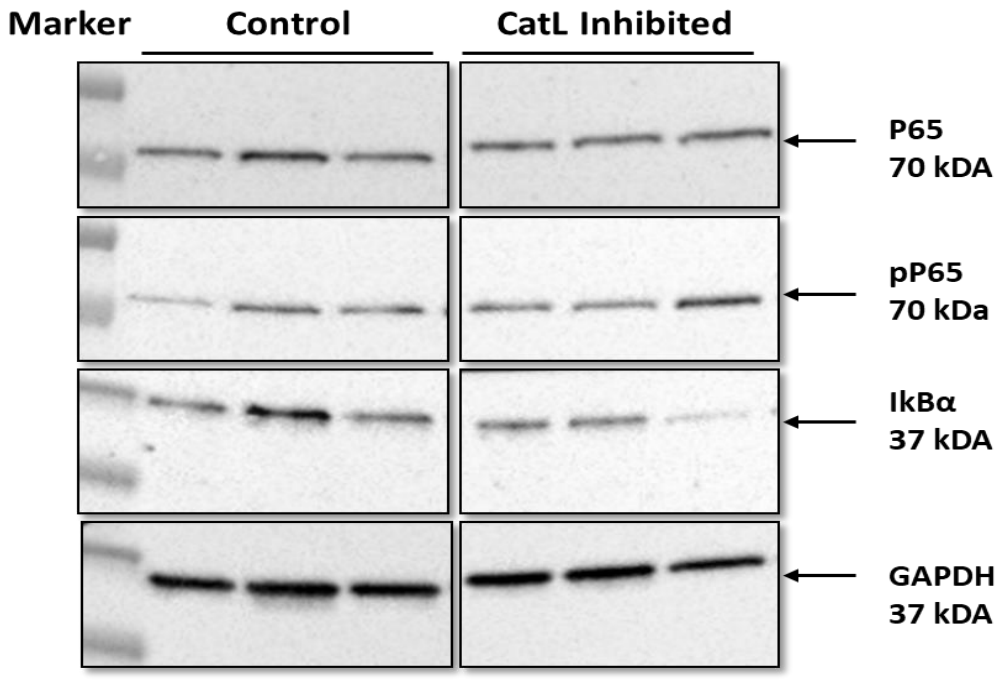

Figure 3.13 Representative western blot image of control vs. cathepsin L inhibited lysates from one independent replicates with three technical replicates on it. The membrane was probe with Anti-P65 (1:500 dilution), Anti Iκβα (1:500 dilution) and phosphorylated p65 (pP65) (1:500 dilution). GAPDH (1:30,000 dilution) was used as a loading control.

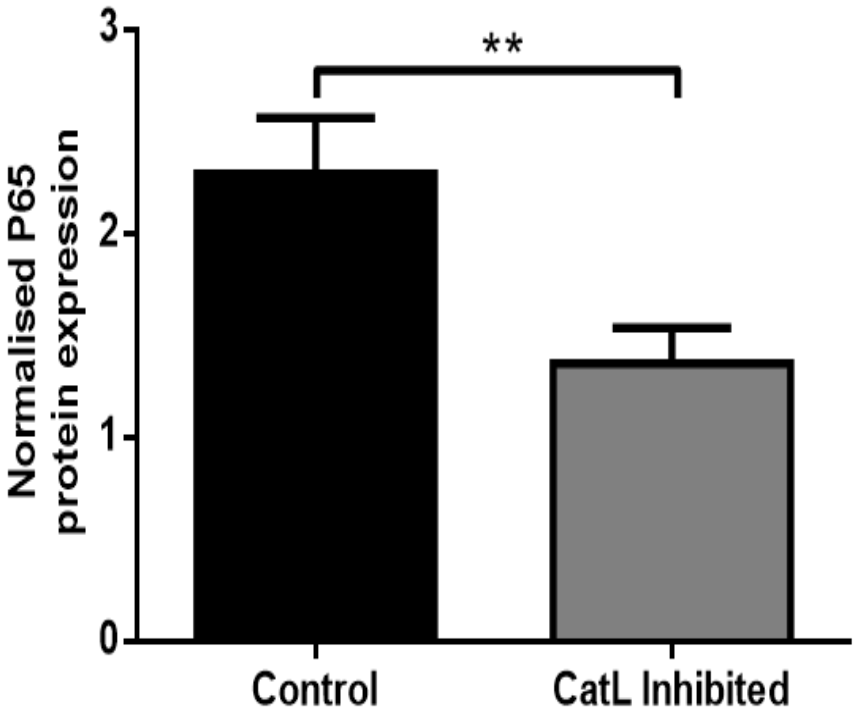

Figure 3.14 P65 protein expression in control and cathepsin L inhibited (CatL Inhibited) ARPE-19 cells. Graph represents average value of P65 protein expression normalised to GAPDH as loading control with error bars indicating ±S.E.M where n=4 (T-test, **p=0.006).

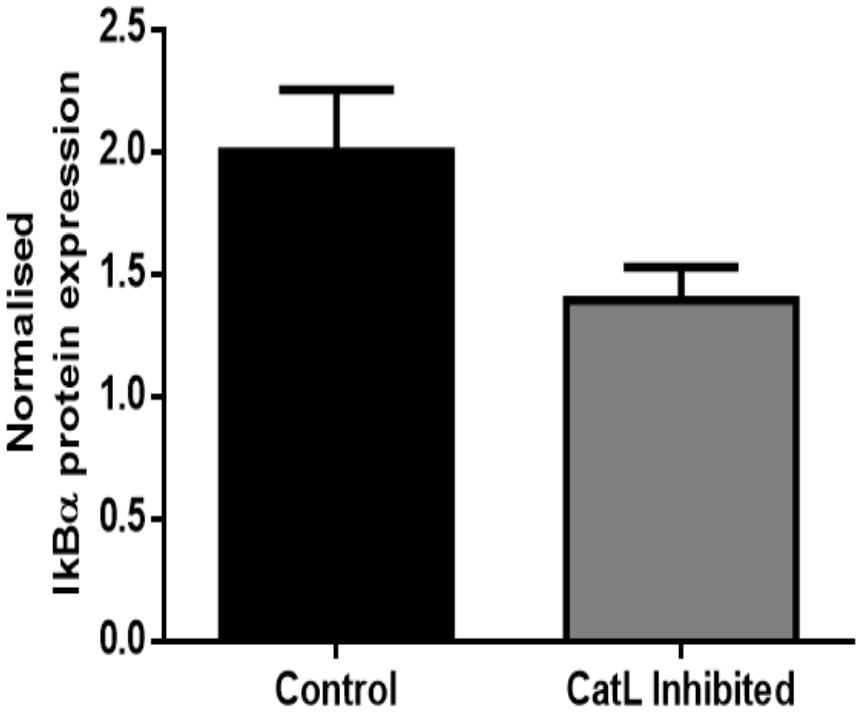

Figure 3.15 Iκβα protein expression in control and cathepsin L inhibited (CatL Inhibited) ARPE-19 cells. Graph represents average value of Iκβα protein expression normalised to GAPDH as loading control where error bars indicating ±S.E.M with n=4 (T-test, *p*=0.131).

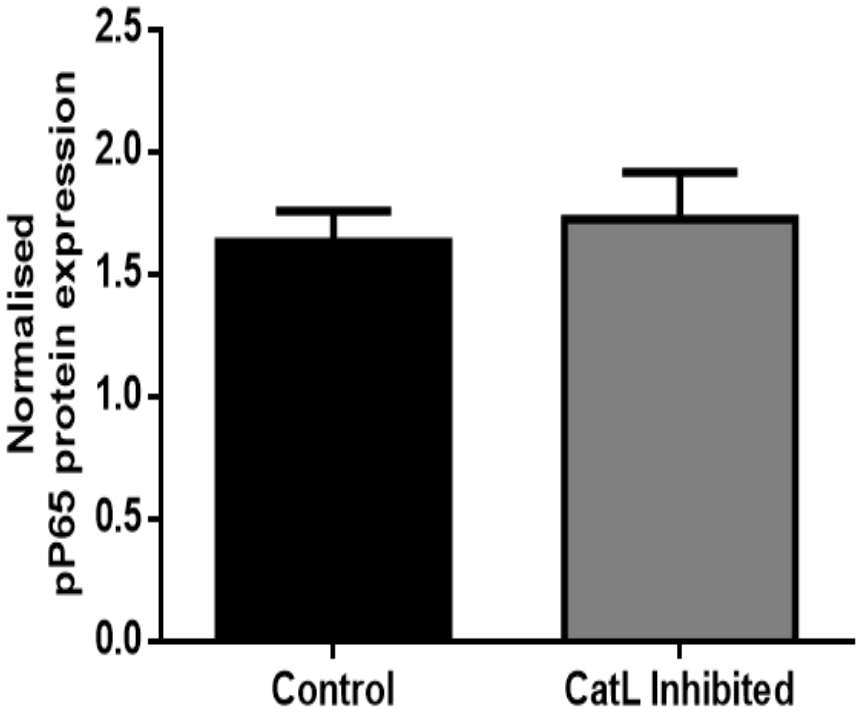

Figure 3.16 pP65 protein expression in control and cathepsin L inhibited (CatL Inhibited) ARPE-19 cells. Graph represents average value of P65 protein expression normalised to GAPDH as loading control with error bars indicating ±S.E.M where n=4 (T-test *p*=0.952).

3.2.4 Overall changes of NF-kB activation in cathepsin L inhibited cells

Changes on NF-κβ activation was further evaluated with the ratio of pP65/P65. No changes were observed in the ratio of P65/Iκβα level (p=0.501) (Figure 3.17). On the contratry, cathepsin L caused a significant increase in the ratio of pP65/P65 in cathepsin L inhibited cells, compared to control with p=0.016 (Figure 3.18). The increase was approximately 80% compared to control cells. The overall increase in this NF-κβ signalling in cathepsin L inhibited cells is due to the shifting profiles of the inactive P65 to its active forms. The increase in the level of activated NF-κβ signalling also suggest a possible favourable effect of cathepsin L in ARPE-19 cells.

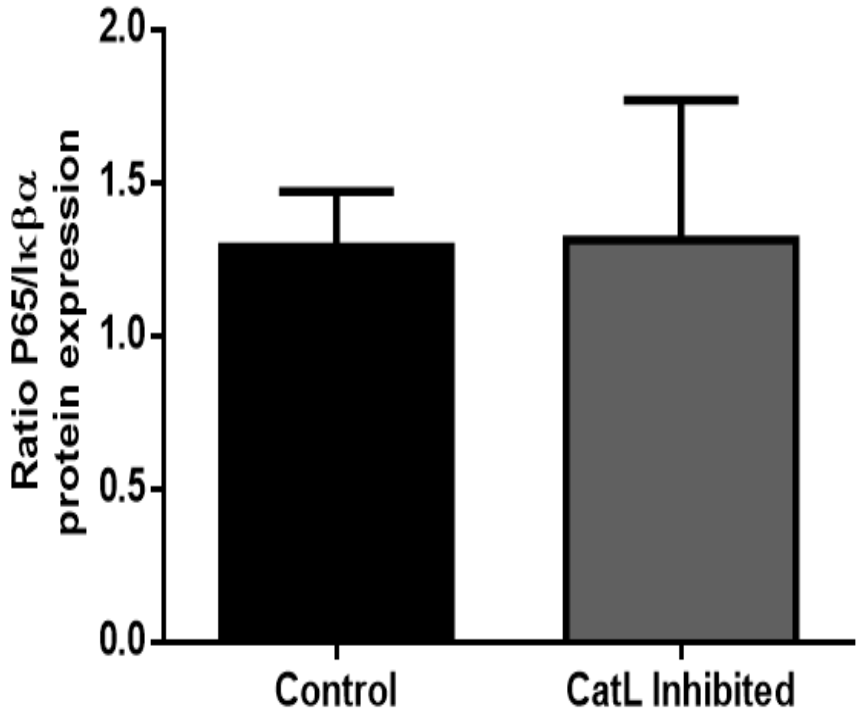

Figure 3.17 Ratio of P65/Iκβα protein expression in control and cathepsin L Inhibited (CatL Inhibited) ARPE-19 cells. Graph represents mean with error bars indicating ± SEM where n=4 (T-test, p=0.501).

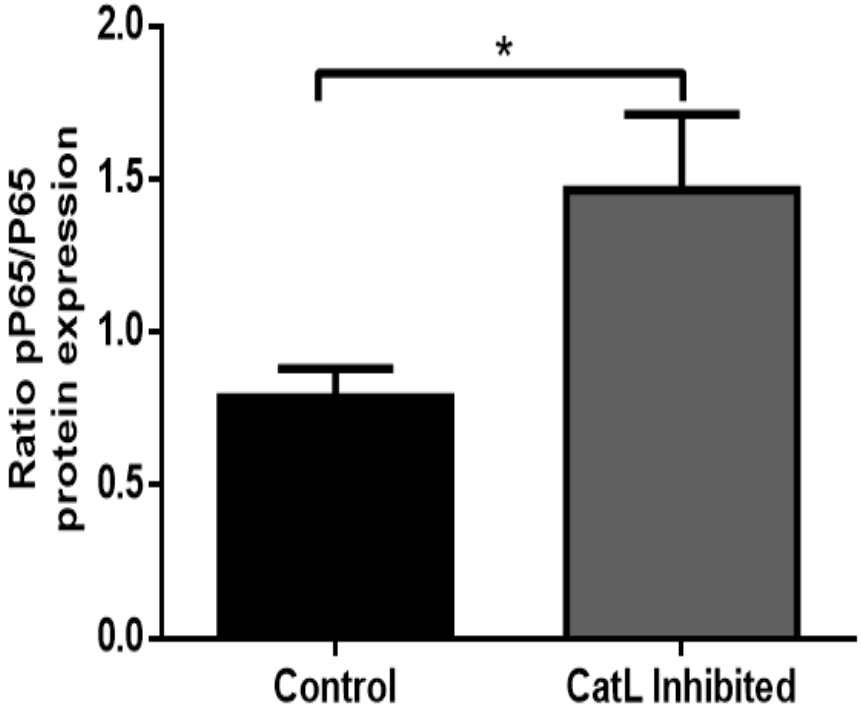

Figure 3.18 Ratio of pP65/P65 protein expression in control and cathepsin L Inhibited (CatL Inhibited) ARPE-19 cells. Graph represents mean with error bars indicating ± SEM with n=4 (T-test, *p*=0.016).

3.3 Effect of TNFα on NF-κβ signalling in cathepsin L inhibited and AGEs-exposed RPE cells

3.3.1 Effect of TNFα on normal RPE cells

TNFα is an oxidative stressor known to activate NF-κβ signalling in cells. The effect of TNFα on RPE cell viability was first assessed using MTT Assay methods. The data is presented in Figure 3.19. Two hours of incubation with 10ng/ml of TNFα did not affect the cell viability of RPE cells (p=0.219).

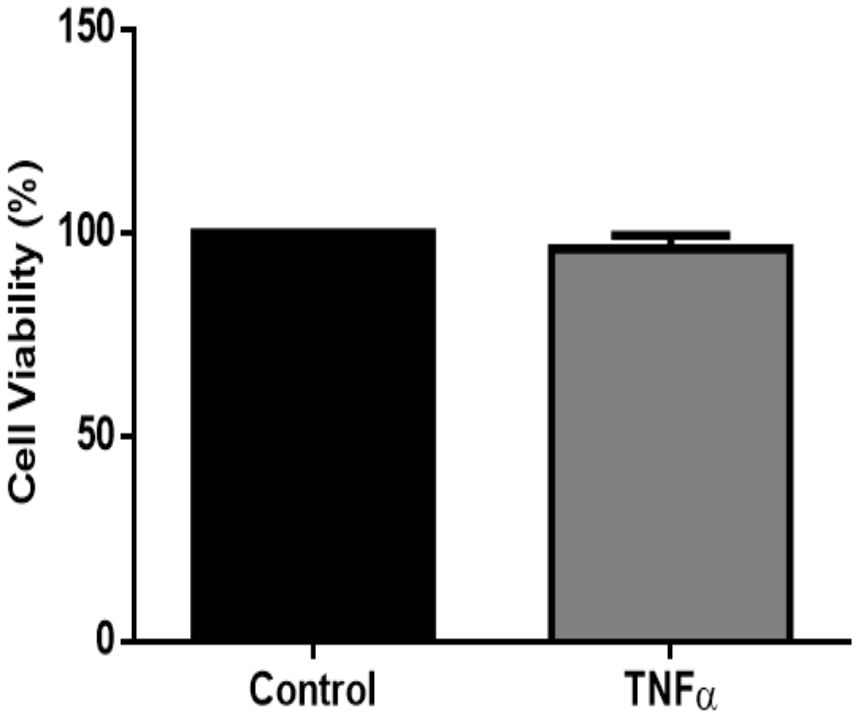

Figure 3.19 The effect of 10ng/ml TNFα on the cells viability of RPE cells. Data displayed as average percentage of cell viability with error bars indicating ± SEM where n=6 (Wilcoxon test, p=0.219).

Next, the effects of TNFα on NF-κβ key effectors without affecting cell viability were tested in normal ARPE-19 cells. ARPE-19 cells were grown till confluent and 10ng/ml TNFα was added to the media for 2 hours. RNA and proteins were isolated and analysis was performed through qPCR and Western blotting. The results are portrayed in Figure 3.20 and Figure 3.22 below. The representative blot is shown in Figure 3.21. The qPCR data showed no change in total P65 (p=0.151) but a significant increase in Iκβα (p=0.016) at mRNA levels. However, western blotting results showed TNFα increased the level of P65 (p<0.0001) and phosphorylated p65 (p=0.003) in RPE cells. This suggests an increase in NF-κβ signalling in RPE cells due to TNFα stimulation. Furthermore, the level of Iκβα protein was also significantly increased in cells with TNFα exposure (p<0.0001) in line with its increase at mRNA level.

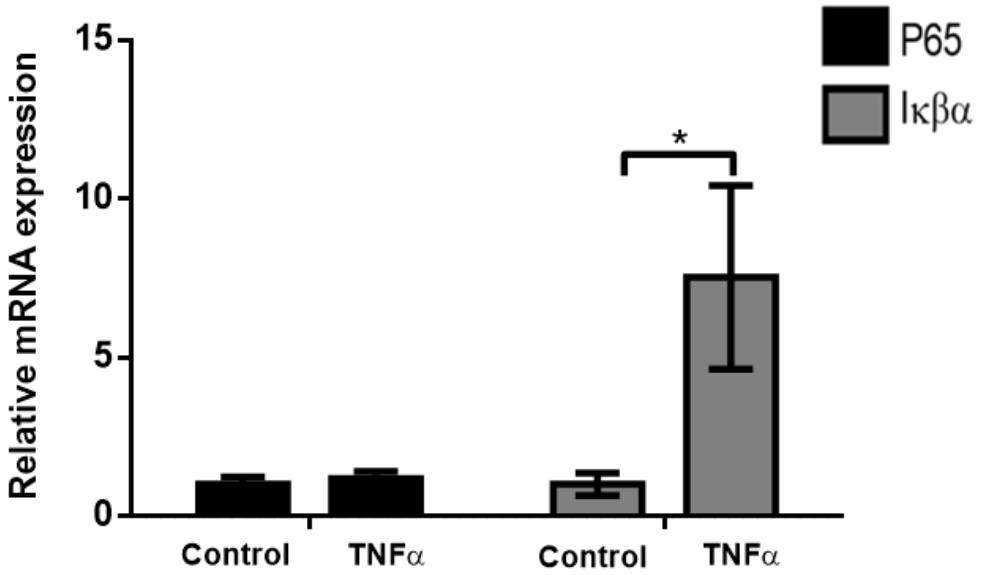

Figure 3.20 **mRNA expression of P65 and Iκβα in ARPE-19 cells after 2hours incubation with 10ng/ml TNFα stimulation. The values presented as means with error bars indicating ± SEM where n=5 (T-test, *p=0.016).**

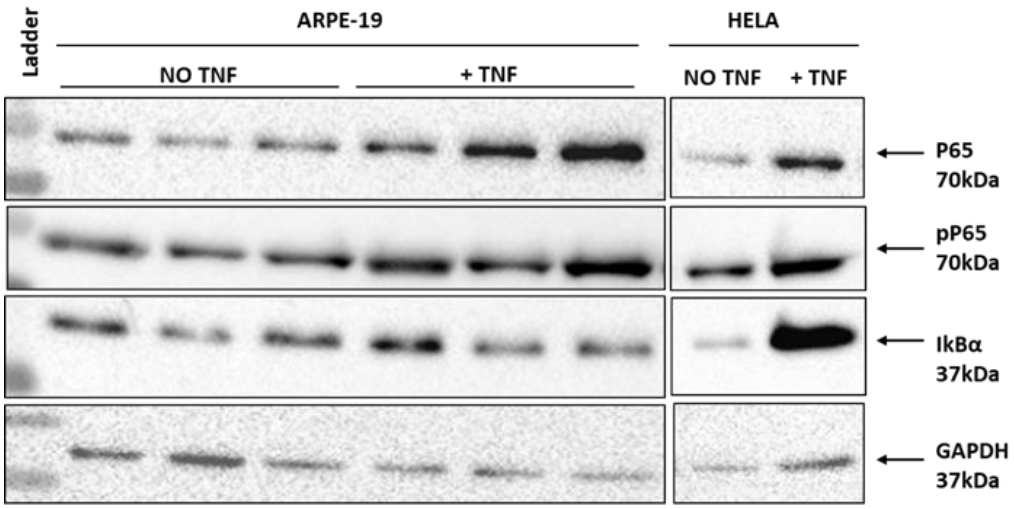

Figure 3.21 Representative blot image of ARPE-19 cells with and without TNFα treatment. The membrane was probed with Anti-P65 (1:500 dilution), Anti Iκβα (1:500 dilution) and phosphorylated p65 (pP65) (1:500 dilution). GAPDH (1:30,000 dilution) was used as a loading control.

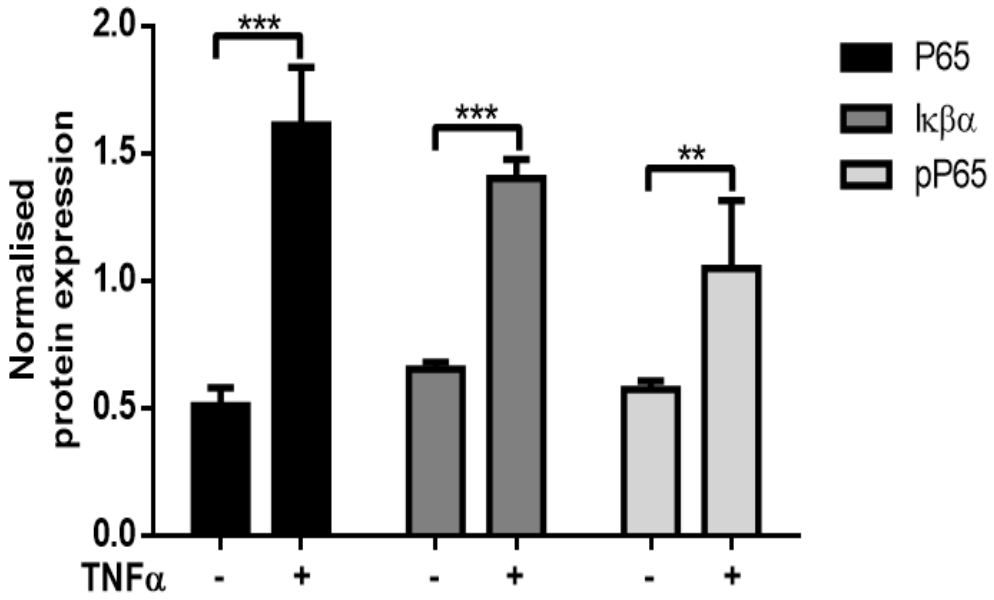

Figure 3.22 Protein expression of P65, Iκβα and pP65 in ARPE-19 after 2hours incubation with 10ng/ml TNFα stimulation. The values presented as means with error bars indicating ± SEM where n=4. (T-test, *****p*<0.005, ******p*<0.0001).

3.3.2 Effect of TNFα on NF-κβ signalling key effector's in cathepsin L inhibited cells

3.3.2.1 Effect of TNFα on NF-κβ signalling key effector's mRNA expression in cathepsin L inhibited cells

Next, with the knowledge that cathepsin L may have a possible protective effect on the RPE cells, we sought to observe if the effect of cathepsin L inhibition on the NF-κβ signalling is altered in the presence of TNFα treatment. Cells were treated with Cathepsin L Inhibitor for 8 hours and TNFα was added 2 hours before harvesting. RNA was harvested for qPCR analysis. qPCR results of five independent experiments is displayed in Figure 3.23 and Figure 3. 24.

Analysis on the P65 mRNA expression showed no changes (p=0.151) in control cells with TNFα exposure. However, a 55% increase in P65 mRNA expression was observed in cathepsin L inhibited cells after TNFα exposure, with a p value of 0.028. A significant increase in Iκβα mRNA expression was noted in both control cells (p=0.016) and cathepsin L inhibited (p=0.008) cells after TNFα treatment. A 95% increase in Iκβα mRNA expression was observed in cathepsin L inhibited cells after TNFα exposure. Comparison between cells without cathepsin L inhibition and with cathepsin L inhibition using Kruskal-Wallis test also showed significant changes in both P65 and Iκβα with p-value of 0.090 and 0.025.

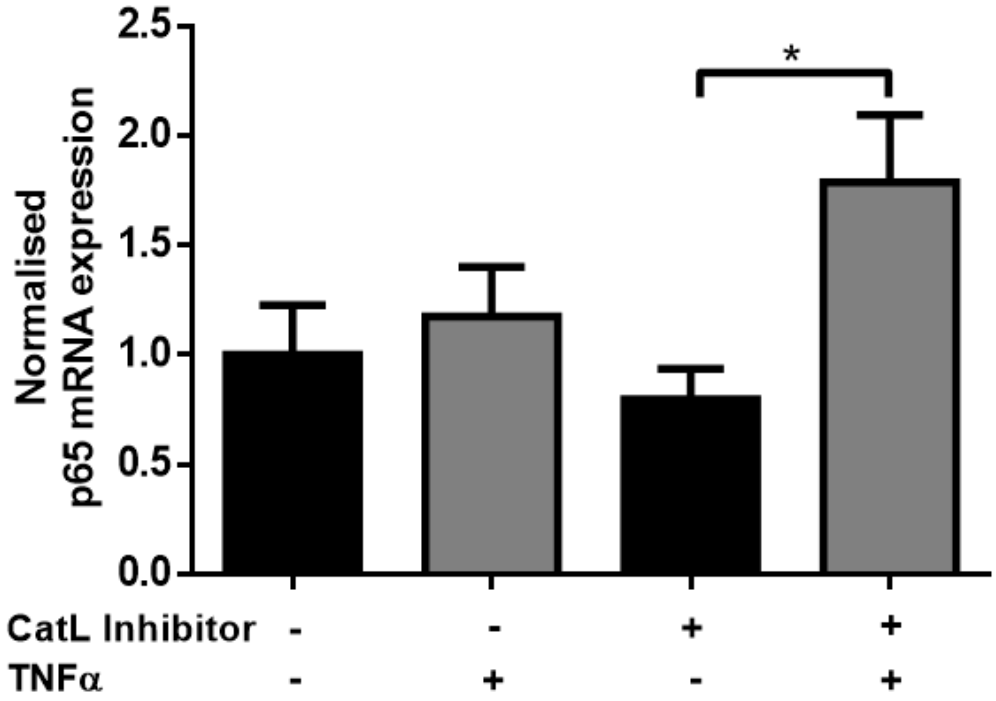

Figure 3.23 P65 mRNA expression in TNF*α*-stimulated control and Cathepsin L inhibited cells. Graph represents as mean with error bars indicating ± SEM where n=5. (T-test, *p<0.050).

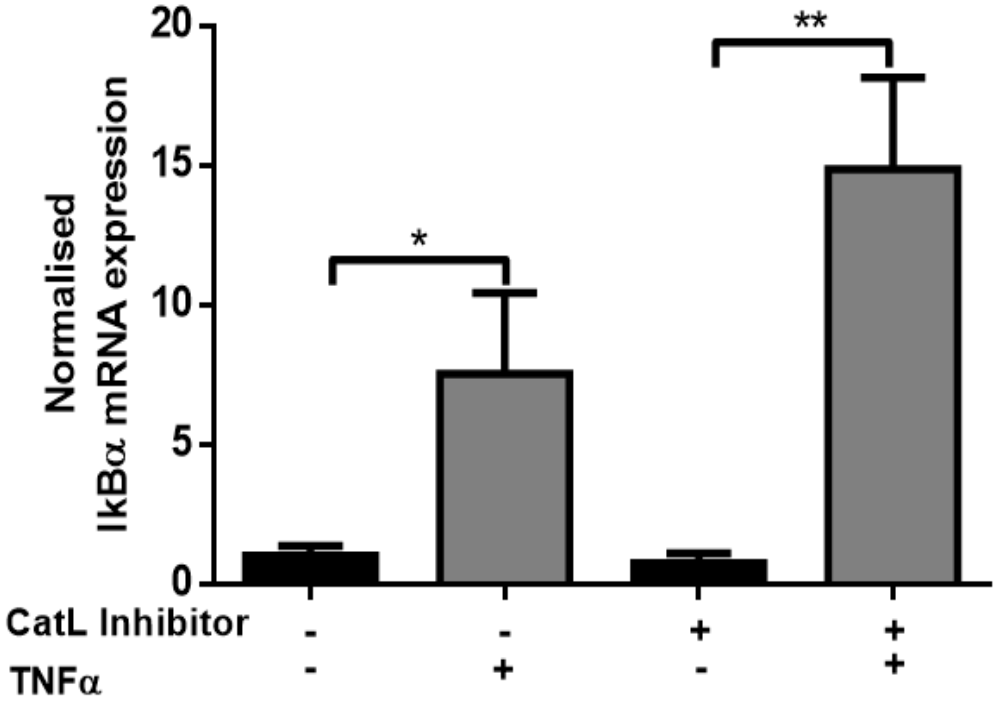

Figure 3.24 Iκβα mRNA expression in TNFα-stimulated control and Cathepsin L inhibited cells. Graph represents as mean with error bars indicating ± SEM where n=5. (T-test, *p<0.050, **p=0.010).

3.3.2.2 Effect of TNFα on protein expression of NF-κβ signalling in cathepsin L inhibited RPE cells

In order to reaffirm the changes caused by TNFα as seen on the mRNA expression level, protein samples were prepared and subjected to immunoblotting. Figure 3.25 shows a representative blots of those sample probed for P65, Iκβα and pP65 antibodies. Analysed protein expression data of three independent experiments were illustrated in Figure 3.26, Figure 3.27 and Figure 3.28 below.

A significant increase in level of total p65 and Iκβα proteins were observed in both control and cathepsin L treated group after TNFα stimulation. There was an increase of 3.7 fold of total P65 protein expression in control group after TNFα exposure ($p<0.001$). But only 2 fold of increase was noted in cathepsin L inhibited group after TNFα treatment ($p<0.001$). There was a significant difference in the increase of P65 protein expression after TNFα exposure in the control group compared to the cathepsin L inhibited group as analysed using Kruskall-Wallis test ($p<0.001$). The increase in TNFα-induced P65 in cathepsin L inhibited cells is 2 times lower as compared to control cells as shown in Figure 3.26.

There was a 1.7-fold and 2.3-fold increase in Iκβα level after TNFα treatment in control groups ($p= 0.009$) and cathepsin L inhibited group respectively ($p<0.001$) (Figure 3.27). Comparing the increase in Iκβα protein expression in control and cathepsin L inhibited group, the increase of Iκβα in cathepsin L inhibited cells is 1-fold higher compared to control cells. However, the differences was not statistically significant.

Analysis on the effect of TNFα on activated pP65 proteins (pP65) shows significant increase in both control and cathepsin L inhibited group Figure 3.28 with a *p*-value of 0.015 and 0.026 in the groups respectively. There was no significant changes

of pP65 increase in cathepsin L inhibited group compared to control group after TNFα exposure.

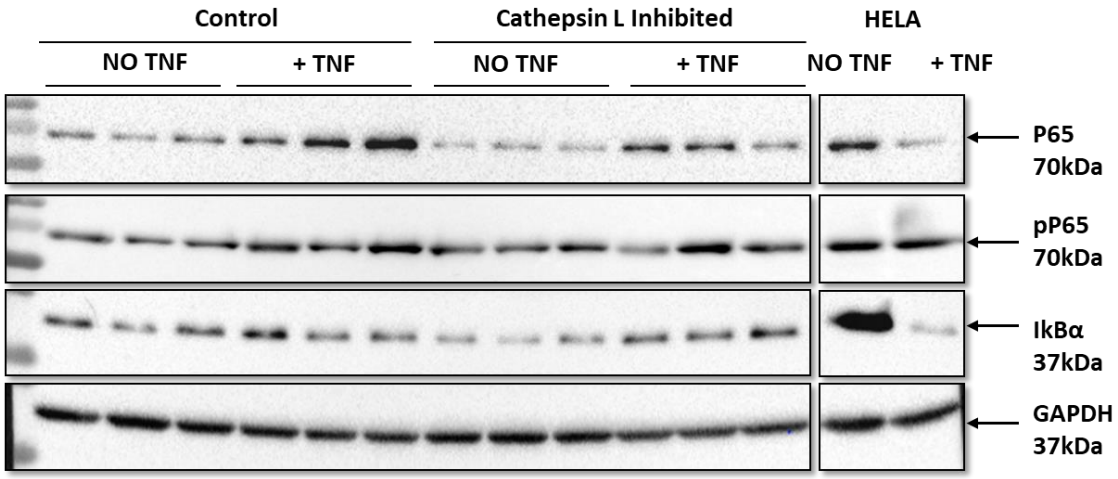

Figure 3.25 Representative blot image of control and cathepsin L inhibited samples with and without TNFα treatment. The membrane was probe with Anti-P65 (1:500 dilution), Anti Iκβα (1:500 dilution) and phosphorylated p65 (pP65) (1:500 dilution). GAPDH (1:30,000 dilution) was used as a loading control.

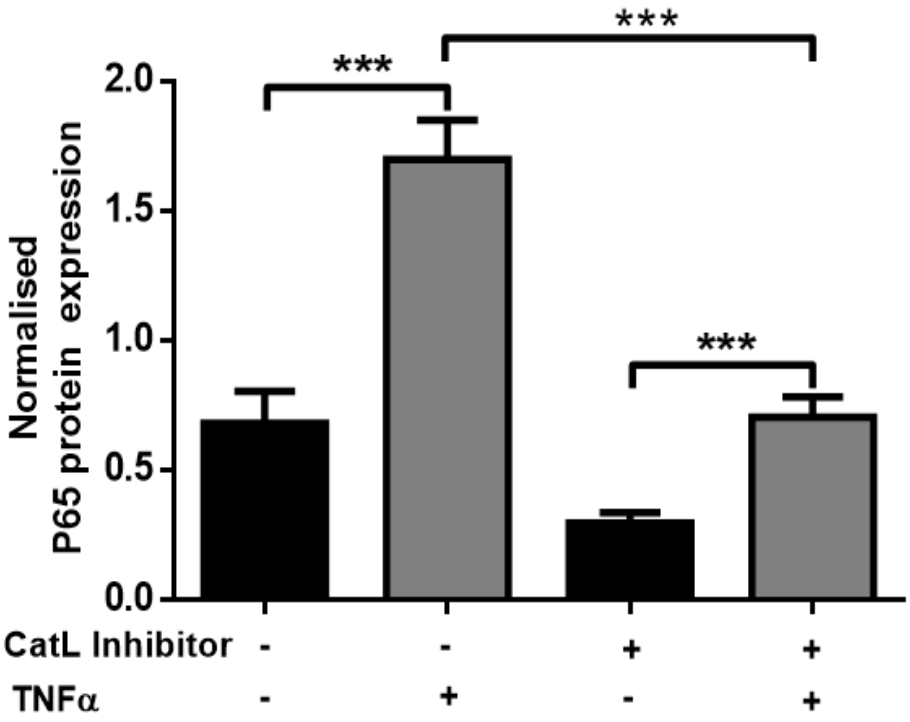

Figure 3.26 P65 protein expression of TNFα-induced control and cathepsin L inhibited ARPE-19 cells. Graph represents average value of P65 protein expression normalised to GAPDH as loading control with error bars indicating ±S.E.M with n=4 (T-test and One Way Annova, ***p<0.001).

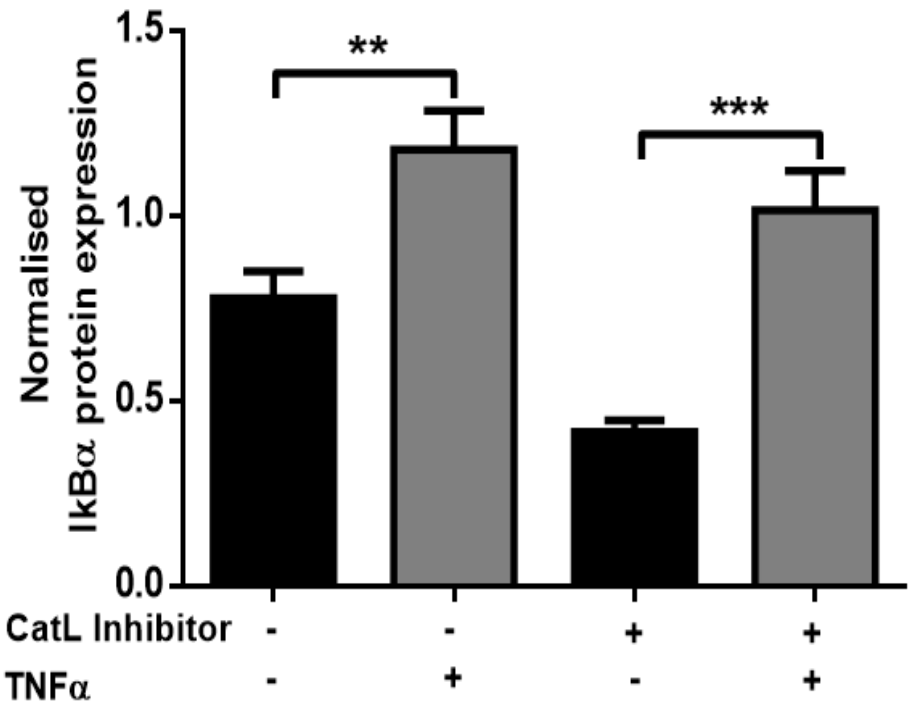

Figure 3.27 Iκβα protein expression of TNFα-induced control and cathepsin L inhibited ARPE-19 cells. Graph represents average value of Iκβα protein expression normalised to GAPDH as loading control with error bars indicating ±S.E.M with n=4 (T-test, *****p*<0.01, ******p*<0.001).

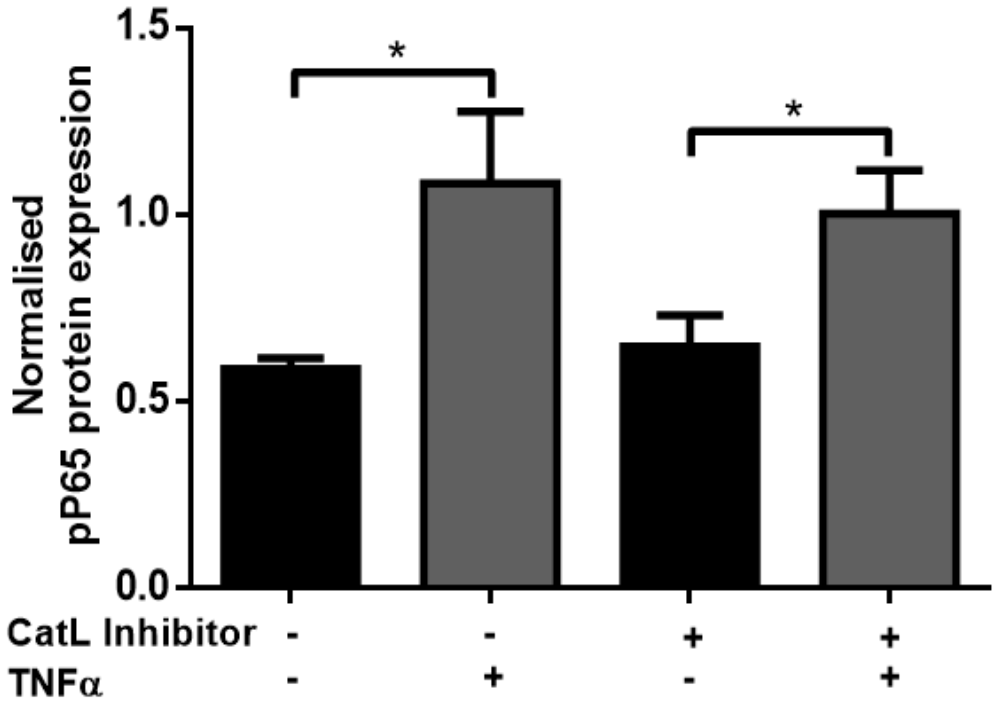

Figure 3.28 pP65 protein expression of TNFα-induced control and cathepsin L inhibited ARPE-19 cells. Graph represents average value of pP65 protein expression normalised to GAPDH as loading control with error bars indicating ±S.E.M with n=4 (T-test, *p<0.050).

3.3.2.3 Overall TNFα-induced NFκβ signalling in cathepsin L inhibited RPE cells

Finally, to see the overall TNFα-induced NF-κβ alteration in cathepsin L exposed cells, we looked into the fold increase of the activation in both cathepsin L inhibited and control group Figure 3.29. No significant differences was observed in the fold change increase of TNFα-induced NF-κβ in cathepsin L inhibited cells compared to control.

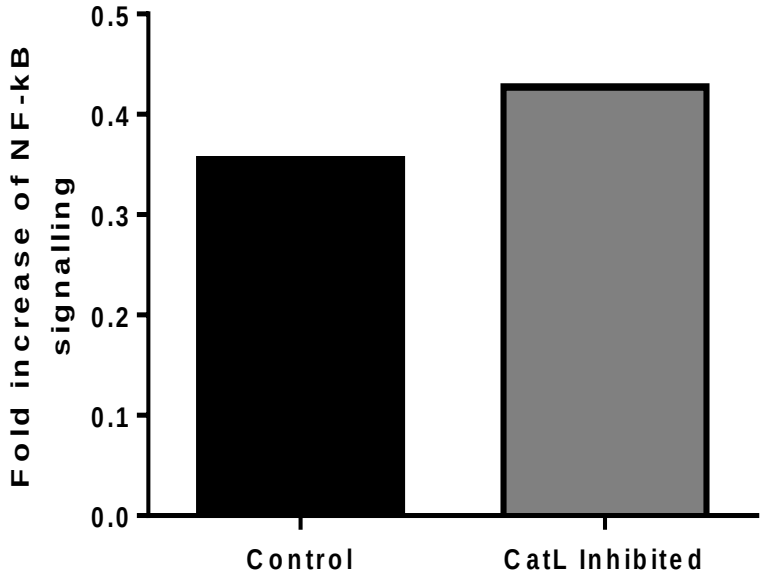

Figure 3.29 Fold increase of TNFα-induced NF-κβ activation in control cells vs. cathepsin L inhibited cells (T-test, n=4).

3.3.3 Effect of TNFα induced NF-kB signalling in AGEs –exposed RPE cells

3.3.3.1 Effect of TNFα on total p65 and Iκβα mRNA expression in AGEs exposed RPE

No significant changes in P65 mRNA expression were observed in both control (p= 0.657) and cathepsin L inhibited (p= 0.829) group in the presence of TNFα (Figure 3.30). However, a significant increase in Iκβα mRNA expression was observed after TNFα treatment in both non-AGEs and AGEs group with a p value of 0.007. Approximately 4-fold increase in Iκβα expression was seen in both groups with TNFα treatment (Figure 3.31). The significant increase in Iκβα expression after TNFα insult suggest an increase in NF-κβ signalling and the increase in Iκβα mRNA expression as a possible result of negative feedback loop of the NF-κβ signalling.

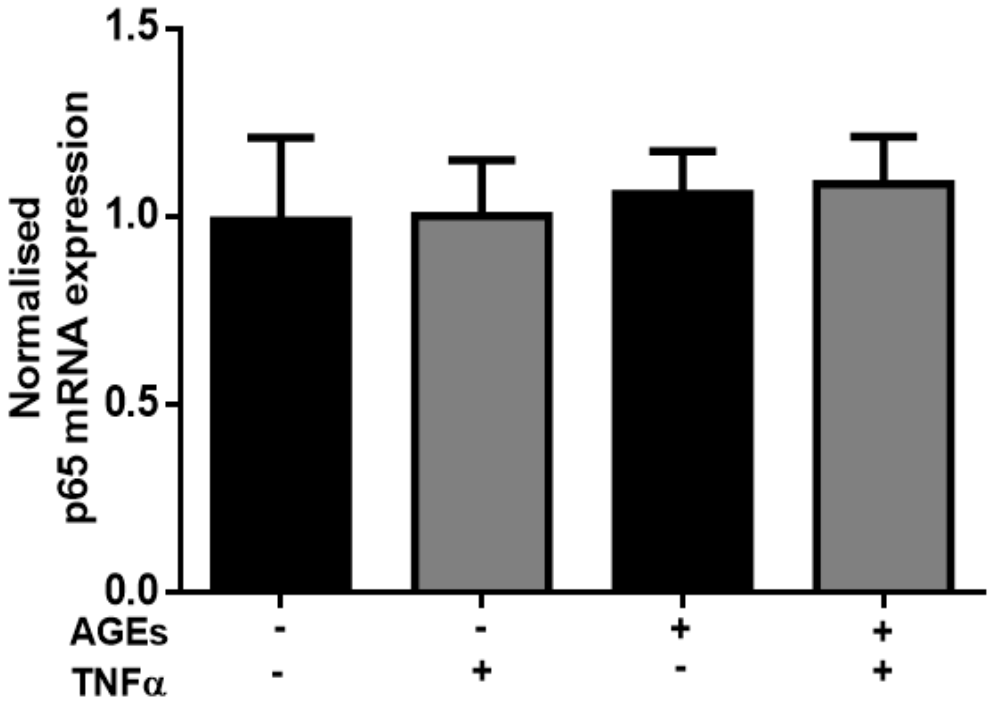

Figure 3.30 P65 mRNA expression in TNFα-stimulated control and AGEs-exposed ARPE-19 cells. The mRNA expression of P65 was normalised to β-actin and β-tubulin. Graph is presented as means with error bars indicating ± SEM where n=4 (T-test, n=4).

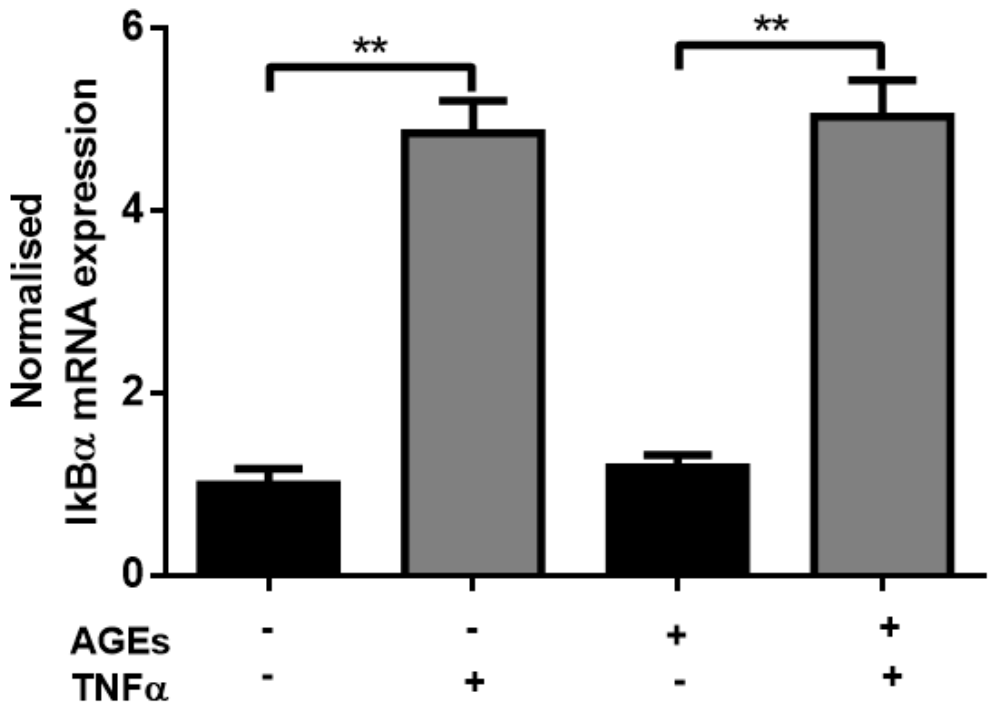

Figure 3.31 Iκβα mRNA expression in TNFα-stimulated control and AGEs-exposed ARPE-19 cells. Graph is presented as means with error bars indicating ± SEM where n=4 (T-test, **p<0.01).

3.3.3.2 Effect of TNFα stimulation on NF-κβ signalling key effectors protein in AGEs exposed RPE cells

With marked changes in the Iκβα mRNA expression upon TNFα insults, we next evaluate the possible changes by TNFα on the NF-κβ protein expression. RPE lysate was prepare in Laemmli lysis buffer and was subjected for immunoblotting with P65, Iκβα and pP65 antibodies. GAPDH was used as a loading control. A representative blot of the control and AGEs-exposed cells with and without the presence of TNFα is illustrated in Figure 3.32.

No changes in total P65 protein expression were observed in either control or AGEs-exposed cells after TNFα treatment (Figure 3.33). On the contrary, significant increase in Iκβα and pP65 was observed in both control and AGEs-exposed group in the presence of TNFα in cells (Figure 3.34 and Figure 3.35). There was about 1.5-fold increase in Iκβα in control cells after TNFα exposure and 2.7-fold increase was observed in the AGEs-exposed group with p-value of 0.003 and <0.001 respectively. Increase of Iκβα protein expression in AGEs-exposed group is almost double to the control group. The pP65 expression increase for about 4-fold in control group and 6-fold increase in AGEs-exposed cells after TNFα stimulation with p-value of 0.001 in both group.

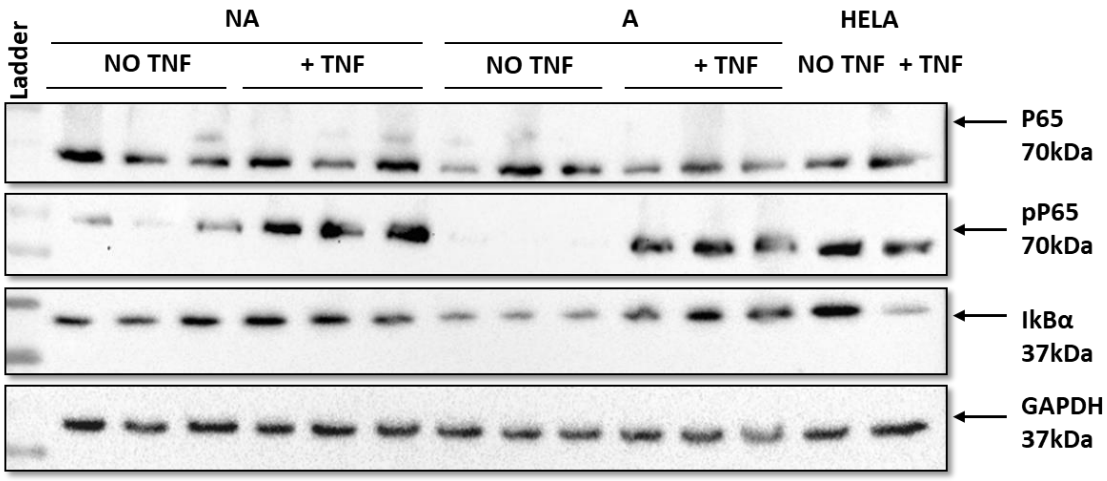

Figure 3.32 Representative blot image of control and AGEs-exposed ARPE-19 samples with and without TNFα treatment. The membrane was probe with Anti-P65 (1:500 dilution), Anti Iκβα (1:500 dilution) and phosphorylated p65 (pP65) (1:500 dilution). GAPDH (1:30,000 dilution) was used as a loading control.

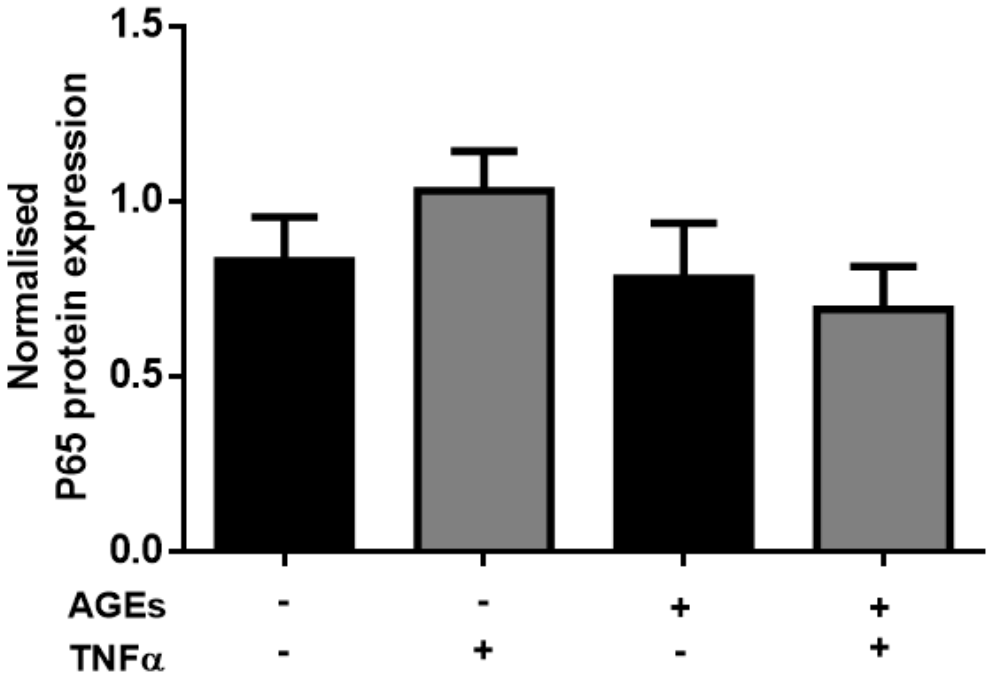

Figure 3.33 P65 protein expression in TNFα-stimulated control and AGEs-exposed ARPE-19 cells. The protein expression of P65 was normalised to GAPDH. Graph is presented as means with error bars indicating ± SEM where n=4.

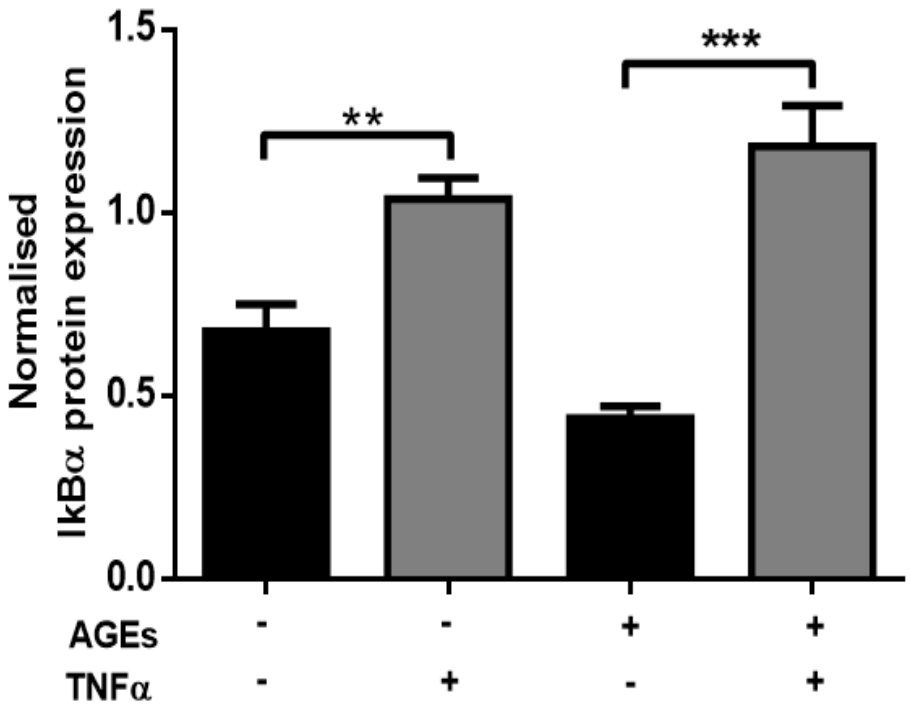

Figure 3.34 Iκβα protein expression in TNFα-stimulated control and AGEs-exposed ARPE-19 cells. Graph is presented as means with error bars indicating ± SEM where n=4 (T-test, **p = 0.01, ***p=0.001).

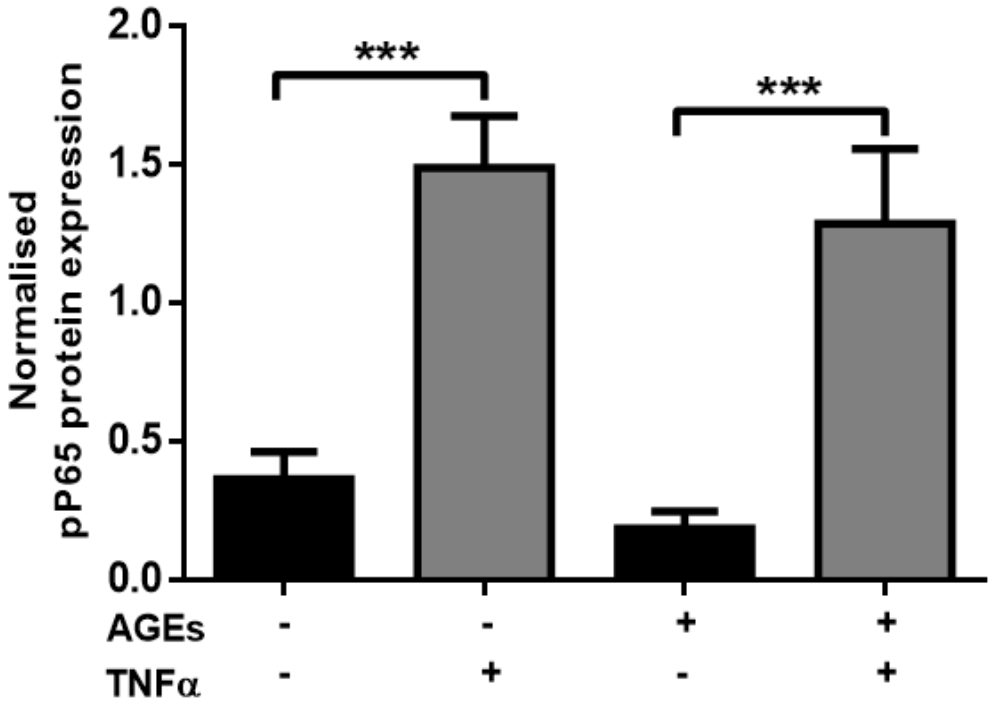

Figure 3.35 pP65 protein expression in TNFα-stimulated control and AGEs-exposed ARPE-19 cells. Graph is presented as means with error bars indicating ± SEM where n=4 (T-test, ***p<0.001).

3.3.3.3 Overall changes of NF-κβ signalling pathway in TNFα-induced AGEs exposed cells

In order to see the overall changes of NF-κβ signalling pathway in TNFα-induced AGEs exposed cells, we looked into ratio pP65/P65 in the cells, a 3-fold increase was noted in control group (p=0.005) and 10-fold increase was perceived in AGEs-exposed cells (p =0.001) (Figure 3. 36). The fold increase of TNFα-induced NF-κβ was 3-fold higher in the AGEs-exposed cells compared to control as shown in Figure 3. 37. No alteration was seen in the ratio of P65/Iκβα in control group, p=0.239 (Figure 3.38). However, a significant reduction was observed in the AGEs-exposed group after TNF treatment (p=0.002).

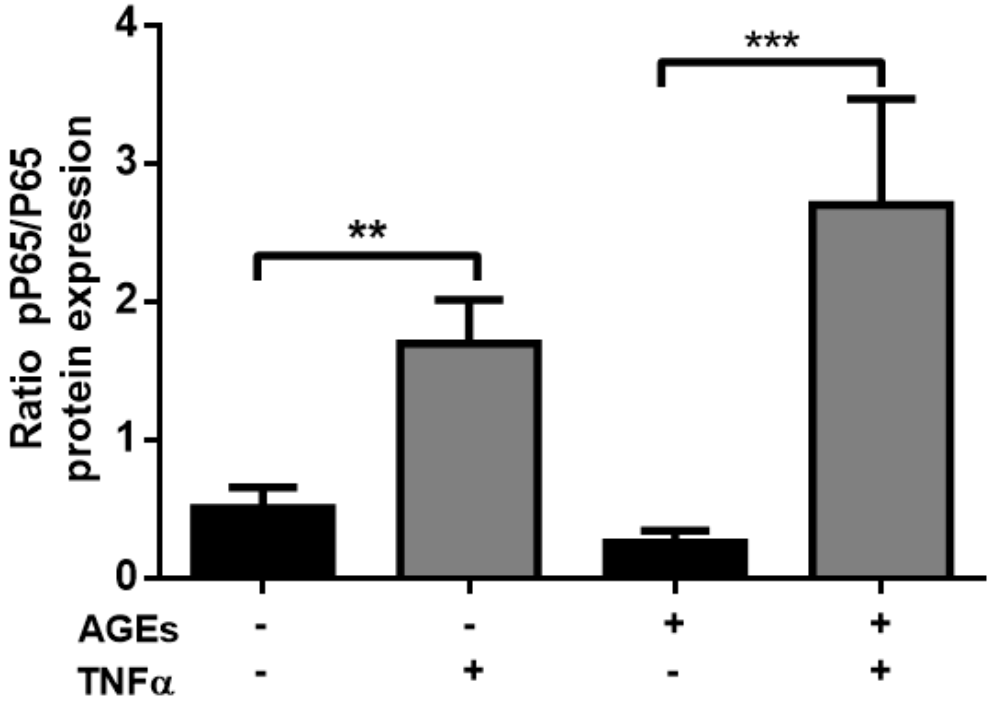

Figure 3.36 Ratio of pP65/P65 normalised to GAPDH in control cells vs. AGEs-exposed cells with and without the presence of TNFα in RPE cells. Bar graph represents average ratio of pP65/P65 with error bars indicating ± SEM where n=4 (T-test, **p<0.010, ***p<0.001).

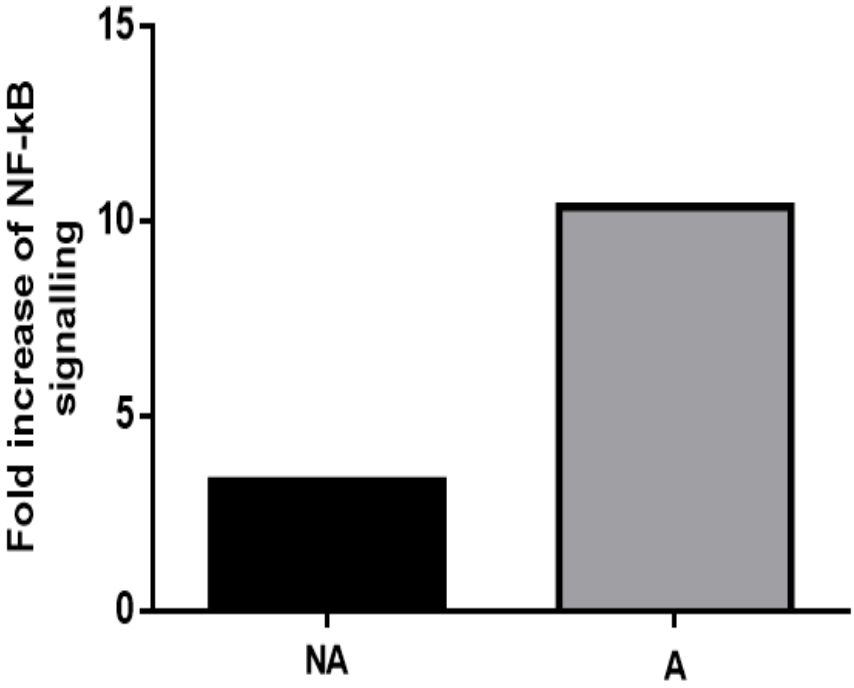

Figure 3.37 Fold increase of TNFα-induced NF-κβ activation in control cells vs. AGEs –exposed RPE cells (n=4).

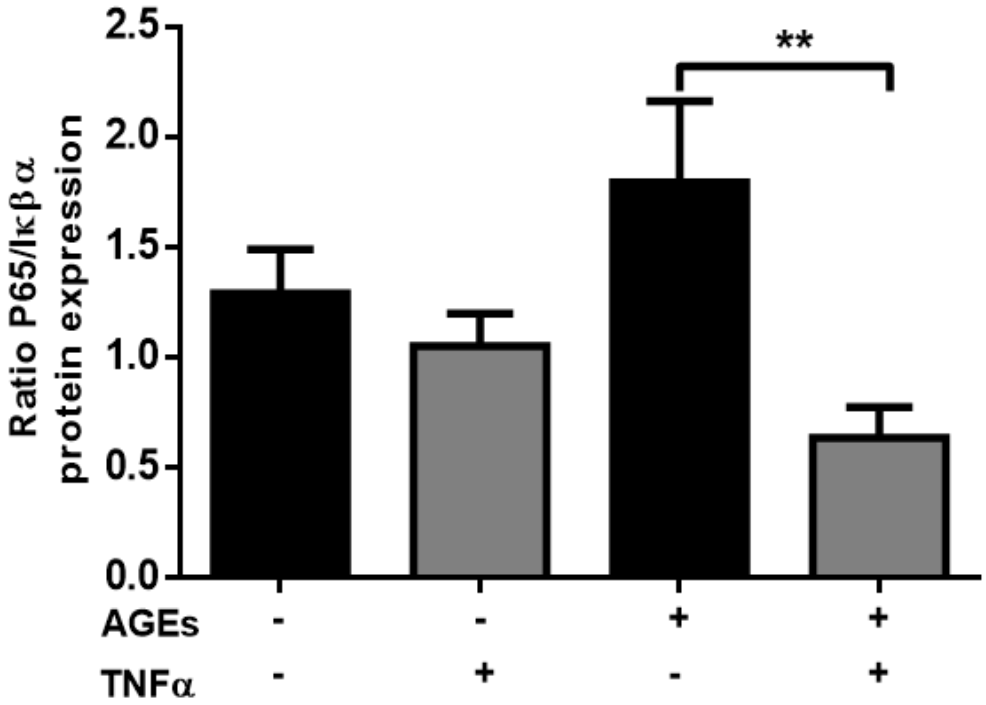

Figure 3.38 Ratio of P65/Iκβα normalised to GAPDH in control cells vs. AGEs-exposed cells with and without the presence of TNFα in RPE cells. Bar graph represents average ratio of P65/Iκβα with error bars indicating ± SEM where n=4 (T-test, **p<0.01).

3.4 Neuroprotective effect of thymoquinone on TNFα-induced NF-κβ signalling in RPE cells

3.4.1 Dose response curve for thymoquinone on RPE cells

Thymoquinone, a flavonoid known for its anti-oxidant properties, is also found to be associated with the NF-κβ signalling. To date, there has been no published data on the effects of the thymoquinone compound on ARPE-19 cells. Thus, in this study, we sought to study possible neuroprotective effect of thymoquinone on NF-κβ signalling in the ageing of RPE.

First, a dose-response curve was plotted to assess the cellular toxicity of thymoquinone on ARPE-19 cells. Briefly, ARPE-19 cells were cultured in 96-well plate for 24 hours. On the next day, cells were treated with different concentrations of thymoquinone, ranging between 0.1µM up to 250uM at four different time points; 0 hours, 2hours, 6 hours and 24 hours. Thymoquinone stock solution was dissolved in 100% DMSO. In order to prevent a false positive result, the percentage of DMSO in each well was standardised to a final concentration of only 0.1%, including control cells (vehicle). Cell viability was performed by adding the MTT reagent as described in section 2.5. At first, the cells were treated with a high dosage of thymoquinone ranging from 10µM up to 250µM. However, due to its toxicity, a lower concentration of thymoquinone dosage ranging between 0.1µM to 25µM were later tested.

Cell viability results are displayed in Figure 3.39. Thymoquinone concentration of 25µM and higher were toxic to ARPE-19 cells. At 25µM, there was a 30% reduction in cell viability with a p value <0.0001. A concentration of 10µM thymoquinone was safe to be used in ARPE-19 without affecting its viability, with approximately 10% reduction in cell viability (p=0.380). From this data, two concentrations of thymoquinone; 0.1µM and 10µM were chosen to be used in the subsequent

experiments. Figure 3.41 shows the effect of thymoquinone on cell viability in ARPE-19 cells, both with and without the presence of TNFα stimulation. Earlier, we showed that TNFα on its own does not affect the viability of ARPE-19 cells, and in here TNFα and thymoquinone was shown to be safe and non-toxic, when used together in ARPE-19 cells (Figure 3.40), EGCG was used as a positive control in these experiments, as it has been shown that EGCG has the ability to protect RPE cells from oxidative stressors, including TNFα (Li et al., 2013; Thichanpiang & Wongprasert, 2015).

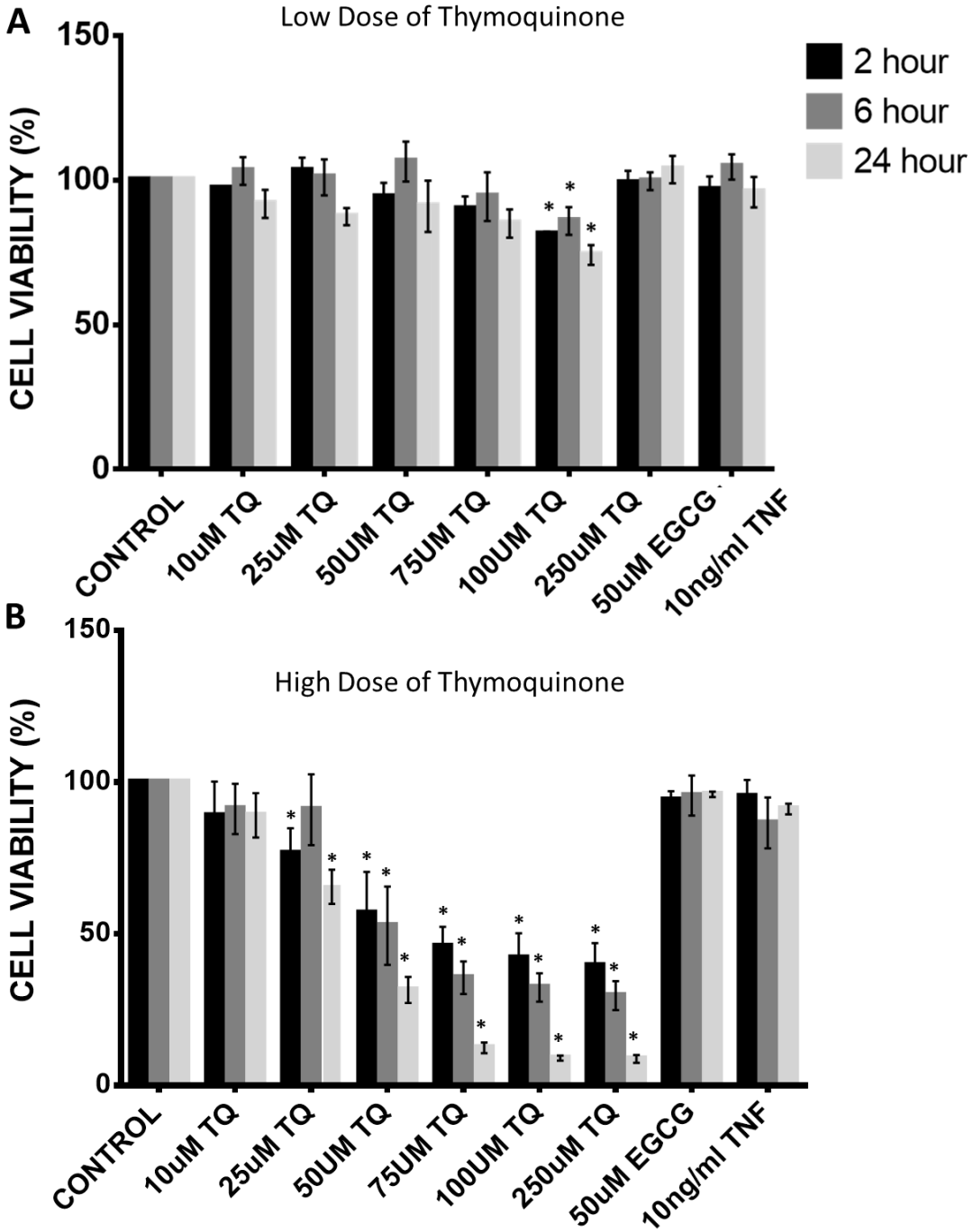

Figure 3.39 Cell viability studies of ARPE-19 cells tested with different concentrations of thymoquinone at three different time points (2, 6 and 24 hours). A) Cell viability of RPE cells in a lower doses of thymoquinone (0.1µM-50µM) B) Cell viability of ARPE-19 cells in high doses of thymoquinone (10µM-250µM). Data presented as mean ± SEM with five independent replicates (n=5) (T-test, *p<0.050).

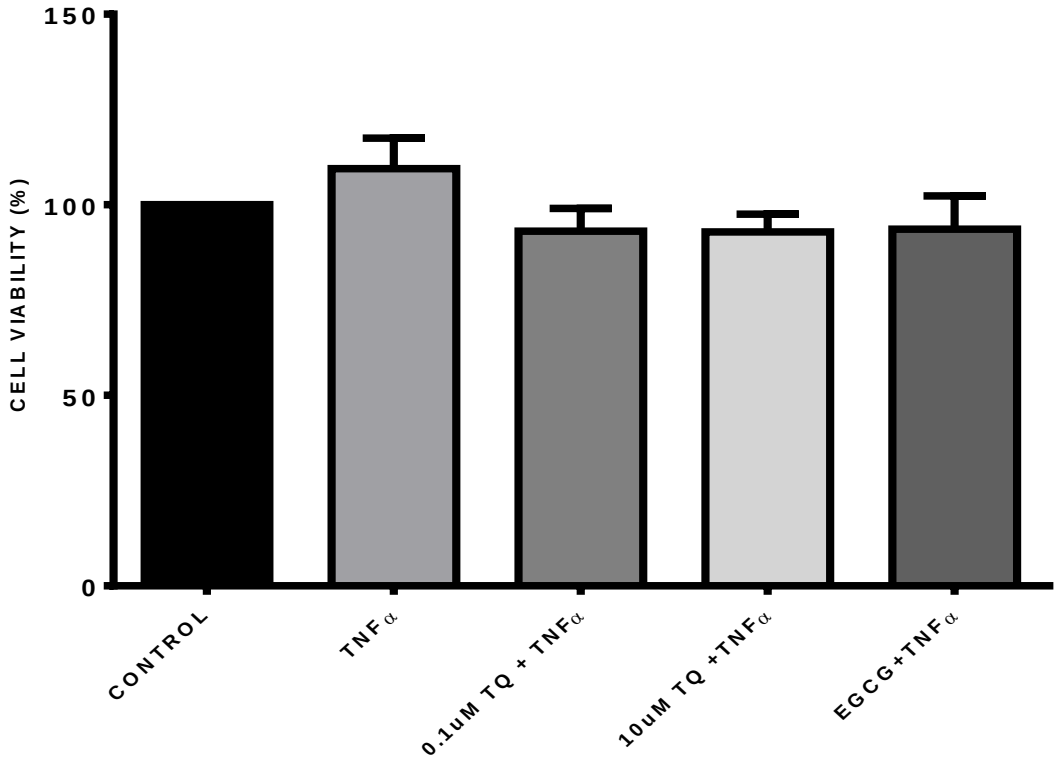

Figure 3.40 Effect of thymoquinone on ARPE-19 cells viability with or without the presence of TNFα stimuli. Data presented as mean ± SEM with three independent replicates (One-way ANNOVA).

3.4.2 Effect of thymoquinone on TNFα induced NF-κβ signalling in ageing RPE cells

As from the previous results in section 3.3 above, ARPE-19 cells exposed to AGEs are more susceptible to TNFα insults. Thus, the possible protective effect of thymoquinone was tested on ARPE-19 cells which were grown on membranes induced with AGEs, both with and without the presence of TNFα. The possibly protective effects of thymoquinone on the NF-κβ signalling in TNFα exposed ageing ARPE-19 cells were studied. The ARPE-19 cells were allowed to grow on the ageing matrix for 14 days as previously described and later, thymoquinone and TNFα were added prior to harvesting.

qPCR analysis was carried out for P65 and Iκβα genes. Data from three independent replicates showed that thymoquinone attenuate TNF-induced increase of P65 mRNA expression in ARPE-19 cells exposed to AGEs or otherwise. However, only the AGEs-exposed ARPE-19 cells showed statistical significant reduction in P65 mRNA expression (Figure 3.41). 0.1μM and 10μM thymoquinone concentrations reduced the TNFα-induced level of P65 in AGEs-exposed cells by 76% and 60%, with *p*-values of 0.040 and 0.050 respectively. Thymoquinone did not cause any significant changes to TNFα-stimulation in both groups of AGEs and non-AGEs ARPE-19 cells (Figure 3.42).

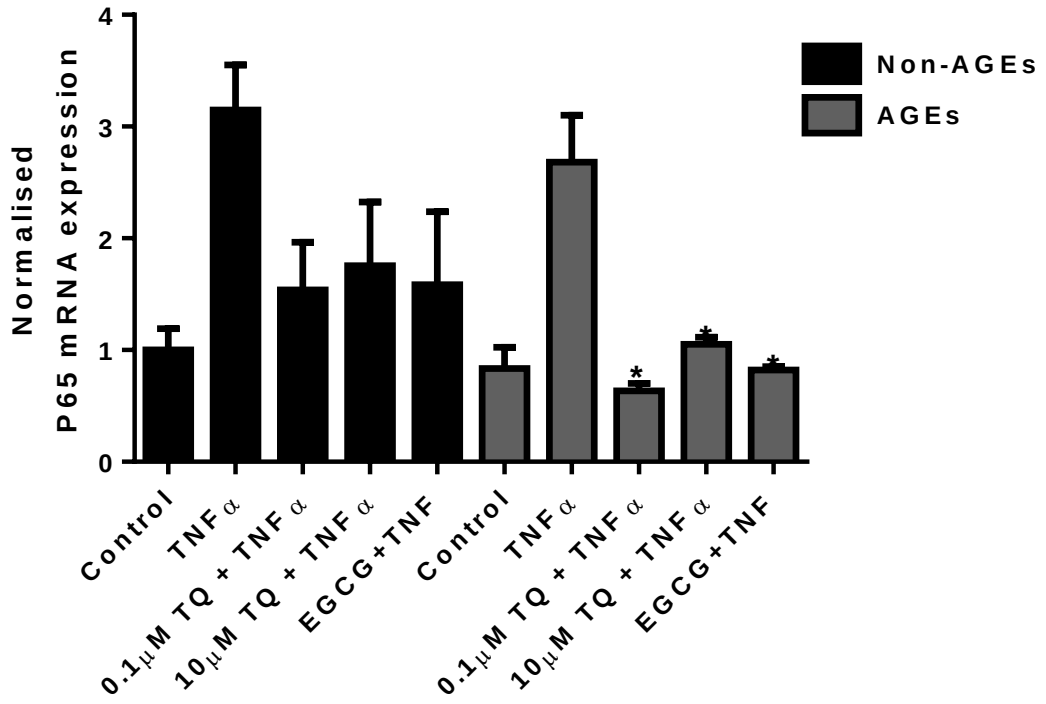

Figure 3.41 Thymoquinone alteration on P65 mRNA expression in TNFα induced non AGEs and AGEs exposed cells. Graph represents mean ± SEM with three independent replicate each (T-test, *p<0.050).

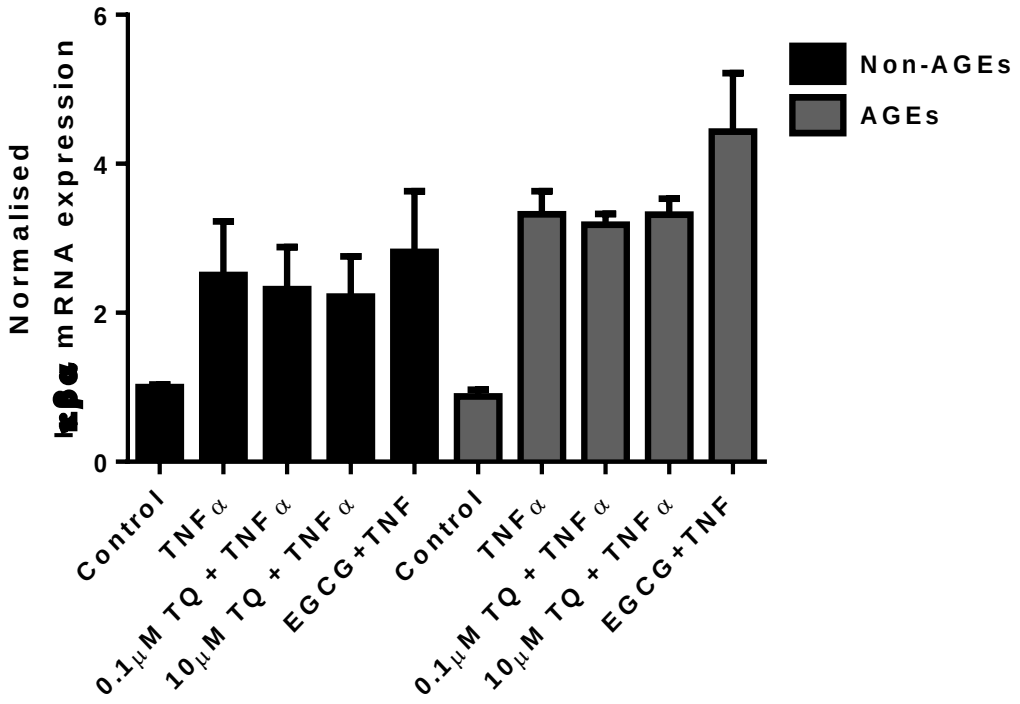

Figure 3.42 Thymoquinone alteration on Iκβα mRNA expression in TNFα induced non-AGEs and AGEs-exposed cells. Graph represents mean ± SEM with three independent replicate each analysed using T-test.

The overall qPCR data above suggests that thymoquinone alters the level of P65 but not Iκβα, in AGEs treated cells with the presence of TNFα. Thus, next, we sought to look at possible alteration of thymoquinone at protein levels in TNFα treated ARPE-19 cells. The representative blot is presented in Figure 3.43. Results show that thymoquinone did not cause any significant differences in P65, Iκβα and pP65 protein levels (Figure 3.44, Figure 3.45 and Figure 3.46).

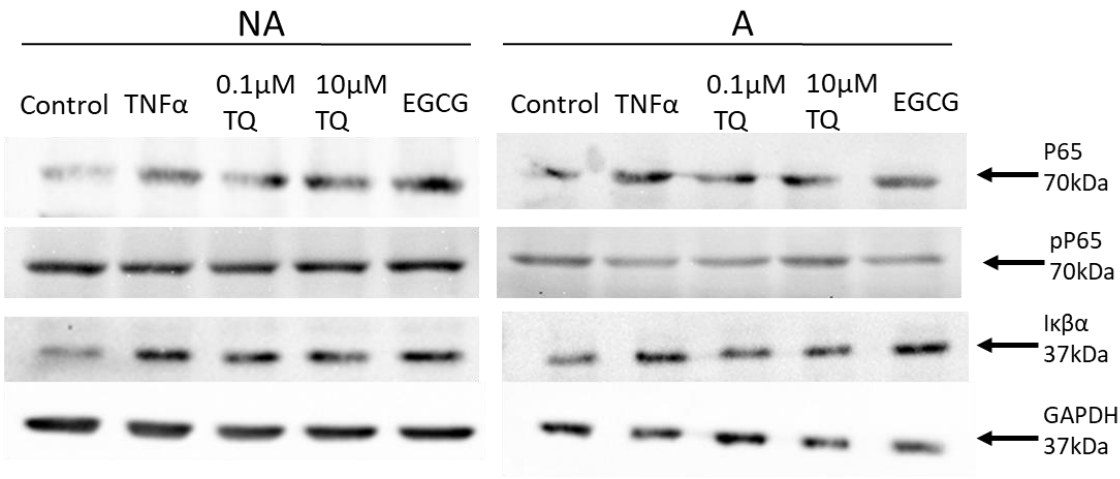

Figure 3.43 Representative western blot image to look for possible protective effect of thymoquinone on TNFα-induced NF-κβ in non –AGEs and AGEs-exposed RPE cells. The membrane was probe with Anti-P65 (1:500 dilution), Anti Iκβα (1:500 dilution) and phosphorylated p65 (pP65) (1:500 dilution). GAPDH (1:30,000 dilution) was used as a loading control.

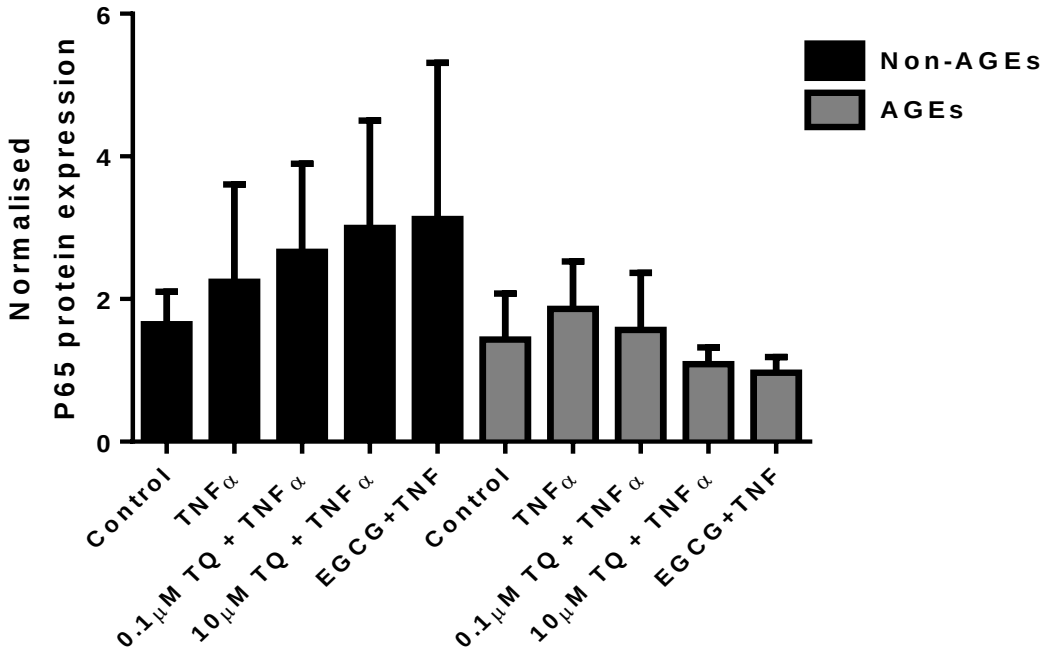

Figure 3.44 Thymoquinone alteration on P65 protein expression in TNFα induced non-AGEs and AGEs exposed cells. Graph represents mean ± SEM with three independent replicate each analysed using T-test.

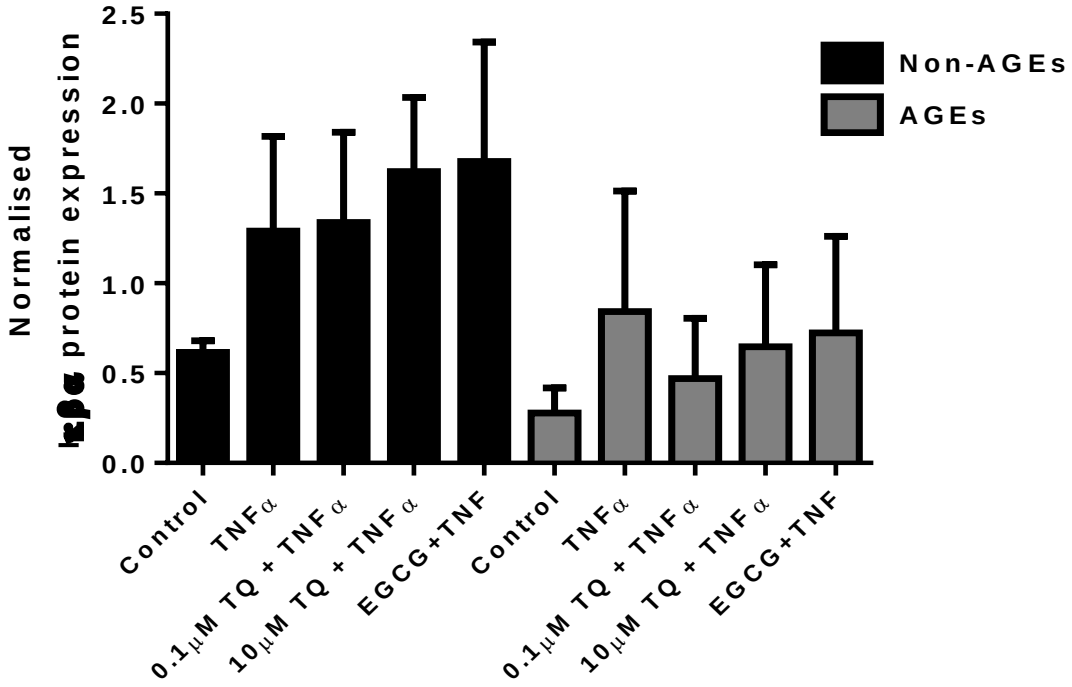

Figure 3.45 Thymoquinone alteration on Iκβα protein expression in TNFα induced non-AGEs and AGEs exposed cells. Graph represents mean ± SEM with three independent replicate analysed using T-test.

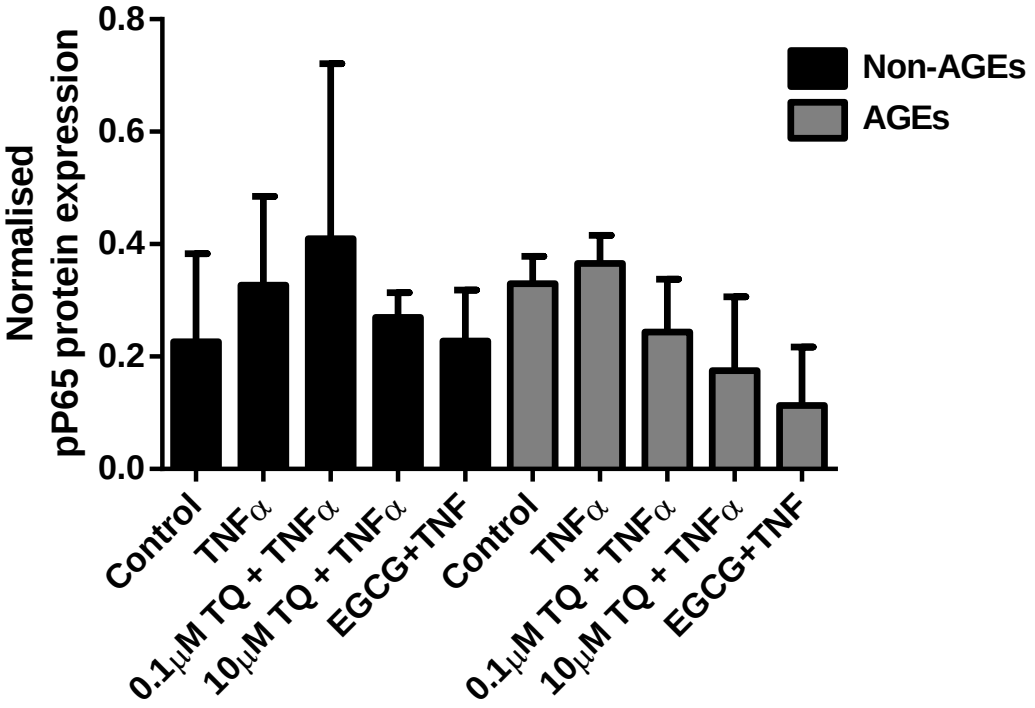

Figure 3.46 Thymoquinone alteration on pP65 protein expression in TNFα induced non-AGEs and AGEs exposed cells. Graph represents mean ± SEM with three independent replicate analysed using T-test.

In summary, thymoquinone showed significant attenuation of TNFα-induced rise of P65 mRNA levels but no change in Iκβα mRNA expression. Western blot analysis showed corresponding decrease in P65, Iκβα and pP65 protein levels especially in AGEs-exposed ARPE-19 cells, however these changes were not statistically significant.

CHAPTER 4: DISCUSSION

4.1 Summary of findings

In this study, we sought to investigate the associations of AGEs, cathepsin L and NF-κβ signalling in ARPE-19 cells. Considering the fact that, both AGEs and cathepsin L can regulate NF-κβ activity and reduction of cathepsin L was seen in AGEs-exposed ARPE-19 cells, it is possible that AGEs exert their effects on the NF-κβ signalling pathway, at least in part, due to modulation of cathepsin L levels.

First, we evaluated the effect of AGEs on the NF-κβ signalling pathway in ARPE-19 cells. One major finding in this study was that AGEs downregulates NF-κβ signalling pathway in human RPE cells. Significant reduction in level of P65, Iκβα and pP65 was observed in the presence of AGEs. However, when treated with TNFα, there was an exaggerated response to an oxidative stressor (TNFα) in cells exposed to AGEs.

In the previous study from the group, in which cathepsin profiling in AGEs exposed cells was performed, cathepsin L expression and activity was found to be downregulated with AGEs exposure. Since cathepsins have also been shown to be associated with NF-kB signalling pathway, the role of cathepsin L in NF-κβ signalling was assessed through the use of cathepsin L inhibition. Cathepsin L inhibition caused downregulation of the NF-κβ signalling in RPE cells, with significant reduction of P65 expression. In addition, there was a reduction in response to TNFα stimulation by cathepsin L.

Finally, the possible protective effect of thymoquinone was determined in AGEs-exposed RPE cells with and without the presence of TNFα. However, thymoquinone did not show any protective effect against TNFα-induced NF-κβ signalling.

4.2 The use of AGEs-exposed RPE cells as an *in vitro* model of AMD

In the present study, ARPE-19 cells were grown on a layer of ECM to mimic the Bruch's membrane in which the RPE resides in their natural environment. Bruch's membrane undergoes structural and physiological changes with age, including changes in chemical composition and increase of structural thickness (Okubo et al., 1999). Thickening of Bruch's membrane, in part, will result in the reduction of choroidal blood flow, which affects the transport of waste materials out of the RPE cells, thus resulting in a higher accumulation of waste product which impairs the RPE homeostasis (Zarbin, 2004).

AGEs formation on the ECM layer in this study was induced through the use of chemical, glycoaldehyde. Glycoaldehyde is an intermediate for the formation of AGEs structure, as seen in N (epsilon)-(carboxymethyl) lysine (CML) (Nagai et al., 2000). The degree of AGEs induced by this models *in vitro* has already been described elsewhere (Stitt et al., 2004; Glenn et al., 2009; Glenn & Stitt, 2009). Stitt et al (Stitt et al., 2004) tested the GA-derived fluorescent on control and AGEs ECM through the use of spectrofluorometer at 370 to 440 excitation and emission wavelength. Increased CML has been observed with glycoaldehyde treatment in a dose and time dependent manner (Stitt et al., 2004), which is in line with increase observation of AGEs autoflourescent in human Bruch's membrane observed by Glen et al (Glenn et al., 2009). CML accumulation resulted in the disruption of Bruch's membrane, triggers the growth of blood vessel and induces choroidal neovascularisation (CNV) formation (Ishibashi et al., 1998; Zarbin, 2004; Tian et al., 2005; Yamada et al., 2006). In a study investigating the localisation of CML in ageing eyes, CML accumulation was observed in soft drusen of all ageing cells, but its localisation into RPE was only observed in wet AMD patients (Ishibashi et al., 1998). These evidences show that the use of glycoaldehyde to induce

AGEs on ECM used in this study as an AMD model was a relevant physiological choice.

ARPE-19 cells were seeded on the glycoaldehyde-induced matrigel and allowed to grow for two weeks, when the cells formed a confluent monolayer in both control and AGEs-treated group. The reason for the 2-week time point was to allow the cells in both groups to become confluent and comparable to each other. In addition, the two-week time point was chosen in order to accommodate the decrease in cathepsin L activity as previously studied (Sharif et al., 2018). The modification of the ECM was carry out as stated by (Glenn et al., 2009). In order to maintain variability effect of AGEs to the cells, the chemicals such as glycoaldehyde and sodium borohydride solution used in the preparation of ECM were freshly prepared each time to ensure the maximum activity of the solutions. Apart from that, incubation time, number of washes as well as quantity of washes were also taken into account to reduce variability to the experiments.

When we compared the growth rate of the RPE cells in this model, AGEs-exposed RPE cells in our 2-week models exhibited a slower growth rate and low cells population in the first week of culture as compared to the non-AGEs RPE cells, although both of them were seeded with the same number of cells at Day 0. The slower growth rate and lower cell population in AGEs-exposed group might be due to cell death when it was first seeded onto the membrane, thus the surviving cells had to adapt to the AGEs, and later grow at the same rate as the non-AGEs cells.

Morphologically, the RPE grown on AGEs-exposed ECM were shown to have a little less cobblestoned-appearance compared to control cells. This observation was also reported by Glen et al who demonstrated a slight morphological and physiological difference in the appearance of cells grown on non-AGEs and with AGEs exposure (Glenn et al., 2009). Due to the post-mitotic nature of RPE, remaining RPE tends to

stretch themselves to fill the spaces which had become vacant as a result from dead RPE cells during normal ageing (Feeney-Burns et al., 1984; Del Priore et al., 2002). Non-AGEs cells showed typical ARPE-19 characteristics with tight junction formation, fully formed smooth and rough endoplasmic reticulum, polyribosomes, mitochondria and lysosomal like inclusion (Dunn et al., 1996; Glenn et al., 2009). In comparison, AGEs-exposed RPE showed less tight junction properties with large lipid-like inclusion bodies as seen in ageing and AMD RPE cells (Glenn et al., 2009).

4.3 Reduction in NF-κβ signalling pathway activation signals parainflammatory reaction of AGEs-exposed RPE cells

One mechanism by which AGEs cause age-related changes is through binding to its receptor, such as RAGE. RAGE has been found to be up-regulated with ageing and higher RAGE was found in AMD patients (Howes et al., 2004; Yamada et al., 2006). Binding of AGEs to RAGE is assumed to be a potential mechanism which linked oxidative stress and induction of inflammation, a potential mechanism of AMD (Yamada et al., 2006). Howes et al (Howes et al., 2004) speculated that AGE and RAGE is involved in mediation of local inflammatory response associated with AMD.

Binding of AGEs to RAGE has been shown to activate the NF- κβ signalling pathway, a master regulator of inflammation (Yan et al., 1994; Lin et al., 2012; Lin et al., 2013). Investigation into the effects of AGEs on NF-kB binding capability using placenta membrane showed that AGEs are capable of increasing DNA binding and transcription of pro-inflammatory cytokines such as TNFα, IL-1β and IL-8 (Lappas et al., 2007). The increase of AGEs and RAGE has been shown to strongly correlate with AMD and the binding activates the NF-κβ pathway and induce apoptosis in RPE cells (Howes et al., 2004; Lin et al., 2012). Observation on the AGEs change in primary cultured RPE cells has shown up-regulation of NF-κβ related cytokines such as GM-

CSF and CXCL11 (Lin et al., 2013). Apart from that, in the same study, VEGF, a cytokine that is strongly associated with wet AMD progression, also has been shown to be up-regulated by almost twice with AGEs compared to control cells (Lin et al., 2013).

In this current study, we investigate the effect of AGEs on the NF-κβ key signalling effectors; P65, Iκβα and phosphorylated P65 (pP65). Cells were exposed to AGEs for 2 weeks and changes in the NF- κβ were measured. From the aforementioned evidences (Howes et al., 2004; Lappas et al., 2007; Lin et al., 2012; Lin et al., 2013), it was hypothesised that AGEs exposure to RPE cells would leads to activation of NF-κβ signalling. However, our data indicates a reduction effect of AGEs on the NF-κβ signalling pathway. The summary of our results is shown in Figure 4.1. Observations on the expression levels of P65, Iκβα, and phosphorylated P65 through immunoblotting revealed a significant decreased in the three proteins. Our finding is contrary to findings by Lan et al which showed that AGEs significantly increase pP65 with no change in level of P65 in mouse pancreatic islet endothelial cell line MS1 cells as compared to control cells (Lan et al., 2015). However, the differences observed may be explained by (1) their method of inducing AGEs differs from the method used in this study and (2) NF-κβ respond to AGEs stimulus may be dependent on cell types. In other words, endothelial cells may react differently to ARPE-19 cells when exposed to AGEs in culture.

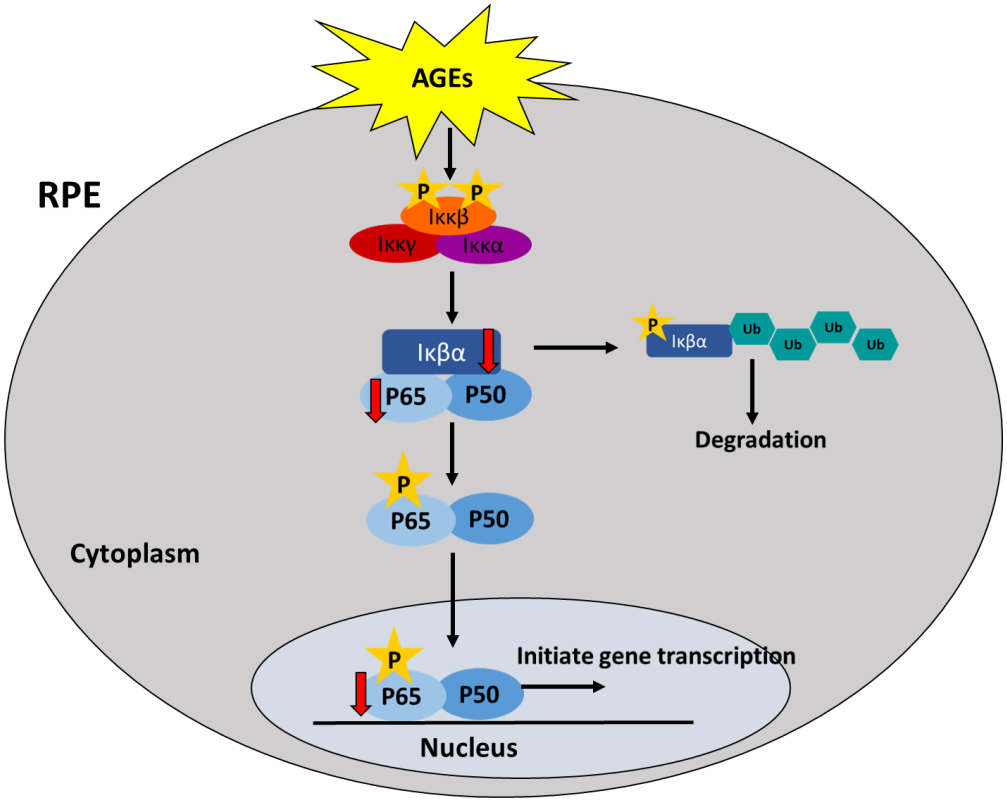

Figure 4.1 The effect of AGEs on NF-κβ signalling pathway in 2-weeks AGEs model. Figure was from own drawing.

In addition, the reduction effect of NF- κβ signalling seen in this cell culture model is thought to be due to a state of para-inflammation. The term 'para-inflammation' was first proposed by Medzhitov in 2008 (Medzhitov, 2008), and is defined as an adaptive response of cells or tissue to protect themselves against oxidative stress and maintain its adequate functionality. In a para-inflammatory state, cells are in a state between healthy homeostasis and chronic inflammation. If the stress persist, the balance will be tipped and cells will suffer from chronic inflammation leading to cell or tissue damage (Lin et al., 2013). Xu et al proposed that the para-inflammation may actually contribute to age-related retinal pathologies including AMD (Xu et al., 2009).

In our study, exposure of ARPE-19 cells to AGEs for 2 weeks is very likely to have create a parainflammatory state, where cells are trying to protect themselves by preventing the activation of NF-κβ signalling pathway. The association of parainflammation and AGEs in RPE in AMD has been described previously (Lin et al.,

2013; Nita et al., 2014). Lin and collegues (Lin et al., 2013) performed a differential gene expression in order to study the effects of AGEs on anti- and pro-inflammatory pathway in human RPE cells. Their data revealed 41 up and 18-down regulation of various anti- and pro-inflammatory genes. Out of these genes, there were upregulation of anti-inflammatory cytokines including IL10, IL1ra, and IL9 and proinflammatory cytokines including IL4, IL15, and IFN-γ. Apart from that, other proinflammatory cytokines including IL8, MCP1, and IP10 were underexpressed with AGE stimulation of human cultured RPE cells. These cytokines are novel genes associated with AMD pathogenesis and candidate marker of inflammatory events in the outer retina which are modulated through NF-κβ signalling pathway. The pattern of up- and down-regulation of this inflammatory cytokines after 24 hour AGEs exposure are a result of the cells' adaptive response towards low grade stress accumulated in Bruch's membrane or parainflammation (Lin et al., 2013; Nita et al., 2014).

4.4 TNF-α induced NF-κβ activation shifting the para-inflammatory state to chronic inflammation

As mentioned above, 2-weeks AGEs exposure on RPE display an adaptive response of cells towards oxidative stress known a parainflammation. However, this balance can be tipped to chronic inflammation with an excessive and pro-long exposure to sources of stress. In order to test that, TNFα has been used to challenge the inflammation in RPE cells. TNFα is a cell signalling protein essential in inducing an inflammatory response (Al-Gayyar & Elsherbiny, 2013). In AMD, higher expression of TNFα has been found in neovascular AMD eyes (Al-Gayyar & Elsherbiny, 2013). TNFα is able to disrupt RPE barrier function through upregulation of VEGF and promoting angiogenesis (Giraudo et al., 1998; Cha et al., 2007; Terasaki et al., 2013). In AMD, VEGF has been found to be upregulated and enhanced the formation of CNV as seen in late stage of AMD (Matsuoka et al., 2004; Tsai et al., 2006).

Binding of TNFα to its receptors, such as TNFR-1 and TNFR-2 appears to be one of key steps in the NF-κβ signalling pathway. Korthagen et al (Korthagen et al., 2015) performed a microanalysis to study the RPE-specific response to TNFα. They reported that more than 150 genes were differentially expressed in response to TNFα, and most of the genes were associated with NF-κβ signalling pathway.

ARPE-19 cells with and without AGEs exposure were later exposed to 10ng/ml TNFα stimulus and samples were analysed for changes in NF-κβ signalling pathway key effectors. Results indicate a significant increase of TNFα-induced NF-κβ activation in both AGEs-exposed and non-AGEs exposed RPE cells. These was observed with significant increase in level pP65 and Iκβα protein expression levels. The data is summarized in Figure 4.2. In addition, looking into fold increase induced by TNFα, a higher increased was observed in AGEs-exposed RPE cells compared to control cells which means the AGEs-exposed cells are more vulnerable to inflammatory cytokines compared to young ones. This data also indicates the shifting of response of cells from parainflammation to chronic inflammation. Exposure to AGEs only resulted in dampening of NF-κβ signalling, but incubation with TNFα tipped the balance and exposed the cells to chronic inflammation. Chronic TNFα exposure has been shown to alter RPE cells and allow them to resemble the pathology in AMD (Touhami et al., 2018).

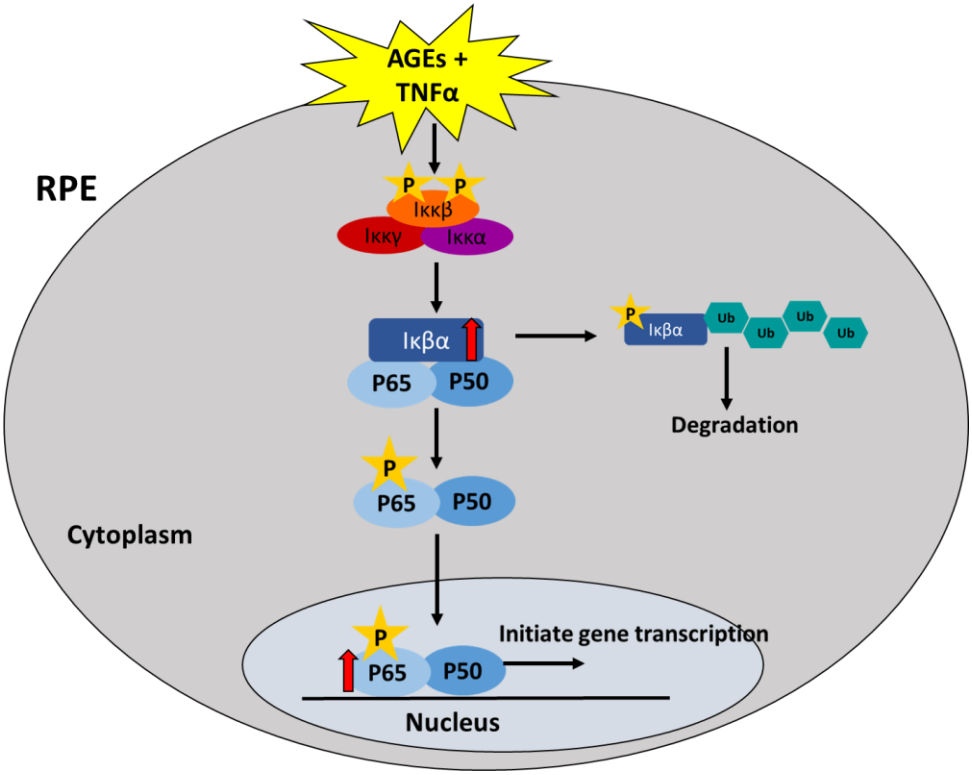

Figure 4.2 The effect of TNFα on NF-κβ signalling pathway in AGEs-exposed RPE cells. Image was from own drawing.

4.5 Role of Cathepsin L in NF-κβ signalling and RPE

. Lysosomal enzymes are important in clearing waste products from cells and maintaining the cells homeostasis. Lysosomal proteases such as cathepsins are responsible in digesting extracellular material (Turk et al., 2012). These extracellular debris are taken-up by endocytosis and subsequently they form intracellular material as a result of autophagy (Stoka et al., 2005; Repnik et al., 2012; Stoka et al., 2016). Cathepsins has been found to be altered with ageing (Wyczalkowska-Tomasik & Paczek, 2012; Stoka et al., 2016). Cathepsins B, L and S are most often mentioned (Wendt et al., 2008; Wyczalkowska-Tomasik & Paczek, 2012). Cathepsin expression and regulation might be cells specific, because different cells shows different levels of expression with regards to ageing. Downregulation of cathepsin L and unaltered level of cathepsin B has been observed in senescent rats' brain tissues (Nakanishi et al., 1994). In contrast, cathepsin B protein and activity levels was found to be increased in the livers of ageing rats (Keppler et al., 2000). In a rat's brain, the level of cathepsin B, E and D is higher in aged rats compared to young rats, however cathepsin L level decreased with age (Nakanishi et al., 1994; Nakanishi et al., 1997). The increase of cathepsin D and E in aged rat brain was thought to be associated with lipofuscinogenesis as these cathepsins has been found to co-localise with lipofuscin (Nakanishi et al., 1997; Okada et al., 2015). The data together sum up the importance of cathepsins in cells and their regulation is dependent on types and location of the cell.

In the RPE, lysosomal enzymes is important in phagocytosis and autophagy processes. The age related decrease in these degradative capacity impairs the autaphagic clearance of photoreceptor outer segment and protein aggregates, which eventually leads to accumulation of lipofuscin and drusen observed in AMD (Shamsi & Boulton, 2001; Ferrington et al., 2016). Out of the twelve cathepsins in the cathepsins family, cathepsin D has been among the most widely studied in the RPE cells. The importance

of cathepsin D in RPE has been noted from the observation in which cathepsin D deficient mice showed signs of vision loss (Koike et al., 2003). Inhibition of cathepsin D also has been shown to impair the degradative capacity of photoreceptor outer segment and leads to accumulation of debris in RPE as seen in drusen of ageing cells (Rakoczy et al., 1997; Rakoczy et al., 1999).

Cathepsin D was found to be downregulated with AGEs in RPE cells (Glenn et al., 2009b; Sharif et al., 2018). In addition, a recent study in our group also revealed a downregulation of cathepsin L with AGEs in RPE cells (Sharif et al., 2018). Cathepsin L belongs to cysteine protease family. It is mainly located in the lysosomes, however, it can also be found in nucleus, cytoplasm and extracellular matrix (Brix et al., 2008). Cathepsin L participates in protein degradation of functional proteins in lysosomes as well as other physiological processes including autophagy and apoptosis (Sun et al., 2013).

Cathepsin L has been shown to play a role in matrix degradation, invasion and neovascularization (Urbich et al., 2005; Sugita et al., 2009). Urbich et al (Urbich et al., 2005) demonstrated that cathepsin L is required for endothelial progenitor cell-induced neovascularization in mouse hind limb model. In AMD, cathepsin L was thought to play a significant role in extracellular environment of Bruch's membrane and the development of choroidal neovascularisation during wet AMD progression (Alizadeh et al., 2006; Shimada et al., 2010). Shimada and colleagues (Shimada et al., 2010) revealed that cathepsin L inhibition leads to significant reduction in size of neovascularization in cathepsin L deficiency mice. In the eye, Bruch's membrane extracellular matrix provides a physical barrier to restrict movement of cells within the eye and prevent retinal angiogenesis (Bird, 1993; Chong et al., 2005; Shimada et al., 2010). Thus, the process of extracellular matrix degradation is important to initiate CNV. Cathepsin L

may be involved in AMD through degradation of the extracellular matrix in Bruch membrane, which facilitates the invasion of choroidal blood vessels into the RPE space, forming choroidal neovascular membrane seen in wet AMD.

Given their high metabolic rate, the RPE cells are highly susceptible to oxidative stress and inflammation (Plafker et al., 2012; Datta et al., 2017). In this situation, cathepsin L are shown to regulate the complement pathway in the RPE to protect against exogenous and endogenous insults (Liszewski et al., 2013; Minton, 2013; Satyam et al., 2017; Jakoš et al., 2019). In AMD, complement components such as C3, C5b-9, CFB and CFH has been detected in drusen and AMD lesion (Anderson et al., 2010; Gehrs et al., 2010; Xu & Chen, 2016; Chrzanowska et al., 2018; Katschke et al., 2018; Maugeri et al., 2018). The complement pathway consists of over 30 small proteins produced in liver as an inactive precursor and released to the circulation for tissue distribution (Xu & Chen, 2016). Once the precursor has reach its tissue destination, it requires two critical steps for full activation; C3 cleavage and C5 cleavage (Sim & Tsiftsoglou, 2004; Xu & Chen, 2016). Recent evidence shows that cathepsin L is involved in C3 cleavage of the precursor proteins into active C3a and C3b fragments (Liszewski et al., 2013). Activated complement factor is necessary for cell survival. With the reduction in cathepsin L expression in AGEs-exposed RPE cells (Sharif et al., 2018), the activation of complement factor is compromised, which leads to accumulation of drusens leading to increases in cellular inflammation (Charbel Issa et al., 2011; Brandstetter et al., 2015).

Apart from that, cathepsin L also has been associated with NF-κβ signalling pathway (Xiang et al., 2011; Wang et al., 2013; Yang et al., 2015; de Mingo et al., 2016; Xu et al., 2018). Cathepsin L expression was found to be positively correlated with level of NF-κβ in Parkinson's disease patients (Xu et al., 2018). Cathepsin L plays

a dual role in NF-κβ signaling. It can acts as either an inducer or suppressor of the NF-κβ signalling pathway. In an *in vitro* study for Parkinson's disease, neuroblastoma cells treated with neurotoxin 6-hydroxydopamine (6-OHDA) revealed an increased in cathepsin L expression in cells accompanied by increased of NF-κβ activation and reduced cell viability. Increased of NF-κβ activation was seen through increased of phosphorylated P65 and increased in Iκβα degradation (Xiang et al., 2011).

In another study, Wang et al (Wang et al., 2013) investigated the role of cathepsin L in Quinolic Acid (QA)-induced NF-κβ activation in rat striatal neurons to study neurodegeneration diseases. Again, their study also showed that increased in cathepsin L expression was accompanied by increased in P65 nuclear translocation and Iκβα degradation in QA-treated cells as compared to control cells. Inhibition of cathepsin L in cells through usage of Z-FF-FMK (inhibitor of cathepsin B and L) suppressed the QA-induced NF-κβ activation (Wang et al., 2013). Taking the two studies together, it can be concluded that cathepsin L is involved in NF-κβ activation, and inhibition of cathepsin L can reverse the effect and protect the cells from activation NF-κβ signalling.

On the other hand, the ability of cathepsin L in suppressing the NF-κβ signaling pathway was observed by Tang et al (Tang et al., 2009). Their study was focused on cardiac hyperthrophy where cathepsin L was reduced. They proposed that cathepsin L may have a neuroprotective capability through blocking of NF-κβ activation. Their data showed that, cardiac hyperthrophy is reduced in overexpressed cathepsin L mice as compared to the wild type. Furthermore, in vitro experiments using cardiomyocytes cells also showed that cathepsin L overexpression can diminished the cardiac hyperthrophy. On top of that, NF-κβ activation and inflammatory responses were also attenuated (Tang et al., 2009). In conclusion, their study showed cathepsin L blocked the NF-κβ signalling, and inhibition of cathepsin L may results in initiation of early

inflammation. The representative diagram on the dual role of cathepsin L on NF-κβ signalling regulation is shown on Figure 4.2.

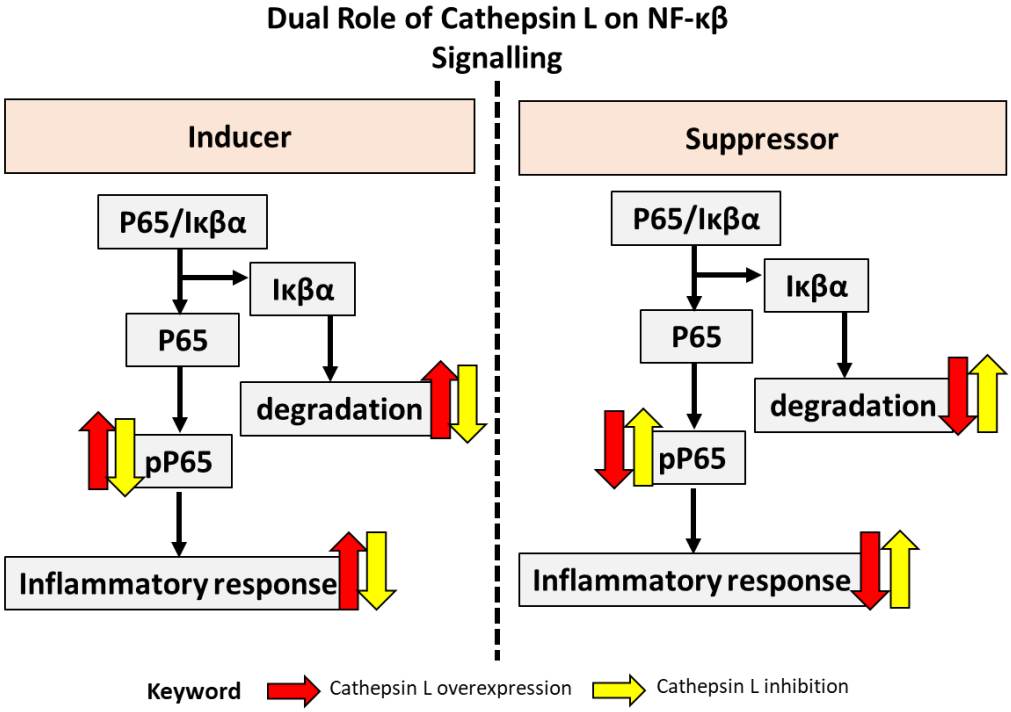

Figure 4.3 The dual role of cathepsin L in NF-κβ signalling pathway. Image was drawn based on information provided by (Tang et al., 2009; Xiang et al., 2011; Wang et al., 2013).

Taking the facts that cathepsin L was reduced in AGEs-exposed RPE cells and the possible roles of cathepsin L in NF-κβ signalling pathway as mentioned above, it is possible that the dampening of NF-κβ signalling as seen in AGEs-exposed RPE cells is due to the decreased in cathepsin L expression. Thus, we investigate the role cathepsin L on NF-κβ signalling in the RPE cells through the use of cathepsin L inhibitor. Our results show that inhibition of cathepsin L only alters the level of P65 in cells. Significant reduction in P65 expression was observed with no changes to level of pP65 and Iκβα. Observation on the ratio of pP65/P65 shows a significant increase in NF-κβ signalling in cathepsin L inhibited cells, however this overall increase in cathepsin L

inhibited cells was thought to be due to the phosphorylation of the P65 molecules to its active forms. Summary on the effect of cathepsin L inhibition on NF-κβ signalling pathway in RPE cells is shown in Figure 4.3.

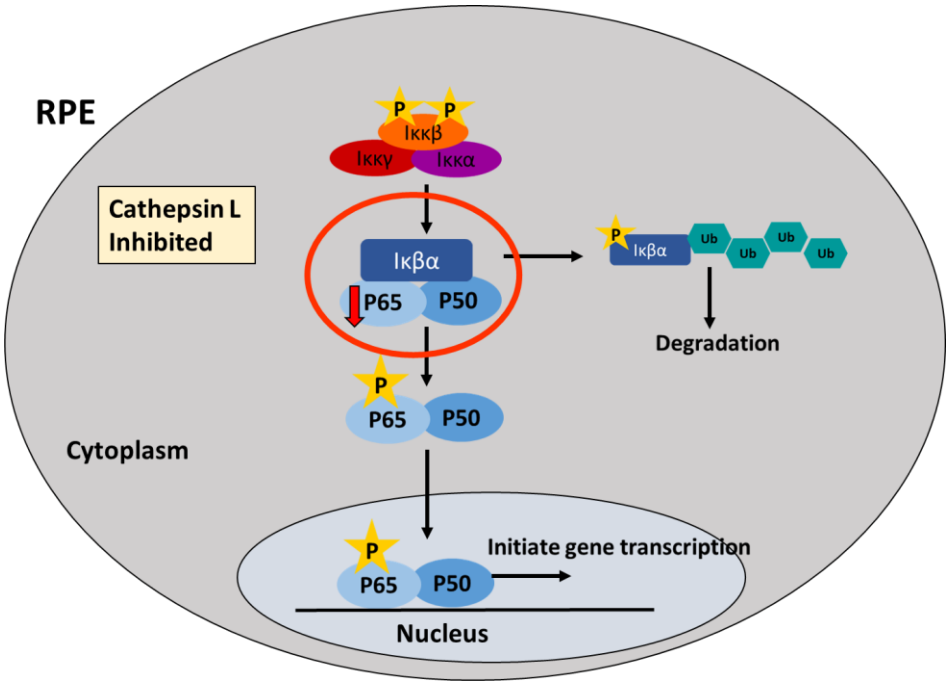

Figure 4.4 The effect of cathepsin L inhibition on NF-κβ signalling pathway. Image was from own drawing.

To further elucidate the role of cathepsin L in NF-κβ signalling in RPE cells, the cathepsin L inhibited RPE cells were stimulated with TNFα. Stimulation of cathepsin L inhibited cells with TNFα revealed an increase of P65, Iκβα and pP65 expression level. However, no changes was observed when comparing the average fold of NF-κβ activation caused by TNFα in cathepsin L inhibited cells compared to controls. These data propose that cathepsin L alone is not sufficient to make the cells more vulnerable to proinflammatory stimuli (TNFα) and inhibition of cathepsin L might exert a potential anti-inflammatory effects. Taking the data of TNFα-exposed in AGEs and cathepsin L-inhibited cells together, we anticipated that AGEs modulation in NF-κβ signalling in

RPE cells is in part due to reduction of cathepsin L. The data of the present study on effect of AGEs of NF-κβ signalling is summarized in Figure 4.4.

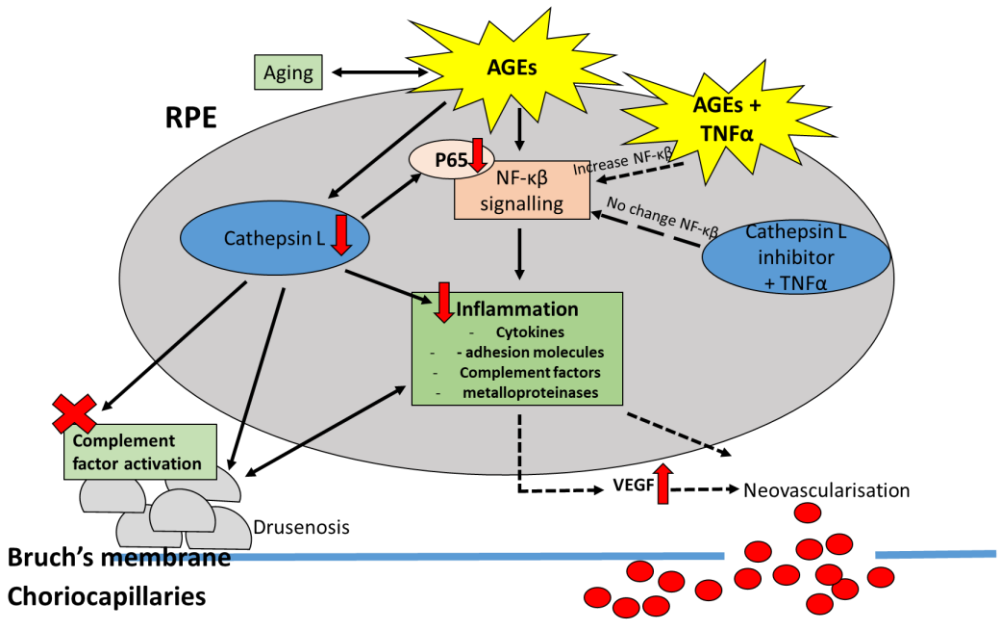

Figure 4.5 The association of cathepsin L and AGEs on NF-κβ signalling in RPE cells in regards to AMD pathogenesis. Image was from own drawing.

Further studies to elucidate the exact mechanism of cathepsin L regulation in AGEs-induced NF-κβ signalling are still needed in order to further understand the mechanism of vision loss in AMD. Cathepsin L has always been proposed to be an upstream, regulator of NF-κβ activation (Yang et al., 2015). In line with this, our study shows cathepsin L modulates the level of P65 which is one of the upstream regulator of NF-κβ signalling. However, since NF-κβ is highly dependent on its inhibitor, Iκβα, it is still possible that cathepsin L modulate NF-κβ through Iκβα proteolysis (Wang et al., 2013). However, the negative feedback loop of NF-κβ signalling in transcribing new Iκβα into the cells may occur and hence the changes in the key effector proteins may not be clearly observed (Scott et al., 1993; Chiao et al., 1994; Kearns et al., 2006; Fagerlund et al., 2015).

In addition, it is important to note that there was a study demonstrated the regulatory loop where cathepsin acts as a downstream target gene of NF-κβ signalling (Biswas et al., 2003; Wang et al., 2013). The study was carried out in murine C2C12 skeletal myoblast cells. However, this study was focused on of NF-κβ-mediated cathepsin L. Here, we are addressing the opposite, i.e. cathepsin L mediated modulation of NF-κβ signalling. The role of cathepsin L NF-κβ signalling might differ between cell types. The current changes seen in this study may only be applicable for RPE cells and not in others. Our data suggest that dampening of AGEs on NF-κβ may in part is due to the decrease in level of cathepsin L in cells, however cathepsin L most likely interacts with other complex or network to regulate NF-κβ either directly or indirectly.

4.6 Thymoquinone as possible NF-κβ signalling suppressor

Thymoquinone is a bioactive compound found in the seeds oil of Nigella sativa. Thymoquinone has been shown to exhibit anti-inflammatory properties including in reducing the inflammatory effect caused by TNFα (Sayed & Morcos, 2007; Umar et al., 2015). Thymoquinone has been shown to modulate NF-κβ in various cell lines through decrease in pP65, reduction in Iκβα degradation and suppression of the pP65 DNA binding capability in a concentration and time dependent manner (Mohamed et al., 2005; El Gazzar et al., 2007; Sayed & Morcos, 2007; Sethi et al., 2008; Velagapudi et al., 2017a). In a study on the neuroprotective effect of thymoquinone on BV2 cells, thymoquinone has been shown to inhibit NF-κβ-dependent signalling through modulation of Iκβα phosphorylation and NF-κβ binding to DNA (Velagapudi et al., 2017a). In the same study, thymoquinone was shown to inhibit LPS-induced NF-κβ in BV2 cells. To our knowledge, this is the first study carried out to evaluate the neuroprotective effect of thymoquinone on NF-κβ signalling in RPE cells. Our data indicated thymoquinone are ineffective against TNFα-induced NF-κβ activation in AGEs-exposed RPE cells. Thus, this current study cannot conclude the effect of

thymoquinone on NF-κβ signalling in RPE cells. Further study shall be carried out to elucidate the protective effect of other anti-oxidant and anti-inflammatory agent on TNFα-induced NF-κβ signalling thus suggesting a new theraupeutic target for AMD disease.

4.7 Study limitation and future research direction

ARPE-19 cell line is a spontaneously transformed cell lines derived from a 19-years old male who suffered a head trauma after a vehicle accident (Dunn et al., 1996). It is extensively used in RPE research as it has been shown to portray a normal karyotype as the normal RPE (Samuel et al., 2017). Analysis on the RPE markers also showed the presence of RPE65 and CRALBP expression in both mRNA and protein levels (Kuznetsova et al., 2014). However, some RPE features are lost in ARPE-19 cells. The most prominent one is the loss of pigmentation (Ablonczy et al., 2011; Hellinen et al., 2019). Normal RPE cells in human body are heavily pigmented, which provide antioxidant properties but ARPE-19 cells in culture loses its characteristic pigmentation (Ablonczy et al., 2011). However, it is worthwhile to note that ARPE-19 cells grown for a longer duration (4 months) is shown to developed native RPE phenotypes (Samuel et al., 2017). Although with some study reported on the differences in genetic profiling between primary RPE and ARPE-19 cell, the ARPE-19 is thought the most appropriate cells to represent RPE as it still exhibits characteristic features of a primary human RPE cells (Cai & Del Priore, 2006). In addition, ARPE-19 has been frequently used to study retinal disorder including AMD disease (Kauppinen et al., 2012; Alrashed et al., 2014; Govindaraju et al., 2017). In this project RPE cells with passage number 25-35 was used in the experiment. The maintenance of the cells was carried out strictly to ATCC recommended protocols to make sure the cells did not become senescent. Any cells that shows a different morphology and growth rate was discarded to maintain the quality of cells. Apart from that, the cells used in this study was also tested for mycoplasma

contamination on a regular basis to reduce false positive results as mycoplasma contaminated cells can compromised the cell physiology (Nikfarjam & Farzaneh, 2012).

In this study, we only investigated the role of cathepsin L in NF-κβ signalling through cathepsin L inhibition experiments. To further elucidate the important role of cathepsin L in RPE cells, we proposed to also include overexpression of cathepsin L in cells. This will further elucidate the role of cathepsin L NF-κβ signaling pathway in the ARPE-19 cells. Overexpression of cathepsin L can be performed by transfection method of the RPE cells using cathepsin L expression plasmid. The cathepsin L-expressed plasmid can also be tagged with fluorescent tag, which can be used to monitor the localisation of cathepsin L in cells, thus provides further understanding on the role of cathepsin L in RPE cells. Tagged plasmid construction protocol can be referred to the work of Tamhane et al (Tamhane et al., 2015).

We only measured the NF-κβ activation through western blotting and qPCR analysis. Three antibodies were used in western blotting which are P65, Iκβα and pP65 which are the main key player of the signalling pathway. It would also be good to include other player of NF-κβ in order to fully understand the changes in the signalling pathway such as IKKs, and different phosphorylation site of P65. Apart from Ser536, P65 subunit has 10 other phosphorylation sites, however, Ser536 and Ser276 are the two best understood phosphorylation sites (Christian et al., 2016). The reason we chose Ser536 site in this study is because the Ser536 phosphorylation site was shown to be associate with apoptosis in cells. In addition, TNFα-induced NF-κβ activation also was shown to be associated with Ser536 phosphorylation site (Moreno et al., 2010). Different phosphorylation sites are reported to affect different biological processes. Activation at Ser536 was shown to be involved in apoptosis and cell growth. Meanwhile activation at Ser276 leads to inhibition of apoptosis (Christian et al., 2016).

Although thymoquinone has been shown to protect other cells from NF-κβ signalling, the reaction was ineffective in RPE cells. It would be possible also to test other antioxidant such as ascorbic acid (Cárcamo et al., 2002) and beta-carotene (Palozza et al., 2003). The ascorbic acid has been shown to attenuate oxidative stress level in diabetic aged-rats (Yin et al., 2011; Wei et al., 2014). Carcamo et al (Cárcamo et al., 2002) reported that ascorbic acid inhibits TNFα-induced activation of NF-κβ in few cell lines: HeLa, monocytic U937, myeloid leukemia HL-60, breast MCF-7 and primary endothelial HUVEC cells, in a dose dependent manner through inhibition of Iκβα phosphorylation, thus reducing the level of phosphorylated NF-κβ in cells. In addition, beta carotene also has been demonstrated to suppress NF-κβ activation in LPS-stimulated macrophages through blocking of P65 nuclear translocation and inhibiting the Iκβα phosphorylation and degradation (Bai et al., 2005).

Finally, with the important function of RPE in phagocytosis of photoreceptor outer segment and autophagy, the next research direction can be focused to see the effect the AGEs models on these two cellular events. This may shed further light in understanding the relationship of cathepsin L and AGEs accumulation in this AMD cell culture model.

CHAPTER 5: CONCLUSION

In summary, NF-κβ signalling pathway is reduced when exposed to AGEs and this response is exaggerated with TNFα stimulation. The increased susceptibility of ARPE-19 cells exposed to AGEs to pro-inflammatory stimuli suggests that senescent cells appear to be more susceptible to damage, and this explains the AMD development in the elderly. In view of the findings that showed AGEs downregulates cathepsin L in RPE cells, and both the AGEs and cathepsin L are involved in NF-κβ signalling pathway, we evaluated the role of cathepsin L in NF-κβ signalling pathway in AGEs-exposed RPE cells. Our results showed that the role of cathepsin L in the NF-κβ signalling in RPE cells is through modulation of P65 level. Inhibition of cathepsin L cause a significant reduction in P65 expression and reduce the response to TNFα stimulation. However, cathepsin L alone was not able to make cells more susceptible towards pro-inflammatory stimuli as seen in AGEs-exposed cells. Thus, we conclude the changes seen in NF-κβ signalling on AGEs–exposed RPE cells is in part due to the downregulation of cathepsin L in cells. However, studies working to elucidate the exact mechanisms involved in cathepsin L regulation of NF-κB pathway regulation are still required. Further understanding on how cathepsin L is involved in NF-κβ may provide new insights into the development of AMD. Lastly, thymoquinone did not show any significant effects on the NF-κβ pathway. Taking these data together, we shows the involvement of cathepsin L in NF-κβ signalling pathway in RPE cells in relation to ageing and AMD. These data provide a new insight linking age-related stressors, particularly AGEs, to cathepsin L and NF-kB signalling pathway in RPE cells, thus to provide a deeper understanding of the pathogenesis of AMD disease.

REFERENCES

Abdelsalam, A., Del Priore, L., & Zarbin, M. A. (1999). Drusen in age-related macular degeneration: pathogenesis, natural course, and laser photocoagulation-induced regression. *Surv Ophthalmol, 44*(1), 1-29.

Ablonczy, Z., Dahrouj, M., & Marneros, A. G. (2014). Progressive dysfunction of the retinal pigment epithelium and retina due to increased VEGF-A levels. *Faseb j, 28*(5), 2369-2379. doi:10.1096/fj.13-248021

Ablonczy, Z., Dahrouj, M., Tang, P. H., Liu, Y., Sambamurti, K., Marmorstein, A. D., & Crosson, C. E. (2011). Human Retinal Pigment Epithelium Cells as Functional Models for the RPE In Vivo. *Investigative ophthalmology & visual science, 52*(12), 8614-8620. doi:10.1167/iovs.11-8021

Ahmed, N. (2005). Advanced glycation endproducts—role in pathology of diabetic complications. *Diabetes Research and Clinical Practice, 67*(1), 3-21. doi:http://dx.doi.org/10.1016/j.diabres.2004.09.004

Al-Gayyar, M. M., & Elsherbiny, N. M. (2013). Contribution of TNF-alpha to the development of retinal neurodegenerative disorders. *Eur Cytokine Netw, 24*(1), 27-36. doi:10.1684/ecn.2013.0334

Alexopoulou, L., Holt, A. C., Medzhitov, R., & Flavell, R. A. (2001). Recognition of double-stranded RNA and activation of NF-[kappa]B by Toll-like receptor 3. *Nature, 413*(6857), 732-738.

Alizadeh, P., Smit-McBride, Z., Oltjen, S. L., & Hjelmeland, L. M. (2006). Regulation of cysteine cathepsin expression by oxidative stress in the retinal pigment epithelium/choroid of the mouse. *Exp Eye Res, 83*(3), 679-687.

Alrashed, F., Bennett, A., Kerr, I., & Foss, A. (2014). Use of ARPE-19 cell line as an in-vitro model for age related macular degeneration. *Investigative ophthalmology & visual science, 55*(13), 628-628.

Anderson, D. H., Radeke, M. J., Gallo, N. B., Chapin, E. A., Johnson, P. T., Curletti, C. R., . . . Johnson, L. V. (2010). The pivotal role of the complement system in aging and age-related macular degeneration: hypothesis re-visited. *Prog Retin Eye Res, 29*(2), 95-112. doi:10.1016/j.preteyeres.2009.11.003

Ansari, M. W., & Nadeem, A. (2016). *Atlas of ocular anatomy*: Springer.

Ao, J., Wood, J. P., Chidlow, G., Gillies, M. C., & Casson, R. J. (2018). Retinal pigment epithelium in the pathogenesis of age-related macular degeneration and photobiomodulation as a potential therapy? *Clin Exp Ophthalmol, 46*(6), 670-686. doi:10.1111/ceo.13121

Appelqvist, H., Wäster, P., Kågedal, K., & Öllinger, K. (2013). The lysosome: from waste bag to potential therapeutic target. *Journal of molecular cell biology, 5*(4), 214-226.

Aradhya, S., & Nelson, D. L. (2001). NF-κB signaling and human disease. *Current Opinion in Genetics & Development, 11*(3), 300-306. doi:http://doi.org/10.1016/S0959-437X(00)00194-5

Arjamaa, O., Nikinmaa, M., Salminen, A., & Kaarniranta, K. (2009). Regulatory role of HIF-1α in the pathogenesis of age-related macular degeneration (AMD). *Ageing Research Reviews, 8*(4), 349-358. doi:https://doi.org/10.1016/j.arr.2009.06.002

Ayoub, T., & Patel, N. (2009). Age-related macular degeneration. *Journal of the Royal Society of Medicine, 102*(2), 56-61. doi:10.1258/jrsm.2009.080298

Badary, O. A., Taha, R. A., Gamal El-Din, A. M., & Abdel-Wahab, M. H. (2003). Thymoquinone Is a Potent Superoxide Anion Scavenger. *Drug and Chemical Toxicology, 26*(2), 87-98. doi:10.1081/DCT-120020404

Bai, S.-K., Lee, S.-J., Na, H.-J., Ha, K.-S., Han, J.-A., Lee, H., . . . Kim, Y.-M. (2005). β-Carotene inhibits inflammatory gene expression in lipopolysaccharide-stimulated macrophages by suppressing redox-based NF-κB activation. *Experimental &Amp; Molecular Medicine, 37*, 323. doi:10.1038/emm.2005.42

Barquet, L. A. (2015). [Role of VEGF in diseases of the retina]. *Arch Soc Esp Oftalmol, 90 Suppl 1*, 3-5. doi:10.1016/s0365-6691(15)30002-2

Basta, G., Lazzerini, G., Massaro, M., Simoncini, T., Tanganelli, P., Fu, C., . . . De Caterina, R. (2002). Advanced Glycation End Products Activate Endothelium Through Signal-Transduction Receptor RAGE. *A Mechanism for Amplification of Inflammatory Responses, 105*(7), 816-822. doi:10.1161/hc0702.104183

Basta, G., Schmidt, A. M., & De Caterina, R. (2004). Advanced glycation end products and vascular inflammation: implications for accelerated atherosclerosis in diabetes. *Cardiovasc Res, 63*(4), 582-592. doi:10.1016/j.cardiores.2004.05.001

Bazan, N. G. (2007). Homeostatic Regulation of Photoreceptor Cell Integrity: Significance of the Potent Mediator Neuroprotectin D1 Biosynthesized from Docosahexaenoic Acid The Proctor Lecture. *Investigative ophthalmology & visual science, 48*(11), 4866-4881. doi:10.1167/iovs.07-0918

Beatty, S., Koh, H.-H., Phil, M., Henson, D., & Boulton, M. (2000). The role of oxidative stress in the pathogenesis of age-related macular degeneration. *Survey of ophthalmology, 45*(2), 115-134.

Beg, A. A., & Baldwin, A. S. (1993). The I kappa B proteins: multifunctional regulators of Rel/NF-kappa B transcription factors. *Genes & development, 7*(11), 2064-2070.

Beg, A. A., & Baltimore, D. (1996). An essential role for NF-kB in preventing TNF-alpha-induced cell death. *Science, 274*(5288), 782.

Berman, E. R. (1994). Retinal pigment epithelium: lysosomal enzymes and aging. *Br J Ophthalmol, 78*(2), 82-83.

Besharse, J. C., Hollyfield, J. G., & Rayborn, M. E. (1977). Photoreceptor outer segments: accelerated membrane renewal in rods after exposure to light. *Science, 196*(4289), 536-538.

Bhatia, S. K., Rashid, A., Chrenek, M. A., Zhang, Q., Bruce, B. B., Klein, M., . . . Nickerson, J. M. (2016). Analysis of RPE morphometry in human eyes. *Mol Vis, 22*, 898-916.

Bhattacharya, S., Chaum, E., Johnson, D. A., & Johnson, L. R. (2012). Age-related susceptibility to apoptosis in human retinal pigment epithelial cells is triggered by disruption of p53–Mdm2 association. *Investigative ophthalmology & visual science, 53*(13), 8350-8366.

Bhutto, I., & Lutty, G. (2012). Understanding age-related macular degeneration (AMD): Relationships between the photoreceptor/retinal pigment epithelium/Bruch's membrane/choriocapillaris complex. *Molecular aspects of medicine, 33*(4), 295-317. doi:http://doi.org/10.1016/j.mam.2012.04.005

Bhutto, I. A., McLeod, D. S., Hasegawa, T., Kim, S. Y., Merges, C., Tong, P., & Lutty, G. A. (2006). Pigment epithelium-derived factor (PEDF) and vascular endothelial growth factor (VEGF) in aged human choroid and eyes with age-related macular degeneration. *Exp Eye Res, 82*(1), 99-110. doi:10.1016/j.exer.2005.05.007

Bian, Q., Gao, S., Zhou, J., Qin, J., Taylor, A., Johnson, E. J., . . . Shang, F. (2012). Lutein and zeaxanthin supplementation reduces photooxidative damage and modulates the expression of inflammation-related genes in retinal pigment epithelial cells. *Free Radical Biology and Medicine, 53*(6), 1298-1307. doi:http://dx.doi.org/10.1016/j.freeradbiomed.2012.06.024

Bierhaus, A., Chevion, S., Chevion, M., Hofmann, M., Quehenberger, P., Illmer, T., . . . Nawroth, P. P. (1997). Advanced glycation end product-induced activation of NF-kappaB is suppressed by alpha-lipoic acid in cultured endothelial cells. *Diabetes, 46*(9), 1481-1490.

Bierhaus, A., Humpert, P. M., Morcos, M., Wendt, T., Chavakis, T., Arnold, B., . . . Nawroth, P. P. (2005). Understanding RAGE, the receptor for advanced glycation end products. *Journal of Molecular Medicine, 83*(11), 876-886. doi:10.1007/s00109-005-0688-7

Bierhaus, A., Schiekofer, S., Schwaninger, M., Andrassy, M., Humpert, P. M., Chen, J., . . . Nawroth, P. P. (2001). Diabetes-associated sustained activation of the transcription factor nuclear factor-kappaB. *Diabetes, 50*(12), 2792-2808.

Biesemeier, A., Schraermeyer, U., & Eibl, O. (2011). Chemical composition of melanosomes, lipofuscin and melanolipofuscin granules of human RPE tissues. *Exp Eye Res, 93*(1), 29-39. doi:10.1016/j.exer.2011.04.004

Bird, A. (1993). Choroidal neovascularisation in age-related macular disease. *Br J Ophthalmol, 77*(10), 614.

Biswas, G., Anandatheerthavarada, H. K., Zaidi, M., & Avadhani, N. G. (2003). Mitochondria to nucleus stress signaling: a distinctive mechanism of NFκB/Rel activation through calcineurin-mediated inactivation of IκBβ. *The Journal of cell biology, 161*(3), 507-519. doi:10.1083/jcb.200211104

Boesze-Battaglia, K., & Goldberg, A. F. X. (2002). Photoreceptor renewal: a role for peripherin/rds. *International review of cytology, 217*, 183-225. doi:10.1016/s0074-7696(02)17015-x

Bokov, A., Chaudhuri, A., & Richardson, A. (2004). The role of oxidative damage and stress in aging. *Mech Ageing Dev, 125*(10-11), 811-826. doi:10.1016/j.mad.2004.07.009

Bonilha, V. L. (2008). Age and disease-related structural changes in the retinal pigment epithelium. *Clinical Ophthalmology (Auckland, N.Z.), 2*(2), 413-424. doi:10.2147/opth.s2151

Bosch, E., Horwitz, J., & Bok, D. (1993). Phagocytosis of outer segments by retinal pigment epithelium: phagosome-lysosome interaction. *Journal of Histochemistry & Cytochemistry, 41*(2), 253-263. doi:doi:10.1177/41.2.8419462

Boulton, M., & Dayhaw-Barker, P. (2001). The role of the retinal pigment epithelium: Topographical variation and ageing changes. *Eye, 15*(3), 384-389.

Boulton, M., Docchio, F., Dayhaw-Barker, P., Ramponi, R., & Cubeddu, R. (1990). Age-related changes in the morphology, absorption and fluorescence of melanosomes and lipofuscin granules of the retinal pigment epithelium. *Vision Research, 30*(9), 1291-1303. doi:http://doi.org/10.1016/0042-6989(90)90003-4

Boulton, M., & Wassell, J. (1998). Ageing of the human retinal pigment epithelium. In *Retinal pigment epithelium and macular diseases* (pp. 19-28): Springer.

Boulton, M. E. (2013). Ageing of the Retina and Retinal Pigment Epithelium. In F. G. Holz, D. Pauleikhoff, R. F. Spaide, & A. C. Bird (Eds.), *Age-related Macular Degeneration* (pp. 45-63). Berlin, Heidelberg: Springer Berlin Heidelberg.

Boulton, M. E. (2014). Studying melanin and lipofuscin in RPE cell culture models. *Exp Eye Res, 126*, 61-67. doi:10.1016/j.exer.2014.01.016

Bowes Rickman, C., Farsiu, S., Toth, C. A., & Klingeborn, M. (2013). Dry age-related macular degeneration: mechanisms, therapeutic targets, and imaging. *Investigative ophthalmology & visual science, 54*(14), ORSF68-ORSF80. doi:10.1167/iovs.13-12757

Brandstetter, C., Holz, F. G., & Krohne, T. U. (2015). Complement component C5a primes retinal pigment epithelial cells for inflammasome activation by lipofuscin-mediated photooxidative damage. *Journal of Biological Chemistry*, jbc. M115. 671180.

Brasier, A. R. (2006). The NF-κB regulatory network. *Cardiovascular Toxicology, 6*(2), 111-130. doi:10.1385/ct:6:2:111

Brasier, A. R., Lu, M., Hai, T., Lu, Y., & Boldogh, I. (2001). NF-κB-inducible BCL-3 expression is an autoregulatory loop controlling nuclear p50/NF-κB1 residence. *Journal of Biological Chemistry, 276*(34), 32080-32093.

Bressler, N. M., Bressler, S. B., & Fine, S. L. (1988). Age-related macular degeneration. *Survey of ophthalmology, 32*(6), 375-413.

Bridges, C. D., Alvarez, R. A., & Fong, S. L. (1982). Vitamin A in human eyes: amount, distribution, and composition. *Investigative ophthalmology & visual science, 22*(6), 706-714.

Bringmann, A., Pannicke, T., Grosche, J., Francke, M., Wiedemann, P., Skatchkov, S. N., . . . Reichenbach, A. (2006). Muller cells in the healthy and diseased retina. *Prog Retin Eye Res, 25*(4), 397-424. doi:10.1016/j.preteyeres.2006.05.003

Brix, K., Dunkhorst, A., Mayer, K., & Jordans, S. (2008). Cysteine cathepsins: cellular roadmap to different functions. *Biochimie, 90*(2), 194-207. doi:10.1016/j.biochi.2007.07.024

Brömme, D., & Wilson, S. (2011). Role of cysteine cathepsins in extracellular proteolysis. In *Extracellular matrix degradation* (pp. 23-51): Springer.

Brunk, U. T., & Terman, A. (2002). Lipofuscin: mechanisms of age-related accumulation and influence on cell function12. *Free Radical Biology and Medicine, 33*(5), 611-619. doi:http://dx.doi.org/10.1016/S0891-5849(02)00959-0

Budancamanak, M., Kanter, M., Demirel, A., Ocakci, A., Uysal, H., & Karakaya, C. (2006). Protective effects of thymoquinone and methotrexate on the renal injury in collagen-induced arthritis. *Archives of Toxicology, 80*(11), 768-776. doi:10.1007/s00204-006-0094-0

Bulloj, A., Duan, W., & Finnemann, S. C. (2013). PI 3-kinase independent role for AKT in F-actin regulation during outer segment phagocytosis by RPE cells. *Exp Eye Res, 113*, 9-18. doi:10.1016/j.exer.2013.05.002

Burton, G. J., & Jauniaux, E. (2011). Oxidative stress. *Best Practice & Research Clinical Obstetrics & Gynaecology, 25*(3), 287-299.

Buschini, E., Piras, A., Nuzzi, R., & Vercelli, A. (2011). Age related macular degeneration and drusen: Neuroinflammation in the retina. *Progress in Neurobiology, 95*(1), 14-25. doi:10.1016/j.pneurobio.2011.05.011

Cai, H., & Del Priore, L. V. (2006). Gene expression profile of cultured adult compared to immortalized human RPE. *Mol Vis, 12*, 1-14.

Carballo, E., Lai, W. S., & Blackshear, P. J. (1998). Feedback inhibition of macrophage tumor necrosis factor-α production by tristetraprolin. *Science, 281*(5379), 1001-1005.

Cárcamo, J. M., Pedraza, A., Bórquez-Ojeda, O., & Golde, D. W. (2002). Vitamin C Suppresses TNFα-Induced NFκB Activation by Inhibiting IκBα Phosphorylation. *Biochemistry, 41*(43), 12995-13002. doi:10.1021/bi0263210

Cardozo, A. K., Heimberg, H., Heremans, Y., Leeman, R., Kutlu, B., Kruhøffer, M., . . . Eizirik, D. L. (2001). A comprehensive analysis of cytokine-induced and nuclear factor-κB-dependent genes in primary rat pancreatic β-cells. *Journal of Biological Chemistry, 276*(52), 48879-48886.

Carmona-Gutierrez, D., Hughes, A. L., Madeo, F., & Ruckenstuhl, C. (2016). Review: The crucial impact of lysosomes in aging and longevity. *Ageing Research Reviews, 32*, 2-12. doi:10.1016/j.arr.2016.04.009

Carpentier, S., Knaus, M., & Suh, M. (2009). Associations between Lutein, Zeaxanthin, and Age-Related Macular Degeneration: An Overview. *Critical Reviews in Food Science and Nutrition, 49*(4), 313-326. doi:10.1080/10408390802066979

Cavallotti, C., & Cerulli, L. (2008). *Age-related changes of the human eye*: Springer Science & Business Media.

Cejka, C., & Cejkova, J. (2015). Oxidative stress to the cornea, changes in corneal optical properties, and advances in treatment of corneal oxidative injuries. *Oxidative Medicine and Cellular Longevity, 2015*.

Cha, H. S., Bae, E. K., Koh, J. H., Chai, J. Y., Jeon, C. H., Ahn, K. S., . . . Koh, E. M. (2007). Tumor necrosis factor-alpha induces vascular endothelial growth factor-C expression in rheumatoid synoviocytes. *J Rheumatol, 34*(1), 16-19.

Chalam, K. V., Khetpal, V., Rusovici, R., & Balaiya, S. (2011). A review: role of ultraviolet radiation in age-related macular degeneration. *Eye Contact Lens, 37*(4), 225-232. doi:10.1097/ICL.0b013e31821fbd3e

Chang, J.-B., Chu, N.-F., Syu, J.-T., Hsieh, A.-T., & Hung, Y.-R. (2011). Advanced glycation end products (AGEs) in relation to atherosclerotic lipid profiles in middle-aged and elderly diabetic patients. *Lipids in Health and Disease, 10*(1), 228. doi:10.1186/1476-511X-10-228

Chapman, N. A., Jacobs, R. J., & Braakhuis, A. J. (2019). Role of diet and food intake in age-related macular degeneration: a systematic review. *Clin Exp Ophthalmol, 47*(1), 106-127. doi:10.1111/ceo.13343

Charbel Issa, P., Chong, N. V., & Scholl, H. P. N. (2011). The significance of the complement system for the pathogenesis of age-related macular degeneration - current evidence and translation into clinical application. *Graefe's archive for clinical and experimental ophthalmology = Albrecht von Graefes Archiv fur klinische und experimentelle Ophthalmologie, 249*(2), 163-174. doi:10.1007/s00417-010-1568-6

Chavakis, T., Bierhaus, A., & Nawroth, P. P. (2004). RAGE (receptor for advanced glycation end products): a central player in the inflammatory response. *Microbes and Infection, 6*(13), 1219-1225. doi:http://dx.doi.org/10.1016/j.micinf.2004.08.004

Chehl, N., Chipitsyna, G., Gong, Q., Yeo, C. J., & Arafat, H. A. (2009). Anti-inflammatory effects of the Nigella sativa seed extract, thymoquinone, in pancreatic cancer cells. *HPB, 11*(5), 373-381. doi:10.1111/j.1477-2574.2009.00059.x

Chen, J., Jing, J., Yu, S., Song, M., Tan, H., Cui, B., & Huang, L. (2016a). Advanced glycation endproducts induce apoptosis of endothelial progenitor cells by activating receptor RAGE and NADPH oxidase/JNK signaling axis. *American journal of translational research, 8*(5), 2169-2178.

Chen, L., Yang, P., & Kijlstra, A. (2002). Distribution, markers, and functions of retinal microglia. *Ocul Immunol Inflamm, 10*(1), 27-39.

Chen, M., Rajapakse, D., Fraczek, M., Luo, C., Forrester, J. V., & Xu, H. (2016b). Retinal pigment epithelial cell multinucleation in the aging eye - a mechanism to repair damage and maintain homoeostasis. *Aging Cell, 15*(3), 436-445. doi:10.1111/acel.12447

Cheung, L. K., & Eaton, A. (2013). Age-Related Macular Degeneration. *Pharmacotherapy: The Journal of Human Pharmacology and Drug Therapy, 33*(8), 838-855.

Chiao, P. J., Miyamoto, S., & Verma, I. M. (1994). Autoregulation of I kappa B alpha activity. *Proc Natl Acad Sci U S A, 91*(1), 28-32.

Chong, N. H. V., Keonin, J., Luthert, P. J., Frennesson, C. I., Weingeist, D. M., Wolf, R. L., . . . Hageman, G. S. (2005). Decreased thickness and integrity of the macular elastic layer of Bruch's membrane correspond to the distribution of lesions associated with age-related macular degeneration. *Am J Pathol, 166*(1), 241-251. doi:10.1016/S0002-9440(10)62248-1

Christian, F., Smith, E. L., & Carmody, R. J. (2016). The Regulation of NF-kappaB Subunits by Phosphorylation. *Cells, 5*(1). doi:10.3390/cells5010012

Chrzanowska, M., Modrzejewska, A., & Modrzejewska, M. (2018). New insight into the role of the complement in the most common types of retinopathy-current literature review. *International journal of ophthalmology, 11*(11), 1856-1864. doi:10.18240/ijo.2018.11.19

Cui, H., Kong, Y., & Zhang, H. (2012). Oxidative stress, mitochondrial dysfunction, and aging. *Journal of signal transduction, 2012*, 646354-646354. doi:10.1155/2012/646354

Curcio, C. A., & Johnson, M. (2013). Structure, function, and pathology of Bruch's membrane. *Retina, 1*(Part 2), 466-481.

Datta, S., Cano, M., Ebrahimi, K., Wang, L., & Handa, J. T. (2017). The impact of oxidative stress and inflammation on RPE degeneration in non-neovascular AMD. *Progress in retinal and eye research, 60*, 201-218. doi:10.1016/j.preteyeres.2017.03.002

de Duve, C., Pressman, B. C., Gianetto, R., Wattiaux, R., & Appelmans, F. (1955). Tissue fractionation studies. 6. Intracellular distribution patterns of enzymes in rat-liver tissue. *Biochemical Journal, 60*(4), 604-617.

de Mingo, A., de Gregorio, E., Moles, A., Tarrats, N., Tutusaus, A., Colell, A., . . . Mari, M. (2016). Cysteine cathepsins control hepatic NF-kappaB-dependent inflammation via sirtuin-1 regulation. *Cell Death Dis, 7*(11), e2464. doi:10.1038/cddis.2016.368

DeGroot, J., Bank, R. A., Bijlsma, J. W. J., TeKoppele, J. M., Verzijl, N., & Lafeber, F. (2004). Advanced glycation endproducts in the development of osteoarthritis. *Arthritis Res Ther, 6*(Suppl 3), 78-78. doi:10.1186/ar1414

Del Priore, L. V., Kuo, Y.-H., & Tezel, T. H. (2002). Age-Related Changes in Human RPE Cell Density and Apoptosis Proportion In Situ. *Investigative ophthalmology & visual science, 43*(10), 3312-3318.

Delcourt, C., Carrière, I., Ponton-Sanchez, A., Fourrey, S., Lacroux, A., Papoz, L., & Group, f. t. P. S. (2001). Light Exposure and the Risk of Age-Related Macular Degeneration: The Pathologies Oculaires Liées à l'Age (POLA) Study. *JAMA Ophthalmology, 119*(10), 1463-1468. doi:10.1001/archopht.119.10.1463

DelMonte, D. W., & Kim, T. (2011). Anatomy and physiology of the cornea. *Journal of Cataract & Refractive Surgery, 37*(3), 588-598.

Delori, F. C., Goger, D. G., & Dorey, C. K. (2001). Age-related accumulation and spatial distribution of lipofuscin in RPE of normal subjects. *Invest Ophthalmol Vis Sci, 42*(8), 1855-1866.

Derk, J., MacLean, M., Juranek, J., & Schmidt, A. M. (2018). The Receptor for Advanced Glycation Endproducts (RAGE) and Mediation of Inflammatory Neurodegeneration. *Journal of Alzheimer's disease & Parkinsonism, 8*(1), 421. doi:10.4172/2161-0460.1000421

Ding, H., Ji, X., Chen, R., Ma, T., Tang, Z., Fen, Y., & Cai, H. (2015). Antifibrotic properties of receptor for advanced glycation end products in idiopathic pulmonary fibrosis. *Pulm Pharmacol Ther, 35*, 34-41. doi:10.1016/j.pupt.2015.10.010

Donato, A. J., Black, A. D., Jablonski, K. L., Gano, L. B., & Seals, D. R. (2008). Aging is associated with greater nuclear NF kappa B, reduced I kappa B alpha, and increased expression of proinflammatory cytokines in vascular endothelial cells of healthy humans. *Aging Cell, 7*(6), 805-812. doi:10.1111/j.1474-9726.2008.00438.x

Donato, A. J., Eskurza, I., Silver, A. E., Levy, A. S., Pierce, G. L., Gates, P. E., & Seals, D. R. (2007). Direct evidence of endothelial oxidative stress with aging in humans: relation to impaired endothelium-dependent dilation and upregulation of nuclear factor-kappaB. *Circ Res, 100*(11), 1659-1666. doi:10.1161/01.RES.0000269183.13937.e8

Donoso, L. A., Kim, D., Frost, A., Callahan, A., & Hageman, G. (2006). The role of inflammation in the pathogenesis of age-related macular degeneration. *Surv Ophthalmol, 51*(2), 137-152. doi:10.1016/j.survophthal.2005.12.001

Drenth, H., Zuidema, S. U., Krijnen, W. P., Bautmans, I., van der Schans, C., & Hobbelen, H. (2017). Association between advanced glycation end-products and functional performance in Alzheimer's disease and mixed dementia. *Int Psychogeriatr, 29*(9), 1525-1534. doi:10.1017/s1041610217000886

Dunaief, J. L., Dentchev, T., Ying, G.-S., & Milam, A. H. (2002). The Role of Apoptosis in Age-Related Macular Degeneration. *JAMA Ophthalmology, 120*(11), 1435-1442. doi:10.1001/archopht.120.11.1435

Dunn, K., Aotaki-Keen, A., Putkey, F., & Hjelmeland, L. (1996). ARPE-19, a human retinal pigment epithelial cell line with differentiated properties. *Exp Eye Res, 62*(2), 155-170.

El-Hifnawi, E., BenEzra, D., Reichenbach, A., & Hettlich, H. J. (1995). Distribution of cathepsin D in human ocular tissue: An immunohistochemical study. *Annals of Anatomy - Anatomischer Anzeiger, 177*(6), 515-523. doi:https://doi.org/10.1016/S0940-9602(11)80083-X

El Gazzar, M., El Mezayen, R., Marecki, J. C., Nicolls, M. R., Canastar, A., & Dreskin, S. C. (2006). Anti-inflammatory effect of thymoquinone in a mouse model of allergic lung inflammation. *International Immunopharmacology, 6*(7), 1135-1142. doi:http://dx.doi.org/10.1016/j.intimp.2006.02.004

El Gazzar, M. A., El Mezayen, R., Nicolls, M. R., & Dreskin, S. C. (2007). Thymoquinone attenuates proinflammatory responses in lipopolysaccharide-activated mast cells by modulating NF-kappaB nuclear transactivation. *Biochimica et Biophysica Acta (BBA) - General Subjects, 1770*(4), 556-564. doi:http://dx.doi.org/10.1016/j.bbagen.2007.01.002

Euler, T., Haverkamp, S., Schubert, T., & Baden, T. (2014). Retinal bipolar cells: elementary building blocks of vision. *Nature Reviews Neuroscience, 15*, 507. doi:10.1038/nrn3783

https://www.nature.com/articles/nrn3783#supplementary-information

Fagerlund, R., Behar, M., Fortmann, K. T., Lin, Y. E., Vargas, J. D., & Hoffmann, A. (2015). Anatomy of a negative feedback loop: the case of IkBa. *JR Soc. Interface, 12*(110), 1-8.

Farazdaghi, M. K., & Ebrahimi, K. B. (2019). Role of the Choroid in Age-related Macular Degeneration: A Current Review. *Journal of ophthalmic & vision research, 14*(1), 78-87. doi:10.4103/jovr.jovr_125_18

Feeney-Burns, L., Hilderbrand, E. S., & Eldridge, S. (1984). Aging human RPE: morphometric analysis of macular, equatorial, and peripheral cells. *Invest Ophthalmol Vis Sci, 25*(2), 195-200.

Ferrington, D. A., Sinha, D., & Kaarniranta, K. (2016). Defects in retinal pigment epithelial cell proteolysis and the pathology associated with age-related macular degeneration. *Progress in retinal and eye research, 51*, 69-89. doi:https://doi.org/10.1016/j.preteyeres.2015.09.002

Filocamo, M., & Morrone, A. (2011). Lysosomal storage disorders: Molecular basis and laboratory testing. *Human genomics, 5*, 156-169. doi:10.1186/1479-7364-5-3-156

Finnemann, S. C., Bonilha, V. L., Marmorstein, A. D., & Rodriguez-Boulan, E. (1997). Phagocytosis of rod outer segments by retinal pigment epithelial cells requires alpha(v)beta5 integrin for binding but not for internalization. *Proc Natl Acad Sci U S A, 94*(24), 12932-12937.

Flatt, T. (2012). A new definition of aging? *Frontiers in genetics, 3*, 148-148. doi:10.3389/fgene.2012.00148

Fletcher, D. C., Schuchard, R. A., & Renninger, L. W. (2012). Patient Awareness of Binocular Central Scotoma in Age-Related Macular Degeneration. *Optometry and Vision Science, 89*(9), 1395-1398. doi:10.1097/OPX.0b013e318264cc77

Folgar, F. A., Yuan, E. L., Sevilla, M. B., Chiu, S. J., Farsiu, S., Chew, E. Y., & Toth, C. A. (2016). Drusen Volume and Retinal Pigment Epithelium Abnormal Thinning Volume Predict 2-Year Progression of Age-Related Macular Degeneration. *Ophthalmology, 123*(1), 39-50.e31. doi:10.1016/j.ophtha.2015.09.016

Ford, K. M., Saint-Geniez, M., Walshe, T., Zahr, A., & D'Amore, P. A. (2011). Expression and role of VEGF in the adult retinal pigment epithelium. *Investigative ophthalmology & visual science, 52*(13), 9478-9487. doi:10.1167/iovs.11-8353

Fraser-Bell, S., Donofrio, J., Wu, J., Klein, R., Azen, S. P., & Varma, R. (2005). Sociodemographic factors and age-related macular degeneration in Latinos: the Los Angeles Latino Eye Study. *Am J Ophthalmol, 139*(1), 30-38. doi:10.1016/j.ajo.2004.08.029

Fraternale, A., Crinelli, R., Casabianca, A., Paoletti, M. F., Orlandi, C., Carloni, E., . . . Magnani, M. (2013). Molecules Altering the Intracellular Thiol Content Modulate NF-kB and STAT-1/IRF-1 Signalling Pathways and IL-12 p40 and IL-27 p28 Production in Murine Macrophages. *PLoS One, 8*(3), e57866. doi:10.1371/journal.pone.0057866

Friedman, D. S., O'colmain, B., Munoz, B., Tomany, S., McCarty, C., De Jong, P., . . . Kempen, J. (2004). Prevalence of age-related macular degeneration in the United States. *Arch ophthalmol, 122*(4), 564-572.

Friedrichson, T., Kalbach, H. L., Buck, P., & van Kuijk, F. J. (1995). Vitamin E in macular and peripheral tissues of the human eye. *Curr Eye Res, 14*(8), 693-701. doi:10.3109/02713689508998497

Frohlich, S. J. (2005). [Age-related macula degeneration and diabetic retinopathy -- differences in optic rehabilitation]. *Klin Monbl Augenheilkd, 222*(4), 337-341. doi:10.1055/s-2005-858089

Gao, H., & Hollyfield, J. G. (1992). Aging of the human retina. Differential loss of neurons and retinal pigment epithelial cells. *Invest Ophthalmol Vis Sci, 33*(1), 1-17.

Garhart, C., & Lakshminarayanan, V. (2012). Anatomy of the Eye. In J. Chen, W. Cranton, & M. Fihn (Eds.), *Handbook of Visual Display Technology* (pp. 73-83): Springer Berlin Heidelberg.

Gauthier, S., Kaur, G., Mi, W., Tizon, B., & Levy, E. (2011). Protective mechanisms by cystatin C in neurodegenerative diseases. *Frontiers in bioscience (Scholar edition), 3*, 541-554.

Gehrs, K. M., Anderson, D. H., Johnson, L. V., & Hageman, G. S. (2006). Age-related macular degeneration--emerging pathogenetic and therapeutic concepts. *Annals of medicine, 38*(7), 450-471. doi:10.1080/07853890600946724

Gehrs, K. M., Jackson, J. R., Brown, E. N., Allikmets, R., & Hageman, G. S. (2010). Complement, Age-Related Macular Degeneration and a Vision of the Future. *JAMA Ophthalmology, 128*(3), 349-358. doi:10.1001/archophthalmol.2010.18

Gheorghe, A., Mahdi, L., & Musat, O. (2015). AGE-RELATED MACULAR DEGENERATION. *Romanian journal of ophthalmology, 59*(2), 74-77.

Gilmore, T. D. (2006). Introduction to NF-κB: players, pathways, perspectives. *Oncogene, 25*(51), 6680-6684.

Giraudo, E., Primo, L., Audero, E., Gerber, H.-P., Koolwijk, P., Soker, S., . . . Bussolino, F. (1998). Tumor necrosis factor-α regulates expression of vascular endothelial growth factor receptor-2 and of its co-receptor neuropilin-1 in human vascular endothelial cells. *Journal of Biological Chemistry, 273*(34), 22128-22135.

Gkogkolou, P., & Böhm, M. (2012). Advanced glycation end products: Key players in skin aging? *Dermato-endocrinology, 4*(3), 259-270. doi:10.4161/derm.22028

Glenn, J. V., Mahaffy, H., Wu, K. Q., Smith, G., Nagai, R., Simpson, D. A. C., . . . Stitt, A. W. (2009). *Advanced Glycation End Product (AGE) Accumulation on Bruch's Membrane: Links to Age-Related RPE Dysfunction*.

Glenn, J. V., & Stitt, A. W. (2009). The role of advanced glycation end products in retinal ageing and disease. *Biochimica et Biophysica Acta (BBA) - General Subjects, 1790*(10), 1109-1116. doi:http://dx.doi.org/10.1016/j.bbagen.2009.04.016

Goh, S.-Y., & Cooper, M. E. (2008). The role of advanced glycation end products in progression and complications of diabetes. *The Journal of Clinical Endocrinology & Metabolism, 93*(4), 1143-1152.

Goldin, A., Beckman, J. A., Schmidt, A. M., & Creager, M. A. (2006). Advanced Glycation End Products. *Sparking the Development of Diabetic Vascular Injury, 114*(6), 597-605. doi:10.1161/circulationaha.106.621854

Golestaneh, N., Chu, Y., Xiao, Y.-Y., Stoleru, G. L., & Theos, A. C. (2017). Dysfunctional autophagy in RPE, a contributing factor in age-related macular degeneration. *Cell Death Dis, 8*(1), e2537. doi:10.1038/cddis.2016.453

Gómez-Sintes, R., Ledesma, M. D., & Boya, P. (2016). Lysosomal cell death mechanisms in aging. *Ageing Research Reviews, 32*, 150-168. doi:https://doi.org/10.1016/j.arr.2016.02.009

Gong, X., Draper, C. S., Allison, G. S., Marisiddaiah, R., & Rubin, L. P. (2017). Effects of the Macular Carotenoid Lutein in Human Retinal Pigment Epithelial Cells. *Antioxidants (Basel), 6*(4). doi:10.3390/antiox6040100

Govindaraju, V. K., Bodas, M., & Vij, N. (2017). Cigarette smoke induced autophagy-impairment regulates AMD pathogenesis mechanisms in ARPE-19 cells. *PLoS One, 12*(8), e0182420. doi:10.1371/journal.pone.0182420

Grimm, S., Horlacher, M., Catalgol, B., Hoehn, A., Reinheckel, T., & Grune, T. (2012). Cathepsins D and L reduce the toxicity of advanced glycation end products. *Free Radical Biology and Medicine, 52*(6), 1011-1023. doi:http://dx.doi.org/10.1016/j.freeradbiomed.2011.12.021

Group, A.-R. E. D. S. R. (2000). Risk factors associated with age-related macular degeneration: a case-control study in the age-related eye disease study: age-related eye disease study report number 3. *Ophthalmology, 107*(12), 2224-2232.

Grzebyk, E., Knapik-Kordecka, M., & Piwowar, A. (2013). Advanced glycation end-products and cathepsin cysteine protease in type 2 diabetic patients. *Pol Arch Med Wewn, 123*(7-8), 364-370.

Guha, S., Coffey, E. E., Lu, W., Lim, J. C., Beckel, J. M., Laties, A. M., . . . Mitchell, C. H. (2014). Approaches for detecting lysosomal alkalinization and impaired degradation in fresh and cultured RPE cells: Evidence for a role in retinal degenerations. *Exp Eye Res, 126*, 68-76. doi:https://doi.org/10.1016/j.exer.2014.05.013

Guilbaud, A., Niquet-Leridon, C., Boulanger, E., & Tessier, F. J. (2016). How Can Diet Affect the Accumulation of Advanced Glycation End-Products in the Human Body? *Foods (Basel, Switzerland), 5*(4), 84. doi:10.3390/foods5040084

Guillonneau, X., Bryckaert, M., Launay-Longo, C., Courtois, Y., & Mascarelli, F. (1998). Endogenous FGF1-induced Activation and Synthesis of Extracellular Signal-regulated Kinase 2 Reduce Cell Apoptosis in Retinal-pigmented Epithelial Cells. *Journal of Biological Chemistry, 273*(35), 22367-22373. doi:10.1074/jbc.273.35.22367

Guo, J. D., Zhao, X., Li, Y., Li, G. R., & Liu, X. L. (2018). Damage to dopaminergic neurons by oxidative stress in Parkinson's disease. *International journal of molecular medicine, 41*(4), 1817-1825.

Guo, P.-C., Dong, Z., Zhao, P., Zhang, Y., He, H., Tan, X., . . . Xia, Q. (2015). Structural insights into the unique inhibitory mechanism of the silkworm protease inhibitor serpin18. *Scientific reports, 5*, 11863. doi:10.1038/srep11863

https://www.nature.com/articles/srep11863#supplementary-information

Gupta, S. C., Sundaram, C., Reuter, S., & Aggarwal, B. B. (2010). Inhibiting NF-κB Activation by Small Molecules As a Therapeutic Strategy. *Biochim Biophys Acta, 1799*(10-12), 775-787. doi:10.1016/j.bbagrm.2010.05.004

Hageman, G. S., Luthert, P. J., Victor Chong, N. H., Johnson, L. V., Anderson, D. H., & Mullins, R. F. (2001). An integrated hypothesis that considers drusen as biomarkers of immune-mediated processes at the RPE-Bruch's membrane interface in aging and age-related macular degeneration. *Prog Retin Eye Res, 20*(6), 705-732.

Haider, S. H., Oskuei, A., Crowley, G., Kwon, S., Lam, R., Riggs, J., . . . Nolan, A. (2019). Receptor for advanced glycation end-products and environmental exposure related obstructive airways disease: a systematic review. *European Respiratory Review, 28*(151), 180096. doi:10.1183/16000617.0096-2018

Hammond, B. R., Johnson, B. A., & George, E. R. (2014). Oxidative photodegradation of ocular tissues: Beneficial effects of filtering and exogenous antioxidants. *Exp Eye Res, 129*, 135-150. doi:https://doi.org/10.1016/j.exer.2014.09.005

Handa, J. T., Reiser, K. M., Matsunaga, H., & Hjelmeland, L. M. (1998). The advanced glycation endproduct pentosidine induces the expression of PDGF-B in human retinal pigment epithelial cells. *Exp Eye Res, 66*(4), 411-419.

Handa, J. T., Verzijl, N., Matsunaga, H., Aotaki-Keen, A., Lutty, G. A., te Koppele, J. M., . . . Hjelmeland, L. M. (1999). Increase in the advanced glycation end product pentosidine in Bruch's membrane with age. *Invest Ophthalmol Vis Sci, 40*(3), 775-779.

Harman, D. (1981). The aging process. *Proceedings of the National Academy of Sciences of the United States of America, 78*(11), 7124-7128.

Hayasaka, S. (1983). Lysosomal enzymes in ocular tissues and diseases. *Survey of ophthalmology, 27*(4), 245-258. doi:http://dx.doi.org/10.1016/0039-6257(83)90125-X

Hayasaka, S., Hara, S., & Mizuno, K. (1975). Distribution and some properties of cathepsin D in the retinal pigment epithelium. *Exp Eye Res, 21*(4), 307-313. doi:http://doi.org/10.1016/0014-4835(75)90041-X

Hayden, M. S., & Ghosh, S. (2004). Signaling to NF-κB. *Genes & development, 18*(18), 2195-2224.

Helenius, M., Hänninen, M., Lehtinen, S. K., & Salminen, A. (1996). Aging-induced up-regulation of nuclear binding activities of oxidative stress responsive NF-kB transcription factor in mouse cardiac muscle. *Journal of Molecular and Cellular Cardiology, 28*(3), 487-498. doi:10.1006/jmcc.1996.0045

Hellinen, L., Hagström, M., Knuutila, H., Ruponen, M., Urtti, A., & Reinisalo, M. (2019). Characterization of artificially re-pigmented ARPE-19 retinal pigment epithelial cell model. *Scientific reports, 9*(1), 13761. doi:10.1038/s41598-019-50324-8

Hemmi, H., Takeuchi, O., Kawai, T., Kaisho, T., Sato, S., Sanjo, H., . . . Akira, S. (2000). A Toll-like receptor recognizes bacterial DNA. *Nature, 408*(6813), 740-745.

Hernández-Zimbrón, L. F., Zamora-Alvarado, R., Velez-Montoya, R., Zenteno, E., Gulias-Cañizo, R., Quiroz-Mercado, H., & Gonzalez-Salinas, R. (2018). Age-related macular degeneration: new paradigms for treatment and management of AMD. *Oxidative Medicine and Cellular Longevity, 2018*.

Herrmann, R. K., Robison, W. G., Jr., & Bieri, J. G. (1984). Deficiencies of vitamins E and A in the rat: lipofuscin accumulation in the choroid. *Invest Ophthalmol Vis Sci, 25*(4), 429-433.

Higgins, W. J., Fox, D. M., Kowalski, P. S., Nielsen, J. E., & Worrall, D. M. (2010). Heparin enhances serpin inhibition of the cysteine protease cathepsin L. *J Biol Chem, 285*(6), 3722-3729. doi:10.1074/jbc.M109.037358

Hoesel, B., & Schmid, J. A. (2013). The complexity of NF-κB signaling in inflammation and cancer. *Molecular cancer, 12*(1), 1.

Holt, D. J., & Grainger, D. W. (2011). Multinucleated giant cells from fibroblast cultures. *Biomaterials, 32*(16), 3977-3987. doi:10.1016/j.biomaterials.2011.02.021

Howes, K. A., Liu, Y., Dunaief, J. L., Milam, A., Frederick, J. M., Marks, A., & Baehr, W. (2004). Receptor for advanced glycation end products and age-related macular degeneration. *Investigative ophthalmology & visual science, 45*(10), 3713-3720.

Hu, Y., Baud, V., Delhase, M., Zhang, P., Deerinck, T., Ellisman, M., . . . Karin, M. (1999). Abnormal morphogenesis but intact IKK activation in mice lacking the IKKα subunit of IκB kinase. *Science, 284*(5412), 316-320.

Ida, H., Ishibashi, K., Reiser, K., Hjelmeland, L. M., & Handa, J. T. (2004). Ultrastructural aging of the RPE-Bruch's membrane-choriocapillaris complex in the D-galactose-treated mouse. *Invest Ophthalmol Vis Sci, 45*(7), 2348-2354. doi:10.1167/iovs.03-1337

Im, E., & Kazlauskas, A. (2007). The role of cathepsins in ocular physiology and pathology. *Exp Eye Res, 84*(3), 383-388. doi:10.1016/j.exer.2006.05.017

Imamura, Y., Noda, S., Hashizume, K., Shinoda, K., Yamaguchi, M., Uchiyama, S., . . . Tsubota, K. (2006). Drusen, choroidal neovascularization, and retinal pigment epithelium dysfunction in SOD1-deficient mice: a model of age-related macular degeneration. *Proceedings of the National Academy of Sciences, 103*(30), 11282-11287.

Inana, G., Murat, C., An, W., Yao, X., Harris, I. R., & Cao, J. (2018). RPE phagocytic function declines in age-related macular degeneration and is rescued by human umbilical tissue derived cells. *Journal of Translational Medicine, 16*(1), 63. doi:10.1186/s12967-018-1434-6

Ishibashi, T., Murata, T., Hangai, M., Nagai, R., Horiuchi, S., Lopez, P. F., . . . Ryan, S. J. (1998). Advanced glycation end products in age-related macular degeneration. *Archives of ophthalmology, 116*(12), 1629-1632.

Ivanov, I. V., Mappes, T., Schaupp, P., Lappe, C., & Wahl, S. (2018). Ultraviolet radiation oxidative stress affects eye health. *J Biophotonics, 11*(7), e201700377. doi:10.1002/jbio.201700377

Jakoš, T., Pišlar, A., Jewett, A., & Kos, J. (2019). Cysteine Cathepsins in Tumor-Associated Immune Cells. *Frontiers in Immunology, 10*(2037). doi:10.3389/fimmu.2019.02037

Joachim, N., Mitchell, P., Younan, C., Burlutsky, G., Cheng, C.-Y., Cheung, C. M. G., . . . Wang, J. J. (2014). Ethnic Variation in Early Age-Related Macular Degeneration Lesions Between White Australians and Singaporean Asians. *Investigative ophthalmology & visual science, 55*(7), 4421-4429. doi:10.1167/iovs.14-14476

Kaarniranta, K., & Salminen, A. (2009). NF-κB signaling as a putative target for ω-3 metabolites in the prevention of age-related macular degeneration (AMD). *Experimental Gerontology, 44*(11), 685-688. doi:http://doi.org/10.1016/j.exger.2009.09.002

Kaarniranta, K., Salminen, A., Haapasalo, A., Soininen, H., & Hiltunen, M. (2011). Age-related macular degeneration (AMD): Alzheimer's disease in the eye? *Journal of Alzheimer's Disease, 24*(4), 615-631.

Kandarakis, S. A., Piperi, C., Topouzis, F., & Papavassiliou, A. G. (2014). Emerging role of advanced glycation-end products (AGEs) in the pathobiology of eye diseases. *Progress in retinal and eye research, 42*, 85-102.

Kanter, M. (2009). Protective effects of thymoquinone on streptozotocin-induced diabetic nephropathy. *J Mol Histol, 40*(2), 107-115. doi:10.1007/s10735-009-9220-7

Kanwar, M., Chan, P.-S., Kern, T. S., & Kowluru, R. A. (2007). Oxidative Damage in the Retinal Mitochondria of Diabetic Mice: Possible Protection by Superoxide Dismutase. *Investigative ophthalmology & visual science, 48*(8), 3805-3811. doi:10.1167/iovs.06-1280

Karin, M. (1999). How NF-κB is activated: the role of the IκB kinase (IKK) complex. *Oncogene, 18*(49).

Kasahara, E., Lin, L.-R., Ho, Y.-S., & Reddy, V. N. (2005). SOD2 protects against oxidation-induced apoptosis in mouse retinal pigment epithelium: implications for age-related macular degeneration. *Investigative ophthalmology & visual science, 46*(9), 3426-3434.

Kasper, M., & Funk, R. H. W. (2001). Age-related changes in cells and tissues due to advanced glycation end products (AGEs). *Arch Gerontol Geriatr, 32*(3), 233-243. doi:http://dx.doi.org/10.1016/S0167-4943(01)00103-0

Katschke, K. J., Xi, H., Cox, C., Truong, T., Malato, Y., Lee, W. P., . . . van Lookeren Campagne, M. (2018). Classical and alternative complement activation on photoreceptor outer segments drives monocyte-dependent retinal atrophy. *Scientific reports, 8*(1), 7348. doi:10.1038/s41598-018-25557-8

Katz, M. L. (2002). Potential role of retinal pigment epithelial lipofuscin accumulation in age-related macular degeneration. *Arch Gerontol Geriatr, 34*(3), 359-370. doi:http://dx.doi.org/10.1016/S0167-4943(02)00012-2

Kauppinen, A., Niskanen, H., Suuronen, T., Kinnunen, K., Salminen, A., & Kaarniranta, K. (2012). Oxidative stress activates NLRP3 inflammasomes in ARPE-19 cells—Implications for age-related macular degeneration (AMD). *Immunology Letters, 147*(1–2), 29-33. doi:http://doi.org/10.1016/j.imlet.2012.05.005

Kawasaki, R., Wang, J. J., Aung, T., Tan, D. T., Mitchell, P., Sandar, M., . . . Wong, T. Y. (2008). Prevalence of age-related macular degeneration in a Malay population: the Singapore Malay Eye Study. *Ophthalmology, 115*(10), 1735-1741.

Kay, P., Yang, Y. C., & Paraoan, L. (2013). Directional protein secretion by the retinal pigment epithelium: roles in retinal health and the development of age-related macular degeneration. *J Cell Mol Med, 17*(7), 833-843. doi:10.1111/jcmm.12070

Kearns, J. D., Basak, S., Werner, S. L., Huang, C. S., & Hoffmann, A. (2006). IkappaBepsilon provides negative feedback to control NF-kappaB oscillations, signaling dynamics, and inflammatory gene expression. *The Journal of cell biology, 173*(5), 659-664. doi:10.1083/jcb.200510155

Kennedy, C. J., Rakoczy, P. E., & Constable, I. J. (1995). Lipofuscin of the retinal pigment epithelium: A review. *Eye, 9*(6), 763-771.

Keppler, D., Walter, R., Perez, C., & Sierra, F. (2000). Increased expression of mature cathepsin B in aging rat liver. *Cell Tissue Res, 302*(2), 181-188.

Kevany, B. M., & Palczewski, K. (2010). Phagocytosis of retinal rod and cone photoreceptors. *Physiology (Bethesda, Md.), 25*(1), 8-15. doi:10.1152/physiol.00038.2009

Khan, J. C., Thurlby, D. A., Shahid, H., Clayton, D. G., Yates, J. R. W., Bradley, M., . . . Bird, A. C. (2006). Smoking and age related macular degeneration: the number of pack years of cigarette smoking is a major determinant of risk for both geographic atrophy and choroidal neovascularisation. *British Journal of Ophthalmology, 90*(1), 75-80. doi:10.1136/bjo.2005.073643

Khoo, H. E., Ng, H. S., Yap, W. S., Goh, H. J. H., & Yim, H. S. (2019). Nutrients for Prevention of Macular Degeneration and Eye-Related Diseases. *Antioxidants (Basel), 8*(4). doi:10.3390/antiox8040085

Kim, E.-K., Kim, H., Vijayakumar, A., Kwon, O., & Chang, N. (2017). Associations between fruit and vegetable, and antioxidant nutrient intake and age-related macular degeneration by smoking status in elderly Korean men. *Nutrition journal, 16*(1), 77-77. doi:10.1186/s12937-017-0301-2

Klein, R., Myers, C. E., Lee, K. E., Gangnon, R. E., Sivakumaran, T. A., Iyengar, S. K., & Klein, B. E. K. (2015). Small Drusen and Age-Related Macular Degeneration: The Beaver Dam Eye Study. *Journal of clinical medicine, 4*(3), 424-440. doi:10.3390/jcm4030425

Klettner, A., Kaya, L., Flach, J., Lassen, J., Treumer, F., & Roider, J. (2015). Basal and apical regulation of VEGF-A and placenta growth factor in the RPE/choroid and primary RPE. *Molecular vision, 21*, 736-748.

Klettner, A., Westhues, D., Lassen, J., Bartsch, S., & Roider, J. (2013). Regulation of constitutive vascular endothelial growth factor secretion in retinal pigment epithelium/choroid organ cultures: p38, nuclear factor kappaB, and the vascular endothelial growth factor receptor-2/phosphatidylinositol 3 kinase pathway. *Molecular vision, 19*, 281-291.

Ko, S. Y., Ko, H. A., Chu, K. H., Shieh, T. M., Chi, T. C., Chen, H. I., . . . Chang, S. S. (2015). The Possible Mechanism of Advanced Glycation End Products (AGEs) for Alzheimer's Disease. *PLoS One, 10*(11), e0143345. doi:10.1371/journal.pone.0143345

Koike, M., Shibata, M., Ohsawa, Y., Nakanishi, H., Koga, T., Kametaka, S., . . . Uchiyama, Y. (2003). Involvement of two different cell death pathways in retinal atrophy of cathepsin D-deficient mice. *Molecular and Cellular Neuroscience, 22*(2), 146-161. doi:https://doi.org/10.1016/S1044-7431(03)00035-6

Kolb, H. (2007a). Glial cells of the retina. In *Webvision: The Organization of the Retina and Visual System [Internet]*: University of Utah Health Sciences Center.

Kolb, H. (2007b). Gross anatomy of the eye. In *Webvision: The Organization of the Retina and Visual System [Internet]*: University of Utah Health Sciences Center.

Kolb, H., Fernandez, E., & Nelson, R. (1995). Photoreceptors--Webvision: The Organization of the Retina and Visual System.

Kolb, H., Fernandez, E., Nelson, R., & Kolb, H. (2007). Gross anatomy of the eye.

Korthagen, N. M., van Bilsen, K., Swagemakers, S. M., van de Peppel, J., Bastiaans, J., van der Spek, P. J., . . . Dik, W. A. (2015). Retinal pigment epithelial cells display specific transcriptional responses upon TNF-alpha stimulation. *Br J Ophthalmol, 99*(5), 700-704. doi:10.1136/bjophthalmol-2014-306309

Kowluru, R. A., Kowluru, V., Xiong, Y., & Ho, Y.-S. (2006). Overexpression of mitochondrial superoxide dismutase in mice protects the retina from diabetes-induced oxidative stress. *Free Radical Biology and Medicine, 41*(8), 1191-1196. doi:https://doi.org/10.1016/j.freeradbiomed.2006.01.012

Kuznetsova, A. V., Kurinov, A. M., & Aleksandrova, M. A. (2014). Cell models to study regulation of cell transformation in pathologies of retinal pigment epithelium. *Journal of ophthalmology, 2014*.

Lambert, N. G., ElShelmani, H., Singh, M. K., Mansergh, F. C., Wride, M. A., Padilla, M., . . . Ambati, B. K. (2016). Risk factors and biomarkers of age-related macular degeneration. *Progress in retinal and eye research, 54*, 64-102. doi:10.1016/j.preteyeres.2016.04.003

Lan, K.-C., Chiu, C.-Y., Kao, C.-W., Huang, k.-h., Wang, C.-C., Huang, K.-T., . . . Hwa Liu, S. (2015). *Advanced Glycation End-Products Induce Apoptosis in Pancreatic Islet Endothelial Cells via NF-κB-Activated Cyclooxygenase-2/Prostaglandin E2 Up-Regulation* (Vol. 10).

Lappas, M., Permezel, M., & Rice, G. E. (2007). Advanced glycation endproducts mediate pro-inflammatory actions in human gestational tissues via nuclear factor-κB and extracellular signal-regulated kinase 1/2. *Journal of Endocrinology, 193*(2), 269-277.

LaVail, M. M. (1976). Rod outer segment disc shedding in relation to cyclic lighting. *Exp Eye Res, 23*(2, Part 2), 277-280. doi:https://doi.org/10.1016/0014-4835(76)90209-8

Lee, E. G., Boone, D. L., Chai, S., Libby, S. L., Chien, M., Lodolce, J. P., & Ma, A. (2000). Failure to regulate TNF-induced NF-κB and cell death responses in A20-deficient mice. *Science, 289*(5488), 2350-2354.

Liang, F.-Q., & Godley, B. F. (2003). Oxidative stress-induced mitochondrial DNA damage in human retinal pigment epithelial cells: a possible mechanism for RPE aging and age-related macular degeneration. *Exp Eye Res, 76*(4), 397-403. doi:http://doi.org/10.1016/S0014-4835(03)00023-X

Liles, M. R., Newsome, D. A., & Oliver, P. D. (1991). Antioxidant enzymes in the aging human retinal pigment epithelium. *Arch ophthalmol, 109*(9), 1285-1288. doi:10.1001/archopht.1991.01080090111033

Lin, T., Cui, J. Z., & Matsubara, J. A. (2012). Advance Glycation End Product and its Role in Age-related Degenerative Diseases of the Eye. *Investigative ophthalmology & visual science, 53*(14), 4285-4285.

Lin, T., Walker, G. B., Kurji, K., Fang, E., Law, G., Prasad, S. S., . . . Matsubara, J. A. (2013). Parainflammation associated with advanced glycation endproduct stimulation of RPE in vitro: Implications for age-related degenerative diseases of the eye. *Cytokine, 62*(3), 369-381. doi:http://dx.doi.org/10.1016/j.cyto.2013.03.027

Lipniacki, T., Paszek, P., Brasier, A. R., Luxon, B., & Kimmel, M. (2004). Mathematical model of NF-κB regulatory module. *Journal of Theoretical Biology, 228*(2), 195-215.

Liszewski, M. K., Kolev, M., Le Friec, G., Leung, M., Bertram, P. G., Fara, A. F., . . . Kemper, C. (2013). Intracellular complement activation sustains T cell homeostasis and mediates effector differentiation. *Immunity, 39*(6), 1143-1157. doi:10.1016/j.immuni.2013.10.018

Liu, N., Raja, S. M., Zazzeroni, F., Metkar, S. S., Shah, R., Zhang, M., . . . Ashton-Rickardt, P. G. (2003). NF-kappaB protects from the lysosomal pathway of cell death. *The EMBO journal, 22*(19), 5313-5322. doi:10.1093/emboj/cdg510

Liu, T., Zhang, L., Joo, D., & Sun, S.-C. (2017). NF-κB signaling in inflammation. *Signal transduction and targeted therapy, 2*, 17023. doi:10.1038/sigtrans.2017.23

Losso, J. N., Bawadi, H. A., & Chintalapati, M. (2011). Inhibition of the formation of advanced glycation end products by thymoquinone. *Food Chem, 128*(1), 55-61. doi:10.1016/j.foodchem.2011.02.076

Lu, L., Hackett, S. F., Mincey, A., Lai, H., & Campochiaro, P. A. (2006). Effects of different types of oxidative stress in RPE cells. *Journal of cellular physiology, 206*(1), 119-125.

Lu, M., Kuroki, M., Amano, S., Tolentino, M., Keough, K., Kim, I., . . . Adamis, A. P. (1998). Advanced glycation end products increase retinal vascular endothelial growth factor expression. *J Clin Invest, 101*(6), 1219-1224. doi:10.1172/jci1277

Luevano-Contreras, C., & Chapman-Novakofski, K. (2010). Dietary advanced glycation end products and aging. *Nutrients, 2*(12), 1247-1265.

Ma, W., Lee, S. E., Guo, J., Qu, W., Hudson, B. I., Schmidt, A. M., & Barile, G. R. (2007). RAGE ligand upregulation of VEGF secretion in ARPE-19 cells. *Investigative ophthalmology & visual science, 48*(3), 1355-1361.

Majji, A. B., Cao, J., Chang, K. Y., Hayashi, A., Aggarwal, S., Grebe, R. R., & Eugene de Juan, J. (2000). Age-Related Retinal Pigment Epithelium and Bruch's Membrane Degeneration in Senescence-Accelerated Mouse. *Investigative ophthalmology & visual science, 41*(12), 3936-3942.

Mao, Y., & Finnemann, S. C. (2012). Essential diurnal Rac1 activation during retinal phagocytosis requires alphavbeta5 integrin but not tyrosine kinases focal adhesion kinase or Mer tyrosine kinase. *Mol Biol Cell, 23*(6), 1104-1114. doi:10.1091/mbc.E11-10-0840

Martin, D. M., Yee, D., & Feldman, E. L. (1992). Gene expression of the insulin-like growth factors and their receptors in cultured human retinal pigment epithelial cells. *Molecular Brain Research, 12*(1), 181-186. doi:https://doi.org/10.1016/0169-328X(92)90082-M

Masuda, T., Shimazawa, M., & Hara, H. (2017). Retinal Diseases Associated with Oxidative Stress and the Effects of a Free Radical Scavenger (Edaravone). *Oxidative Medicine and Cellular Longevity, 2017*, 14. doi:10.1155/2017/9208489

Masuda, T., Wahlin, K., Wan, J., Hu, J., Maruotti, J., Yang, X., . . . Esumi, N. (2014). Transcription factor SOX9 plays a key role in the regulation of visual cycle gene expression in the retinal pigment epithelium. *J Biol Chem, 289*(18), 12908-12921. doi:10.1074/jbc.M114.556738

Matsuoka, M., Ogata, N., Otsuji, T., Nishimura, T., Takahashi, K., & Matsumura, M. (2004). Expression of pigment epithelium derived factor and vascular endothelial growth factor in choroidal neovascular membranes and polypoidal choroidal vasculopathy. *Br J Ophthalmol, 88*(6), 809-815.

Maugeri, A., Barchitta, M., Mazzone, M. G., Giuliano, F., & Agodi, A. (2018). Complement System and Age-Related Macular Degeneration: Implications of Gene-Environment Interaction for Preventive and Personalized Medicine. *BioMed Research International, 2018*.

Mazzoni, F., Safa, H., & Finnemann, S. C. (2014). Understanding photoreceptor outer segment phagocytosis: Use and utility of RPE cells in culture. *Exp Eye Res, 126*(0), 51-60. doi:http://dx.doi.org/10.1016/j.exer.2014.01.010

Medicherla, R., Leers-Sucheta, S., Luo, Y., & Azhar, S. (2002). Age-dependent modulation of NF-κB expression in rat adrenal gland. *Mech Ageing Dev, 123*(9), 1211-1227.

Medzhitov, R. (2008). Origin and physiological roles of inflammation. *Nature, 454*(7203), 428-435. doi:10.1038/nature07201

Miceli, M. V., Liles, M. R., & Newsome, D. A. (1994). Evaluation of oxidative processes in human pigment epithelial cells associated with retinal outer segment phagocytosis. *Exp Cell Res, 214*(1), 242-249. doi:10.1006/excr.1994.1254

Michalska-Małecka, K., Kabiesz, A., Nowak, M., & Śpiewak, D. (2015). Age related macular degeneration – challenge for future: Pathogenesis and new perspectives for the treatment. *European Geriatric Medicine, 6*(1), 69-75. doi:https://doi.org/10.1016/j.eurger.2014.09.007

Minton, K. (2013). The inside story on complement activation. *Nature Reviews Immunology, 14*, 61. doi:10.1038/nri3603

Mohamed, A., Afridi, D. M., Garani, O., & Tucci, M. (2005). Thymoquinone inhibits the activation of NF-kappaB in the brain and spinal cord of experimental autoimmune encephalomyelitis. *Biomed Sci Instrum, 41*, 388-393.

Mookiah, M. R. K., Acharya, U. R., Koh, J. E. W., Chandran, V., Chua, C. K., Tan, J. H., . . . Laude, A. (2014). Automated diagnosis of Age-related Macular Degeneration using greyscale features from digital fundus images. *Computers in*

Biology and Medicine, 53, 55-64. doi:https://doi.org/10.1016/j.compbiomed.2014.07.015

Moreno, R., Sobotzik, J. M., Schultz, C., & Schmitz, M. L. (2010). Specification of the NF-kappaB transcriptional response by p65 phosphorylation and TNF-induced nuclear translocation of IKK epsilon. *Nucleic Acids Res, 38*(18), 6029-6044. doi:10.1093/nar/gkq439

Nagai, R., Matsumoto, K., Ling, X., Suzuki, H., Araki, T., & Horiuchi, S. (2000). Glycolaldehyde, a reactive intermediate for advanced glycation end products, plays an important role in the generation of an active ligand for the macrophage scavenger receptor. *Diabetes, 49*(10), 1714-1723.

Nagi, M. N., Alam, K., Badary, O. A., Al-Shabanah, O. A., Al-Sawaf, H. A., & Al-Bekairi, A. M. (1999). Thymoquinone protects against carbon tetrachloride hetatotoxicity in mice via an antioxidant mechanism. *IUBMB Life, 47*(1), 153-159. doi:10.1080/15216549900201153

Nakanishi, H., Amano, T., Sastradipura, D. F., Yoshimine, Y., Tsukuba, T., Tanabe, K., . . . Yamamoto, K. (1997). Increased expression of cathepsins E and D in neurons of the aged rat brain and their colocalization with lipofuscin and carboxy-terminal fragments of Alzheimer amyloid precursor protein. *J Neurochem, 68*(2), 739-749.

Nakanishi, H., Tominaga, K., Amano, T., Hirotsu, I., Inoue, T., & Yamamoto, K. (1994). Age-Related Changes in Activities and Localizations of Cathepsins D, E, B, and L in the Rat Brain Tissues. *Exp Neurol, 126*(1), 119-128. doi:http://dx.doi.org/10.1006/exnr.1994.1048

Nandrot, E. F., Anand, M., Almeida, D., Atabai, K., Sheppard, D., & Finnemann, S. C. (2007). Essential role for MFG-E8 as ligand for alphavbeta5 integrin in diurnal retinal phagocytosis. *Proc Natl Acad Sci U S A, 104*(29), 12005-12010. doi:10.1073/pnas.0704756104

Nandrot, E. F., Kim, Y., Brodie, S. E., Huang, X., Sheppard, D., & Finnemann, S. C. (2004). Loss of synchronized retinal phagocytosis and age-related blindness in mice lacking alphavbeta5 integrin. *J Exp Med, 200*(12), 1539-1545. doi:10.1084/jem.20041447

Nedić, O., Rattan, S. I. S., Grune, T., & Trougakos, I. P. (2013). Molecular effects of advanced glycation end products on cell signalling pathways, ageing and pathophysiology. *Free Radical Research, 47*(sup1), 28-38. doi:10.3109/10715762.2013.806798

Newsome, D. A., Miceli, M. V., Liles, M. R., Tate, D. J., & Oliver, P. D. (1994). Antioxidants in the retinal pigment epithelium. *Progress in retinal and eye research, 13*(1), 101-123. doi:https://doi.org/10.1016/1350-9462(94)90006-X

Nguyen-Legros, J., & Hicks, D. (2000). Renewal of photoreceptor outer segments and their phagocytosis by theretinal pigment epithelium. In *International review of cytology* (Vol. 196, pp. 245-313): Academic Press.

Ni, J., Yuan, X., Gu, J., Yue, X., Gu, X., Nagaraj, R. H., . . . Proteomic, A. M. D. S. G. (2009). Plasma protein pentosidine and carboxymethyllysine, biomarkers for age-related macular degeneration. *Mol Cell Proteomics, 8*(8), 1921-1933. doi:10.1074/mcp.M900127-MCP200

Nikfarjam, L., & Farzaneh, P. (2012). Prevention and Detection of Mycoplasma Contamination in Cell Culture. *Cell Journal (Yakhteh), 13*(4), 203-212.

Nita, M., Grzybowski, A., Ascaso, F. J., & Huerva, V. (2014). Age-related macular degeneration in the aspect of chronic low-grade inflammation (pathophysiological parainflammation). *Mediators of Inflammation, 2014*.

Nowotny, K., Schröter, D., Schreiner, M., & Grune, T. (2018). Dietary advanced glycation end products and their relevance for human health. *Ageing Research Reviews, 47*, 55-66. doi:https://doi.org/10.1016/j.arr.2018.06.005

Nozaki, M., Raisler, B. J., Sakurai, E., Sarma, J. V., Barnum, S. R., Lambris, J. D., . . . Ambati, J. (2006). Drusen complement components C3a and C5a promote choroidal neovascularization. *Proc Natl Acad Sci U S A, 103*(7), 2328-2333. doi:10.1073/pnas.0408835103

Nylandsted, J., Gyrd-Hansen, M., Danielewicz, A., Fehrenbacher, N., Lademann, U., Høyer-Hansen, M., . . . Jäättelä, M. (2004). Heat shock protein 70 promotes cell survival by inhibiting lysosomal membrane permeabilization. *The Journal of Experimental Medicine, 200*(4), 425-435. doi:10.1084/jem.20040531

Obert, E., Strauss, R., Brandon, C., Grek, C., Ghatnekar, G., Gourdie, R., & Rohrer, B. (2017). Targeting the tight junction protein, zonula occludens-1, with the connexin43 mimetic peptide, αCT1, reduces VEGF-dependent RPE pathophysiology. *Journal of molecular medicine (Berlin, Germany), 95*(5), 535-552. doi:10.1007/s00109-017-1506-8

Oeckinghaus, A., & Ghosh, S. (2009). The NF-κB Family of Transcription Factors and Its Regulation. *Cold Spring Harbor Perspectives in Biology, 1*(4), a000034. doi:10.1101/cshperspect.a000034

Oeckinghaus, A., Hayden, M. S., & Ghosh, S. (2011). Crosstalk in NF-[kappa]B signaling pathways. *Nat Immunol, 12*(8), 695-708.

Okada, R., Wu, Z., Zhu, A., Ni, J., Zhang, J., Yoshimine, Y., . . . Nakanishi, H. (2015). Cathepsin D deficiency induces oxidative damage in brain pericytes and impairs the blood–brain barrier. *Molecular and Cellular Neuroscience, 64*, 51-60. doi:https://doi.org/10.1016/j.mcn.2014.12.002

Okazaki, T., Sakon, S., Sasazuki, T., Sakurai, H., Doi, T., Yagita, H., . . . Nakano, H. (2003). Phosphorylation of serine 276 is essential for p65 NF-κB subunit-dependent cellular responses. *Biochem Biophys Res Commun, 300*(4), 807-812. doi:http://doi.org/10.1016/S0006-291X(02)02932-7

Okubo, A., Rosa, R. H., Jr., Bunce, C. V., Alexander, R. A., Fan, J. T., Bird, A. C., & Luthert, P. J. (1999). The relationships of age changes in retinal pigment epithelium and Bruch's membrane. *Invest Ophthalmol Vis Sci, 40*(2), 443-449.

Organisciak, D. T., Wang, H. M., Li, Z. Y., & Tso, M. O. (1985). The protective effect of ascorbate in retinal light damage of rats. *Invest Ophthalmol Vis Sci, 26*(11), 1580-1588.

Ott, C., Jacobs, K., Haucke, E., Santos, A. N., Grune, T., & Simm, A. (2014). Role of advanced glycation end products in cellular signaling. *Redox Biol, 2*, 411-429.

Palombella, V. J., Rando, O. J., Goldberg, A. L., & Maniatis, T. (1994). The ubiquitinproteasome pathway is required for processing the NF-κB1 precursor protein and the activation of NF-κB. *Cell, 78*(5), 773-785.

Palozza, P., Serini, S., Torsello, A., Di Nicuolo, F., Piccioni, E., Ubaldi, V., . . . Calviello, G. (2003). β-Carotene Regulates NF-κB DNA-Binding Activity by a Redox Mechanism in Human Leukemia and Colon Adenocarcinoma Cells. *The Journal of Nutrition, 133*(2), 381-388. doi:10.1093/jn/133.2.381

Panda-Jonas, S., Jonas, J. B., & Jakobczyk-Zmija, M. (1996). Retinal pigment epithelial cell count, distribution, and correlations in normal human eyes. *American journal of ophthalmology, 121*(2), 181-189.

Paraoan, L., Grierson, I., & Maden, B. E. H. (2000). Analysis of expressed sequence tags of retinal pigment epithelium: cystatin C is an abundant transcript. *Int J Biochem Cell Biol, 32*(4), 417-426.

Paraoan, L., Hiscott, P., Gosden, C., & Grierson, I. (2010). Cystatin C in macular and neuronal degenerations: implications for mechanism(s) of age-related macular degeneration. *Vision Res, 50*(7), 737-742. doi:10.1016/j.visres.2009.10.022

Peng, Y., Kim, J.-M., Park, H.-S., Yang, A., Islam, C., Lakatta, E. G., & Lin, L. (2016). AGE-RAGE signal generates a specific NF-κB RelA "barcode" that directs collagen I expression. *Scientific reports, 6*, 18822.

Penn, J. S., Madan, A., Caldwell, R. B., Bartoli, M., Caldwell, R. W., & Hartnett, M. E. (2008). Vascular endothelial growth factor in eye disease. *Progress in retinal and eye research, 27*(4), 331-371. doi:10.1016/j.preteyeres.2008.05.001

Plafker, S. M., O'Mealey, G. B., & Szweda, L. I. (2012). Mechanisms for countering oxidative stress and damage in retinal pigment epithelium. *International review of cell and molecular biology, 298*, 135-177. doi:10.1016/B978-0-12-394309-5.00004-3

Poché, R. A., & Reese, B. E. (2009). Retinal horizontal cells: challenging paradigms of neural development and cancer biology. *Development (Cambridge, England), 136*(13), 2141-2151. doi:10.1242/dev.033175

Raff, M. C. (1992). Social controls on cell survival and cell death. *Nature, 356*(6368), 397-400. doi:10.1038/356397a0

Ragheb, A., Attia, A., Eldin, W., Elbarbry, F., Gazarin, S., & Shoker, A. (2009). The protective effect of thymoquinone, an anti-oxidant and anti-inflammatory agent, against renal injury: A review. *Saudi Journal of Kidney Diseases and Transplantation, 20*(5), 741-752.

Rakoczy, P. E., Lai, C. M., Baines, M., Grandi, S. D., Fitton, J. H., & Constable, I. J. (1997). Modulation of cathepsin D activity in retinal pigment epithelial cells. *Biochemical Journal, 324*(3), 935-940. doi:10.1042/bj3240935

Rakoczy, P. E., Sarks, S. H., Daw, N., & Constable, I. J. (1999). Distribution of cathepsin D in human eyes with or without age-related maculopathy. *Exp Eye Res, 69*(4), 367-374. doi:10.1006/exer.1999.0700

Ramasamy, R., Vannucci, S. J., Du Yan, S. S., Herold, K., Yan, S. F., & Schmidt, A. M. (2005). Advanced glycation end products and RAGE: a common thread in aging, diabetes, neurodegeneration, and inflammation. *Glycobiology, 15*(7), 16R-28R.

Rando, R. R. (2001). The biochemistry of the visual cycle. *Chemical Reviews, 101*(7), 1881-1896.

Rathnasamy, G., Foulds, W. S., Ling, E. A., & Kaur, C. (2019). Retinal microglia - A key player in healthy and diseased retina. *Prog Neurobiol, 173*, 18-40. doi:10.1016/j.pneurobio.2018.05.006

Reichenbach, A., & Bringmann, A. (2013). New functions of Muller cells. *Glia, 61*(5), 651-678. doi:10.1002/glia.22477

Remington, L. A., & Goodwin, D. (2011). *Clinical anatomy of the visual system E-Book*: Elsevier Health Sciences.

Repnik, U., Stoka, V., Turk, V., & Turk, B. (2012). Lysosomes and lysosomal cathepsins in cell death. *Biochimica et Biophysica Acta (BBA)-Proteins and Proteomics, 1824*(1), 22-33.

Rex, T. S., Tsui, I., Hahn, P., Maguire, A. M., Duan, D., Bennett, J., & Dunaief, J. L. (2004). Adenovirus-mediated delivery of catalase to retinal pigment epithelial cells protects neighboring photoreceptors from photo-oxidative stress. *Hum Gene Ther, 15*(10), 960-967. doi:10.1089/hum.2004.15.960

Robison, W. G., Jr, & Kuwabara, T. (1977). Vitamin A storage and peroxisomes in retinal pigment epithelium and liver. *Investigative ophthalmology & visual science, 16*(12), 1110-1117.

Roth, W., Deussing, J., Botchkarev, V. A., Pauly-Evers, M., Saftig, P., Hafner, A., . . . Peters, C. (2000). Cathepsin L deficiency as molecular defect of furless: hyperproliferation of keratinocytes and pertubation of hair follicle cycling. *The FASEB journal, 14*(13), 2075-2086. doi:10.1096/fj.99-0970com

Rothwarf, D. M., Zandi, E., Natoli, G., & Karin, M. (1998). IKK-γ is an essential regulatory subunit of the IκB kinase complex. *Nature, 395*(6699), 297-300.

Rózanowska, M., Bober, A., Burke, J. M., & Sarna, T. (1997). The role of retinal pigment epithelium melanin in photoinduced oxidation of ascorbate. *Photochemistry And Photobiology, 65*(3), 472-479.

Różanowski, B., Cuenco, J., Davies, S., Shamsi, F., Zadlo, A., Dayhaw-Barker, P., . . . Boulton, M. (2008). The Phototoxicity of Aged Human Retinal Melanosomes. *Photochemistry And Photobiology, 84*, 650-657. doi:10.1111/j.1751-1097.2007.00259.x

Rudolf, M., Schloetzer–Schrehardt, U., Michels, S., Aherrahou, Z., Doehring, L. C., Kaczmarek, P., . . . Schmidt–Erfurth, U. (2005). Lipid Accumulation in Bruch's Membrane Is Associated With an Increased Expression of Vascular Endothelial Growth Factor (VEGF) in the Choriocapillaries. *Investigative ophthalmology & visual science, 46*(13), 1213-1213.

Rudzińska, M., Parodi, A., Soond, S. M., Vinarov, A. Z., Korolev, D. O., Morozov, A. O., . . . Zamyatnin, A. A. (2019). The Role of Cysteine Cathepsins in Cancer Progression and Drug Resistance. *International Journal of Molecular Sciences, 20*(14), 3602.

Ryeom, S. W., Sparrow, J. R., & Silverstein, R. L. (1996). CD36 participates in the phagocytosis of rod outer segments by retinal pigment epithelium. *J Cell Sci, 109 (Pt 2)*, 387-395.

Saccà, S. C., Cutolo, C. A., Ferrari, D., Corazza, P., & Traverso, C. E. (2018). The Eye, Oxidative Damage and Polyunsaturated Fatty Acids. *Nutrients, 10*(6), 668. doi:10.3390/nu10060668

Sadigh, S., Cideciyan, A. V., Sumaroka, A., Huang, W. C., Luo, X., Swider, M., . . . Jacobson, S. G. (2013). Abnormal Thickening as well as Thinning of the Photoreceptor Layer in Intermediate Age-Related Macular Degeneration. *Investigative ophthalmology & visual science, 54*(3), 1603-1612. doi:10.1167/iovs.12-11286

Saint-Geniez, M., Kurihara, T., Sekiyama, E., Maldonado, A. E., & D'Amore, P. A. (2009). An essential role for RPE-derived soluble VEGF in the maintenance of the choriocapillaris. *Proceedings of the National Academy of Sciences of the United States of America, 106*(44), 18751-18756. doi:10.1073/pnas.0905010106

Sakurai, H., Chiba, H., Miyoshi, H., Sugita, T., & Toriumi, W. (1999). IκB kinases phosphorylate NF-κB p65 subunit on serine 536 in the transactivation domain. *Journal of Biological Chemistry, 274*(43), 30353-30356.

Samuel, W., Jaworski, C., Postnikova, O. A., Kutty, R. K., Duncan, T., Tan, L. X., . . . Redmond, T. M. (2017). Appropriately differentiated ARPE-19 cells regain phenotype and gene expression profiles similar to those of native RPE cells. *Molecular vision, 23*, 60.

Sanes, J. R., & Masland, R. H. (2015). The types of retinal ganglion cells: current status and implications for neuronal classification. *Annu Rev Neurosci, 38*, 221-246. doi:10.1146/annurev-neuro-071714-034120

Sarks, S. H., Arnold, J. J., Killingsworth, M. C., & Sarks, J. P. (1999). Early drusen formation in the normal and aging eye and their relation to age related maculopathy: a clinicopathological study. *British Journal of Ophthalmology, 83*(3), 358-368. doi:10.1136/bjo.83.3.358

Sarna, T., Burke, J. M., Korytowski, W., Różanowska, M., Skumatz, C. M. B., Zaręba, A., & Zaręba, M. (2003). Loss of melanin from human RPE with aging: possible role of melanin photooxidation. *Exp Eye Res, 76*(1), 89-98. doi:https://doi.org/10.1016/S0014-4835(02)00247-6

Sasaki, N., Fukatsu, R., Tsuzuki, K., Hayashi, Y., Yoshida, T., Fujii, N., . . . Makita, Z. (1998). Advanced glycation end products in Alzheimer's disease and other neurodegenerative diseases. *Am J Pathol, 153*(4), 1149-1155. doi:10.1016/s0002-9440(10)65659-3

Sato, E., Mori, F., Igarashi, S., Abiko, T., Takeda, M., Ishiko, S., & Yoshida, A. (2001). Corneal advanced glycation end products increase in patients with proliferative diabetic retinopathy. *Diabetes care, 24*(3), 479-482.

Satyam, A., Kannan, L., Matsumoto, N., Geha, M., Lapchak, P. H., Bosse, R., . . . Tsokos, G. C. (2017). Intracellular Activation of Complement 3 Is Responsible for Intestinal Tissue Damage during Mesenteric Ischemia. *The Journal of Immunology, 198*(2), 788-797. doi:10.4049/jimmunol.1502287

Saudek, D. M., & Kay, J. (2003). Advanced glycation endproducts and osteoarthritis. *Curr Rheumatol Rep, 5*(1), 33-40.

Sayed, A. A., & Morcos, M. (2007). Thymoquinone decreases AGE-induced NF-kappaB activation in proximal tubular epithelial cells. *Phytother Res, 21*(9), 898-899. doi:10.1002/ptr.2177

Schmidt, A. M., Yan, S. D., Yan, S. F., & Stern, D. M. (2000). The biology of the receptor for advanced glycation end products and its ligands. *Biochimica et Biophysica Acta (BBA) - Molecular Cell Research, 1498*(2–3), 99-111. doi:http://dx.doi.org/10.1016/S0167-4889(00)00087-2

Schraermeyer, U., & Heimann, K. (1999). Current understanding on the role of retinal pigment epithelium and its pigmentation. *Pigment cell research, 12*(4), 219-236.

Schutt, F., Bergmann, M., Holz, F. G., & Kopitz, J. (2003). Proteins Modified by Malondialdehyde, 4-Hydroxynonenal, or Advanced Glycation End Products in Lipofuscin of Human Retinal Pigment Epithelium. *Investigative ophthalmology & visual science, 44*(8), 3663-3668. doi:10.1167/iovs.03-0172

Scott, M. L., Fujita, T., Liou, H. C., Nolan, G. P., & Baltimore, D. (1993). The p65 subunit of NF-kappa B regulates I kappa B by two distinct mechanisms. *Genes Dev, 7*(7a), 1266-1276.

Seidler, D. G., Schwegler, J. S., & Liesenhoff, H. (1999). Expression of fibroblast growth factors 1 and 2 in a human retinal pigment epithelium cell line (K1034). *Ophthalmic Res, 31*(4), 280-286. doi:10.1159/000055548

Semba, R. D., Nicklett, E. J., & Ferrucci, L. (2010). Does accumulation of advanced glycation end products contribute to the aging phenotype? *The journals of gerontology. Series A, Biological sciences and medical sciences, 65*(9), 963-975. doi:10.1093/gerona/glq074

Sen, R., & Baltimore, D. (1986). Multiple nuclear factors interact with the immunoglobulin enhancer sequences. *Cell, 46*(5), 705-716. doi:http://dx.doi.org/10.1016/0092-8674(86)90346-6

Sergejeva, O., Botov, R., Liutkevičienė, R., & Kriaučiūnienė, L. (2016). Genetic factors associated with the development of age-related macular degeneration. *Medicina, 52*(2), 79-88.

Sethi, G., Ahn, K. S., & Aggarwal, B. B. (2008). Targeting Nuclear Factor-κB Activation Pathway by Thymoquinone: Role in Suppression of Antiapoptotic Gene Products and Enhancement of Apoptosis. *Molecular Cancer Research, 6*(6), 1059-1070. doi:10.1158/1541-7786.mcr-07-2088

Shamsi, F. A., & Boulton, M. (2001). Inhibition of RPE lysosomal and antioxidant activity by the age pigment lipofuscin. *Investigative ophthalmology & visual science, 42*(12), 3041-3046.

Sharif, U., Mahmud, N. M., Kay, P., Yang, Y. C., Harding, S. P., Grierson, I., . . . Paraoan, L. (2018). Advanced glycation end products-related modulation of cathepsin L and NF-κB signalling effectors in retinal pigment epithelium lead to augmented response to TNFα. *J Cell Mol Med, 0*(0). doi:doi:10.1111/jcmm.13944

Sharma, C., Kaur, A., Thind, S. S., Singh, B., & Raina, S. (2015). Advanced glycation End-products (AGEs): an emerging concern for processed food industries. *Journal of food science and technology, 52*(12), 7561-7576. doi:10.1007/s13197-015-1851-y

Shimada, N., Ohno-Matsui, K., Iseki, S., Koike, M., Uchiyama, Y., Wang, J., . . . Morita, I. (2010). Cathepsin L in Bone Marrow-Derived Cells Is Required for Retinal and Choroidal Neovascularization. *Am J Pathol, 176*(5), 2571-2580. doi:10.2353/ajpath.2010.091027

Silachev, D. N., Plotnikov, E. Y., Zorova, L. D., Pevzner, I. B., Sumbatyan, N. V., Korshunova, G. A., . . . Zorov, D. B. (2015). Neuroprotective effects of mitochondria-targeted plastoquinone and thymoquinone in a rat model of brain ischemia/reperfusion injury. *Molecules, 20*(8), 14487-14503.

Silverman, S. M., & Wong, W. T. (2018). Microglia in the Retina: Roles in Development, Maturity, and Disease. *Annu Rev Vis Sci, 4*, 45-77. doi:10.1146/annurev-vision-091517-034425

Sim, R. B., & Tsiftsoglou, S. A. (2004). Proteases of the complement system. *Biochem Soc Trans, 32*(Pt 1), 21-27. doi:10.1042/bst0320021

Simo, R., Villarroel, M., Corraliza, L., Hernandez, C., & Garcia-Ramirez, M. (2010). The retinal pigment epithelium: something more than a constituent of the blood-retinal barrier--implications for the pathogenesis of diabetic retinopathy. *J Biomed Biotechnol, 2010*, 190724. doi:10.1155/2010/190724

Smerdon, D. (2000). Anatomy of the eye and orbit. *Current Anaesthesia & Critical Care, 11*(6), 286-292.

Snell, R. S., & Lemp, M. A. (2013). *Clinical anatomy of the eye*: John Wiley & Sons.

Snodderly, D. M. (1995). Evidence for protection against age-related macular degeneration by carotenoids and antioxidant vitamins. *The American journal of clinical nutrition, 62*(6), 1448S-1461S.

Sparrow, J. R., & Boulton, M. (2005). RPE lipofuscin and its role in retinal pathobiology. *Exp Eye Res, 80*(5), 595-606.

Sparrow, J. R., Hicks, D., & Hamel, C. P. (2010). The retinal pigment epithelium in health and disease. *Current molecular medicine, 10*(9), 802-823. doi:10.2174/156652410793937813

Spilsbury, K., Garrett, K. L., Shen, W.-Y., Constable, I. J., & Rakoczy, P. E. (2000). Overexpression of vascular endothelial growth factor (VEGF) in the retinal pigment epithelium leads to the development of choroidal neovascularization. *Am J Pathol, 157*(1), 135-144.

Spira, D., Stypmann, J., Tobin, D. J., Petermann, I., Mayer, C., Hagemann, S., . . . Reinheckel, T. (2007). Cell Type-specific Functions of the Lysosomal Protease Cathepsin L in the Heart. *Journal of Biological Chemistry, 282*(51), 37045-37052. doi:10.1074/jbc.M703447200

Starnes, A. C., Huisingh, C., McGwin, G., Jr., Sloan, K. R., Ablonczy, Z., Smith, R. T., . . . Ach, T. (2016). Multi-nucleate retinal pigment epithelium cells of the human macula exhibit a characteristic and highly specific distribution. *Vis Neurosci, 33*, e001. doi:10.1017/s0952523815000310

Starr, J. M., & Starr, R. J. (2014). Chapter 2 - Skin Aging and Oxidative Stress. In V. R. Preedy (Ed.), *Aging* (pp. 15-22). San Diego: Academic Press.

Stitt, A. W. (2001). Advanced glycation: an important pathological event in diabetic and age related ocular disease. *British Journal of Ophthalmology, 85*(6), 746-753.

Stitt, A. W. (2005). The Maillard reaction in eye diseases. *Annals of the New York Academy of Sciences, 1043*(1), 582-597.

Stitt, A. W., Hughes, S. J., Canning, P., Lynch, O., Cox, O., Frizzell, N., . . . Gardiner, T. A. (2004). Substrates modified by advanced glycation end-products cause dysfunction and death in retinal pericytes by reducing survival signals mediated by platelet-derived growth factor. *Diabetologia, 47*(10), 1735-1746. doi:10.1007/s00125-004-1523-3

Stoeckle, C., Gouttefangeas, C., Hammer, M., Weber, E., Melms, A., & Tolosa, E. (2009). Cathepsin W expressed exclusively in CD8+ T cells and NK cells, is secreted during target cell killing but is not essential for cytotoxicity in human CTLs. *Experimental hematology, 37*, 266-275. doi:10.1016/j.exphem.2008.10.011

Stoka, V., Turk, B., & Turk, V. (2005). Lysosomal cysteine proteases: structural features and their role in apoptosis. *IUBMB Life, 57*(4-5), 347-353.

Stoka, V., Turk, V., & Turk, B. (2016). Lysosomal cathepsins and their regulation in aging and neurodegeneration. *Ageing Research Reviews, 32*, 22-37. doi:http://dx.doi.org/10.1016/j.arr.2016.04.010

Strauss, O. (2005). The retinal pigment epithelium in visual function. *Physiological reviews, 85*(3), 845-881.

Sugita, S., Horie, S., Nakamura, O., Maruyama, K., Takase, H., Usui, Y., . . . Mochizuki, M. (2009). Acquisition of T Regulatory Function in Cathepsin L-Inhibited T Cells by Eye-Derived CTLA-2α during Inflammatory Conditions. *The Journal of Immunology, 183*(8), 5013-5022. doi:10.4049/jimmunol.0901623

Sun, K., Cai, H., Tezel, T. H., Paik, D., Gaillard, E. R., & Del Priore, L. V. *Bruch's membrane aging decreases phagocytosis of outer segments by retinal pigment epithelium*.

Sun, K., Cai, H., Tezel, T. H., Paik, D., Gaillard, E. R., & Del Priore, L. V. (2007). Bruch's membrane aging decreases phagocytosis of outer segments by retinal pigment epithelium. *Mol Vis, 13*, 2310-2319.

Sun, L., Huang, T., Xu, W., Sun, J., Lv, Y., & Wang, Y. (2017). Advanced glycation end products promote VEGF expression and thus choroidal neovascularization via Cyr61-PI3K/AKT signaling pathway. *Scientific reports, 7*(1), 14925. doi:10.1038/s41598-017-14015-6

Sun, M., Ouzounian, M., de Couto, G., Chen, M., Yan, R., Fukuoka, M., . . . Liu, P. P. (2013). Cathepsin-L ameliorates cardiac hypertrophy through activation of the autophagy-lysosomal dependent protein processing pathways. *J Am Heart Assoc, 2*(2), e000191. doi:10.1161/jaha.113.000191

Sun, S.-C. (2017). The non-canonical NF-κB pathway in immunity and inflammation. *Nature reviews. Immunology, 17*(9), 545-558. doi:10.1038/nri.2017.52

Tafani, M., Di Vito, M., Frati, A., Pellegrini, L., De Santis, E., Sette, G., . . . Russo, M. A. (2011a). Pro-inflammatory gene expression in solid glioblastoma microenvironment and in hypoxic stem cells from human glioblastoma. *J Neuroinflammation, 8*, 32. doi:10.1186/1742-2094-8-32

Tafani, M., Schito, L., Pellegrini, L., Villanova, L., Marfe, G., Anwar, T., . . . Russo, M. A. (2011b). Hypoxia-increased RAGE and P2X7R expression regulates tumor cell invasion through phosphorylation of Erk1/2 and Akt and nuclear translocation of NF-κB. *Carcinogenesis, 32*(8), 1167-1175. doi:10.1093/carcin/bgr101

Tak, P. P., & Firestein, G. S. (2001). NF-κB: a key role in inflammatory diseases. *Journal of Clinical Investigation, 107*(1), 7-11.

Takeda, K., Takeuchi, O., Tsujimura, T., Itami, S., Adachi, O., Kawai, T., . . . Akira, S. (1999). Limb and skin abnormalities in mice lacking IKKα. *Science, 284*(5412), 313-316.

Tamhane, T., Wolters, B. K., Illukkumbura, R., Maelandsmo, G. M., Haugen, M. H., & Brix, K. (2015). Construction of a plasmid coding for green fluorescent protein tagged cathepsin L and data on expression in colorectal carcinoma cells. *Data Brief, 5*, 468-475. doi:10.1016/j.dib.2015.09.022

Tang, Q., Cai, J., Shen, D., Bian, Z., Yan, L., Wang, Y.-X., . . . Wang, W. (2009). Lysosomal cysteine peptidase cathepsin L protects against cardiac hypertrophy through blocking AKT/GSK3β signaling. *Journal of Molecular Medicine, 87*(3), 249-260. doi:10.1007/s00109-008-0423-2

Tao, C., & Zhang, X. (2014). Development of astrocytes in the vertebrate eye. *Developmental dynamics : an official publication of the American Association of Anatomists, 243*(12), 1501-1510. doi:10.1002/dvdy.24190

Telegina, D. V., Kozhevnikova, O. S., Bayborodin, S. I., & Kolosova, N. G. (2017a). Contributions of age-related alterations of the retinal pigment epithelium and of glia to the AMD-like pathology in OXYS rats. *Scientific reports, 7*(1), 41533. doi:10.1038/srep41533

Telegina, D. V., Kozhevnikova, O. S., & Kolosova, N. G. (2017b). Molecular mechanisms of cell death in retina during development of age-related macular degeneration. *Advances in Gerontology, 7*(1), 17-24. doi:10.1134/S2079057017010155

Terasaki, H., Kase, S., Shirasawa, M., Otsuka, H., Hisatomi, T., Sonoda, S., . . . Sakamoto, T. (2013). TNF-α Decreases VEGF Secretion in Highly Polarized RPE Cells but Increases It in Non-Polarized RPE Cells Related to Crosstalk between JNK and NF-κB Pathways. *PLoS One, 8*(7), e69994. doi:10.1371/journal.pone.0069994

Thornton, J., Edwards, R., Mitchell, P., Harrison, R. A., Buchan, I., & Kelly, S. P. (2005). Smoking and age-related macular degeneration: a review of association. *Eye, 19*(9), 935-944. doi:10.1038/sj.eye.6701978

Thorpe, S., & Baynes, J. (2003). Maillard reaction products in tissue proteins: new products and new perspectives. *Amino acids, 25*(3-4), 275-281.

Tian, J., Ishibashi, K., Ishibashi, K., Reiser, K., Grebe, R., Biswal, S., . . . Handa, J. T. (2005). Advanced glycation endproduct-induced aging of the retinal pigment epithelium and choroid: a comprehensive transcriptional response. *Proceedings of the National Academy of Sciences of the United States of America, 102*(33), 11846-11851.

Tian, S.-W., Ren, Y., Pei, J.-Z., Ren, B.-C., & He, Y. (2017). Pigment epithelium-derived factor protects retinal ganglion cells from hypoxia-induced apoptosis by preventing mitochondrial dysfunction. *International journal of ophthalmology, 10*(7), 1046-1054. doi:10.18240/ijo.2017.07.05

Tieri, P., Termanini, A., Bellavista, E., Salvioli, S., Capri, M., & Franceschi, C. (2012). Charting the NF-κB Pathway Interactome Map. *PLoS One, 7*(3), e32678. doi:10.1371/journal.pone.0032678

Tokarz, P., Kaarniranta, K., & Blasiak, J. (2013). Role of antioxidant enzymes and small molecular weight antioxidants in the pathogenesis of age-related macular degeneration (AMD). *Biogerontology, 14*(5), 461-482. doi:10.1007/s10522-013-9463-2

Tong, J. P., & Yao, Y. F. (2006). Contribution of VEGF and PEDF to choroidal angiogenesis: a need for balanced expressions. *Clin Biochem, 39*(3), 267-276. doi:10.1016/j.clinbiochem.2005.11.013

Touhami, S., Beguier, F., Augustin, S., Charles-Messance, H., Vignaud, L., Nandrot, E. F., . . . Sahel, J.-A. (2018). Chronic exposure to tumor necrosis factor alpha induces retinal pigment epithelium cell dedifferentiation. *J Neuroinflammation, 15*(1), 85.

Trellu, S., Courties, A., Jaisson, S., Friguet, B., Houard, X., Erkhirch, F. P., . . . Sellam, J. (2017). Accumulation of advanced glycation end-products (AGEs) in osteoarthritic cartilage is related to an impairment of the adaptative mechanism of glyoxalase-1. *Osteoarthritis and Cartilage, 25*, S86. doi:10.1016/j.joca.2017.02.134

Tsai, D. C., Charng, M. J., Lee, F. L., Hsu, W. M., & Chen, S. J. (2006). Different plasma levels of vascular endothelial growth factor and nitric oxide between patients with choroidal and retinal neovascularization. *Ophthalmologica, 220*(4), 246-251. doi:10.1159/000093079

Tsin, A., Betts-Obregon, B., & Grigsby, J. (2018). Visual cycle proteins: Structure, function, and roles in human retinal disease. *J Biol Chem, 293*(34), 13016-13021. doi:10.1074/jbc.AW118.003228

Turk, V., Stoka, V., Vasiljeva, O., Renko, M., Sun, T., Turk, B., & Turk, D. (2012). Cysteine cathepsins: From structure, function and regulation to new frontiers. *Biochimica et Biophysica Acta (BBA) - Proteins and Proteomics, 1824*(1), 68-88. doi:http://dx.doi.org/10.1016/j.bbapap.2011.10.002

Turk, V., Turk, B., & Turk, D. (2001). Lysosomal cysteine proteases: facts and opportunities. *The EMBO journal, 20*(17), 4629-4633.

Uhlik, M., Good, L., Xiao, G., Harhaj, E. W., Zandi, E., Karin, M., & Sun, S.-C. (1998). NF-κB-inducing kinase and IκB kinase participate in human T-cell leukemia virus I Tax-mediated NF-κB activation. *Journal of Biological Chemistry, 273*(33), 21132-21136.

Umar, S., Hedaya, O., Singh, A. K., & Ahmed, S. (2015). Thymoquinone inhibits TNF-α-induced inflammation and cell adhesion in rheumatoid arthritis synovial fibroblasts by ASK1 regulation. *Toxicology and Applied Pharmacology, 287*(3), 299-305. doi:10.1016/j.taap.2015.06.017

Umar, S., Zargan, J., Umar, K., Ahmad, S., Katiyar, C. K., & Khan, H. A. (2012). Modulation of the oxidative stress and inflammatory cytokine response by thymoquinone in the collagen induced arthritis in Wistar rats. *Chemico-Biological Interactions, 197*(1), 40-46. doi:http://dx.doi.org/10.1016/j.cbi.2012.03.003

Urbich, C., Heeschen, C., Aicher, A., Sasaki, K., Bruhl, T., Farhadi, M. R., . . . Dimmeler, S. (2005). Cathepsin L is required for endothelial progenitor cell-induced neovascularization. *Nat Med, 11*(2), 206-213. doi:10.1038/nm1182

VandenLangenberg, G. M., Mares-Perlman, J. A., Klein, R., Klein, B. E. K., Brady, W. E., & Palta, M. (1998). Associations between Antioxidant and Zinc Intake and the 5-Year Incidence of Early Age-related Maculopathy in the Beaver Dam Eye Study. *American Journal of Epidemiology, 148*(2), 204-214. doi:10.1093/oxfordjournals.aje.a009625

Vanderbeek, B. L., Zacks, D. N., Talwar, N., Nan, B., Musch, D. C., & Stein, J. D. (2011). Racial differences in age-related macular degeneration rates in the United States: a longitudinal analysis of a managed care network. *American journal of ophthalmology, 152*(2), 273-282.e273. doi:10.1016/j.ajo.2011.02.004

Velagapudi, R., Kumar, A., Bhatia, H. S., El-Bakoush, A., Lepiarz, I., Fiebich, B. L., & Olajide, O. A. (2017a). Inhibition of neuroinflammation by thymoquinone requires activation of Nrf2/ARE signalling. *Int Immunopharmacol, 48*, 17-29. doi:10.1016/j.intimp.2017.04.018

Velagapudi, R., Kumar, A., Bhatia, H. S., El-Bakoush, A., Lepiarz, I., Fiebich, B. L., & Olajide, O. A. (2017b). Inhibition of neuroinflammation by thymoquinone requires activation of Nrf2/ARE signalling. *International Immunopharmacology, 48*, 17-29. doi:https://doi.org/10.1016/j.intimp.2017.04.018

Velilla, S., García-Medina, J. J., García-Layana, A., Dolz-Marco, R., Pons-Vázquez, S., Pinazo-Durán, M. D., . . . Gallego-Pinazo, R. (2013). Smoking and age-related macular degeneration: review and update. *Journal of ophthalmology, 2013*, 895147-895147. doi:10.1155/2013/895147

Verma, S., Dixit, R., & Pandey, K. C. (2016). Cysteine Proteases: Modes of Activation and Future Prospects as Pharmacological Targets. *Frontiers in pharmacology, 7*.

Verstrepen, L., Bekaert, T., Chau, T.-L., Tavernier, J., Chariot, A., & Beyaert, R. (2008). TLR-4, IL-1R and TNF-R signaling to NF-κB: variations on a common theme. *Cellular and Molecular Life Sciences, 65*(19), 2964-2978. doi:10.1007/s00018-008-8064-8

Vistoli, G., De Maddis, D., Cipak, A., Zarkovic, N., Carini, M., & Aldini, G. (2013). Advanced glycoxidation and lipoxidation end products (AGEs and ALEs): an overview of their mechanisms of formation. *Free Radic Res, 47 Suppl 1*, 3-27. doi:10.3109/10715762.2013.815348

Wang, A. L., Lukas, T. J., Yuan, M., Du, N., Tso, M. O., & Neufeld, A. H. (2009). Autophagy and exosomes in the aged retinal pigment epithelium: possible relevance to drusen formation and age-related macular degeneration. *PLoS One, 4*(1), e4160. doi:10.1371/journal.pone.0004160

Wang, F., Rendahl, K. G., Manning, W. C., Quiroz, D., Coyne, M., & Miller, S. S. (2003). AAV-mediated expression of vascular endothelial growth factor induces

choroidal neovascularization in rat. *Investigative ophthalmology & visual science, 44*(2), 781-790.

Wang, X., Martindale, J., Liu, Y., & Holbrook, N. (1998). The cellular response to oxidative stress: influences of mitogen-activated protein kinase signalling pathways on cell survival. *Biochem. J, 333,* 291-300.

Wang, Y.-R., Qin, S., Han, R., Wu, J.-C., Liang, Z.-Q., Qin, Z.-H., & Wang, Y. (2013). Cathepsin L Plays a Role in Quinolinic Acid-Induced NF-Kb Activation and Excitotoxicity in Rat Striatal Neurons. *PLoS One, 8*(9), e75702. doi:10.1371/journal.pone.0075702

Wang, Y., Gao, H., Zhang, W., Zhang, W., & Fang, L. (2015). Thymoquinone inhibits lipopolysaccharide-induced inflammatory mediators in BV2 microglial cells. *Int Immunopharmacol, 26*(1), 169-173. doi:10.1016/j.intimp.2015.03.013

Wang, Y., Shen, D., Wang, V. M., Yu, C. R., Wang, R. X., Tuo, J., & Chan, C. C. (2012). Enhanced apoptosis in retinal pigment epithelium under inflammatory stimuli and oxidative stress. *Apoptosis, 17*(11), 1144-1155. doi:10.1007/s10495-012-0750-1

Watanabe, S., Hayakawa, T., Wakasugi, K., & Yamanaka, K. (2014). Cystatin C protects neuronal cells against mutant copper-zinc superoxide dismutase-mediated toxicity. *Cell Death Dis, 5,* e1497. doi:10.1038/cddis.2014.459

Waugh, N., Loveman, E., Colquitt, J., Royle, P., Yeong, J. L., Hoad, G., & Lois, N. (2018). Treatments for dry age-related macular degeneration and Stargardt disease: a systematic review.

Wei, W., Li, L., Zhang, Y., Geriletu, Yang, J., Zhang, Y., & Xing, Y. (2014). Vitamin C Protected Human Retinal Pigmented Epithelium from Oxidant Injury Depending on Regulating SIRT1. *The Scientific World Journal, 2014,* 750634. doi:10.1155/2014/750634

Wendt, W., Lubbert, H., & Stichel, C. C. (2008). Upregulation of cathepsin S in the aging and pathological nervous system of mice. *Brain Res, 1232*, 7-20. doi:10.1016/j.brainres.2008.07.067

Wertz, I. E., O'rourke, K. M., Zhou, H., Eby, M., Aravind, L., Seshagiri, S., . . . Boone, D. L. (2004). De-ubiquitination and ubiquitin ligase domains of A20 downregulate NF-κB signalling. *Nature, 430*(7000), 694-699.

Westmoreland, B. F., Lemp, M. A., & Snell, R. S. (1998). Clinical Anatomy of the Eye. In: Blackwell Publishers.

Witmer, A., Vrensen, G., Van Noorden, C., & Schlingemann, R. (2003). Vascular endothelial growth factors and angiogenesis in eye disease. *Progress in retinal and eye research, 22*(1), 1-29.

Wong, W. L., Su, X., Li, X., Cheung, C. M. G., Klein, R., Cheng, C.-Y., & Wong, T. Y. (2014). Global prevalence of age-related macular degeneration and disease

burden projection for 2020 and 2040: a systematic review and meta-analysis. *The Lancet Global Health, 2*(2), e106-e116.

Woo, C. C., Kumar, A. P., Sethi, G., & Tan, K. H. B. (2012). Thymoquinone: Potential cure for inflammatory disorders and cancer. *Biochemical pharmacology, 83*(4), 443-451. doi:http://dx.doi.org/10.1016/j.bcp.2011.09.029

Wyczalkowska-Tomasik, A., & Paczek, L. (2012). Cathepsin B and L activity in the serum during the human aging process: cathepsin B and L in aging. *Arch Gerontol Geriatr, 55*(3), 735-738. doi:10.1016/j.archger.2012.05.007

Xiang, B., Fei, X., Zhuang, W., Fang, Y., Qin, Z., & Liang, Z. (2011). Cathepsin L is involved in 6-hydroxydopamine induced apoptosis of SH-SY5Y neuroblastoma cells. *Brain Res, 1387*, 29-38. doi:10.1016/j.brainres.2011.02.092

Xie, J., Mendez, J. D., Mendez-Valenzuela, V., & Aguilar-Hernandez, M. M. (2013). Cellular signalling of the receptor for advanced glycation end products (RAGE). *Cell Signal, 25*(11), 2185-2197. doi:10.1016/j.cellsig.2013.06.013

Xu, H., & Chen, M. (2016). Targeting the complement system for the management of retinal inflammatory and degenerative diseases. *European Journal of Pharmacology, 787*, 94-104. doi:10.1016/j.ejphar.2016.03.001

Xu, H., Chen, M., & Forrester, J. V. (2009). Para-inflammation in the aging retina. *Prog Retin Eye Res, 28*(5), 348-368. doi:10.1016/j.preteyeres.2009.06.001

Xu, L., Sheng, J., Tang, Z., Wu, X., Yu, Y., Guo, H., . . . Zhou, J. (2005). Cystatin C prevents degeneration of rat nigral dopaminergic neurons: in vitro and in vivo studies. *Neurobiology Of Disease, 18*(1), 152-165. doi:http://doi.org/10.1016/j.nbd.2004.08.012

Xu, S., Zhang, H., Yang, X., Qian, Y., & Xiao, Q. (2018). Inhibition of cathepsin L alleviates the microglia-mediated neuroinflammatory responses through caspase-8 and NF-kappaB pathways. *Neurobiol Aging, 62*, 159-167. doi:10.1016/j.neurobiolaging.2017.09.030

Yamada, Y., Ishibashi, K., Ishibashi, K., Bhutto, I. A., Tian, J., Lutty, G. A., & Handa, J. T. (2006). The expression of advanced glycation endproduct receptors in rpe cells associated with basal deposits in human maculas. *Exp Eye Res, 82*(5), 840-848.

Yamaoka, S., Courtois, G., Bessia, C., Whiteside, S. T., Weil, R., Agou, F., . . . Israël, A. (1998). Complementation cloning of NEMO, a component of the IκB kinase complex essential for NF-κB activation. *Cell, 93*(7), 1231-1240.

Yan, S. D., Schmidt, A. M., Anderson, G. M., Zhang, J., Brett, J., Zou, Y. S., . . . Stern, D. (1994). Enhanced cellular oxidant stress by the interaction of advanced glycation end products with their receptors/binding proteins. *J Biol Chem, 269*(13), 9889-9897.

Yang, N., Wang, P., Wang, W.-j., Song, Y.-z., & Liang, Z.-q. (2015). Inhibition of cathepsin L sensitizes human glioma cells to ionizing radiation in vitro through

NF-κB signaling pathway. *Acta Pharmacologica Sinica, 36*(3), 400-410. doi:10.1038/aps.2014.148

Yin, J., Thomas, F., Lang, J. C., & Chaum, E. (2011). Modulation of oxidative stress responses in the human retinal pigment epithelium following treatment with vitamin C. *J Cell Physiol, 226*(8), 2025-2032. doi:10.1002/jcp.22532

Yorston, D. (2014). Anti-VEGF drugs in the prevention of blindness. *Community eye health, 27*(87), 44-46.

Younessi, P., & Yoonessi, A. (2011). Advanced Glycation End-Products and Their Receptor-Mediated Roles: Inflammation and Oxidative Stress. *Iranian Journal of Medical Sciences, 36*(3), 154-166.

Yu, C. C., Nandrot, E. F., Dun, Y., & Finnemann, S. C. (2012). Dietary antioxidants prevent age-related retinal pigment epithelium actin damage and blindness in mice lacking alphavbeta5 integrin. *Free Radic Biol Med, 52*(3), 660-670. doi:10.1016/j.freeradbiomed.2011.11.021

Zafrilla, P., Losada, M., Perez, A., Caravaca, G., & Mulero, J. (2013). Biomarkers of oxidative stress in patients with wet age related macular degeneration. *The journal of nutrition, health & aging, 17*(3), 219-222.

Zarbin, M. A. (2004). Current concepts in the pathogenesis of age-related macular degeneration. *Archives of ophthalmology, 122*(4), 598-614. doi:10.1001/archopht.122.4.598

Zhang, Q., Ames, J. M., Smith, R. D., Baynes, J. W., & Metz, T. O. (2009). A perspective on the Maillard reaction and the analysis of protein glycation by mass spectrometry: probing the pathogenesis of chronic disease. *Journal of proteome research, 8*(2), 754-769. doi:10.1021/pr800858h

LIST OF PUBLICATIONS AND PAPERS PRESENTED

Publication

"AGE-related modulation of cathepsin L and NF-κβ signaling effectors in retinal pigment epithelium leads to augmented response to TNFα"

*Umar Sharif, *Nur Musfirah Mahmud, Paul Kay, Yit C. Yang, Simon P. Harding, Ian Grierson, Tengku Ain Kamalden, Malcolm J. Jackson, Luminita Paraoan.

Published in Journal of Cellular and Molecular Medicine (19 October 2018)

Conference and Scientific Meetings Attended

1. Modulation of cathepsin L expression and NF-κβ signalling pathway effectors by advanced glycation end-products in retinal pigment epithelial cells

   N.M. Mahmud, U. Sharif, P. Kay, T.A. Kamalden, Y.C. Yang, S. Harding, L. Paraoan

   Poster presentation, ARVO 2016, Seattle, USA

2. "Does NF-κβ Signalling in the Ageing Retinal Pigment Epithelium (RPE) lead to lysosomal regulation?"

   N.M. Mahmud, T.A. Kamalden, L. Paraoan

   Oral Presentation, Institute of Ageing and Chronic Disease (IACD), University of Liverpool, UK

3. “Modulation of cathepsin L expression and NF-κβ signalling pathway effectors by advanced glycation end-products in retinal pigment epithelial cells”

   N.M. Mahmud, U. Sharif, P. Kay, T.A. Kamalden, Y.C. Yang, S. Harding, L. Paraoan

   Pre- ARVO, Oral presentation, Institute of Ageing and Chronic Disease (IACD), University of Liverpool, UK

4. “Cathepsin L Expression, Advanced Glycation Endproducts and NF-κβ signaling in RPE cells”

   N.M. Mahmud, T.A. Kamalden, L. Paraoan

   Rapid Fire Oral and Poster Presentation, Department of Eye and Vision Science (DEVS), University of Liverpool, UK.

5. ”Autophagy/Mitophagy in Age Related Macular Degeneration”

   N.M. Mahmud, T.A. Kamalden, L. Paraoan

   Post ARVO, Oral Presentation, Institute of Ageing and Chronic Disease (IACD), University of Liverpool, UK

APPENDIX

Appendix A: Buffers and Reagent Used in Research

A. Laemmli Lysis Buffer (for lysing cells).

(0.128M β-mercaptoethanol, 40mM Tris, 10%glycerol, 1%SDS, 0.01% bromophenol blue)

10ml 10% SDS

10ml glycerol

10ml β-mercaptoethanol 16ml 0.25M Tris pH6.8

1ml 0.1% bromophenol blue (1mg in 1ml, or a few specs)

Solution was made up to 100ml with distilled water.

B. Laemmli loading buffer

(10x, 62.5mM Tris pH 6.8, 0.625M β-mercaptoethanol, 10% glycerol, 2%SDS, 0.00125% bromophenol blue)

0.8ml Glycerol

3.0ml water

2.0ml 0.25M TrisHcl pH 6.8

1.6ml 10% SDS

0.4ml β-mercaptoethanol

Solution was made to 8ml stock and a few specs of bromophenol blue was added to give its color. Later, ¼ volume of loading buffer was added to sample before heating (used at 2x)

C. Resolving gel buffer for SDS-PAGE (Tris-Hcl 3M pH 8.85, 100ml stock)

36.33g Tris

Initially, 80ml of distilled water was added to the Tris powder and stirred to dissolve. pH was calibrated to 8.85 using Hcl. Finally, distilled water as added to a total volume of 100ml.

D. Stacking gel for SDS-PAGE (0.25M Tris-Hcl pH6.8)

3.028g Tris

Initially, 80ml of distilled water was added to the Tris powder and stirred to dissolve. pH was calibrated to 6.8 using Hcl. Finally, distilled water as added to a total volume of 100ml.

E. 10% Ammonium persulphate (APS)

0.05g APS powder

500µl of distilled water was added to the powder and vortex until fully dissolved.

F. 10% Sodium Dodecyl Sulphate Solution (SDS)

50g SDS powder

The SDS powder was handled in the fumehood as it can cause serious respiratory problems. 500ml of water was added to the powder and stirred until it is fully dissolve.

G. 5x running buffer for SDS-PAGE Electrophoresis (1L)

(0.125M Tris, 1.25M Glycine, 0.5%SDS)

15.1g Tris base

94g Glycine

50ml 10% SDS

Solution was made by mixing all the components above and the volume was adjusted to 1L. The running buffer was used at 1x during experiments. Thus, appropriate volume of stock solution was later added to distilled water to get the 1x concentration.

H. Transfer Buffer for western blotting

233ml 100% ethanol

100ml 5x running buffer

Solution was made by adding the required volume of ethanol and running buffer. Volume was adjusted to 1L with addition of distilled water.

I. 10x Tris-buffered Saline (10x TBS)

(0.2M Tris, pH7.6)

24.2g Tris

80g NaCl

Initially, 800ml of distilled water was added to the solution and pH was calibrated using Hcl solution. Then, the total volume of the solution was adjusted to 1L with distilled water.

J. Blocking Buffer for Immunoblotting

(0.02M Tris Nacl pH7.6, 0.1% Tween-20 with 5%(w/v) non-fat dry milk)

5g non fat dry powdered milk/ Bovine Serum Albumin powder

100ml wash buffer (TBS-tween)

Membranes were blocked either in 5% milk or 5% BSA dissolved in TBS –tween solution.

K. Wash Buffer (TBS-tween) for Wwestern Blot's Membrane Washing

(0.2M Tris M Nacl pH7.6, 0.1% Tween-20)

100ml 10x TBS

1ml Tween-20

Solution was made up to 1L using distilled water.

L. Stripping Buffer for Western Blot Membrane

10.4ml 3M Tris solution (Resolving gel buffer)

100ml 10% SDS

Initially, solution was made up to 300ml with distilled water. pH was adjusted to 6.7 with Hcl. Finally, the volume was adjusted to 500ml with distilled water. 175µl of β-mercaptoethanol was added to every 25ml of stock solution just before use.

M. Agarose Gel for Electrophoresis

1.5g Agarose powder/ tablet

Solution was made up to 100ml with 1X TBE electrophoresis buffer in a flask.

N. 10X Tris-Borate-EDTA (TBE) Electrophoresis Buffer

108g Tris

55g Orthoboric Acid (B (OH) 3)

2.92g EDTA

Solution was made up to 1L with distilled water. Stock solution was diluted to 1x working concentration just before use.